8 Vessel Failure Frequencies Estimated for Oconee Unit 1, Beaver Valley Unit 1, and Palisades

8.1 Chapter Structure

In this chapter, we describe the results of our probabilistic calculations for Oconee Unit 1, Beaver Valley Unit 1, and Palisades.
Section 8.2 details the plant-specific features of each analysis, including both methodology and input variables. In Section 8.3, we present the values of frequency of crack initiation (FCI) and through-wall cracking frequency (TWCF) that we have estimated for these three plants, and we discuss the characteristics of the distributions from which these values are derived.
In Section 8.4, we examine the material features that contribute most significantly, and those that do not contribute at all, to the magnitude of the FCI and TWCF values. A key output of this section is a methodology to express the embrittlement level of different plants on an equivalent basis. In Section 8.5, we both identify the classes of transients (e.g., LOCAs, MSLBs, and so on) that contribute most significantly, and those that do not contribute at all, to the level of PTS challenge at a particular plant. Using this information along with methodology developed in Section 8.4 allows us to determine if plant-specific factors need to be considered when assessing the level of challenge posed to plants by different transient classes. The chapter concludes with Section 8.6, which summarizes our findings and indicates factors that need to be considered if these findings are to be considered generally applicable to all PWRs. Issues of general applicability are examined in more detail in Chapter 9.

8.2 Plant-Specific Features of Analysis

8.2.1 PRA

8.2.1.1 Analysis Methodology

In the case of both the Oconee and Beaver Valley PRA analyses, NRC contractors were responsible for both constructing the PRA models and binning the overcooling sequences into "case" sequences. The PRA models were constructed from scratch, largely based on information learned from the 1980s PTS work, but with numerous improvements. The HRA portion of the PRA was also initially performed by the NRC contractors. The corresponding licensees provided information about each plant and answered both written and verbal questions as the PRA model and the PRA/HRA evolved. In each case, two plant visits took place: one early in the process to gather plant information, and a second when interim results were available to allow licensee review and input.

In contrast, the PRA/HRA analysis for Palisades derived mostly from an existing licensee PRA model that already included overcooling sequences. NRC contractors provided comments on the existing PRA model, a model that was subsequently modified by the licensee in response to these comments. Once the revised PRA model was satisfactory to both the licensee and NRC contractors, the HRA portion of the analysis was conducted as a collaborative effort. This HRA information was included in the Palisades PRA model, and sequence binning and frequency estimates were subsequently performed primarily by the licensee with NRC contractor review, input, and slight modification. Two plant visits were also conducted for the Palisades analysis: the first for initial project and

plant familiarization, and the second for conducting the collaborative HRA. As for the other two plant analyses, numerous discussions were held between the Palisades staff and NRC Contractors as the PRA model and PRA/HRA evolved. Hence, while the same overall approach was followed to construct all three PRA/HRA models, the origin of these models and the key personnel responsible for constructing them varied from plant-to-plant

8.2.1.2 Inputs

The plant-specific PRAs described in Section 8.2.1.1 led to the definition of a master list of thermal-hydraulic transients. A sub-set of these transients from this list was defined as the "base case" for each plant, which represents our best mathematical description of the conditions at the plant that could produce a PTS challenge to vessel integrity. TH cases from the master list were eliminated from the base case for a number of reasons, including the following:

- Certain transients were binned together, making some TH runs redundant, or
- Sensitivity studies revealed that certain TH cases did not need to be passed on, or
- The minimum temperature remained above 400°F (204°C) within the first ≈170 minutes. Experience gained from previous analysis of PTS has repeatedly demonstrated that transients need to be at least this severe to make any contribution at all to the calculated through-wall cracking frequency. Later examination of TWCF estimates for all base case transients revealed that many transients having lower minimum temperatures still made no contribution to TWCF, thus demonstrating the appropriateness of this screening limit.

The details of each plant-specific PRA are summarized in other reports [***Kolaczkowski-Oco, Whitehead-BV, Whitehead-Pal***]. Appendix A provides the master list of transients for all three plants, and also lists the frequency values for the base-case transients.

8.2.2 TH

This section describes the RELAP5 models developed for the Oconee-1, Beaver Valley Unit 1, and Palisades plants. The TH analysis methodology is similar for the three plants. In each case, the best available RELAP5 input model was used as the starting point to expedite the model development process. For Oconee, the base model was that used in the code scaling, applicability and uncertainty (CSAU) study. For Beaver Valley, the base model was the H.B. Robinson-2 model used in the original PTS study in the mid 1980s. This model was revised by Westinghouse to reflect the Beaver Valley plant configuration. For Palisades, the base model was obtained from Nuclear Management Corporation, the operators of the Palisades plant. This model was originally developed and documented by Siemens Power Corporation to support analysis of the loss of electrical load event for Palisades.

The RELAP5 models for the Oconee, Beaver Valley, and Palisades plants are detailed representations of the power plants and include all major components for both the primary and secondary plant systems. RELAP5 heat structures are used throughout the models to represent structures such as the fuel, vessel wall, vessel internals, and steam generator tubes. The reactor vessel nodalization includes the downcomer, lower plenum, core inlet, core, core bypass, upper plenum and upper head regions. Plant-specific features, such as the reactor vessel vent valves, are included as appropriate.

The downcomer model used in each plant utilizes a two-dimensional nodalization. This approach was used to capture the possible temperature variation in the downcomer due to the injection of cold ECCS water into each of the cold legs. Capturing this temperature variation in the downcomer is not possible with the original one-dimensional downcomer. In the revised models, the downcomer is divided into six azimuthal regions for each plant.

The safety injection systems modeled for the Oconee, Palisades, and Beaver Valley plants include high-pressure injection (HPI),

low-pressure injection (LPI), other ECCS components (e.g., accumulators, core flood tanks (CFTs), safety injection tanks (SITs) depending on the plant designation), and makeup/letdown, as appropriate.

The secondary coolant system models include steam generators, main and auxiliary/emergency feedwater, steam lines, safety valves, main steam isolation valves (as appropriate), and turbine bypass and stop valves.

Each of the models was updated to reflect the current plant configuration including updating system setpoints (to best estimate values) and modifying control logic to reflect current operating procedures. Other changes to the models include the addition of control blocks to calculate parameters for convenience or information only (e.g., items such as minimum downcomer temperature). The Oconee, Beaver Valley, and Palisades models were then initialized to simulate hot full power and hot zero power plant operation for the purpose of establishing satisfactory steady-state conditions from which the PTS transient event sequence calculations are started.

In RELAP5 simulations of LOCA event sequences for the Oconee and Palisades plants during which all of the reactor coolant pumps are tripped and the loss of primary coolant system inventory is sufficient to interrupt coolant loop natural circulation flow, a circulating flow was observed between the two cold legs on the same coolant loop. The circulations mix coolant in the reactor vessel downcomer, cold leg and SG outlet plenum regions. These RELAP5 cold-leg circulations were originally reported during the first PTS evaluation study [Fletcher 84, Spiggs 85] and are significant for the PTS application. When the circulation is present the calculated reactor vessel downcomer fluid temperature benefits from the warming effects created by mixing the cold HPI fluid with the warm steam generator outlet plenum fluid. When the circulation is not present the calculated reactor vessel downcomer fluid temperature more directly feels the influence of the cold HPI fluid. Note that both the Oconee and Palisades plants have a "2x4" configuration with two cold legs and one hot leg in each coolant loop. In contrast, the Beaver Valley plant has a single hot and cold leg per coolant loop and this type of circulating flow is not seen. (See Section 6.3.2 for a further discussion of this issue.)

Certain experiments used in the assessment exhibited apparent indications of cold leg circulations very similar to those simulated with RELAP5. However, the experimental evidence was not judged to be conclusive and concerns (related to circulation initiation and the scalability of the behavior from the sub-scale experiment to full-scale plant configurations) remain regarding the veracity of these circulations. Because of these concerns and because the effect of including cold leg circulations in the RELAP5 simulations is nonconservative for PTS (i.e., it results in warmer reactor vessel downcomer temperatures), same-loop cold leg circulations were prevented in the RELAP5 PTS plant simulations for LOCA events. The cold leg circulations were prevented by implementing large reverse flow loss coefficients (1.0E5, based on the cold leg pipe flow area) in the reactor coolant pump regions of the RELAP5 model. The model change is implemented at the time during the event sequence when the reactor coolant pump coast-down is complete.

A tabulation of the key parameters for the three study plants relevant to PTS is presented in Table 8.1, while [***Arcieri-Base***] explains the TH models in detail.

8.2.3 PFM

A separate report [***Dickson-Base***] provides full details of the plant-specific input values for each of the three plants. These inputs include the following:

- Composition and Mechanical Property Data: As detailed in Section 7.7.1.2 of this report and in Appendix D of [***EricksonKirk-PFM***] FAVOR models the uncertainty in the input variables of Cu, Ni, P, unirradiated RT_{NDT}, and unirradiated Charpy upper shelf energy. The data on which the distributions that

FAVOR samples are based are drawn from *all data available* for the entire population of RPV-grade ferritic steels and their weldments. Consequently, these distributions overestimate (sometimes significantly so) the degree of uncertainty in these input variables relative to that characteristic of a *particular* weld, plate, or forging in a *particular* PWR. The mean values of Cu, Ni, P, unirradiated RT_{NDT}, and unirradiated Charpy upper shelf energy about which these distributions are located are modeled as being specific to the particular welds, plates, and forgings in the particular plants. These input values, which are summarized in Table 8.2 are drawn from the NRC's Reactor Vessel Integrity Database [RVID2]. RVID2 was developed based on information obtained from licensee responses to NRC Generic Letter 92-01, Revision 1 and its 1995 supplement [GL9201R1, Strosnider 94, GL9201R1S1]. GL-92-01 was issued to resolve questions arising out of the staff's review of the Yankee Rowe PWR in the early 1990s. In reviewing the licensee's submittal, the staff noted that chemical composition and reference temperature information was not available for the specific materials from which Yankee was constructed. To prevent occurrence of this problem at other plants GL-92-01 required licensees to provide to the NRC all of their vessel-specific composition and mechanical property data. The 1995 supplement to GL-92-01 [GL9201R1S1] continued and broadened this data collection effort when the staff noted that licensees were not always able to consider all pertinent data in their submittals because of both proprietary issues associated with some data sets and because no single source of all the material property data needed to support reactor vessel integrity evaluations existed. As the consolidation of all the data obtained in response to GL-92-01 Rev. 1 (and its 1995 supplement) the information in RVID2 (and, consequently, in Table 8.2) provides a sound basis for the compositional and mechanical property models adopted in FAVOR.

- Flaw Data: As described in Section 7.5 and detailed by [***Simonen***], flaw distributions have been derived that apply to domestic PWRs in general. Nonetheless, these distributions have certain plant-specific aspects. Table 8.3 summarizes the variables that quantify the plant-specific features of the flaw distribution, and the basis for these variables.
- Locations of Welds, Plates, and Forgings within the Vessel Beltline, and Fluence: Plant-specific information is needed regarding the spatial arrangement of the different welds, plates, and forgings and on the variation of fluence throughout the beltline region of the vessels. Figure 8.1 provides an example of such information for Oconee Unit 1; see [***Dickson-Base***] for full details. Information regarding the spatial arrangement of the different welds, plates, and forgings is taken from construction drawings while fluence estimates are based on RG1.190 procedures. (See Section 7.6 of this report and [***EricksonKirk-PFM***] for details.)

Only those factors discussed above are defined on a plant-specific basis in this analysis. All other features not mentioned are justified as generic and treated as such. Details on models and variables treated generically can be found in Chapter 7, as well as in [***EricksonKirk-PFM***, ***EricksonKirk-SS***].

8.3 Estimated Values of FCI and TWCF

This section begins with a presentation of our estimates of the annual frequencies of crack initiation (FCI) and through-wall cracking (TWCF) resulting from PTS for our three study plants for a range of embrittlement conditions (Section 8.3.1). We then examine the characteristics of the distributions that underlie these FCI and TWCF values (Section 8.3.2).

8.3.1 Overall Results

Table 8.4 presents FAVOR Version 04.1 estimates of the mean annual *FCI* and mean annual *TWCF* for Oconee Unit 1, Beaver Valley Unit 1, and Palisades at 32 and 60 EFPY[‡‡‡]. To estimate values of these metrics close to the *TWCF* limit of $1x10^{-6}$ events/year proposed in Chapter 10, it was necessary to increase the amount of irradiation damage beyond that likely during operational lifetimes currently considered possible. To do so, we performed analyses for some very long operating lifetimes (designated as Ext-A and Ext-B in the table), thereby increasing the fluence and, consequently, the irradiation damage. The range of irradiation exposures examined includes conditions both below and above the current 10 CFR 50.61 RT_{PTS} screening limits.

The results in Table 8.4 demonstrate that even at the end of license extension (60 operational years, or 48 EFPY at an 80% capacity factor) the mean estimated through-wall cracking frequency (*TWCF*) does not exceed $2x10^{-8}$/year. Considering that the Beaver Valley and Palisades RPVs are constructed from some of the most irradiation-sensitive materials in commercial reactor service today, these results suggest that, provided operating practices do not change dramatically in the future, the operating reactor fleet is in little danger of exceeding the *TWCF* acceptance criterion of $5x10^{-6}$/yr expressed by Regulatory Guide 1.154 [RG 1.154][§§§], even after license extension.

8.3.2 Distribution Characteristics

To present our analysis results for all three plants in as compact a format as possible, we report only mean values of FCI and TWCF in Table 8.4. Nonetheless, since a systematic treatment of uncertainties is key to our objective of developing a risk-informed revision to 10 CFR 50.61, it is important to examine the characteristics of the distributions that underlie these mean values. As illustrated in Figure 8.2 using Beaver Valley as a characteristic example, the TWCF distributions are both very broad and highly skewed toward zero. As described in the following sections, both the skewness and the spread in these results are expected because both of these characteristics result directly from the physical features of cleavage fracture.

8.3.2.1 Skewness in the TWCF Distribution

The skewness in the TWCF distributions illustrated in Figure 8.2 results directly from the physical nature of cleavage crack initiation and arrest. The crack initiation (K_{Ic}) and crack arrest (K_{Ia}) toughness distributions both have finite lower bound values that are physically justified [***ErickssonKirk-PFM***]. The following three mathematical conditions all lead to a likelihood of through-wall cracking that is zero *by definition* (not just a very small number):

- If the applied-K_I value for a particular FAVOR simulation run (i.e., a particular crack in a particular location subjected to a particular TH transient) never exceeds the 0^{th} percentile K_{Ic} value, then the crack has zero probability of crack initiation and (consequently) zero probability of through-wall cracking.
- If the applied-K_I value for a particular simulation run exceeds the 0^{th} percentile K_{Ic} value, but exceeds it at a time when the applied-K_I value is dropping with time (i.e., $dK_I/dt \leq 0$), then warm pre-stress has occurred and the crack has zero probability of crack initiation and (consequently) zero probability of through-wall cracking.

---

‡‡‡ The table also includes a number of different reference temperature metrics, the significance of which is discussed in Section 8.4.

§§§ Specifically, Section 9 of Regulatory Guide 1.154 makes the following statement: *"This Regulatory Guide outlines the analyses that should be performed in support of any request to operate at RT_{PTS} values in excess of 270°F ... and states that the staff's primary acceptance criterion will be licensee demonstration that through-wall cracking frequency will be below $5x10^{-6}$ per reactor year for such operation."*

- If the applied-K_I value for a particular simulation run exceeds the minimum K_{Ic} at a time when the applied-K_I value is increasing with time (i.e., $dK_I/dt > 0$), then the crack has a non-zero probability of crack initiation. However, if while the crack is propagating through the RPV wall, the applied-K_I value falls below the minimum K_{Ia} value then the crack arrest must occur. Such a crack would provide no contribution to the through-wall cracking frequency.

Table 8.1. Summary of Plant Parameters Relevant to the PTS Evaluation

Description	Oconee	Beaver Valley	Palisades
Reactor thermal power	2568 MWt	2660 MWt	2530 MWt
Primary code safety valve opening pressure	17.34 MPa (2515 psia)	17.27 MPa (2505 psia)	Three valves with staggered opening setpoints of 17.24, 17.51 and 17.79 MPa (2500, 2540 and 2580 psia).
Primary code safety valve capacity	Two valves each with a capacity of 43.47 kg/s (345,000 lbm/hr) at 16.89 MPa (2450 psia).	Three valves each with a capacity of 62.77 kg/s (498,206 lbm/hr) at 17.24 MPa (2500 psia).	Three valves each with a capacity of 28.98 kg/s (230,000 lbm/hr) at 17.75 MPa (2575 psia).
Pressurizer PORV opening pressure	17.0 MPa (2465 psia)	The first PORV is controlled by a compensated error signal. The error [pressurizer pressure – 15.51 MPa (2250 psia) is processed with a proportional plus integral controller. This PORV begins to open when the compensated error is $\geq$ 0.69 MPa (100 psi) and closes when the compensated pressure error < 0.62 MPa (90 psi). The second and third PORVs open when the pressurizer pressure is $\geq$ 16.2 MPa (2350 psia) and close when pressure < 16.1 MPa (2340 psia).	Two valves, both with an opening setpoint pressure of 16.55 MPa (2400 psia). Note that closed block valves prevent the function of pressure relief through these valves during normal plant operation.
PORV capacity	Estimated flow rate is 16.03 kg/s (127,000 lbm/hr) at 16.9 MPa (2450 psia).	Three valves each with a capacity of 26.46 kg/s (210,000 lbm/hr) at 16.2 MPa (2350 psia)	Two valves each with a capacity of 61.46 kg/s (487,800 lbm/hr) at 16.55 MPa (2400 psia).

Description	Oconee	Beaver Valley	Palisades
LPI injection actuation setpoint	3.89 MPa (550 psig).	SIAS signal: pressurizer pressure ≤ 12.72 MPa (1845 psia), high steamline DP (steamline pressure < header pressure by 0.69 MPa (100 psi) or more), or steamline pressure ≤ 3.47 MPa (503 psia).	Pressurizer pressure less than 10.98 MPa (1593 psia) with a 27-second time delay.
LPI pump shutoff head	1.48 MPa (214 psia)	1.48 MPa (214.7 psia)	1.501 MPa (217.7 psia).
LPI pump runout flow	504.5 kg/s (1110 lbm/s) total for two pumps.	313.4 kg/s (690.84 lbm/s) total for the three loops.	433.5 kg/s (955.7 lbm/s) total for the four loops.
HPI injection actuation setpoint	11.07 MPa (1605 psia)	SIAS signal: pressurizer pressure ≤12.72 MPa (1845 psia), high steamline DP (steamline pressure < header pressure by 0.69 MPa (100 psi) or more), or steamline pressure ≤3.47 MPa (503 psia).	Pressurizer pressure less than 10.98 MPa (1593 psia) with a 27-second time delay.
HPI pump shutoff head	> 18.61 MPa (2700 psia)	>17.93 MPa (2600 psia)	8.906 MPa (1291.7 psia).
HPI pump runout flow	80.9 kg/s (178.2 lbm/s) total for the four loops.	61.12 kg/s (134.7 lbm/s) total for the three loops.	86.49 kg/s (190.7 lbm/s) total for the four loops.
Reactor coolant pump trip setpoint	No automatic trips on the reactor coolant pump. Operator is assumed to trip RCPs at 0.28 K (0.5°F) subcooling.	No automatic trips on the reactor coolant pumps. Operator is assumed to trip RCPs when the differential pressure between the RCS and the highest SG pressure was less than 2.59 MPa (375 psig).	No automatic pump trips. Procedures instruct the operators to trip two RCPs (one in each loop) if pressurizer pressure falls below 8.96 MPa (1300 psia) and to trip all pumps if RCS subcooling falls below 13.9 K (25°F) or if containment pressure exceeds 0.127 MPa (18.4 psia).
SG safety valve bank opening pressure	The lowest relief valve setpoint is 6.76 MPa (980 psia).	The lowest relief valve setpoint is 7.51 MPa (1090 psig).	The lowest MSSV opening setpoint pressure is 7.097 MPa (1029.3 psia).
SG atmospheric steam dumps opening criteria	Not included in the RELAP5 model.	Opening pressure of 7.24 MPa (1050 psia).	Open to control the RCS average temperature to 551 K (532°F)

Description	Oconee	Beaver Valley	Palisades
Number of main steam isolation valves	None.	One per steam line.	One per steam line.
Location of steamline flow restrictors	None.	Located in SG outlet nozzles.	Located in SG outlet nozzles.
Isolation of turbine-driven EFW/AFW pump during MSLB	Isolated during MSLB by isolation circuitry	Requires manual operator action and would be done if needed to maintain SG level	Requires manual operator action and would be done if needed to maintain SG level.
Analyzed range of SI water temperature	Base case model assumptions for HPI and LPI nominal feed temperature is 294.3 K (70°F). CFT temperature is 299.8 K (80°F). Sensitivity cases for ECCS temperature due to seasonal variation: Summer Conditions HPI, LPI - 302.6 K (85°F) CFT - 310.9 K (100°F) Winter Conditions HPI, LPI - 277.6 K (40°F) CFT - 294.3 K (70°F)	Base case model assumptions for HPI and LPI nominal feed temperature is 283.1 K (50°F). CFT temperature is 305.4 K (90°F). Sensitivity cases for ECCS temperature due to seasonal variation: Summer Conditions HPI, LPI – 285.9 K (55°F) CFT – 313.7 K (105°F)	Base case model assumptions for HPI and LPI nominal feed temperature is 304.2 K (87.9°F). SIT temperature is 310.9 K (100°F). Sensitivity cases for ECCS temperature due to seasonal variation: Summer Conditions HPI, LPI - 310.9 K (100°F) SIT - 305.4 K (90°F) Winter Conditions HPI, LPI - 277.6 K (40°F) SIT - 288.7 K (60°F)
Refueling water storage tank water volume	Borated water storage tank water volume is 327,000 gallons (1,237,695 l)	Tank's useable volume is between 1627.7 and 1669.4 m^3 (430,000 and 441,000 gallons).	889.5 m^3 (235,000 gallons)
Containment spray actuation setpoint and flow rate	Total containment spray flow rate is 3,000 gpm (11355 lpm (1500 gpm/pump, 5678 lpm/pump)	Total containment spray flow is 334.4 liter/s (5300 gpm)	Containment spray is activated on high containment pressure at 0.127 MPa (18.4 psia). Total containment spray rate is 229.8 liters/s (3643 gpm).
CFT/accumulator water volume	2 tanks each with a water volume of 28,579 liters (7550 gallons)	3 accumulators each with a liquid volume of 29,299 liters (7740 gallons)	4 SITs each with a water volume of 29450 liters (7780 gallons).
CFT/SIT/ accumulator discharge pressure	4.07 MPa (590 psia)	4.47 MPa (648 psia)	1.48 MPa (214.7 psia)

Table 8.2. Plant specific material values drawn from the RVID2 database [RVID2]

Product Form	Heat	Beltline	$\sigma_{flow(u)}$ [ksi]	$RT_{NDT(u)}$ [°F]			Composition[2]			$USE_{(u)}$ [ft-lb]
				$RT_{NDT(u)}$ Method	$RT_{NDT(u)}$ Value	$\sigma_{(u)}$ Value	Cu	Ni	P	
Beaver Valley 1, (Designer: Westinghouse, Manufacturer: CE) Coolant Temperature = 547°F, Vessel Thickness = 7-7/8-in.										
PLATE	C4381-1	INTERMEDIATE SHELL B6607-1	83.8	MTEB 5-2	43	0	0.14	0.62	0.015	90
	C4381-2	INTERMEDIATE SHELL B6607-2	84.3	MTEB 5-2	73	0	0.14	0.62	0.015	84
	C6292-2	LOWER SHELL B7203-2	78.8	MTEB 5-2	20	0	0.14	0.57	0.015	84
	C6317-1	LOWER SHELL B6903-1	72.7	MTEB 5-2	27	0	0.2	0.54	0.01	80
LINDE 1092 WELD	305414	LOWER SHELL AXIAL WELD 20-714	75.3	Generic	-56	17	0.337	0.609	0.012	98
	305424	INTER SHELL AXIAL WELD 19-714	79.9	Generic	-56	17	0.273	0.629	0.013	112
LINDE 0091 WELD	90136	CIRC WELD 11-714	76.1	Generic	-56	17	0.269	0.07	0.013	144
Oconee 1, (Designer and Manufacturer: B&W) Coolant Temperature = 556°F, Vessel Thickness = 8.44-in.										
FORGING	AHR54 (ZV2861)	LOWER NOZZLE BELT	(4)	B&W Generic	3	31	0.16	0.65	0.006	109
PLATE	C2197-2	INTERMEDIATE SHELL	(4)	B&W Generic	1	26.9	0.15	0.5	0.008	81
	C2800-1	LOWER SHELL	(4)	B&W Generic	1	26.9	0.11	0.63	0.012	81
	C2800-2	LOWER SHELL	69.9	B&W Generic	1	26.9	0.11	0.63	0.012	119
	C3265-1	UPPER SHELL	75.8	B&W Generic	1	26.9	0.1	0.5	0.015	108
	C3278-1	UPPER SHELL	(4)	B&W Generic	1	26.9	0.12	0.6	0.01	81
LINDE 80 WELD	1P0962	INTERMEDIATE SHELL AXIAL WELDS SA-1073	79.4	B&W Generic	-5	19.7	0.21	0.64	0.025	70
	299L44	INT./UPPER SHL CIRC WELD (OUTSIDE 39%) WF-25	(4)	B&W Generic	-7	20.6	0.34	0.68	(3)	81
	61782	NOZZLE BELT/INT. SHELL CIRC WELD SA-1135	(4)	B&W Generic	-5	19.7	0.23	0.52	0.011	80
	71249	INT./UPPER SHL CIRC WELD (INSIDE 61%) SA-1229	76.4	ASME NB-2331	10	0	0.23	0.59	0.021	67
	72445	UPPER/LOWER SHELL CIRC WELD SA-1585	(4)	B&W Generic	-5	19.7	0.22	0.54	0.016	65
	8T1762	LOWER SHELL AXIAL WELDS SA-1430	75.5	B&W Generic	-5	19.7	0.19	0.57	0.017	70
	8T1762	UPPER SHELL AXIAL WELDS SA-1493	(4)	B&W Generic	-5	19.7	0.19	0.57	0.017	70
	8T1762	LOWER SHELL AXIAL WELDS SA-1426	75.5	B&W Generic	-5	19.7	0.19	0.57	0.017	70
Palisades, (Designer and Manufacturer: CE) Coolant Temperature = 532°F, Vessel Thickness = 8½-in.										
PLATE	A-0313	D-3803-2	(4)	MTEB 5-2	-30	0	0.24	0.52	0.01	87
	B-5294	D-3804-3	(4)	MTEB 5-2	-25	0	0.12	0.55	0.01	73
	C-1279	D-3803-3	(4)	ASME NB-2331	-5	0	0.24	0.5	0.011	102
	C-1279	D-3803-1	74.7	ASME NB-2331	-5	0	0.24	0.51	0.009	102
	C-1308A	D-3804-1	(4)	ASME NB-2331	0	0	0.19	0.48	0.016	72
	C-1308B	D-3804-2	(4)	MTEB 5-2	-30	0	0.19	0.5	0.015	76

Product Form	Heat	Beltline	$\sigma_{flow(u)}$ [ksi]	$RT_{NDT(u)}$ [°F]			Composition[2]			$USE_{(u)}$ [ft-lb]
				$RT_{NDT(u)}$ Method	$RT_{NDT(u)}$ Value	$\sigma_{(u)}$ Value	Cu	Ni	P	
LINDE 0124 WELD	27204	CIRC. WELD 9-112	76.9	Generic	-56	17	0.203	1.018	0.013	98
LINDE 1092 WELD	34B009	LOWER SHELL AXIAL WELD 3-112A/C	76.1	Generic	-56	17	0.192	0.98	(3)	111
	W5214	LOWER SHELL AXIAL WELDS 3-112A/C	72.9	Generic	-56	17	0.213	1.01	0.019	118
	W5214	INTERMEDIATE SHELL AXIAL WELDS 2-112 A/C	72.9	Generic	-56	17	0.213	1.01	0.019	118

Notes:

(1) Information taken directly from the July 2000 release of the NRC's Reactor Vessel Integrity (RVID2) database.
(2) These composition values are as reported in RVID2. In FAVOR calculations these values should be treated as the central tendency of the Cu, Ni, and P distributions detailed in [***EricksonKirk-PFM***].
(3) No values of phosphorus are recorded in RVID2 for these heats. A generic value of 0.012 should be used, which is the mean of 826 phosphorus values taken from the surveillance database used by Eason et al. to calibrate the embrittlement trend curve.
(4) No values strength measurements are available in PREP4 for these heats [PREP]. A value of 77 ksi should be used, which is the mean of other flow strength values reported in this Table.

Table 8.3. Summary of vessel specific inputs for the flaw distribution

Variable		Oconee	Beaver Valley	Palisades	Calvert Cliffs	Notes
Inner Radius (to cladding)	[in]	85.5	78.5	86	86	Vessel specific info
Base Metal Thickness	[in]	8.438	7.875	8.5	8.675	Vessel specific info
Total Wall Thickness	[in]	8.626	8.031	8.75	8.988	Vessel specific info

Variable			Oconee	Beaver Valley	Palisades	Calvert Cliffs	Notes
SAW Weld	Volume fraction	[%]	97%				100% - SMAW% - REPAIR%
	Thru-Wall Bead Thickness	[in]	0.1875	0.1875	0.1875	0.1875	All plants report plant-specific dimensions of 3/16-in.
	Truncation Limit	[in]	1				Judgment. Approx. 2X the size of the largest non-repair flaw observed in PVRUF & Shoreham.
	Buried or Surface	--	All flaws are buried				Observation
	Orientation	--	Circ flaws in circ welds, axial flaws in axial welds.				Observation: Virtually all of the weld flaws in PVRUF & Shoreham were aligned with the welding direction because they were lack of sidewall fusion defects.
	Density basis	--	Shoreham density				Highest of observations
	Aspect ratio basis	--	Shoreham & PVRUF observations				Statistically similar distributions from Shoreham and PVRUF were combined to provide more robust estimates, when based on judgment the amount data were limited and/or insufficient to identify different trends for aspect ratios for flaws in the two vessels.
	Depth basis	--	Shoreham & PVRUF observations				Statistically similar distributions combined to provide more robust estimates

Variable			Oconee	Beaver Valley	Palisades	Calvert Cliffs	Notes
SMAW Weld	Volume fraction	[%]	1%				Upper bound to all plant-specific info provided by Steve Byrne (Westinghouse – Windsor).
	Thru-Wall Bead Thickness	[in]	0.21	0.20	0.22	0.25	Oconee is generic value based on average of all plants specific values (including Shoreham & PVRUF data). Other values are plant-specific as reported by Steve Byrne.
	Truncation Limit	[in]	1				Judgment. Approx. 2X the size of the largest non-repair flaw observed in PVRUF & Shoreham.

	Buried or Surface	--	All flaws are buried	Observation
	Orientation	--	Circ flaws in circ welds, axial flaws in axial welds.	Observation: Virtually all of the weld flaws in PVRUF & Shoreham were aligned with the welding direction because they were lack of sidewall fusion defects.
	Density basis	--	Shoreham density	Highest of observations
	Aspect ratio basis	--	Shoreham & PVRUF observations	Statistically similar distributions from Shoreham and PVRUF were combined to provide more robust estimates, when based on judgment the amount data were limited and/or insufficient to identify different trends for aspect ratios for flaws in the two vessels.
	Depth basis	--	Shoreham & PVRUF observations	Statistically similar distributions combined to provide more robust estimates

Variable			Oconee	Beaver Valley	Palisades	Calvert Cliffs	Notes
Repair	Volume fraction	[%]	2%				Judgment. A rounded integral percentage that exceeds the repaired volume observed for Shoreham and for PVRUF, which was 1.5%.
	Thru-Wall Bead Thickness	[in]	0.14				Generic value: As observed in PVRUF and Shoreham by PNNL.
	Truncation Limit	[in]	2				Judgment. Approx. 2X the largest repair flaw found in PVRUF & Shoreham. Also based on maximum expected width of repair cavity.
	Buried or Surface	--	All flaws are buried				Observation
	Orientation	--	Circ flaws in circ welds, axial flaws in axial welds.				The repair flaws had complex shapes and orientations that were not aligned with either the axial or circumferential welds; for consistency with the available treatments of flaws by the FAVOR code, a common treatment of orientations was adopted for flaws in SAW/SMAW and repair welds.
	Density basis	--	Shoreham density				Highest of observations

	Aspect ratio basis	--	Shoreham & PVRUF observations	Statistically similar distributions from Shoreham and PVRUF were combined to provide more robust estimates, when based on judgment the amount data were limited and/or insufficient to identify different trends for aspect ratios for flaws in the two vessels.
	Depth basis	--	Shoreham & PVRUF observations	Statistically similar distributions combined to provide more robust estimates

	Variable		Oconee	Beaver Valley	Palisades	Calvert Cliffs	Notes
Cladding	Actual Thickness	[in]	0.188	0.156	0.25	0.313	Vessel specific info
	# of Layers	[#]	1	2	2	2	Vessel specific info
	Bead Width	[in]	1				Bead widths of 1 to 5-in. characteristic of machine deposited cladding. Bead widths down to ½-in. can occur over welds. Nominal dimension of 1-in. selected for all analyses because this parameter is not expected to influence significantly the predicted vessel failure probabilities. May need to refine this estimate later, particularly for Oconee who reported a 5-in bead width.
	Truncation Limit	[in]	Actual clad thickness rounded to the nearest 1/100th of the total vessel wall thickness				Judgment & computational convenience
	Surface flaw depth in FAVOR	[in]	0.259	0.161	0.263	0.360	
	Buried or Surface	--	All flaws are surface breaking				Judgment. Only flaws in cladding that would influence brittle fracture of the vessel are brittle. Material properties assigned to clad flaws are that of the underlying material, be it base or weld.
	Orientation	--	All circumferential.				Observation: All flaws observed in PVRUF & Shoreham were lack of inter-run fusion defects, and cladding is always deposited circumferentially
	Density basis	--	No surface flaws observed. Density is 1/1000th that of the observed buried flaws in cladding of vessels examined by PNNL. If there is more than one clad layer then there are no clad flaws.				Judgment
	Aspect ratio basis	--	Observations on buried flaws				Judgment
	Depth basis	--	Depth of all surface flaws is the actual clad thickness rounded up to the nearest 1/100th of the total vessel wall thickness.				Judgment.

Variable			Oconee	Beaver Valley	Palisades	Calvert Cliffs	Notes
Plate	Truncation Limit	[in]	0.433				Judgment. Twice the depth of the largest flaw observed in all PNNL plate inspections.
	Buried or Surface	--	All flaws are buried				Observation
	Orientation	--	Half of the simulated flaws are circumferential, half are axial.				Observation & Physics: No observed orientation preference, and no reason to suspect one (other than laminations which are benign.
	Density basis	--	1/10 of small weld flaw density, 1/40 of large weld flaw density of the PVRUF data				Judgment. Supported by limited data.
	Aspect ratio basis	--	Same as for PVRUF welds				Judgment
	Depth basis	--	Same as for PVRUF welds				Judgment. Supported by limited data.

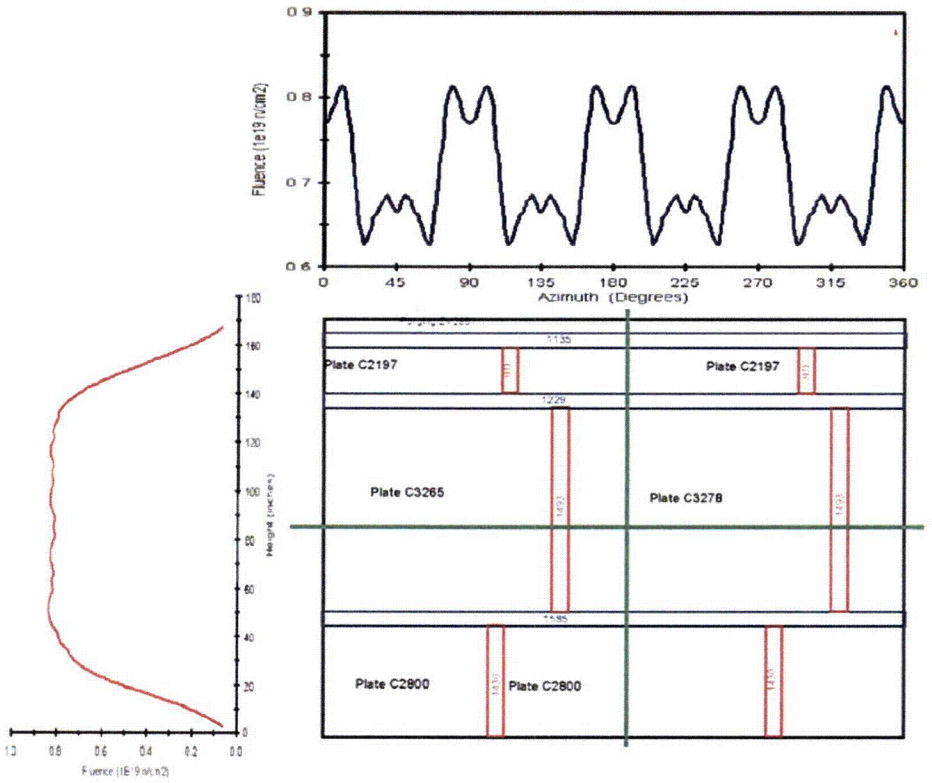

Figure 8.1. Rollout diagram of beltline materials and representative fluence maps for Oconee

Table 8.4. Mean crack initiation and through-wall cracking frequencies estimated for Oconee Unit 1, Beaver Valley Unit 1, using FAVOR Version 04.1

Plant	EFPY[1]	RT_{PTS} [°F][2]	Axial Weld Fusion Line Reference Temperatures [°F]			Reference Temperatures Evaluated at Max Fluence on Vessel ID [°F]		Mean FCI [events/ year]	Mean TWCF [events/ year]
			Max RT_{NDT} in an Axial Weld	Max RT_{NDT} in a Plate	Weld Length Weighted Max RT_{NDT}	Plate	Circ Weld		
Oconee	32	221	152	76	134	79	175	1.29E-10	2.30E-11
	60	250	171	86	149	89	193	1.02E-09	6.47E-11
	Ext-Oa	323	232	131	200	136	251	1.01E-07	1.30E-09
	Ext-Ob	329	263	161	227	170	281	5.24E-07	1.16E-08
Beaver Valley	32	280	155	192	171	243	83	1.32E-07	8.89E-10
	60	299	175	210	188	272	102	5.19E-07	4.84E-09
	Ext-Ba	308	188	225	203	301	121	1.71E-06	2.02E-08
	Ext-Bb	312	207	250	226	354	155	8.87E-06	3.00E-07
Palisades	32	283	212	180	210	189	201	5.22E-08	4.90E-09
	60	311	230	196	227	205	215	1.23E-07	1.55E-08
	Ext-Pa	358	277	246	271	259	254	7.46E-07	1.88E-07
	Ext-Pb	372	333	316	324	335	301	4.47E-06	1.26E-06

1. All plants were analyzed for operational durations of 32 and 60 EFPY (or 40 and 75 operational years, respectively, at an 80% capacity factor. Each plant was also analyzed at two extended embrittlement levels (Ext-Oa and Ext-Ob for Oconee, for example) with the aim of obtaining mean through-wall cracking frequency values closer to the $1x10^{-6}$ limit proposed in Chapter 10.
2. RT_{PTS} is defined as per the equations and procedures of 10 CFR 50.61. Limiting materials in Oconee, Beaver Valley, and in Palisades are circumferential weld SA-1229, plate 6317-1, and axial weld 2-112 A/C, respectively.

In practice, these mathematical conditions are satisfied most of the time in the Monte Carlo simulations conducted using FAVOR (78% of the time in Beaver Valley at 32 EFPY, for example) because the simulated crack is small, the simulated toughness is high, and the simulated TH transient does not produce a very severe stress state in the RPV wall. However, on rare occasions, a larger crack will be simulated in a lower toughness material and subjected to a more severe transient. In these situations, the likelihood of developing a through-wall crack is higher. However, this combined sampling of the upper tails of many distributions happens only rarely.

8.3.2.2 Large Spread in the TWCF Distribution

The TWCF distributions illustrated in Figure 8.2 are very broad, spanning three or mode orders of magnitude from minimum to maximum. This characteristic again relates to the physics of cleavage fracture. As discussed in Section 8.3.2.1, the absolute lower bounds associated with both the K_{Ic} and K_{Ia} distributions leads to a large number of the Monte Carlo simulations producing a through-wall cracking probability that is, *by definition*, zero. However, on rare occasions, the tails of many distributions are sampled in the same simulation run, resulting in a larger crack being simulated to occur in a lower toughness material. This combined

possibility of both zero and higher probabilities of TWCF leads to TWCF distributions that are naturally broad. As illustrated in Figure 8.2, the TWCF distributions tend to compress as the plants age because the more embrittled materials in these plants are less likely to produce through-wall cracking frequencies that are either very low, or zero.

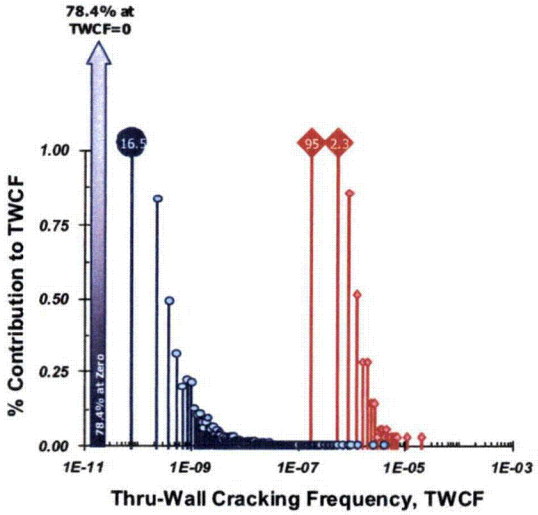

Figure 8.2. Typical distribution of through-wall cracking frequency (as calculated for Beaver Valley at 32 EFPY (blue circles) and for extended embrittlement conditions (red diamonds)

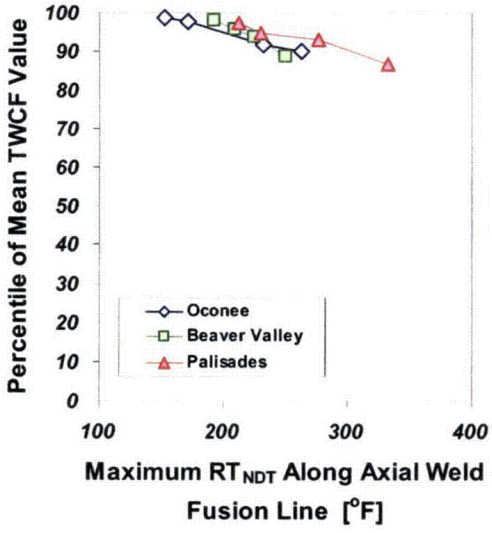

Figure 8-3. TWCF distribution percentile corresponding to the mean value

Because of the skewness characteristic of the TWCF distributions, the mean values reported in Table 8.4 do not lie close to the median value of the underlying distributions. In fact, as illustrated in Figure 8-3, mean TWCF values generally correspond to the ~90th percentile (and usually higher) over the range of embrittlement studied. Thus, the mean TWCF values are appropriately used to establish a revised PTS screening limit suitable for regulatory use.

8.4 Material Factors Contributing to FCI and TWCF

This section begins (in Section 8.4.1) with a discussion of the flaws simulated by FAVOR to exist in the RPV and the toughness properties that control the behavior of those flaws (i.e., if the flaw initiates, if the flaw propagates through the RPV wall). These considerations lead to several proposed "reference temperature metrics" that are can be used to correlate and/or predict the likelihood of fracture occurring in the various regions (axial weld, circumferential weld, plate) of the RPV beltline. We then discuss (in Section 8.4.2) the contribution of the various RPV beltline regions to the estimated FCI and TWCF values. In Section 8.4.3, we propose a procedure that accounts, at least approximately, for the different embrittlement levels in the three study plants to enable the comparison of similar transients at different plants presented in Section 8.5. We conclude in Section 8.4.4 with a discussion of how these results differ from those reported in December 2002 [***Kirk 12-02***].

8.4.1 Flaws Simulated by FAVOR, and Reference Temperature Metrics

When performing a structural flaw assessment, the location of the flaw or flaws being assessed needs to be known (along with many other factors) so that the resistance to fracture of the material at the flaw location can be either measured or estimated. The situation in this study differs somewhat from a routine flaw assessment because the flaws are simulated, and because hundreds upon thousands of flaws are being assessed. Nonetheless, the objective here

is to correlate and/or predict the metrics that quantify the vessel's resistance to fracture:

CPI Conditional Probability of Crack Initiation. This is the probability that a crack will grow from its original size, conditioned on the assumed occurrence of a particular transient.

CPTWC Conditional Probability of Through-Wall Cracking. This is the probability that a crack will grow from its original size to the point that it propagates completely through the vessel wall, conditioned on the assumed occurrence of a particular transient.

FCI Frequency of Crack Initiation. This is the matrix product of the CPI value for each transient (including its uncertainty distribution) with the estimated frequency of that transient occurring (including its uncertainty distribution). FCI values are expressed per year.

TWCF Through-Wall Cracking Frequency. This is the matrix product of the CPTWC value for each transient (including its uncertainty distribution) with the estimated frequency of that transient occurring (including its uncertainty distribution). TWCF values are expressed per year.

In order to correlate and/or predict these metrics to quantify the vessel's resistance to fracture, some measure of the resistance of the materials in the vessel to fracture at the location of these many flaws is needed. A reference temperature (*RT*) establishes the resistance of a material to fracture, the variability in this resistance, and how this resistance varies with temperature. As described in [***ErickssonKirk-PFM***] and as illustrated schematically in Figure 8-4, a reference temperature is commonly thought of as positioning the cleavage fracture toughness transition curve on the temperature axis. However, because relationships exist that establish the position of the arrest transition curve and of the upper shelf curve with respect to the cleavage reference temperature (see [***ErickssonKirk-PFM***] for a full discussion), the toughness of ferritic steels can be fully descried by this single reference temperature. Since *RT* values can be estimated from information on vessel materials available in the RVID database [RVID2] and from information available from surveillance programs implemented under Appendix H to 10 CFR Part 50, they provide a way to estimate the resistance of vessel materials to fracture and how this resistance diminishes with increased neutron irradiation.

Figure 8-5 illustrates the location and orientation of the flaws that are simulated to exist in the RPV and the relationship between these flaw locations and the azimuthal and axial variations of fluence. (See [***ErickssonKirk-PFM***] and [***Simonen***] for a more detailed explanation of the technical bases for these flaw locations and orientations.) The information in Figure 8-5 is summarized as follows for each of the simulated flaw populations:

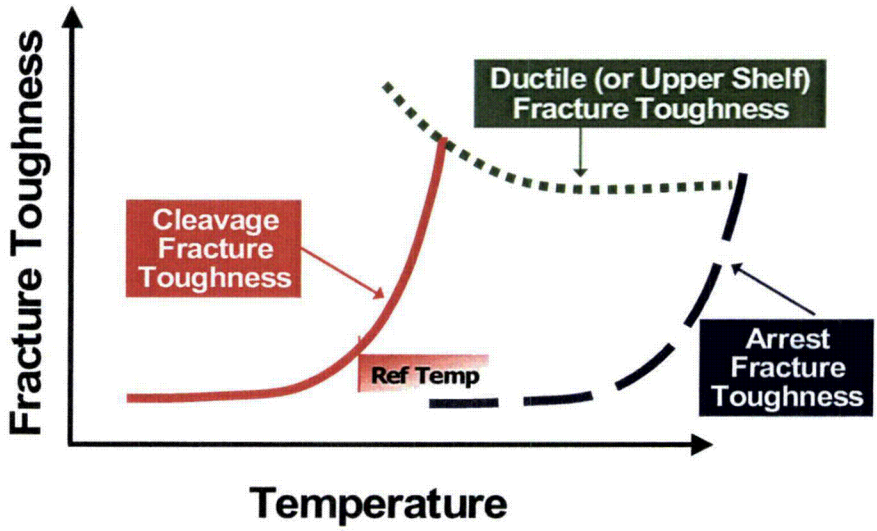

Figure 8-4. Relationship between a reference temperature (RT) and various measure of resistance to fracture (fracture toughness). This is a schematic illustration of temperature dependence only; scatter in fracture toughness is not shown.

- Embedded Axial Weld Flaws: The overwhelming majority of flaws in axial welds are lack of fusion defects, which occur on the weld fusion lines. Consequently, all of these flaws are oriented axially. The behavior of these flaws (i.e., if the flaw initiates, if the flaw propagates through the RPV wall) is controlled by the less tough of the plate or weld that lie on either side of the flaws. As illustrated in Figure 8-5, the axial fluence variation is relatively minor along most of the axial weld fusion line length. However, the large azimuthal fluence variation can expose each axial weld fusion line to have different fluences. The likelihood of vessel fracture from axial weld flaws depends upon (1) the total number of axial weld flaws (which scales with fusion line area), and (2) the fluence to which these flaws are subjected. Consequently, an appropriate metric to correlate/predict the likelihood of fracture from axial weld flaws would be weighted to account for variations in axial weld length and fluence level. Mathematically, the reference temperature metric for axial welds (RT_{AW}) is defined as follows:

$$\text{Eq. 8-1} \quad RT_{AW} = \frac{\sum_{i=1}^{nafl} RT^{i}_{MAX-AW} \cdot \ell^{i}_{FL}}{\sum_{i=1}^{nfl} \ell^{i}_{FL}}$$

where

$nafl$	is the number of axial weld fusion lines in the vessel beltline region,
ℓ_{FL}	is the length of a particular fusion line in the vessel beltline region, and
$RT_{MAX\text{-}AW}$	is evaluated for each of the axial weld fusion lines using the following formula. In the formula the symbol ϕt_{FL} refers to the maximum fluence occurring along a particular axial weld fusion line, and ΔT_{30} is the shift in the Charpy V-Notch 30-ft-lb energy produced by irradiation at ϕt_{FL}.

$$RT_{MAX-AW} \equiv MAX\left\{\left(RT^{plate}_{NDT(u)} + \Delta T^{plate}_{30}\left(\phi t_{FL}\right)\right), \left(RT^{axialweld}_{NDT(u)} + \Delta T^{axialweld}_{30}\left(\phi t_{FL}\right)\right)\right\}$$

- Embedded Circumferential Weld Flaws: The overwhelming majority of flaws in circumferential welds are lack of fusion defects, which occur on the weld fusion lines. Consequently, all of these flaws are oriented circumferentially. The behavior of these flaws (i.e., if the flaw initiates, if the flaw propagates through the RPV wall) is controlled by the less tough of the plate or weld that lie on either side of the flaws. As illustrated in Figure 8-5, the azimuthal fluence variation ensures that these circumferential weld cracks will somewhere be subjected to the maximum fluence that occurs anywhere on the vessel ID. Flaws are equally likely to occur at any position around the circumference of the RPV, and the initiation / propagation of fracture from such flaws is more likely at higher fluences. Consequently, an appropriate metric to correlate/predict the likelihood of fracture from circumferential weld flaws would be a weighted average of the largest RT_{NDT} value associated with each circumferential weld fusion line when irradiated to the maximum ID fluence. Mathematically, the reference temperature metric for circumferential welds (RT_{CW}) is defined as follows:

$$\text{Eq. 8-2} \quad RT_{CW} = \frac{\sum_{i=1}^{ncfl} RT^{i}_{MAX-CW}}{ncfl}$$

where

$ncfl$ is the number of circumferential weld fusion lines in the vessel beltline region,

$RT_{MAX\text{-}CW}$ is evaluated for each of the circumferential weld fusion lines using the following formula. In the formula the symbol ϕt_{MAX} refers to the maximum fluence occurring over the ID in the vessel beltline region, and ΔT_{30} is the shift in the Charpy V-Notch 30 ft-lb energy produced by irradiation at ϕt_{MAX}.

$$RT_{MAX-CW} \equiv MAX\left\{\left(RT^{plate}_{NDT(u)} + \Delta T^{plate}_{30}\left(\phi t_{MAX}\right)\right), \left(RT^{circweld}_{NDT(u)} + \Delta T^{circweld}_{30}\left(\phi t_{MAX}\right)\right)\right\}$$

It should be noted that at an equivalent embrittlement level, the likelihood of a circumferential weld flaw leading to through-wall cracking of the vessel is much lower than for an axial weld flaw. Even though circumferential and axial weld flaws are the same size because they are drawn from the same distribution, the variation of crack driving force through the wall of a cylindrical RPV differs considerably for circumferential and for axial flaws. Cheverton et al. describe how the application of a cold thermal shock to the inner diameter of a cylinder containing a flaw produces bending of the cylinder wall [Cheverton 85a]. This bending, originating from the contraction of the cold metal at and near the ID and the resistance to this contraction provided by the hotter metal deeper into the thickness of the cylinder, tends to be much larger for infinite length axial flaws than for infinite length circumferential flaws. A cylindrical geometry with an infinite axial flaw is asymmetric while a cylindrical geometry with an infinite circumferential flaw is symmetric. The asymmetry associated with the axial flaw degrades the cylinder's resistance to bending much more than the symmetric circumferential flaw (see Figure 8-6). It is for this reason that the applied-K_I of an axially oriented flaw continues to increase for cracks extending much deeper into the vessel wall than does the applied-K_I for a circumferentially oriented flaw (see Figure 8.7). The driving force peak that occurs for circumferential cracks provides a natural crack arrest mechanism that occurs in all RPVs because of their cylindrical geometry. Conversely, the applied driving force for axial flaws continues to increase as their depth increases, which leads directly to the ability of axial flaws to propagate all the way through the RPV wall.

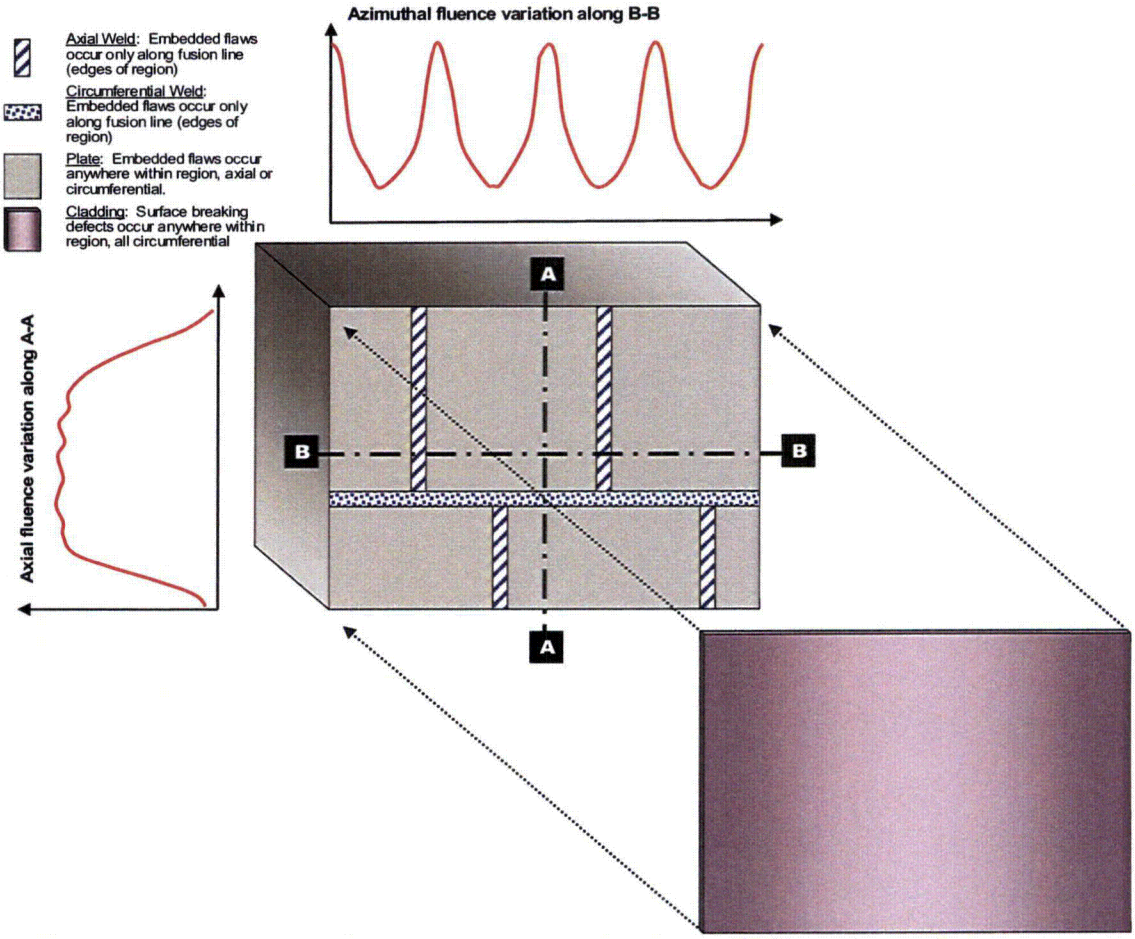

Figure 8-5. Location and orientation of flaws simulated by FAVOR to exist in different regions of the RPV beltline

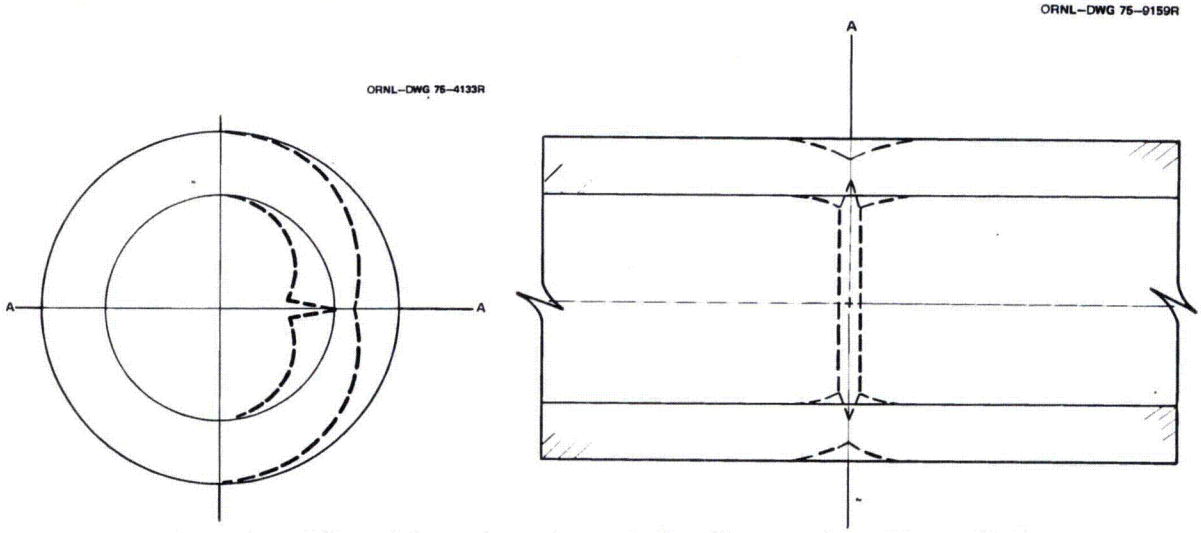

Figure 8-6. Effect of flaw orientation on the bending experienced by a cylinder subjected to a cold thermal shock on the inner diameter.

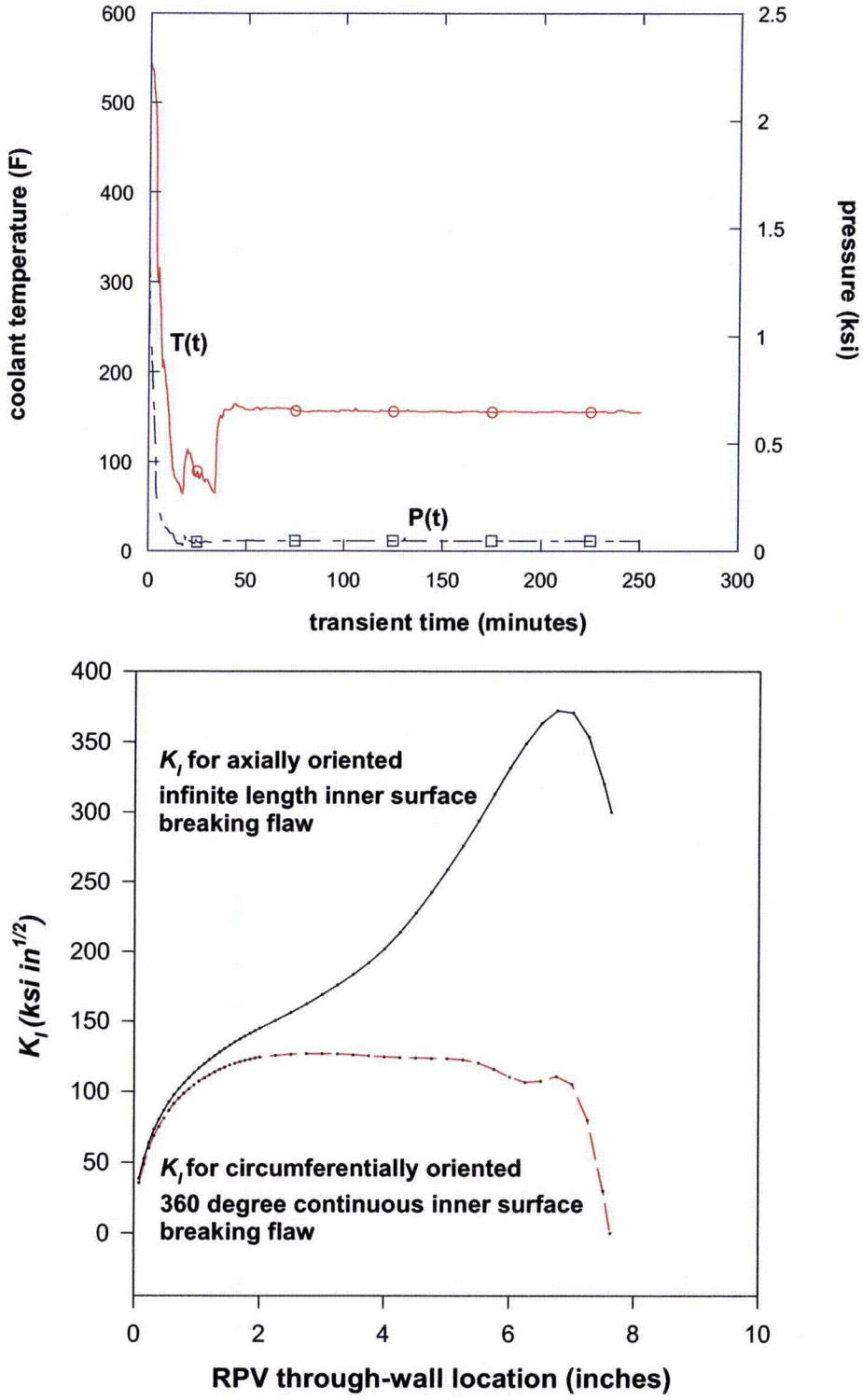

Figure 8.7. Through-wall variation of crack driving force (K_I): axially oriented flaws compared to circumferentially oriented flaws
(Comparison is shown for an 8-inch diameter surge line break in Beaver Valley (Transient #7 – see top plot) at a time 11 minutes after the start of the transient (see bottom plot).)

- Embedded Plate Flaws: Flaws in plates occur predominantly due to no-metallic inclusions. These can occur anywhere within the plate; they have no preferred orientation (i.e., they are equally likely to be axial or circumferential). As illustrated in Figure 8-5, the azimuthal fluence variation makes it certain that every plate will somewhere be subjected to the maximum fluence occurring on the vessel ID. Plate flaws are equally likely to occur at any position in the plate, so initiation / propagation of fracture from such flaws is more likely at higher fluences. Consequently, an appropriate metric to correlate / predict the likelihood of fracture from plate flaws would be a weighted average of the largest RT_{NDT} value associated with each plate when irradiated to the maximum ID fluence. Mathematically, the reference temperature metric for plates (RT_{PL}) is defined as follows:

$$\text{Eq. 8-3} \quad RT_{PL} = \frac{\sum_{i=1}^{npl} RT^{i}_{MAX-PL} \cdot V^{i}_{PL}}{\sum_{i=1}^{npl} V^{i}_{PL}}.$$

where

npl	is the number of plates in the vessel beltline region,
V_{PL}	is the volume of each of these plates,
$RT_{MAX\text{-}PW}$	is evaluated for each plate using the following formula. In the formula the symbol ϕt_{MAX} refers to the maximum fluence occurring over the ID in the vessel beltline region, and ΔT_{30} is the shift in the Charpy V-Notch 30 ft-lb energy produced by irradiation at ϕt_{MAX}.

$$RT_{MAX-PL} \equiv RT^{plate}_{NDT(u)} + \Delta T^{plate}_{30}\left(\phi t_{MAX}\right)$$

It should be noted that at an equivalent embrittlement level, the likelihood of a plate flaw leading to through-wall cracking of the vessel is much lower than for an axial weld flaw for two reasons. First, half of all simulated plate flaws are oriented circumferentially, which reduces their driving force relative to axial flaws (see Figure 8.7). Additionally, plate flaws are generally much smaller than weld flaws. However, the azimuthal variation of fluence makes it virtually certain that some region of the plates will be subjected to a higher fluence (often a much higher fluence) than will the axial weld fusion lines. At some point, this added embrittlement to which the plate flaws are subjected will overcome the smaller plate flaw driving force caused by their smaller size (*vs.* axial weld flaws), causing the fracture of plate flaws to become more likely than the fracture of axial weld flaws.

- Surface-Breaking Flaws in the Stainless Steel Cladding: The only flaws simulated to break the inner diameter surface of the RPV occur because of lack of inner-run fusion between adjacent beads of weld-deposited stainless steel cladding. Since this cladding is always deposited circumferentially, these flaws are always oriented circumferentially, and they can occur anywhere over the entire ID surface of the vessel. All of the simulated flaws have a crack depth equal to the thickness of the cladding layer, so the toughness properties that control the behavior of these flaws (i.e., if the flaw initiates, if the flaw propagates through the RPV wall) are those of the axial weld, circumferential weld, or plate region that lie under the simulated location of the surface flaw. As discussed later in this section, FAVOR reports the contribution of these flaws to FCI and TWCF along with the contribution of the underlying axial weld,

circumferential weld, or plate region. Thus, the contribution of these flaws to FCI and TWCF is addressed by the combination of RT_{AW}, RT_{CW}, and RT_{PL} making an independent reference temperature metric for flaws in cladding unnecessary. Furthermore, the circumferential orientation of these flaws makes their contribution to FCI and TWCF very small[****].

8.4.2 Effect of RPV Beltline Region on FCI and TWCF Values

As illustrated in Figure 8-5, the beltline region of a nuclear RPV is fabricated from different material product forms. All three vessels analyzed here are plate vessels and, therefore, are fabricated from heavy section ferritic steel plates roll formed to produce 120° or 180° degree segments. These segments are joined by axial welds to form a shell course, and then different shell courses are joined by circumferential welds to make the vessel. Two to three shell courses generally make up the beltline region of the vessel. An alternative fabrication practice, which avoids the need for axial welds, is to join ring-forged cylinders with circumferential welds. In Section 9.2, we address application of the results presented in this chapter (for plate vessels) to forged vessels.

In this report, we use the term "regions" to refer to the different product forms (i.e., plates, axial welds, circumferential welds, and forgings) that make up each RPV. As detailed in Table 8.2, each region has unique properties of chemical composition (which controls susceptibility to irradiation embrittlement), strength, and toughness. These properties also vary within the each region, see [***ErickssonKirk-PFM***] and [***Williams***], respectively, for a description of our bases for characterizing this variation and of the statistical models we have adopted in FAVOR for this purpose. Table 8.5 details the relative contributions these different regions make to the FCI and TWCF values reported in Table 8.4, demonstrating that these different regions (and their associated flaw populations) make widely varied contributions to the FCI and TWCF values, as follows:

- Circumferential Flaws: Circumferential flaws are responsible for a large portion of the FCI because the maximum ID fluence always interacts with a potential location of a circumferential flaw, but almost never with the potential location of an axial flaw. The consequential higher embrittlement frequently associated with circumferential flaws ($RT_{CW} > RT_{AW}$) leads directly to their role as dominant initiators[††††]. However, as illustrated in Figure 8.7, differences in how the driving force to fracture varies through-wall in a cylindrical vessel causes most of these initiated circumferential cracks to arrest before they propagate completely through the vessel wall and contribute to the TWCF. For this reason, circumferential cracks do not contribute to TWCF except in a very minor way at very high RT_{CW} values.
- Axial Flaws: Axial flaws are responsible for nearly all of the TWCF. In both Oconee and in Palisades, the toughness associated with the axial weld flaws is less than the toughness associated with the plate flaws ($RT_{AW} > RT_{PL}$) so the axial weld flaws control nearly all of the TWCF. In Beaver Valley, the toughness associated with the plate flaws is less than the toughness associated with the axial weld flaws

[****] At the extremely high embrittlement level simulated by the Ext-Ob analysis of Oconee Unit 1, cladding flaws contributed only 2.5% and 0.01% to the total FCI and TWCF (respectively). At the more realistic embrittlement levels represented by the 32 and 60 EFPY analyses, these flaws made no contribution to either FCI or TWCF.

[††††] This observation regarding the general dominance of circumferential flaws in controlling FCI does not apply to Palisades. In Palisades, the toughness along the axial weld fusion line is less than the toughness along the circumferential weld fusion line (i.e., $RT_{AW} > RT_{CW}$). This occurs because the chemistry of the axial welds in Palisades is more irradiation-sensitive than that of the circumferential welds, increasing their embrittlement despite the lower fluence along the axial weld fusion lines.

($RT_{PL} > RT_{AW}$). Thus, in Beaver Valley, the plate flaws are responsible for some portion of the TWCF. However, they do not completely control the TWCF because weld flaws are much larger than plate flaws. Nonetheless, it is ***always*** the toughness properties that can be associated with axial flaws (i.e., the toughness properties of either the plate or of the axial weld: RT_{AW} and/or RT_{PL}) that control the TWCF. The toughness properties of the circumferential weld (RT_{CW}) play only a minor role and this only for highly embrittled materials (high RT_{CW}).

Table 8.5. Relative contributions of various flaw populations to the FCI and TWCF values estimated by FAVOR Version 04.1

EFPY	Reference Temperatures [°F]			Mean FCI	Mean TWCF	Apportionment by Originating Flaw Population					
						FCI[1]			TWCF[1]		
	RT_{AW}	RT_{CW}	RT_{PL}			Axial Welds	Circ Welds	Plates	Axial Welds	Circ Welds	Plates
Oconee Unit 1											
32	134	136	72	1.29E-10	2.30E-11	33.83%	66.16%	0.00%	100.00%	0.00%	0.00%
60	149	156	83	1.02E-09	6.47E-11	18.64%	81.35%	0.01%	99.90%	0.10%	0.00%
Ext-Oa	200	207	134	1.01E-07	1.30E-09	8.82%	90.82%	0.35%	99.83%	0.16%	0.00%
Ext-Ob	227	229	164	5.24E-07	1.16E-08	8.52%	90.78%	0.71%	99.81%	0.11%	0.08%
Beaver Valley Unit 1											
32	171	243	217	1.32E-07	8.89E-10	2.37%	96.01%	1.61%	68.44%	0.33%	31.23%
60	188	272	244	5.19E-07	4.84E-09	3.01%	94.26%	2.73%	39.19%	0.72%	60.09%
Ext-Ba	203	301	273	1.71E-06	2.02E-08	2.64%	93.04%	4.33%	15.69%	1.74%	82.55%
Ext-Bb	226	354	324	8.87E-06	3.00E-07	2.23%	91.02%	6.75%	9.21%	6.18%	84.62%
Palisades											
32	210	201	165	5.22E-08	4.90E-09	93.79%	6.22%	0.00%	99.95%	0.05%	0.00%
60	227	215	181	1.23E-07	1.55E-08	92.56%	7.44%	0.00%	99.97%	0.04%	0.00%
Ext-Pa	271	259	231	7.46E-07	1.88E-07	84.45%	15.41%	0.15%	99.91%	0.02%	0.08%
Ext-Pb	324	335	293	4.47E-06	1.26E-06	60.24%	38.58%	1.18%	98.62%	0.01%	1.37%

Note: (1) FCI and TWCF percentages may not add to 100% due to rounding.

8.4.3 Embrittlement Normalization between Different Plants

Section 8.5 examines the classes of transients that have the greatest contribution to FCI and TWCF. Part of this discussion focuses on the similarity/difference of the severity associated with the same type of transient at different plants (e.g., does a 4-in. hot leg break have a similar severity at the different analyzed plants, or must plant-specific factors be considered to accurately predict the severity of the transient?). These discussions form the beginning of our assessment of the general applicability of our results to all PWRs — a topic that Chapter 9 addresses in more detail. To perform these plant-to-plant comparisons of transient severity on an equivalent basis, it is important to be able to account for the differences in embrittlement level between the different analyses we performed. We use the reference temperature metrics RT_{AW}, RT_{CW}, and RT_{PL} introduced in Section 8.4.2 for this purpose.

As discussed in Section 8.4.2, the development of a single reference temperature to serve as an embrittlement metric for all plants is complicated by the following two factors:

- The fracture toughness varies widely throughout the pressure vessel (because of the combined influences of different chemistries in different regions and the fluence variation over the vessel ID).
- The distribution of flaws throughout the vessel; their size, location, and orientation; is non-homogeneous (for physically understood reasons).

Nonetheless, the toughness properties associated with axial cracks control the likelihood of developing a through-wall crack. In Oconee and in Palisades, these properties are described completely by RT_{AW} because ~100% of the TWCF is associated with the axial weld flaw population in these plants, irrespective of embrittlement level. The situation in Beaver Valley is more complex because the high fluence levels remote from the axial weld fusion lines and the high irradiation susceptibility of the Beaver Valley materials create a situation where plate flaws and (at very high levels of embrittlement) circumferential weld flaws contribute to the TWCF. To reflect this, the reference temperature for Beaver Valley should lie between RT_{AW} and RT_{PL}. These considerations are reflected in the final column of Table 8.6, which provides the reference temperature values used in Section 8.5. *It should be noted this approach to obtaining a single reference temperature is developed here **only** to support the transient comparisons performed in Section 8.5. Embrittlement metrics useful for estimating the level of PTS risk in PWRs **in general** are discussed and developed in Chapter 11.*

8.4.4 Changes in these Results Relative to those Reported in December 2002

While the specific numerical results reported herein differ from those in our interim report [***Kirk 12-02***], the general trends discussed in this section have not changed substantively from those reported earlier.

8.5 Contributions of Different Transients to the Through-Wall Cracking Frequency

8.5.1 Overview

As a first step toward assessing the transients that contribute most prominently to the overall TWCF, we divided the transients analyzed for each plant (see Appendix A for a complete list) into the following transient classes:

Table 8.6. Reference temperature metric used in Section 8.5.

Plant	EFPY	Reference Temperatures [°F]			TWCF Apportioned by Originating Flaw Population			Reference Temperature for Section 8.5 Comparisons [°F]
		RT_{AW}	RT_{CW}	RT_{PL}	Axial Welds	Circ Welds	Plates	
Oconee	32	134	136	72	100.00%	0.00%	0.00%	134 (=RT_{AW})
	60	149	156	83	99.90%	0.10%	0.00%	149 (=RT_{AW})
	Ext-Oa	200	207	134	99.83%	0.16%	0.00%	200 (=RT_{AW})
	Ext-Ob	227	229	164	99.81%	0.11%	0.08%	227 (=RT_{AW})
Beaver Valley	32	171	243	217	68.44%	0.33%	31.23%	185 (=RT_{AW} + 0.31·{RT_{PL}-RT_{AW}})
	60	188	272	244	39.19%	0.72%	60.09%	222 (=RT_{AW} + 0.61·{RT_{PL}-RT_{AW}})
	Ext-Ba	203	301	273	15.69%	1.74%	82.55%	262 (=RT_{AW} + 0.85·{RT_{PL}-RT_{AW}})
	Ext-Bb	226	354	324	9.21%	6.18%	84.62%	315 (=RT_{AW} + 0.91·{RT_{PL}-RT_{AW}})
Palisades	32	210	201	165	99.95%	0.05%	0.00%	210 (=RT_{AW})
	60	227	215	181	99.97%	0.04%	0.00%	227 (=RT_{AW})
	Ext-Pa	271	259	231	99.91%	0.02%	0.08%	271 (=RT_{AW})
	Ext-Pb	324	335	293	98.62%	0.01%	1.37%	324 (=RT_{AW})

Note: In Section 8.5, when the TWCFs of different plants are compared at "roughly equivalent" embrittlement levels, the results associated with the shaded rows are used.

LOCA Pipe breaks of any diameter on the primary side (see Tables A.1 and A.2)

SO-1 Stuck-open valves (that may later reclose) on the primary side (see Tables A.3 and A.4)

F&B Feed & bleed "LOCA" (see Table A.8)

MSLB Large diameter (or "main") steam line break (see Table A.5)

SO-2 Smaller diameter secondary side breaks, including stuck-open valves (see Table A.7)

SGTR Steam generator tube rupture (see Table A.8)

OVR Overfeed (see Table A.8)

MIX Mixed primary and secondary initiators (see Table A.9)

Figure 8-8, Figure 8-9, and Figure 8-10 illustrate the contribution to the total TWCF of each transient analyzed for Oconee, Beaver Valley, and Palisades, respectively. (Descriptions of the transients that contribute more than 1% to the total TWCF are provided in Table 8.7, Table 8.8, and Table 8.9 for each plant.) These graphical depictions demonstrate that many of the transients analyzed contribute little or nothing to the TWCF while a limited number of transients dominate TWCF. In general, the contributions of primary side pipe breaks (LOCAs) and stuck-open valves on the primary side that may later reclose (SO-1) are the most important, collectively accounting for 70% or more of the total risk (see Figure 8-11). Stuck-open valves on the secondary side (SO-2) and breaks in the main steam line (MSLB) also contribute to TWCF, but to a more limited extent. Feed-and-bleed LOCAs (F&B) and steam generator tube ruptures (SGTR) do not contribute to TWCF in any significant way.

Figure 8-12 illustrates the annual frequencies of occurrence of the most risk-significant classes of

events, where risk-significance is based on the information in Figure 8-8 through Figure 8-10. In Figure 8-12 the division between small and medium and medium and large break LOCAs occurs at approximately 4 and 8-inches (10.16 and 20.32-cm), respectively. Based on this information, the following observations can be made:

- Plant Effects on Frequency: The frequencies associated with Oconee and Beaver Valley are identical because these frequencies were established by the NRC's PRA contractors based on industry-wide data [INEEL99, INEEL00b] and based on limited plant-specific data. It was the view of these analysts that there were not enough differences between these plants and/or plant-specific data to support adoption of plant-specific frequencies. The Palisades frequencies differ slightly from those adopted for the other two plants for several reasons. Different analysts performed the Palisades PRA, so some differences are attributable to different interpretations of available data. Secondly, the Palisades PRA analysts adopted slightly different models to represent PTS risk than were used for the other two plants. Finally, the Palisades PRA analysis made use of some Palisades-specific information. Taken together, the small plant-to-plant frequency differences shown in Figure 8-12 arise, in part, because of both real differences between the plants and differences in modeling or judgment.
- Event Effects on Frequency: SO-2 events occur with the greatest frequency; approximately 0.02/yr. MSLB and SO-1 events are the next most frequent, but are approximately 10 times less likely than SO-2 events. All LOCA events are less likely still, as illustrated in Figure 8-12. The least likely event class is large-break LOCAs, which are approximately 3,000 times less likely than SO-2 events.

In the following subsections, we examine in further detail the four classes of transients that collectively account for virtually all of the TWCF: LOCA, SO-1, MSLB, and SO-2.

Sections 8.5.2 through 8.5.5 are structured as follows:

Step 1. Each section begins with a general description of transients in the class, how the transient progresses, what actions the operators take, and so on.

Step 2. We then review of all of the transients in the class that were modeled in each of the three study plants with the aim of describing how each transient class has been modeled. Additionally, this discussion points out plant-specific similarities/differences in our treatment of the transient class as regards the specific transients selected to represent the class as a whole.

Step 3. We then examine relationships between the systems-based characteristics of the transients in the class (e.g., break size, break location, HPI throttling at 1 *vs.* 10 minutes, etc.) and their thermal-hydraulic signature (i.e., their temporal variation of pressure, temperature, and heat transfer coefficient in the downcomer).

Step 4. The probabilistic fracture mechanics results are then discussed within the context of the thermal-hydraulic understanding developed in Step #2. Specifically we overlay on the TH transients the predicted times at which the vessel fails. This focuses attention on the part of the transient where differences in the TH signature can influence whether the vessel is predicted to fail or not. Particular attention is paid to determining the importance of operator actions in controlling the transient severity, and identifying if the results from these three study plant can be considered to apply to all PWRs *in general.*

Step 5. The discussion of each transient class concludes with a comparison of our current findings to those reported previously [***Kirk 12-02***] and those that established the basis for the current provisions of 10 CFR 50.61 [SECY-82-465].

Finally, in Section 8.5.6, we discuss classes of transients that do not contribute in any significant way to the total TWCF. These include SGTR, feed-and-bleed LOCAs, and transients that include a combination of failures in both the primary and secondary pressure circuits.

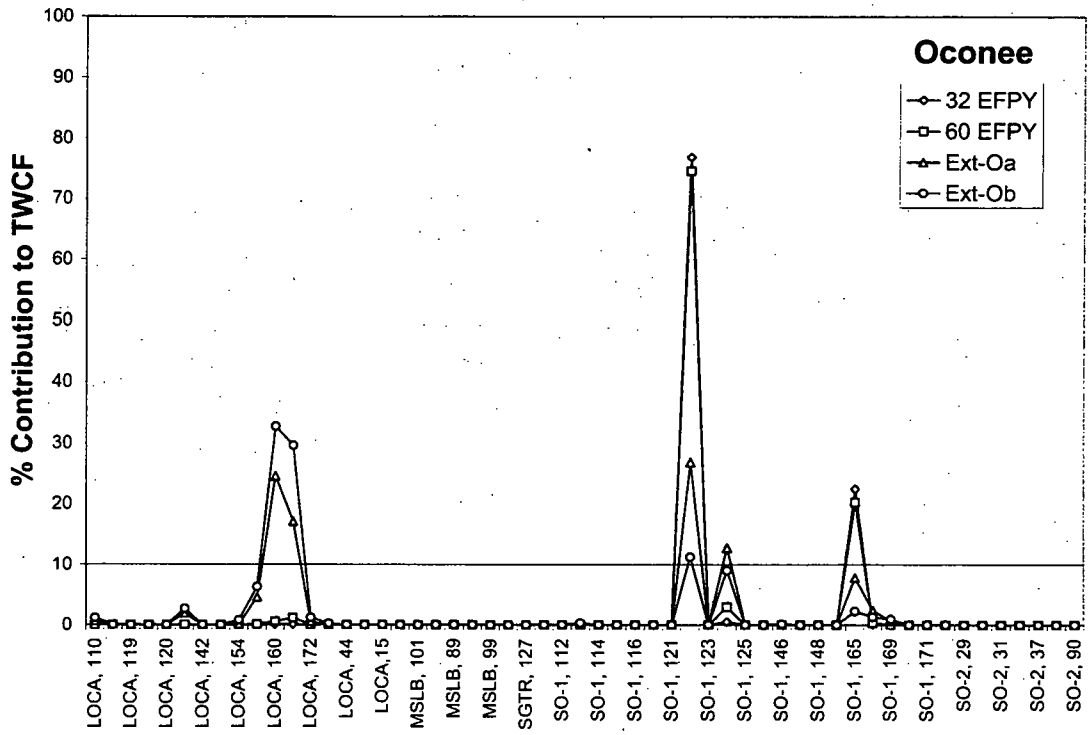

Figure 8-8. Contributions of the different transients to the TWCF in Oconee Unit 1 (Numbers on the abscissa are the TH case numbers, see Appendix A)

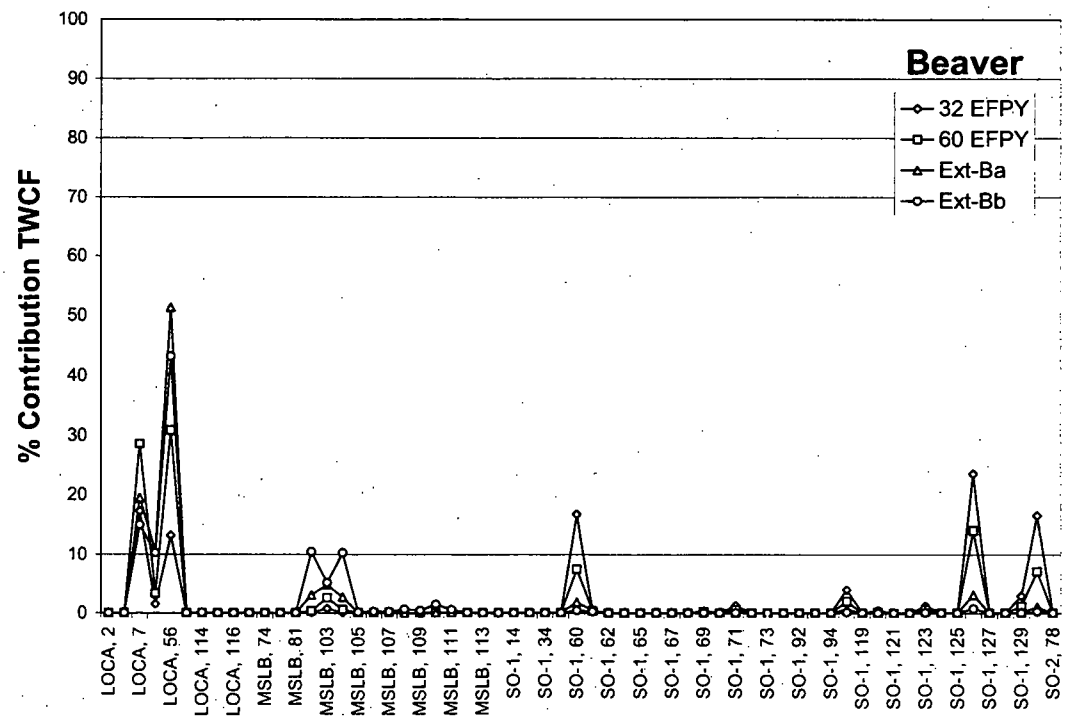

Figure 8-9. Contributions of the different transients to the TWCF in Beaver Valley Unit 1 (Numbers on the abscissa are the TH case numbers, see Appendix A)

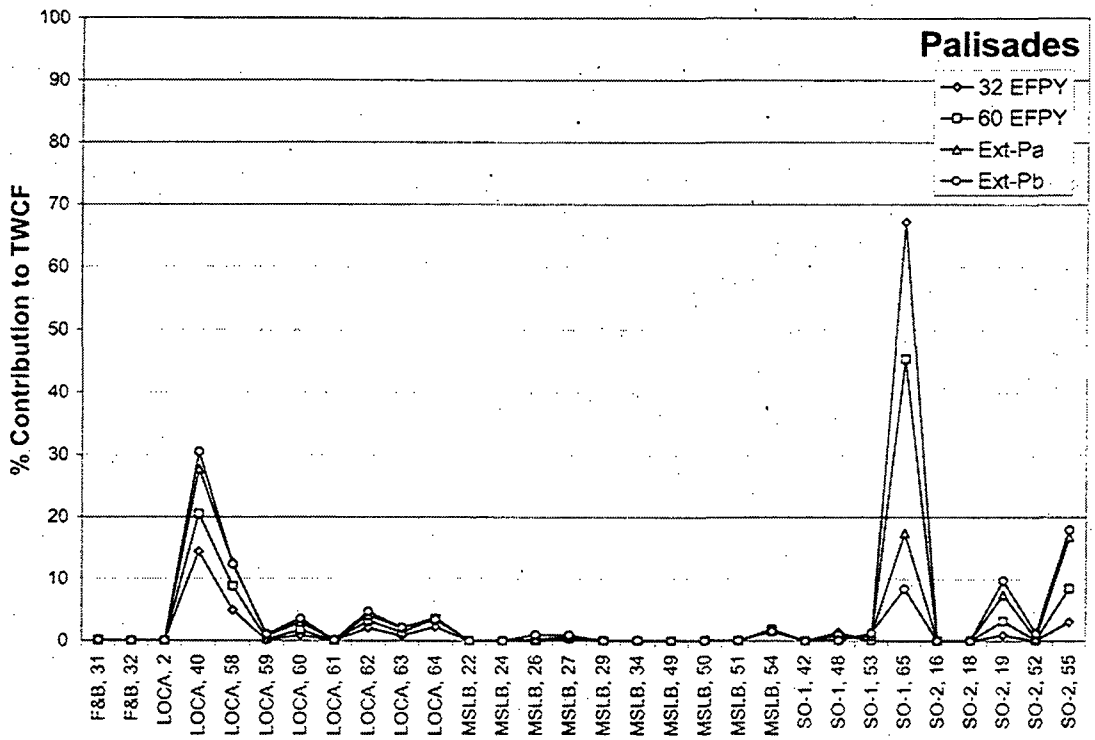

Figure 8-10. Contributions of the different transients to the TWCF in Palisades (Numbers on the abscissa are the TH case numbers, see Appendix A)

Table 8.7. Transients that contribute most significantly to the estimated TWCF of Oconee Unit 1

Class	TH#	System Failure	Operator Action	HZP?	%
SO-1	122	Stuck-open pressurizer safety valve. Valve recloses at 6,000 secs.	Operator throttles HPI at 10 minutes after 2.7 K [5°F] subcooling and 100-in. (254-cm) pressurizer level is reached. (Throttling criteria is 27.8 K [50°F] subcooling.)	Yes	47%
SO-1	165	Stuck-open pressurizer safety valve. Valve recloses at 6,000 secs [RCS low-pressure point].	None	Yes	13%
SO-1	124	Stuck-open pressurizer safety valve. Valve recloses at 3,000 secs.	Operator throttles HPI at 10 minutes after 2.7 K [5°F] subcooling and 100-in. (254-cm) pressurizer level is reached. (Throttling criteria is 27.8 K [50°F] subcooling.)	Yes	6%
SO-1	168	TT/RT with stuck-open pzr SRV. SRV assumed to reclose at 3,000 secs. Operator does not throttle HPI.	None	Yes	1%
LOCA	160	5.66-in. (14.37-cm) surge line break. ECC suction switch to the containment sump included in the analysis.	None	No	15%
LOCA	164	8-in. (20.32-cm) surge line break. ECC suction switch to the containment sump included in the	None	No	12%

Class	TH#	System Failure	Operator Action	HZP?	%[1]
		analysis.			
LOCA	156	16-in. (40.64-cm) hot leg break. ECC suction switch to the containment sump included in the analysis.	None	No	3%
LOCA	141	3.22-in. (8.19-cm) surge line break [Break flow area increased by 30% from 2.83-in. (7.18-cm) break].	None	No	1%

Note: 1. The column headed "%" indicates the contribution of this transient to the TWCF averaged across all four embrittlement levels analyzed.

Table 8.8. Transients that contribute most significantly to the estimated TWCF of Beaver Valley Unit 1

Class	TH#	System Failure	Operator Action	HZP?	%[1]
SO-1	126	Reactor/turbine trip w/one stuck-open pressurizer SRV which recloses at 6,000 s and operator controls HHSI 10 minutes after allowed.	None	No	10%
SO-1	60	Reactor/turbine trip w/one stuck-open pressurizer SRV which recloses at 6,000 s.	None.	No	7%
SO-1	130	Reactor/turbine trip w/one stuck-open pressurizer SRV which recloses at 3,000 s at HZP and operator controls HHSI 10 minutes after allowed.	None	Yes	6%
SO-1	97	Reactor/turbine trip w/one stuck-open pressurizer SRV which recloses at 3,000 s.	None.	Yes	2%
SO-1	129	Reactor/turbine trip w/one stuck-open pressurizer SRV which recloses at 6,000 s at HZP and operator controls HHSI 10 minutes after allowed.	None	Yes	1%
SO-1	123	Reactor/turbine trip w/two stuck-open pressurizer SRVs which reclose at 3,000 s at HZP and operator controls HHSI 10 minutes after allowed.	None	Yes	1%
LOCA	56	4-in. (10.16-cm) surge line break	None	No	35%
LOCA	7	8-in. (20.32-cm) surge line break	None.	No	20%
LOCA	9	16-in. (40.64-cm) hot leg break	None.	No	6%
MSLB	102	Main steam line break with AFW continuing to feed affected generator for 30 minutes.	Operator controls HHSI 30 minutes after allowed. Break is assumed to occur inside containment so that the operator trips the RCPs as a result of adverse containment conditions.	No	4%
MSLB	104	Main steam line break with AFW continuing to feed affected generator for 30 minutes.	Operator controls HHSI 60 minutes after allowed. Break is assumed to occur inside containment so that the operator trips the RCPs as a result of adverse containment conditions.	No	3%
MSLB	103	Main steam line break with AFW continuing to feed affected generator for 30 minutes.	Operator controls HHSI 30 minutes after allowed. Break is assumed to occur inside containment so that the operator trips the RCPs as a result of adverse containment conditions.	Yes	3%

Class	TH#	System Failure	Operator Action	HZP?	%[1]

Note: 1. The column headed "%" indicates the contribution of this transient to the TWCF averaged across all four embrittlement levels analyzed.

Table 8.9. Transients that contribute most significantly to the estimated TWCF of Palisades

Class	TH#	System Failure	Operator Action	HZP?	%
SO-1	65	One stuck-open pressurizer SRV that recloses at 6,000 sec after initiation. Containment spray is assumed not to actuate.	None. Operator does not throttle HPI.	Yes	35%
SO-1	48	Two stuck-open pressurizer SRVs that reclose at 6,000 sec after initiation. Containment spray is assumed not to actuate.	None. Operator does not throttle HPI.	Yes	1%
SO-1	53	Turbine/reactor trip with two stuck-open pressurizer SRVs that reclose at 6,000 sec after initiation. Containment spray is assumed not to actuate.	None. Operator does not throttle HPI.	No	1%
LOCA	40	16-in. (40.64-cm) hot leg break. Containment sump recirculation included in the analysis.	None. Operator does not throttle HPI.	No	23%
LOCA	58	4-in. (10.16-cm) cold leg break. Winter conditions assumed (HPI and LPI injection temp = 40°F (4.44°C), Accumulator temp = 60°F (15.56°C))	None. Operator does not throttle HPI.	No	10%
LOCA	62	8-in. (20.32-cm) cold leg break. Winter conditions assumed (HPI and LPI injection temp = 40°F (4.44°C), Accumulator temp = 60°F (15.56°C))	None. Operator does not throttle HPI.	No	4%
LOCA	64	4-in. (10.16-cm) surge line break. Summer conditions assumed (HPI and LPI injection temp = 100°F (37.78°C), Accumulator temp = 90°F (32.22°C))	None. Operator does not throttle HPI.	No	3%
LOCA	60	2-in. (5.08-cm) surge line break. Winter conditions assumed (HPI and LPI injection temp = 40°F (4.44°C), Accumulator temp = 60°F (15.56°C))	None. Operator does not throttle HPI.	No	2%
LOCA	63	5.66-in. (14.37-cm) cold leg break. Winter conditions assumed (HPI and LPI injection temp = 40°F (4.44°C), Accumulator temp = 60°F (15.56°C))	None. Operator does not throttle HPI.	No	2%
LOCA	59	4-in. (10.16-cm) cold leg break. Summer conditions assumed (HPI and LPI injection temp = 100°F (37.78°C), Accumulator temp = 90°F (32.22°C))	None. Operator does not throttle HPI.	No	1%

Class	TH#	System Failure	Operator Action	HZP?	%
MSLB	54	Main steam line break with failure of both MSIVs to close. Break assumed to be inside containment causing containment spray actuation.	Operator does not isolate AFW on affected SG. Operator does not throttle HPI.	No	2%
MSLB	27	Main steam line break with controller failure resulting in the flow from two AFW pumps into affected steam generator. Break assumed to be inside containment causing containment spray actuation.	Operator starts second AFW pump.	No	1%
SO-2	55	Turbine/reactor trip with 2 stuck-open ADVs on SG-A combined with controller failure resulting in the flow from two AFW pumps into affected steam generator.	Operator starts second AFW pump.	No	12%
SO-2	19	Reactor trip with 1 stuck-open ADV on SG-A.	None. Operator does not throttle HPI.	Yes	5%
Note: 1. The column headed "%" indicates the contribution of this transient to the TWCF averaged across all four embrittlement levels analyzed.					

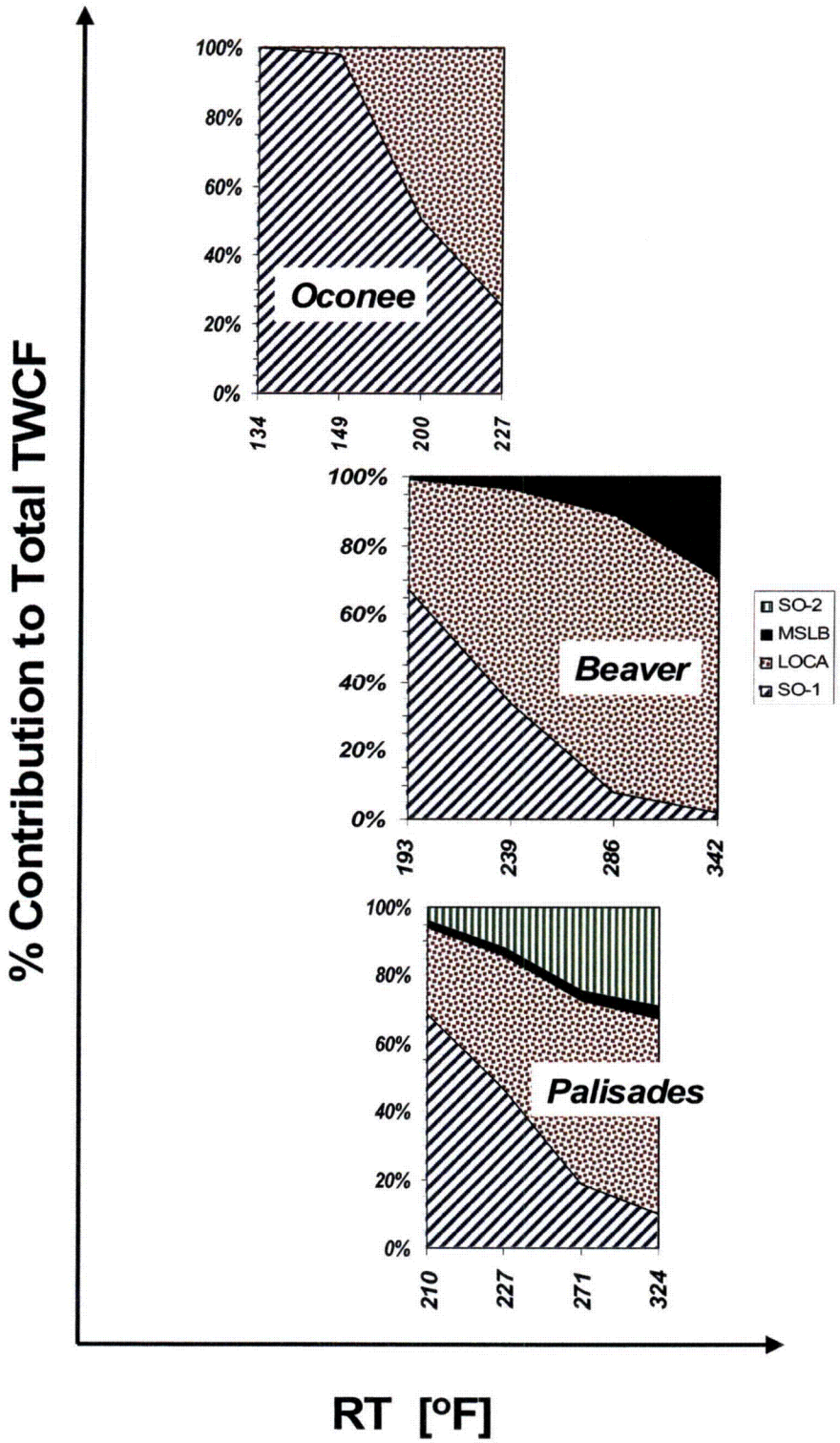

Figure 8-11. Variation in percent contribution to the total TWCF of different transient classes with reference temperature (RT) as defined in Table 8.6. The contributions of feed-and-bleed LOCAs and steam generator tube ruptures were also assessed. These transient classes made no contribution to TWCF, with the exception that feed-and-bleed LOCAs contributed < 0.1% to the TWCF of the Palisades RPV.

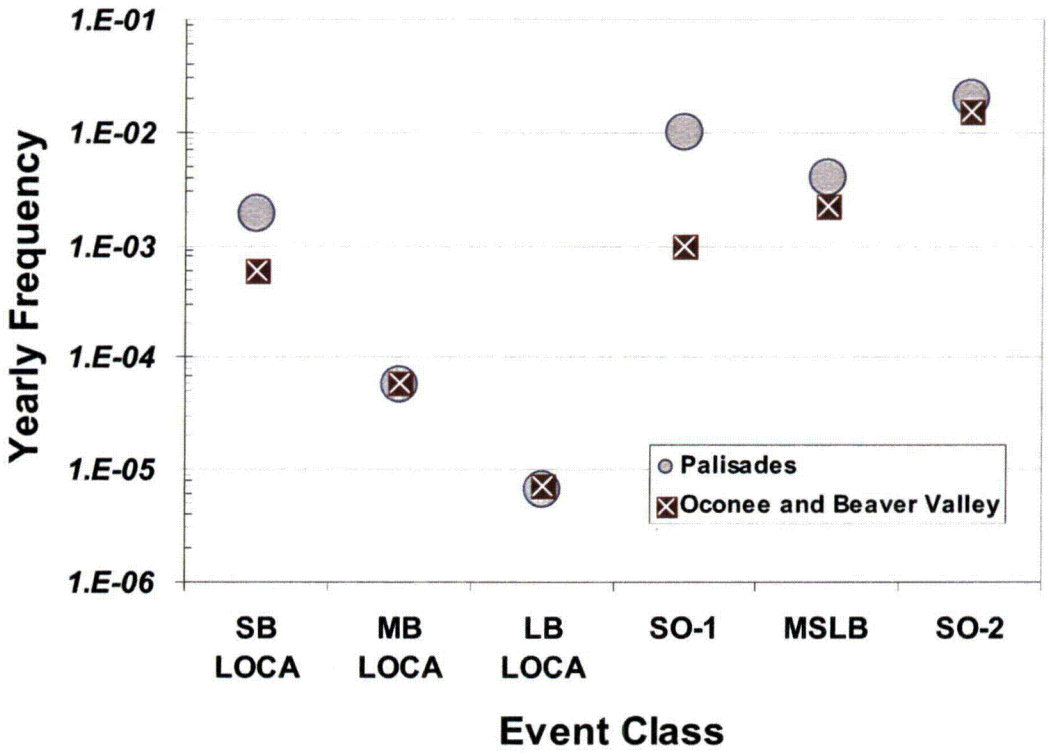

Figure 8-12. Comparison of the annual frequencies of various broad classes of events for full-power conditions

8.5.2 Primary Side Pipe Breaks

8.5.2.1 General Description of a Pipe Break Transient

Following a pipe break, the primary system cools by two mechanisms. The rapid depressurization caused by the break produces a rapid drop in system temperature because, under the saturated conditions that exist once a break occurs, pressure is linked to temperature via the ideal gas law. For large-diameter breaks, this pressure-induced temperature decrease dominates the primary system cooldown. As break size decreases, another cooling mechanism (the temperature and volume of the ECC injection water) becomes important. As indicated in Figure 2.1, ECCS pumps (e.g., HPSI, LPSI, etc.) all inject into the cold leg. Consequently, for cold leg breaks, some of the injection water is lost out of the break, never reaching (or cooling) the downcomer. In this situation, the volume of the cooling water lost is approximately proportional to the number of cold legs. (For example, in a 3-loop plant, if one cold leg breaks, the injection flow reaching the downcomer is diminished by one-third.) Conversely, no cooling water is lost if the break occurs in either the hot leg or in the surge line. For this reason, cold leg breaks tend to be somewhat less severe (at an equivalent diameter) than hot leg or surge line breaks.

The minimum temperature to which the injection water cools the primary can depend on the ambient temperature outside the plant because both the HPSI and LPSI pumps draw from the RWST. In plants where the RWST is outside and uninsulated, the temperature of the cooling water is subject to seasonal temperature variations, which directly impact the portion of the downcomer cooling controlled by safety injection. The effect of seasonal temperature variations on cooling water temperature is a more important factor for smaller diameter breaks.

Additionally, factors such as the total volume of the inventory in the RWST and the pressures at which the safety injection pumps start can differ from plant-to-plant. These features influence the cooldown characteristics of pipe break transients for the following reasons:

- The total volume of the inventory in the RWST controls the time interval over which the ECCS can draw water from this source. If the transient continues after this time, the ECCS has to switch over to recirculation from the containment sump. Since the water in the sump has flowed out of the break, it is generally warmer (~120°F (48.9°C)) than water drawn from the RWST (as low as ~ 40°F (4.4°C) during the winter).
- For breaks of medium to small diameter (approximately 4-in. (10.16-cm) and below) the cooldown rate is sufficiently gradual that it can be influenced by the pressure at which the safety injection pumps start. Plant-specific differences can, therefore, influence the cooldown rate. Differences of this type occurred among the three study plants. Both Oconee and Beaver Valley have high-head HPSI that injects water immediately upon receiving a safety injection actuation signal (at ~ 1,700 psi). In contrast, Palisades has low-head HPSI pumps that inject water when the pressure falls below 1,300 psi.

8.5.2.2 Model of this Transient Class

As detailed in Appendix A, Tables A.1 (break diameters above 3.5-in. (8.9-cm)) and A.2 (break diameters below 3.5-in. (8.9-cm)) our modeling of primary side pipe breaks includes a spectrum of break diameters ranging from 1.4- to 16-in. (3.6- to 40.6-cm) because break size is the single most important factor that controls the rate of system depressurization and (thereby) the severity of the transient. No operator actions are modeled for any break diameter exceeding ≈3-in. (≈7.6-cm) because for these events, the safety injection systems do not fully refill the upper regions of the RCS. Consequently, operators would never take action to shut off the pumps. Other factors modeled include the following:

- break location (for smaller diameter breaks)
- season of the year (for smaller diameter breaks)
- total volume of the RWST inventory (controls the time at which cooling water begins to draw from the sump, which is warmer than the water stored in the RWST)
- pump start setpoints

8.5.2.3 Relationships between System Characteristics and Thermal-Hydraulic Response

8.5.2.3.1 Dominant *vs.* Secondary Factors

Primary side pipe breaks characteristically cause both a rapid cooldown and a rapid depressurization of the primary system. At long times, the temperature of the primary approaches the temperature of the injection water, which can be as low as 35°F (1°C) because it is stored in external tanks. As described in the previous section, the break area (i.e., $\pi \cdot (D_{BREAK}/2)^2$) is the main factor controlling the initial cooldown rate because break area controls the depressurization rate and the two are linked through the ideal gas law. Figure 8.13 illustrates this point for a spectrum of hot leg/surge line breaks in both Beaver Valley and Oconee.

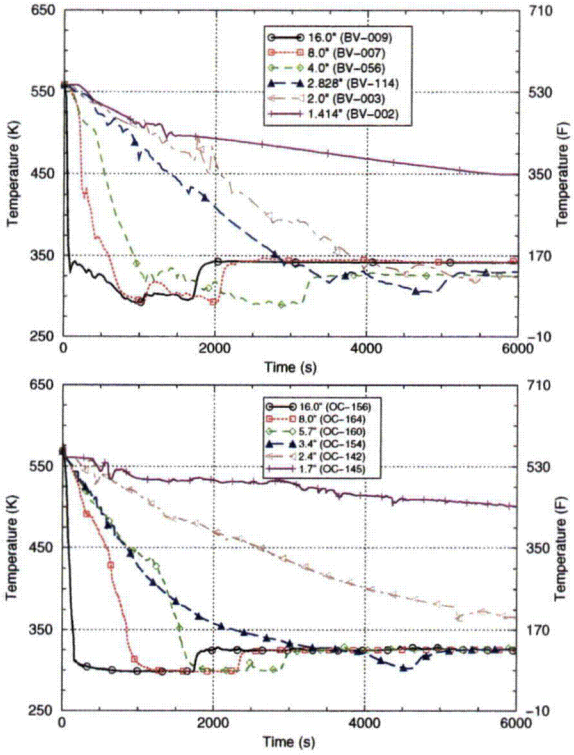

Figure 8.13. Effect of surge line and hot-leg break diameter on the cooldown characteristics of Beaver Valley (top) and Oconee (bottom)

Factors other than break size can alter the cooldown signature somewhat, but are generally less important than the dominating influence of break area. For example:

- Break Location: As described in the previous section, cold leg breaks are expected to be less severe than hot leg breaks at equivalent break diameter due to loss of injection water out of the break. However, as illustrated in Figure 8.14 the effect of break location is not so great as to take a break out of severity order as indicated by break size.
- Injection Water Temperature: Variations in injection water temperature occur both at the time in the transient when the volume of the RWST is exhausted and the HPSI/LPSI pumps start drawing off the sump and as a consequence of seasonal variations. The sudden increase in downcomer temperature evident at approximately 2000 sec. on the 8- and 16-in. diameter break curves in the top graph in Figure 8.13 indicates the time at which the switchover to sump occurs. Figure 8.15 illustrates the effect of seasonal variations on cold leg breaks in Palisades. Again, break diameter is seen to be the dominant factor controlling the initial cooldown rate with seasonal factors playing a less important role.

Relative to differences in cooldown rate between different break sizes, differences in primary system pressure are more modest because safety injection flow cannot fully compensate for the loss of inventory out of these breaks. Figure 8.16 illustrates this point for a range of break sizes in both Oconee and Beaver Valley. Similarly, the effect of break size on differences in the heat transfer coefficient between different breaks is more modest, see Figure 8.17.

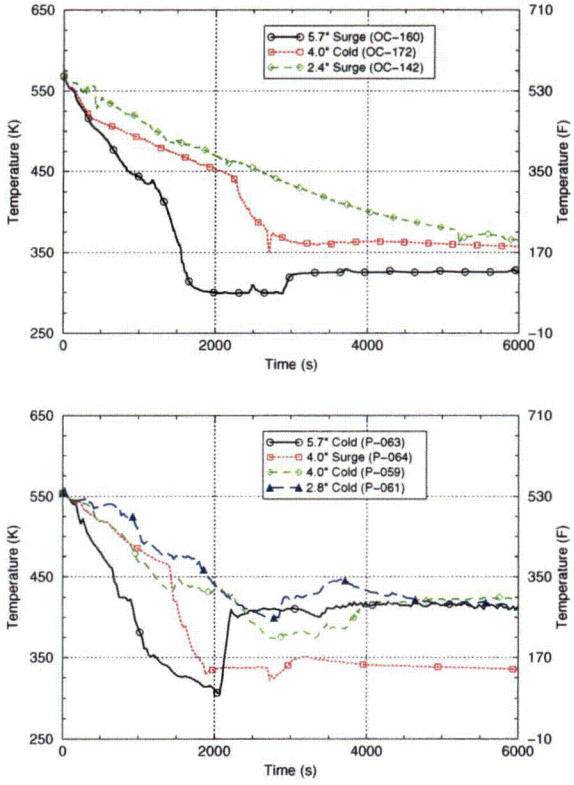

Figure 8.14. Effect of break location on the cooldown characteristics in Oconee (top) and Palisades (bottom)

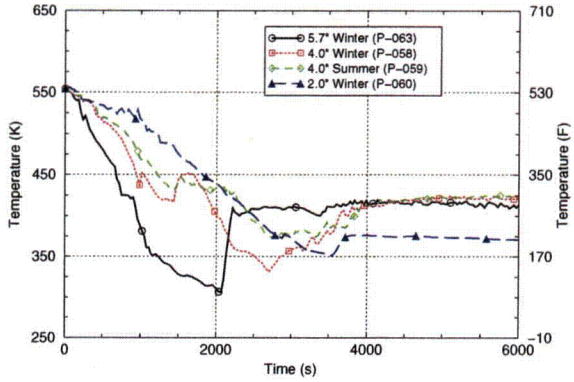

Figure 8.15. Effect of season on the cooldown characteristics of cold leg breaks in Palisades

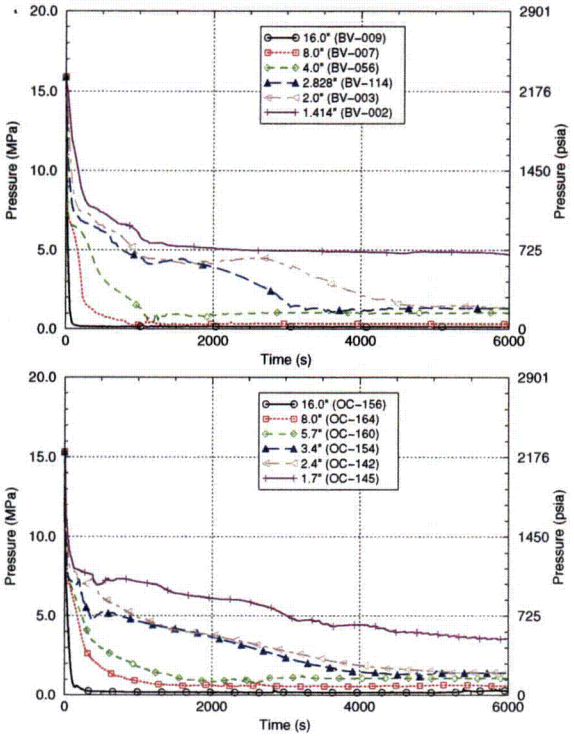

Figure 8.16. Effect of surge line and hot-leg break diameter on the depressurization characteristics of Beaver Valley (top) and Oconee (bottom)

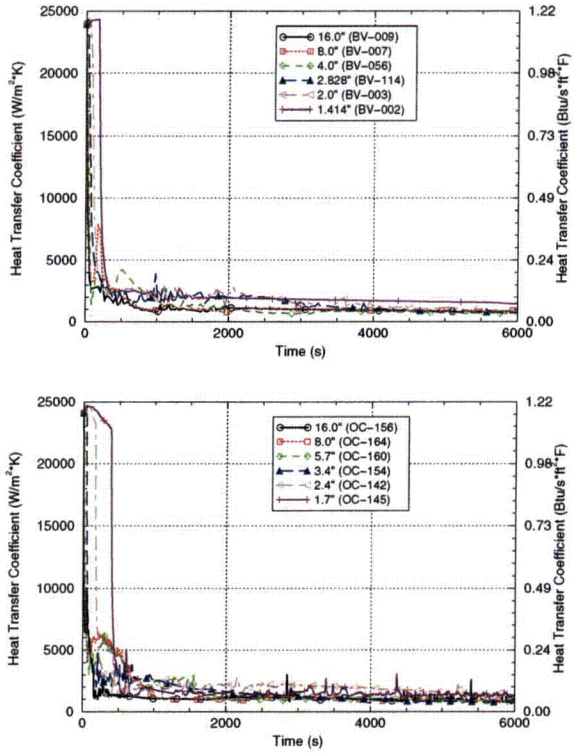

Figure 8.17. Effect of surge line and hot-leg break diameter on the heat transfer coefficient in Beaver Valley (top) and Oconee (bottom)

8.5.2.3.2 Plant-Specific Effects

Figure 8.18 compares the cooldown characteristics of different break sizes across the three plants modeled. For nominally identical conditions between plants (i.e., break size, break location, power level at transient initiation), the response of the three study plants is similar across the entire break size spectrum. This is because the cooldown rate is controlled (mostly) by the size of the break and the overall size, temperature, and pressure of the RPV in which the break occurs. In Figure 8.18, these factors are consistent plant-to-plant.

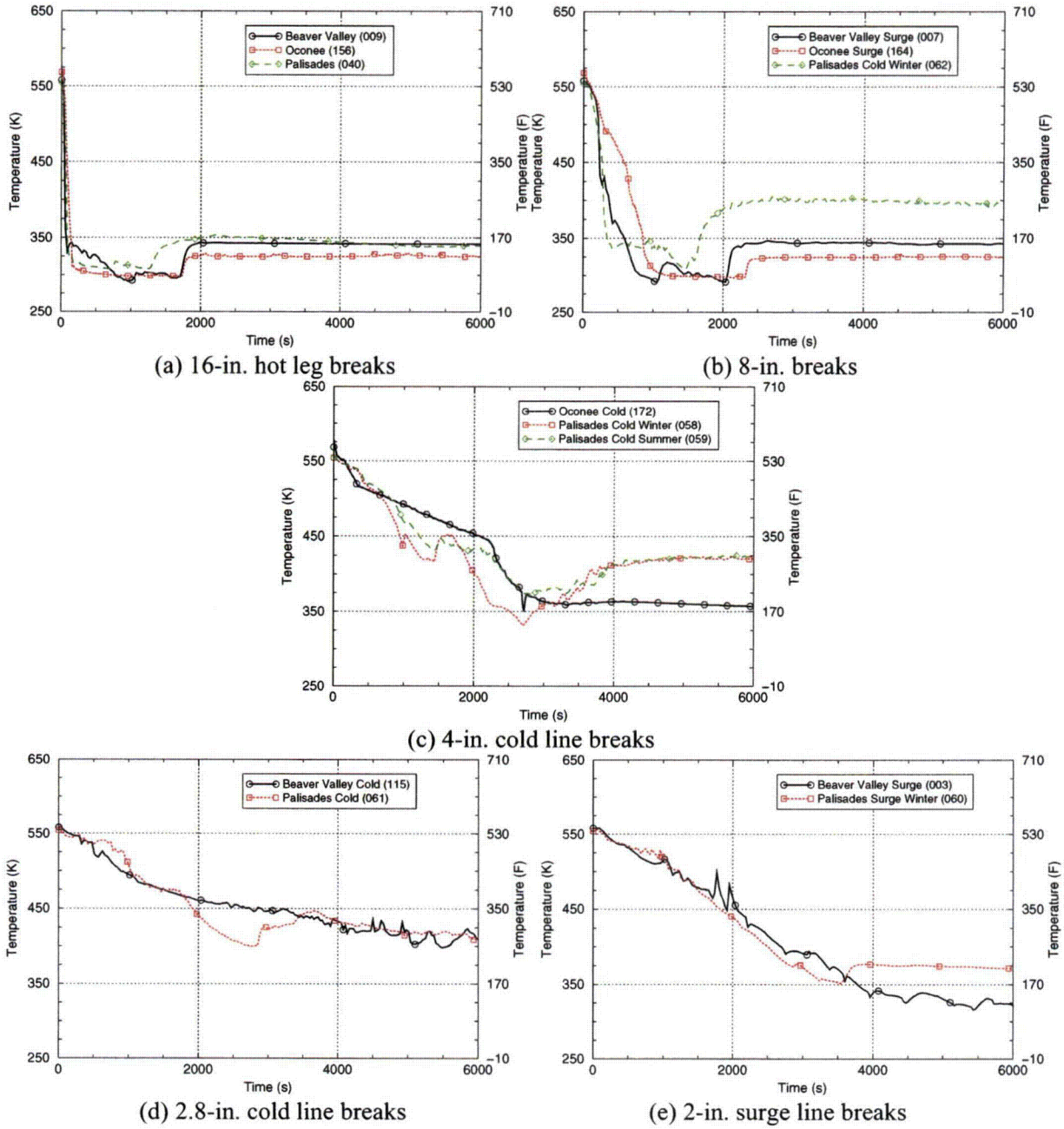

Figure 8.18. Comparison of the cooldown characteristics of the three plants modeled for a spectrum of break diameters

8.5.2.4 Estimates of Vessel Failure Probability

In Section 8.5.2.3, we identified break size as the factor that most significantly influenced the cooldown rate that results from a pipe break, with break location and season of the year playing more limited roles. We examine these factors in the following subsections. Additionally, we discuss differences between the number of cracks initiated by pipe break transients *vs*. those that propagate through the wall, and information concerning the time differential between transient initiation (i.e., pipe break) and vessel failure. The section concludes with an assessment of the applicability of these

findings to assessing the probability of vessel failure due to pipe breaks in general.

In the following subsections, we compare values of CPTWC for different transients taken from Tables A.1 and A.2. To obtain an approximately equivalent level of embrittlement across all plants these comparisons use results for Beaver Valley and for Palisades at 60 EFPY, while Oconee results are taken at the Ext-Ob embrittlement level (see Table 8.6).

8.5.2.4.1 Break Size Effects

Figure 8.19 shows the effect of break size on the CPTWC results for all three plants. Up to a break diameter of ~4- to 5-in. (~10.16- to 12.7-cm), CPTWC depends strongly on break diameter. By comparison, for larger break diameters, the CPTWC is essentially independent of further increases in break diameter. For these larger diameter breaks, the RCS fluid cools faster than the wall of the RPV. In this situation, ***only*** the thermal conductivity of the steel and the thickness of the RPV wall control the thermal stresses and, thus, the severity of the fracture challenge, perturbations to the fluid cooldown rate controlled by the break diameter, break location, and season of the year do not play a role. Thermal conductivity is a physical property, so it is very consistent for all RPV steels. Consequently, the single factor controlling the severity of the fracture challenge for large diameter pipe breaks is the thickness of the RPV wall because higher thermal stresses can develop in thicker walls. This effect of wall thickness is seen in Figure 8.19, where the CPTWC for the thinner vessel (Beaver Valley: 7.875-in (20-cm) thick) is consistently below that of the thicker vessels (Palisades and Oconee both have wall thicknesses of 8½-in) for break sizes above 4- to 5-in. (~10.16- to 12.7-cm). In Section 9.2, we discuss the effects of thickness on vessel failure probability in greater detail.

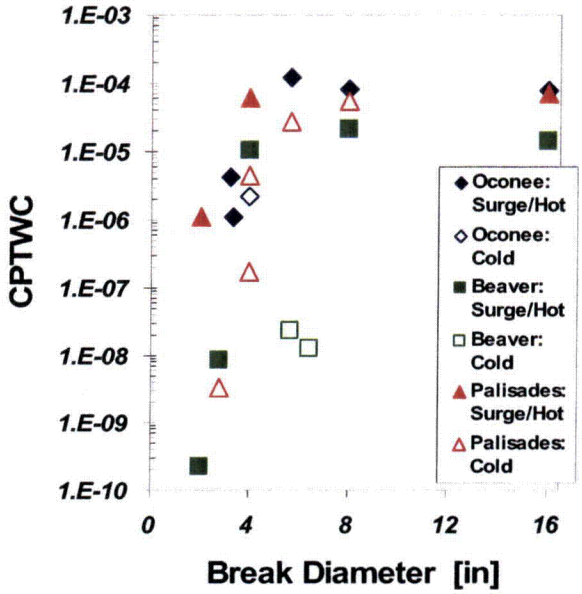

Figure 8.19. Effect of pipe break diameter and break location on the conditional probability of through-wall cracking. (CPTWC taken at approximately equivalent embrittlement levels between plants (Beaver Valley and Palisades at 60 EFPY, Oconee at Ext-Ob))

8.5.2.4.2 Break Location and Seasonal Effects

Figure 8.19 also illustrated the effect of break location. As discussed in Section 8.5.2.2 and illustrated in Figure 8.14, cold leg breaks are less severe than hot leg breaks across the entire break size spectrum because some portion of the ECC flow is lost out of a cold leg break. The magnitude of the influence of break location on CPTWC is negligible for conduction limited conditions (i.e., for large breaks) and increases with decreasing break size because it is for smaller breaks that differences in injection flow can have a significant effect on the fluid cooling rate. In the Palisades analysis the combined effects of break size and of seasonal variations were modeled in more detail than in the other two plants: Figure 8.20 shows these results. Focusing on the 4-in. (10.16-cm) diameter breaks, we see that the surge line break (summer conditions) has a CPTWC approximately 300 times greater than that of a 4-in. (10.16-cm) diameter cold leg break. The effects of seasonal variations are less

important: at the 4-in. (10.16-cm) break size, a cold line break in winter has a CPTWC approximately 20 times greater than a cold line break in summer. It should be noted that seasonal variations are not important at all plants. Some plants have insulated RWSTs which mitigate the effect of outside temperature on the temperature of the ECC injection water.

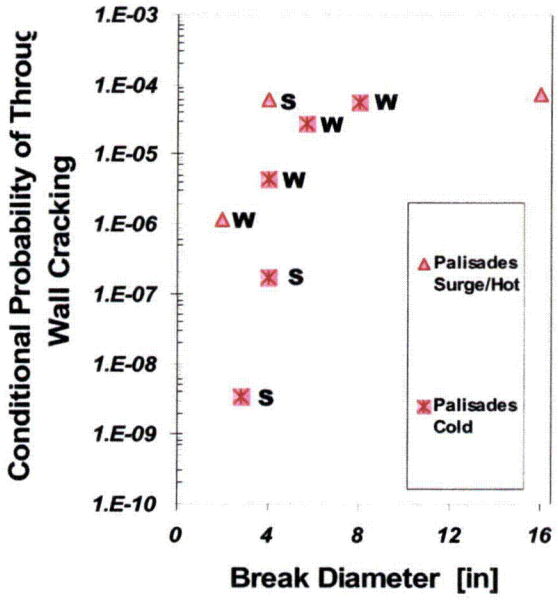

Figure 8.20. Effect of pipe break diameter, break location, and season (S=Summer, W=Winter) on the conditional probability of through-wall cracking for Palisades

8.5.2.4.3 Differences Between Crack Initiation and Vessel Failure for Pipe Break Transients

Because of the lack of a significant pressure component during a pipe break (see Figure 8.16), these transients cause many more crack initiations than they do complete failure of the vessel wall. This is quantified in Figure 8.21 by the ratio of the conditional probability of through-wall cracking to the conditional probability of crack initiation. A ratio of 100% would indicate that all initiated cracks also propagated through the vessel wall.
The maximum ratio for any pipe break analyzed is 12%. while the ratios for the large diameter breaks that contribute most significantly to the through-wall cracking frequency are ~1% for Oconee and Beaver Valley, and ~4% for Palisades. The lower ratios for Oconee and Beaver Valley are caused by the greater dominance of circumferential cracks as initiators in these plants (see Table 8.5).

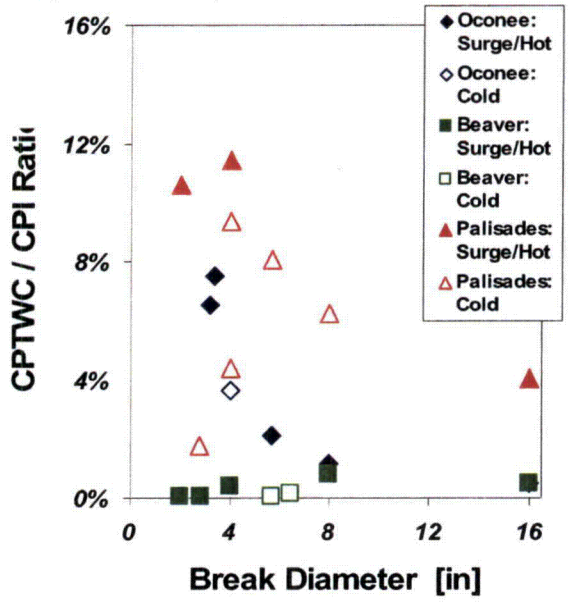

Figure 8.21. Effect of pipe break diameter and break location on the conditional proportion of initiated flaws that propagate through the wall. (CPTWC/CPI ratios taken at approximately equivalent embrittlement levels between plants (Beaver Valley and Palisades at 60 EFPY, Oconee at Ext-Ob).)

8.5.2.4.4 Time Between Pipe Break and Vessel Failure

As illustrated Figure 8.22, there is very little time (particularly for large breaks) between the initiating event (i.e., the pipe breaking) and vessel failure. If failure is going to occur as a consequence of a pipe break, it will happen within ~30 min. (1800 sec.) for 4-in. (10.16-cm) breaks. Vessel failures resulting from larger breaks occur even faster: if an 8-in. (20.32-cm) break fails the vessel, it does so within ~15 min. (900 sec.). These short failure times limit the influence of thermal-hydraulic variations that occur at much longer times (see the plots in Section 8.5.2.3); they also limit the time in which operator action can occur. Additionally, it should be noted that operator actions are not

a factor for pipe break transients because for breaks of diameter ~2-in. (5.08-cm) and greater, there is no action that the operator can take: ECCS flow must continue to keep the core covered.

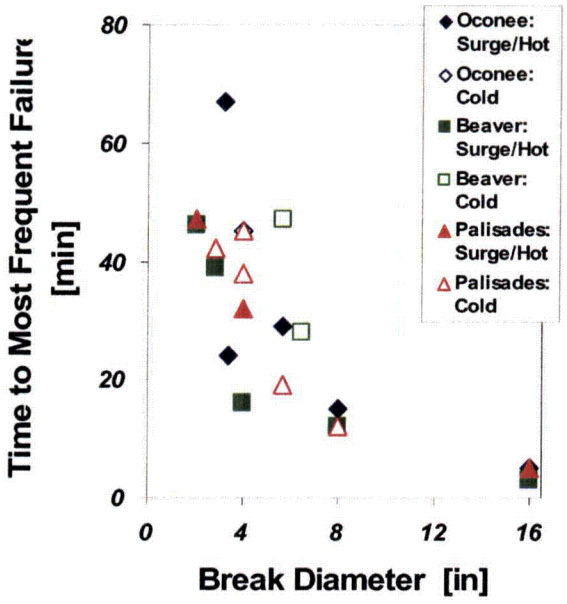

Figure 8.22. Effect of LOCA break diameter and break location on the time at which through-wall cracking occurs (Break times taken at approximately equivalent embrittlement levels between plants (Beaver Valley and Palisades at 60 EFPY, Oconee at Ext-Ob).)

8.5.2.4.5 Applicability of Findings to PWRs in General

While the information presented in this section pertains specifically to the three plants analyzed, the following three factors suggest that these results can be used with confidence to assess the risk of vessel failure arising from pipe break transients for PWRs *in general*:

(1) Larger break sizes control the contribution of pipe breaks to the total estimated TWCF. In the three plants studied break diameters above 5-in. (12.7-cm) account for more than 50% of the TWCF attributable to pipe breaks, with break diameters of 3.5- to 5-in. (8.9- to 12.7-cm) accounting for nearly all of the remainder. As discussed in this section, the severity of larger breaks is more consistent from plant-to-plant than for smaller break diameters.

(2) Operator actions do not play a major role in pipe break transients. Consequently, the transferability of these results to other plants cannot be questioned on the basis of differences in operator training, experience, and so on.

(3) At an equivalent embrittlement level, the TWCF is fairly consistent among the three plants modeled. As a direct consequence of factors 1 and 2, the TWCF attributable only to primary side pipe breaks is reasonably consistent from plant-to-plant (see Figure 8.23).

In Section 9.3, we discuss the applicability of these results to PWRs *in general* in greater detail.

8.5.2.5 Comparison with Previous Studies

8.5.2.5.1 As Reported by [Kirk 12-02]

While the specific numerical results reported herein differ from those in our interim report [***Kirk 12-02***] the general trends discussed in this section have not changed substantively from those reported earlier.

8.5.2.5.2 Studies Providing the Technical Basis of the Current PTS Rule

Our results demonstrating that pipe breaks, particularly large diameter pipe breaks, are dominant contributors to PTS risk represent a substantial change relative to earlier PTS studies [SECY-82-465, ORNL 85a, 86b, 86]. It should, however, be noted that in these earlier studies, large diameter pipe breaks could not contribute to the through-wall cracking frequency because they were excluded *a priori* from the analysis. This exclusion resulted from erroneous assumptions made about the need for significant pressure to drive through-wall cracking, and erroneous interpretation of large-scale tests [Cheverton 85a, Cheverton 85b] as 1:1 surrogates for full-scale PWRs.

(See Appendix A to [***EricksonKirk-PFM***].) Specifically, a series of thermal shock experiments (TSEs) performed at Oak Ridge National Laboratory in the late 1970s and early 1980s demonstrated that thermal shock alone (no pressure was or could be applied to these open-ended cylinders) could drive a cleavage crack almost entirely through the wall of a scaled RPV. (Figure 8-24 shows a post-test photograph of the crack in TSE #6, wherein the crack arrested after propagating 95% of the way through the cylinder wall.) While 95% through-wall cracking is not vessel failure, we do not feel that this evidence adequately justifies the previous judgment that thermal shock alone cannot fail a pressure vessel for the following reasons:

(1) The cylinders tested by ORNL were much thicker (in comparison to their diameter) than commercial PWRs. This increased stiffness makes crack arrest more likely in the experiment than in the actual structure.

(2) The cylinders tested in the ORNL TSEs were fabricated from forgings that tended to have material on the outer diameter that was tougher (lower fracture toughness transition temperature) than on the inner diameter. This toughness gradient, which resulted from the processes used to fabricate the forgings, is not typical of the axial welds that contribute the most to PTS failure frequencies. Again, qualitatively, crack arrest in the TSEs is more likely than in the actual structure.

(3) Because the ORNL TSEs used open-ended cylinders, the pressure component of the loading was zero, *by definition*. However, the results of our PFM calculations (see Figure 8-25) demonstrate that, while low, some pressure is retained within the primary system, even for large diameter breaks.

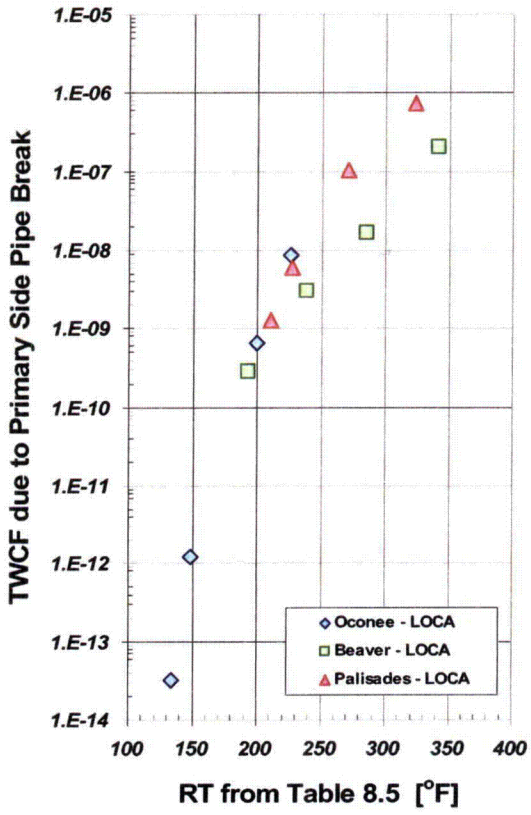

Figure 8.23. The TWCF attributable only to primary side pipe breaks in the three study plants

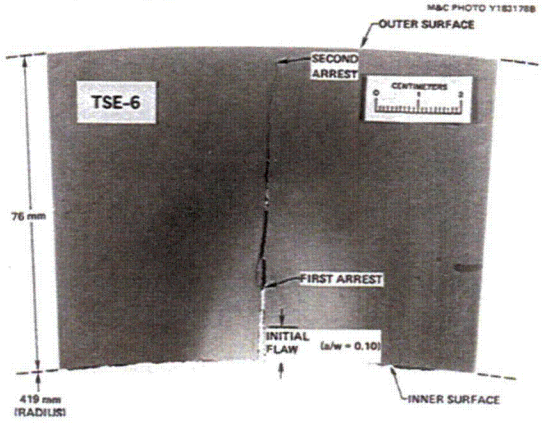

Figure 8-24. Radial profile of arrested crack in TSE 6 [Cheverton 85a] (The crack in this experiment arrested after propagating 95% of the way through the cylinder wall.)

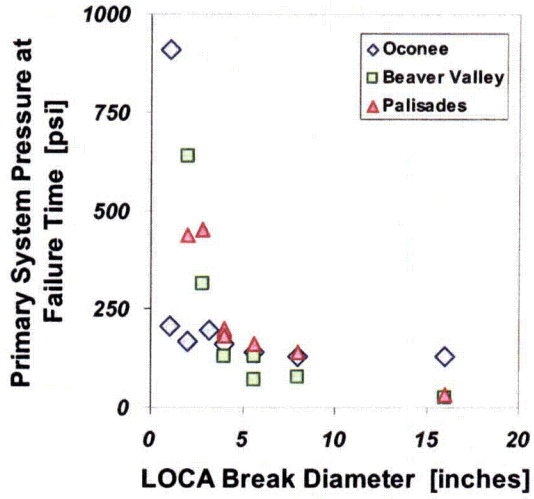

Figure 8-25. Effect of pipe break diameter on the pressure in the primary system at the most likely time of failure

8.5.3 Stuck-Open Valves on the Primary Side (SO-1)

8.5.3.1 General Description of an SO-1 Transient

An SO-1 transient begins with a demand of one or more pressurizer SRVs. In some cases, the SRV opens in response to a real demand, but more often, SRVs open because of a false demand (for example, setpoint drift). Opening of an SRV causes depressurization and consequent rapid cooldown of the RCS. At this stage, other plant equipment actuates and the operators respond in accordance with operating procedures, injecting makeup water to address the loss of primary system coolant caused by the open SRV. Since the makeup water is stored in external tanks at ambient temperature, emergency injection further cools the downcomer wall. At some (random) later time, the stuck-open SRV recloses. When the valve recloses the continued charging and high-pressure injection causes the RCS to begin to refill. For the first ~15 minutes following valve reclosure, both RCS pressure and temperature are stable or increase slightly. During this time, it is unlikely that the primary injection throttling criteria will be met because the primary system is still saturated (i.e., there is no subcooling) and the level in the pressurizer is inadequate to satisfy the throttling criteria. After ~15 minutes, the RCS pressure will rise very quickly (over just a few minutes) as the pressurizer fills as a result of the combined effects of continued primary injection and system heatup. During this rapid repressurization, the primary system throttling criteria will be met, thereby *allowing* the operators to act to control the repressurization rate. The *ability* of operators to throttle injection once they are *allowed* to depends upon how quickly they are able to recognize and react to rapid changes in plant conditions, from a saturated system before bubble collapse to a nearly solid system as and after the bubble collapses. The rapidity of operator response once the throttling criteria are met controls whether, and for how long, the RCS becomes fully repressurized.

8.5.3.2 Model of this Transient Class

Transients modeled in this class (see Table A.3 in Appendix A) include one or more stuck-open pressurizer SRVs or PORVs that may reclose (unstick) later in the transient. The initial cooling rate in these transients is similar to that of a small (~2-in. (5.08-cm) diameter) pipe break, so it is not so rapid as to generate a considerable challenge to the RPV (see Figure 8.19). However, the potential for valve reclosure at some point in the transient leads to the possibility of system repressurization, and this coupled with the thermal stresses from the cooldown and the lowered fracture toughness of the vessel (because of the reduced temperature in the primary system) dramatically increases the severity of this transient class over that associated with small diameter pipe breaks.

Our modeling of this transient class includes the following factors:

- plant power level at transient initiation (full-power *vs.* hot zero power)
- the random time at which valve reclosure is assumed to occur (the possibility of reclosure after both 3,000 and 6,000 seconds was modeled)

- the timing of operator action (i.e., pump throttling) after valve reclosure (modeling considered action taken 1 minute, 10 minutes, and never after the throttling criteria were met)[‡‡‡‡]
- seasonal variations
- more than one valve sticking open
- less than the total number of stuck-open valves subsequently reclosing, or valves only partially sticking open

Scoping analyses revealed the first three of these factors to be of primary importance in establishing the severity of the loading challenge, while the last three factors played very minor roles. Attention, therefore, focused on a more detailed analysis of the first three factors, the effects of which are described in the following section.

8.5.3.3 Relationships between System Characteristics and Thermal-Hydraulic Response

The following three sections (8.5.3.3.1 through 8.5.3.3.3) examine the effects of the following factors, based on the results of a systematic study of these variables performed for Oconee (see Figure 8-26 and Figure 8-27):

- valve reclosure time
- plant power level at transient initiation
- timeliness of operator action once the throttling criteria are met

The results of a somewhat more limited study performed for the Beaver Valley plant can be found in Figure 8-28 through Figure 8-30. Finally, we discuss how well these trends can be expected to apply to other PWRs

[‡‡‡‡] This statement applies only to the models of Beaver Valley and Oconee. Because of hardware differences Palisades was modeled differently (see Section 8.5.3.4.2).

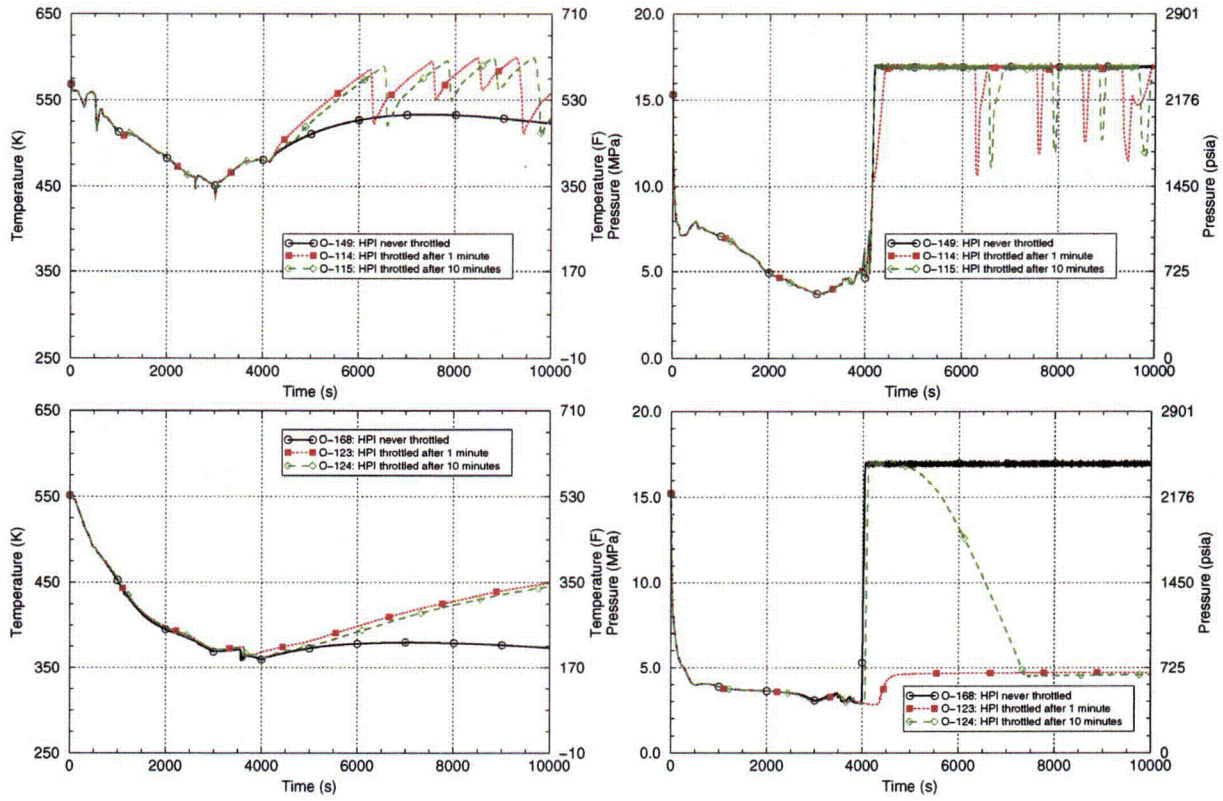

Figure 8-26. Oconee SO-1 transients where the stuck-open SRVs reclose after 3,000 seconds. (Transients in the upper graphs initiate from full power, while transients in the lower graphs initiate from hot zero power.)

8.5.3.3.1 Effect of Valve Reclosure Time on SO-1 Response

Valve reclosure is a random event that can occur at any time after the transient begins. In our model, we have discretized this continuum into the two possibilities of reclosure at 3,000 and 6,000 seconds. These possibilities were selected based on the recognition that the severity of the transient varies with valve reclosure time. Up to some time, transient severity increases with increasing time before reclosure because the temperature of the primary system is dropping (which reduces the fracture toughness) while the thermal stresses are still climbing (because the cooldown is continuing). However, once the RCS has reached its minimum temperature (established by the temperature of the HPI water), the severity of the event begins to reduce because the thermal stresses begin to decline.

The 6,000-second reclosure time was selected to coincide (approximately) with the time of maximum transient severity because it is (approximately) at this time that the RCS temperature reaches its minimum value. The 3,000-second reclosure time was selected because it is not reasonable to assume that all valve reclosures will occur at the worst possible time. The potential for valve reclosure after very long times (in excess of 7,200 seconds, or 2 hours) were not considered because by that time, operators would have initiated new procedures. Since the operators' objective is to stop the transient (i.e., stop dumping irradiated primary system water into containment), they would likely depressurize the steam generators by opening the steam dump valves to cool the secondary side, and they would start low-pressure injection and cool down the RCS to saturation conditions. These actions change the nature of the transient, making it more benign.

Also, they change the probability of operator error. Additional information on valve reclosure times can be found in response to Peer Reviewer Comment #76 in Appendix B to this report.

Figure 8-26 through Figure 8-30 illustrate the effect of valve reclosure at 3,000 *vs.* 6,000 seconds in both Oconee (Figure 8-26 and Figure 8-27) and Beaver Valley (Figure 8-28 through Figure 8-30). The primary difference between these two reclosure times is that the system temperature at the time of repressurization is lower for the 6,000-second case. Because the valve has been open for a longer time, HPI of cold water has continued for a longer time, leading to the colder temperatures in the downcomer. The temperature at the time of repressurization is ≈ 50–75°F (27.7 – 41.7 °C)colder when reclosure occurs after 6,000 sec. *vs.* when reclosure occurs after only 3,000 sec. in Oconee (compare Figure 8-26 to Figure 8-27). In Beaver Valley, the effect of a longer time before reclosure on the temperature at repressurization is more modest (≈25°F or 13.9°C) compare Figure 8-30 to Figure 8-28 and Figure 8-29). Additionally, comparing similar conditions between plants (Figure 8-27 for Oconee *vs.* Figure 8-28 for Beaver Valley) reveals that Beaver Valley cools faster and reaches lower temperatures than Oconee. The origins of these differences between plants are threefold:

- The presence of vent valves at Oconee allows recirculation of water in the downcomer area, leading to higher temperatures in B&W plants.
- The mass flow rate of the PORV in Beaver Valley is 65% greater than that at Oconee (see Table 8.1). Thus, more cooling water is injected into the Beaver Valley RPV in a fixed amount of time, leading to more rapid cooling of the primary system.
- The temperature of the injection water is warmer at Oconee (70°F (21°C)) than it is at Beaver Valley (50°F (10°C)), which leads directly to lower minimum temperatures at Beaver Valley.

Other features of the transient that contribute significantly to its severity (e.g., repressurization or not) are not influenced by valve reclosure time. Whether a plant repressurizes following valve reclosure depends on the plant power level at event initiation, as well as the timeliness of operator action, as discussed in the following two sections.

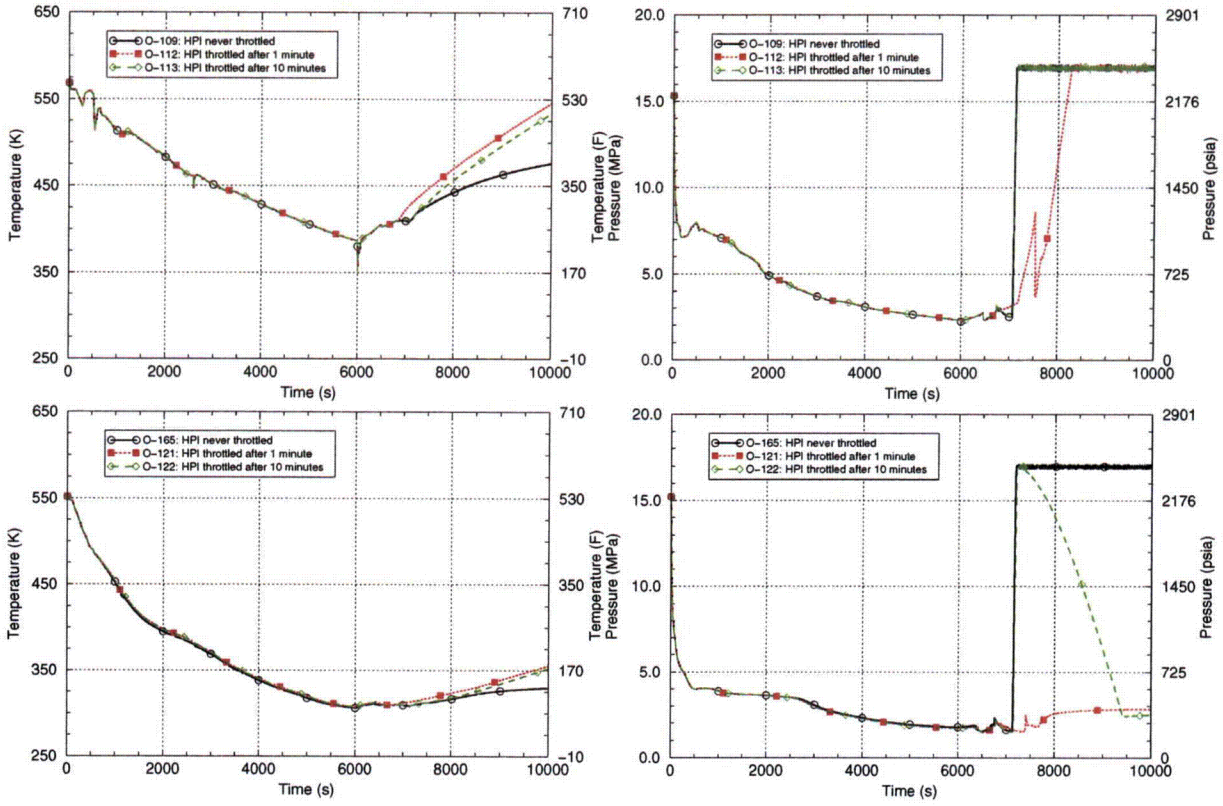

Figure 8-27. Oconee SO-1 transients where the stuck-open SRVs reclose after 6,000 seconds (Transients in the upper graphs initiate from full power, while transients in the lower graphs initiate from hot zero power.)

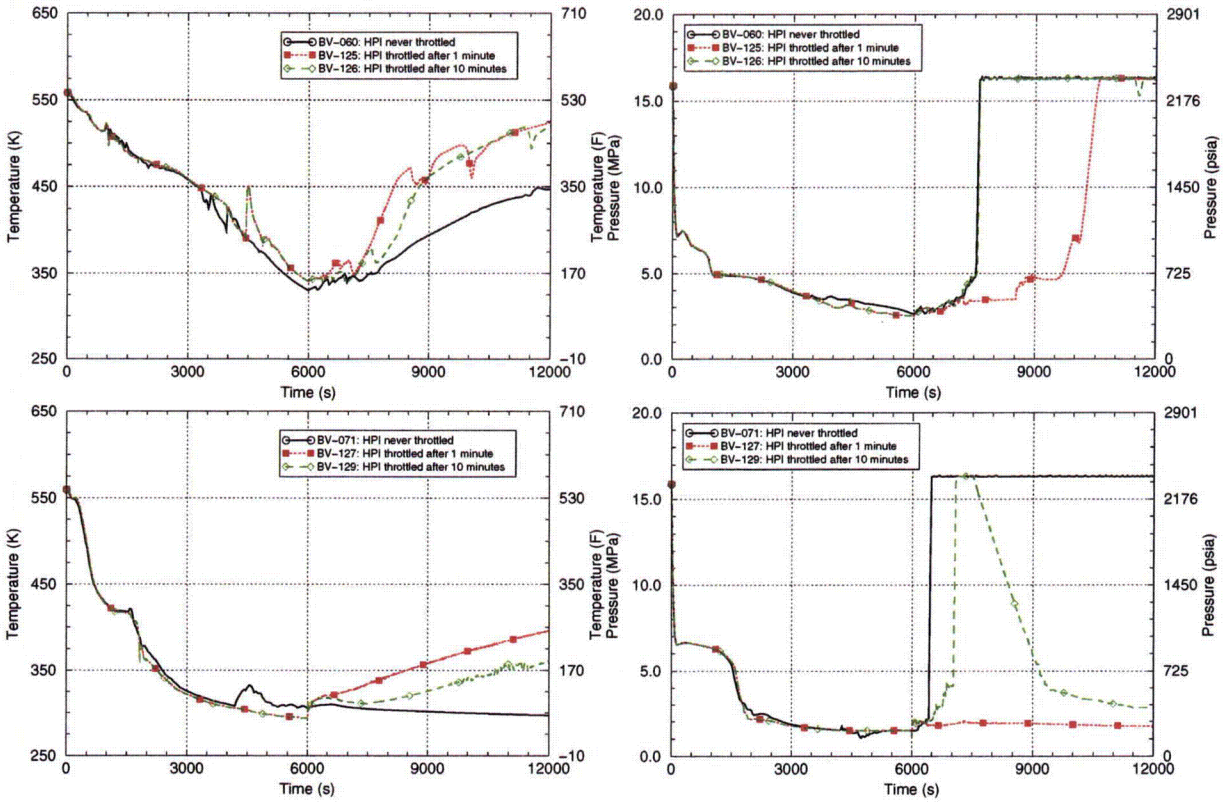

Figure 8-28. Beaver Valley SO-1 transients where a single stuck-open SRV recloses after 6,000 seconds (Transients in the upper graphs initiate from full power, while transients in the lower graphs initiate from hot zero power.)

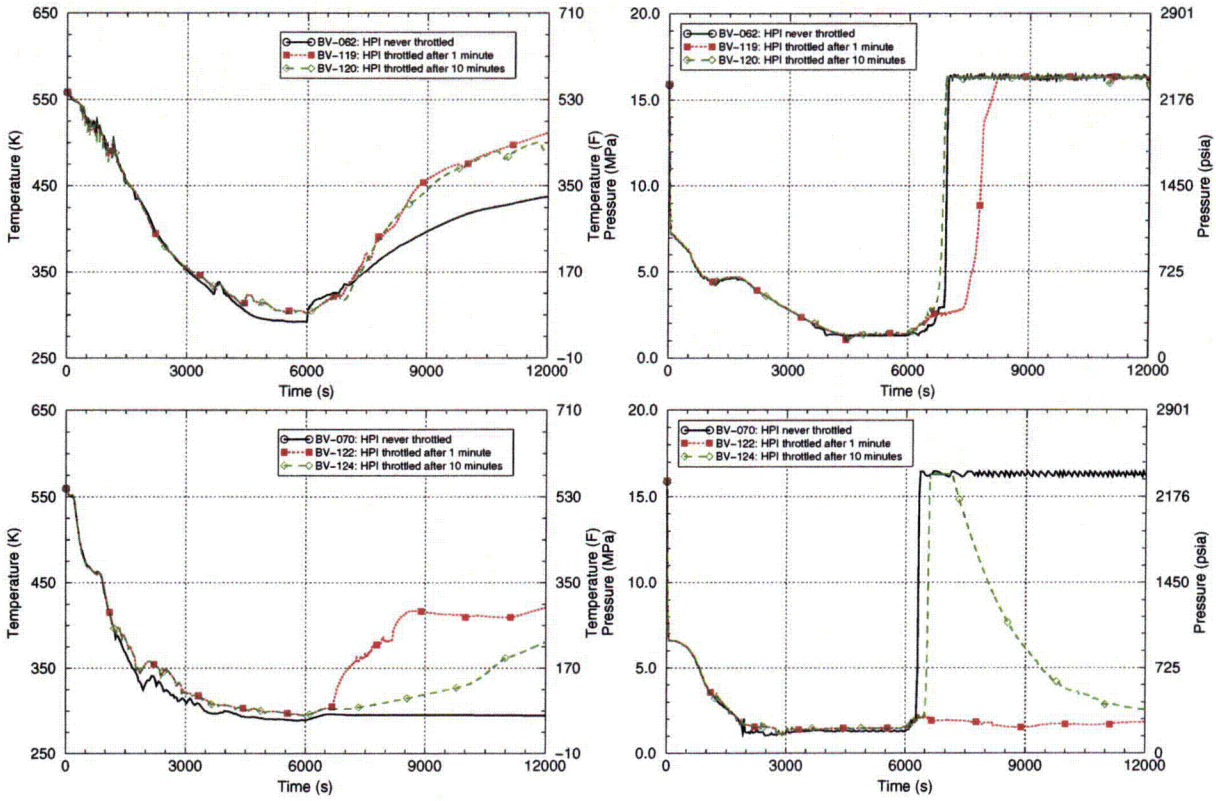

Figure 8-29. Beaver Valley SO-1 transients where a two stuck-open SRVs reclose after 6,000 seconds. (Transients in the upper graphs initiate from full power, while transients in the lower graphs initiate from hot zero power.)

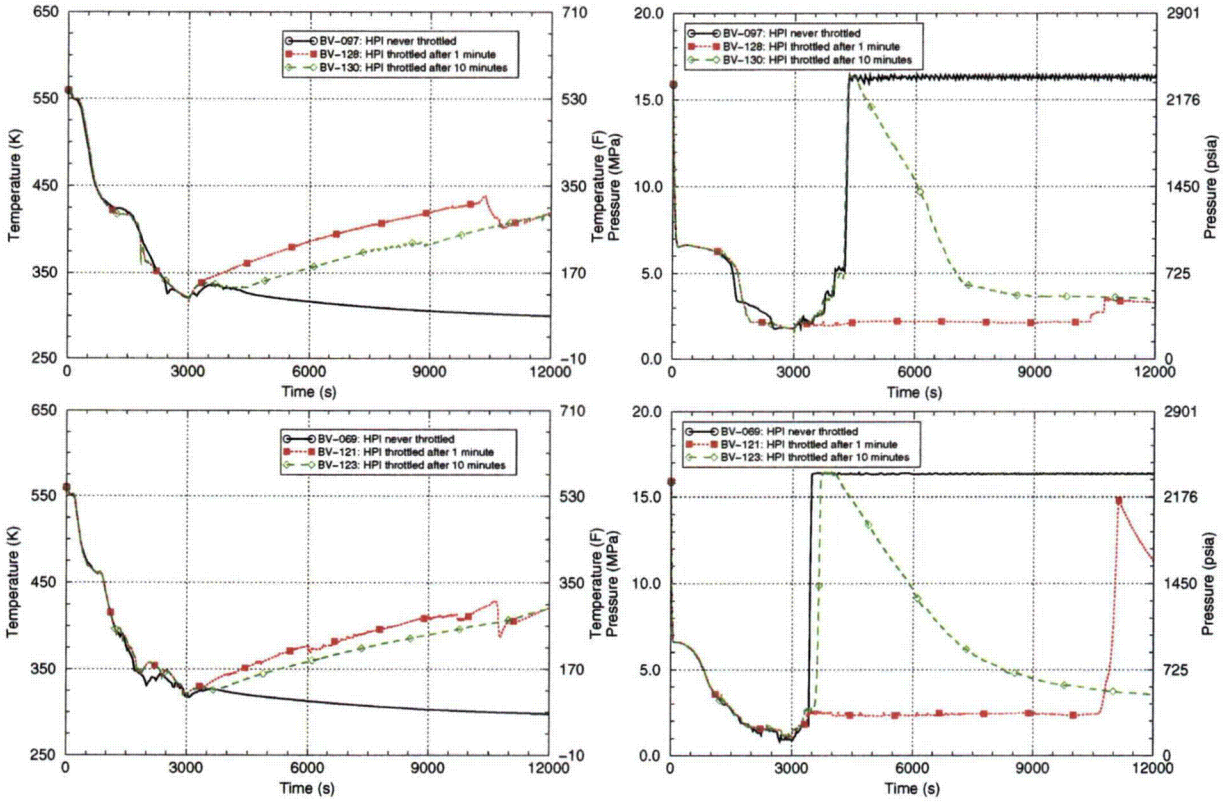

Figure 8-30. Beaver Valley SO-1 transients where stuck-open SRVs recloses after 3,000 seconds (All transients initiate from hot zero power conditions. Transients in the upper graphs have one stuck-open valve, whereas transients in the lower graphs have two stuck-open valves.)

8.5.3.3.2 Effect of Plant Power Level on SO-1 Response

If a plant experiences an SO-1 transient at HZP rather than at full-power conditions, the rate of system cooldown will be more rapid because there is less heat in the system initially. This can be seen in Figure 8-26 and Figure 8-27 by comparing the top graphs (which are initiated from full-power conditions) *vs.* the bottom graphs (which are initiated from HZP conditions). The cooling rate for the HZP transients is considerably more rapid than for the full-power transients. This more rapid cooling rate for HZP transients coupled with the fact that HZP transients begin at lower temperatures than full-power transients makes the temperature at the time or repressurization much lower for HZP transients than it is for full-power transients. These observations are true regardless of the plant considered, and can be expected to hold for all PWRs because of differences in system heat characteristic of HZP *vs.* full-power conditions. For these reasons, SO-1 transients are always more severe when initiated under HZP conditions.

8.5.3.3.3 Effect of Timing of Operator Action on SO-1 Response

Operators are allowed to limit the injection of water to the primary system once certain "throttling criteria" are met. The specific throttling criteria vary from plant-to-plant and from manufacturer to manufacturer, but generally include the following items:

- The subcooling margin must be above some specified minimum to prevent boiling in the primary.
- The level of inventory in the pressurizer must be maintained at or above a certain elevation to keep the pressurizer heaters submerged.

- There may be requirements that the pressure not be falling, to ensure that the operators have regained pressure control of the system (and so can safely begin to reduce injection flow).

These conditions generally cannot be met in an SO-1 transient until the stuck-open valve recloses. As previously noted, how quickly the operator responds after the throttling criteria are satisfied has a significant effect on whether the system repressurizes. Our model considers three possibilities for operator action: 1 minute after the throttling criteria are met, 10 minutes after the throttling criteria are met, and never (no throttling).

The information in Figure 8-26 through Figure 8-30 demonstrates that operator action must be very rapid to prevent the primary from returning to full system pressure for at least some period of time. In all of our analyses, throttling 10 minutes after the throttling criteria were met was too late to prevent rapid repressurization shortly after valve reclosure. When operators throttled 1 minute after the throttling criteria were met and the transient was initiated from full power, the rate of repressurization was sometimes reduced or the time of repressurization delayed, but full system pressure was ultimately regained. It was only in cases where operators throttled within 1 minute *and* the transient initiated from HZP that the operator action prevented system repressurization[§§§§]. This effect of power level on the repressurization response occurs because for HZP there is less heat in the system initially, and because the system is colder at the time of valve reclosure. Pressure and temperature are linked, so the need to heat up the colder water and having less heat to do so inhibits the sudden repressurization.

Certain plant-specific features also influence the effectiveness of operator action. Comparing the results for Oconee (Figure 8-26 and Figure 8-27) and with those for Beaver Valley (Figure 8-28 through Figure 8-30) reveals that, for a fixed throttling time, repressurization is delayed somewhat longer at Beaver Valley than at Oconee. This is a direct consequence of the differences in PORV mass flow rate (65% greater at Beaver Valley) and differences in the injection water temperature (20°F (11°C) colder because of the reduced thermal energy in the RCS (of Beaver Valley relative to Oconee) at the time of value reclosure. Consequently, a given throttling action will be more effective in preventing repressurization at Beaver Valley because throttling limits the reintroduction of thermal energy to the primary, thereby delaying the time at which water solid conditions, and therefore repressurization, occur. It should, however, be noted that these plant-specific differences do not alter significantly the risk-significance of the transient because their most important feature is the return to full system pressure (or not), not small (5–10 minute) variations in when return to full system pressure occurs. Section 8.5.3.4 discusses the risk-significance of SO-1 transients in greater detail.

8.5.3.3.4 Other Factors

In principle, factors other than the time of valve reclosure, the power level at transient initiation, and the timeliness of operator throttling of HPI can affect the TH response of the plant to an SO-1 transient. These factors can include, for example, seasonal variations, more than one valve sticking open, less than the total number of valves that stuck-open reclosing, valves that only partially stick open, and so on. We considered a number of these factors (see Table A.3 of Appendix A), but found their combined likelihood and consequence to be very small relative to the three factors discussed here in detail.

[§§§§] Figure 8-30 (bottom graphs, transient 121) illustrates one case for Beaver Valley at variance with this trend. In this case, rapid operator action has significantly delayed repressurization, but has not stopped it. However, this long delay before repressurization occurs permits considerable warming of the water in the primary system, which reduces significantly the probability of vessel failure. Thus, significant delay of repressurization is nearly as effective as preventing repressurization entirely.

8.5.3.3.5 Plant-Specific Effects on SO-1 Transients

In Sections 8.5.3.3.1 through 8.5.3.3.3, attention focused on transients in Oconee and in Beaver Valley because these plants modeled first and, consequently, the most detailed parametric study was performed on these plant. The plant-specific effects of vent valves, PORV mass flow rate, and injection water temperature have already been discussed. Certain combinations of events were eliminated from the later analyses of Palisades because the insights gained from earlier analysis suggested that the eliminated transients contributed very little or nothing at all to the overall PTS risk. Nonetheless, it is important to assess the degree to which the observations made in Sections 8.5.3.3.1 through 8.5.3.3.3 based on Oconee and Beaver Valley apply to Palisades. Figure 8-31 shows that the cooling rate in the Palisades transient initiated from HZP is less than that at either Oconee or Beaver Valley because the low-heat HPSI pumps at Palisades don't inject as much water as the high-head HPSI pumps at Beaver Valley and Oconee. Nonetheless, this plant-to-plant difference does not alter the trends noted in Sections 8.5.3.3.1 through 8.5.3.3.3 based on Oconee and Beaver Valley results (e.g., HZP transients cool more rapidly than full-power transients, only rapid operator actions taken for transients initiated under HZP conditions can prevent (or significantly delay) repressurization, etc.).

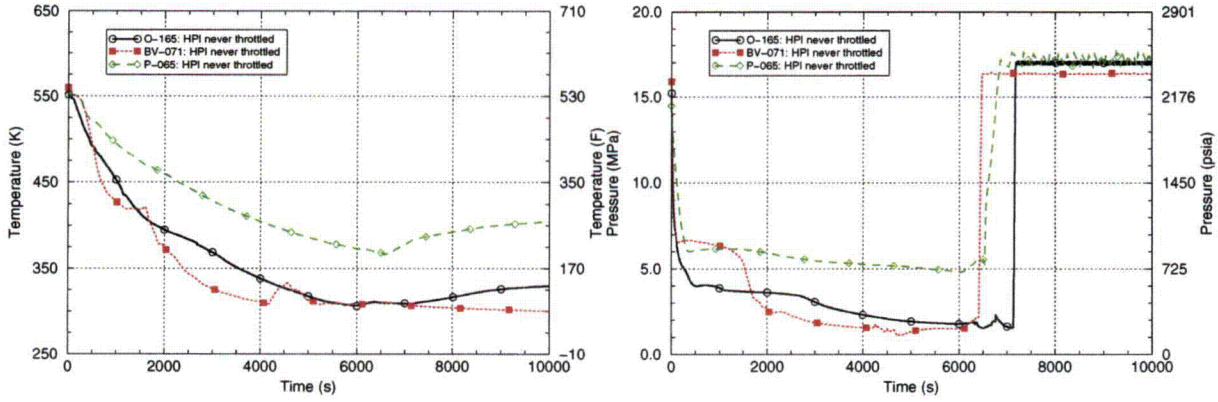

Figure 8-31. Comparison of SO-1 transients between different plants for transients initiated from HZP conditions, valve reclosure after 6,000 sec., and no HPI throttling

8.5.3.4 Estimates of Vessel Failure Probability

8.5.3.4.1 General Observations

In this section, we examine the effect that the time of valve reclosure, the power level at transient initiation, and the timeliness of operator throttling of HPI have on estimated values of CPTWC and on the predicted time of vessel failure during the transient. In Table 8.10, we examine the Oconee transients illustrated in Figure 8-26 and in Figure 8-27 focusing on various indicators of transient severity (i.e., cooling rate, if repressurization occurs or not, and the temperature at the time of repressurization), as well as the CPI, CPTWC, and time of failure values estimated by FAVOR. The following observations follow from the information in the table (these observations also apply to SO-1 transients at other plants):

Table 8.10. Transient severity indicators and estimated values of CPTWC for Oconee at Ext-Ob embrittlement conditions

HPI Throttling	Item	Transient Initiated from Full Power		Transient Initiated from HZP	
		Valve Recloses after 3,000 sec	Valve Recloses after 6,000 sec	Valve Recloses after 3,000 sec	Valve Recloses after 6,000 sec
Never	**Transient #**	**149**	**109**	**168**	**165**
	Average cooling rate over first 2,000 seconds (°F/hr)	308	308	486	486
	Time of repressurization (seconds)	4200	7100	4000	7100
	Temperature at repressurization (°F)	390	270	180	90
	Conditional probability of crack initiation (CPI)	0	1.83E-07	1.10E-04	1.24E-04
	Conditional probability of through-wall cracking (CPTWC)	0	1.83E-07	1.09E-04	1.24E-04
	Time of most failures (seconds)	#N/A	7140	4080	7200
10 minutes after throttling criteria satisfied	**Transient #**	**115**	**113**	**124**	**122**
	Average cooling rate over first 2,000 seconds (°F/hr)	308	308	486	486
	Time of repressurization (seconds)	4200	7100	4050	7100
	Temperature at repressurization (°F)	390	270	190	90
	Conditional probability of crack initiation (CPI)	0	1.42E-07	9.38E-05	1.44E-04
	Conditional probability of through-wall cracking	0	1.31E-07	9.37E-05	1.44E-04
	Time of most failures (seconds)	#N/A	7140	4140	7260
1 minute after throttling criteria satisfied	**Transient #**	**114**	**112**	**123**	**121**
	Average cooling rate over first 2000 seconds (°F/hr)	308	308	486	486
	Time of repressurization (seconds)	4000 – 4400	7100 - 7800	None	None
	Temperature at repressurization (°F)	400 – 440	300 - 405	#N/A	#N/A
	Conditional probability of crack initiation (CPI)	0	0	2.06E-07	2.06E-07
	Conditional probability of through-wall cracking	0	0	1.28E-08	1.28E-08
	Time of most failures (seconds)	#N/A	#N/A	1620	1620

- The occurrence of repressurization does not lead to a non-zero probability of vessel failure unless the temperature of the vessel at the time of repressurization is low enough. The information in Table 8.10 substantiates the general observation that the vessel temperature must be below 400°F (204°C) to produce a non-zero value of CPTWC.
- If a failure occurs, it most often happens between 5 and 20 minutes after the time of valve reclosure, closely following the time of repressurization.
- If repressurization occurs and a crack initiates, the initiated crack fails the vessel almost every time (i.e., the CPTWC is equal to or only slightly less than the CPI). This crack initiation/through-wall crack propagation behavior contrasts sharply with that associated with primary side pipe breaks (see Figure 8.21) where only 5–10% of initiated cracks propagated through-wall. The combination of thermal stresses and pressure in SO-1 transients makes cracks, once initiated, much more likely to propagate all the way through the RPV wall.
- SO-1 transients initiated from HZP conditions have CPTWC values that are ~1000 times higher than the same transient initiated from full-power conditions, this occurring as a consequence of the faster cooling rates and lower temperatures achieved during transients initiated from HZP.
- Valve reclosures after 6,000 seconds exhibit slightly higher CPTWC values than valve reclosures at 3,000 seconds. The effect of higher thermal stresses (for 3,000-second valve reclosures) seems to approximately offset the effect of lower toughness (for 6,000-second valve reclosures).
- For transients initiated from HZP, operator action within 1 minute of reaching the throttling criteria prevents a return to full system pressure, thereby reducing the CPTWC by a factor of ~10,000 relative to the CPTWC generated by repressurization.

8.5.3.4.2 Influence of Operator Actions

The final observation made in the preceding section indicates the potentially significant influence of operator action on the risk-significance of the transient. Consequently, in this section we review the basis for the probabilities assigned to represent the likelihood of operator action in response to this type of transient.

The probabilities assigned to reflect the likelihood of operator action (throttling HPI in this case) after certain times were established based on the expert views of three PRA analysts, with the individual analyst's judgments averaged to provide the consensus view used in our models [***Kolaczkowski-Oco, Whitehead-BV, Whitehead-Pal***]. Table 8.11 summarizes the factors that both favor and impede successful throttling considered by these analysts in formulating their opinions. Table 8.11 also provides the mean probabilities for operator action taken from the consensus distribution. These numbers reflect the analysts' view that throttling within 1 minute of meeting the throttling criteria is somewhat more likely in Oconee than in Beaver Valley, a difference motivated mostly by differences in the simulator observations and procedures followed at the different plants. The numerical throttling probabilities for Palisades are somewhat different from those of Oconee and Beaver Valley because of differences in hardware. At Palisades, HPSI can only charge to approximately 1,250 psi while pressurization between 1,250 psi and full system pressure is achieved via charging pumps. The analysts' took the view that successful throttling of HPSI was very unlikely, whereas successful throttling of charging pumps was very likely.

The plots of pressure *vs.* time (see for example Figure 8-26 and Figure 8-27) indicate that HPI must be throttled within 1 minute of meeting the throttling criteria to prevent repressurization to full system pressure for a HZP transient. Thus, in our model, operators have a 68% chance of preventing repressurization in Oconee, and a 40% chance in Beaver Valley (see Table 8.11).

Our model for Palisades deviates from that suggested by the PRA information in Table 8.11. While the PRA information suggests that repressurization to 1,250 psi is certain and further repressurization is unlikely (happening only 1 time out of 100, on average), the TH sequences selected to represent stuck-open valve transients for Palisades credit *no* operator actions[*****] and, so, all have repressurization to full system pressure. Thus, the TH sequences run and passed to PFM for analysis reflect the following operator action credits for successful throttling of HPI:

- **Oconee** operators successfully throttle HPI and, thereby, prevent return to full system pressure (on average) 68% of the time, provided that the transient initiates from HZP. Since approximately 20% of SO-1 transients occur under HZP conditions, this means that at Oconee operators prevent return to full system pressure for approximately 14% of SO-1 transients.
- **Beaver Valley** operators successfully throttle HPI and, thereby, prevent return to full system pressure (on average) 40% of the time, provided that the transient initiates from HZP. Since approximately 20% of SO-1 transients occur under HZP conditions, this means that at Beaver Valley operators prevent return to full system pressure for approximately 8% of SO-1 transients.
- **Palisades** operators never successfully throttle HPI; therefore, all stuck-open valve transients return to full system pressure once the valve recloses.

These observations indicate that while reasonable and appropriate credit for operator actions has been included in the PRA model, the actual influence of these credits on the estimated values of vessel failure probability attributable to SO-1 transients is small because the operator actions credited only prevent repressurization when SO-1 transients initiate from HZP conditions. Complete removal of operator action credits from the model changes the total risk associated with SO-1 transients only slightly.

[*****] The Palisades model does not subdivide the PRA bins to account for "credit" vs. "no credit" because of our understanding (at the time the model was built) that the estimated TWCF values would be sufficiently low even with this implicit conservatism.

8.5.3.4.3 Applicability of these Findings to PWRs in General

While the information presented in this section pertains specifically to the three plants analyzed, the following factors suggest that these results can be used with confidence to assess the risk of vessel failure arising from pipe break transients for PWRs *in general.*

(1) A major contributor to the risk-significance of SO-1 transients is the return to full system pressure once the valve recloses. The operating and SRV pressures of all PWRs are similar.

(2) While our model includes reasonable and appropriate PRA credits for operator action to throttle HPI, these credits have only a small effect on the estimated probability of vessel failure because the operator actions credited only prevent repressurization when SO-1 transients initiate from HZP conditions. Complete removal of operator action credits from the model changes the total risk associated with SO-1 transients only slightly.

At an equivalent embrittlement level, the TWCF is fairly consistent between the three plants modeled. As a direct consequence of these factors, the TWCF attributable solely to stuck-open primary side valves that later reclose is reasonably consistent from plant-to-plant (see Figure 8.32). In Chapter 9, we discuss the applicability of these results to PWRs *in general* in greater detail.

Table 8.11. Mean operator action probabilities in our modeling of SO-1 transients

Plant	Factors that favor successful throttling	Factors against successful throttling	Mean Probability of successful throttling within *x* minutes after throttling criteria is satisfied		
			x = 1 minute	*x* = 10 minutes	*x* = never (no throttling)
Oconee	Crew is in loss of subcooling procedure (EP-501). Procedure contains many cautions on PTS	Crew might have adopted a LOCA mindset and, therefore, not be attentive to the possibility of rapid repressurization.	68%	27%	5%
	Simulator observations confirm that crews are sensitized to PTS, and that they carefully monitor PTS parameters.	Emergency safeguards logic must be reset before HPI can be throttled, so throttling might be delayed while logic is being reset.			
	High pressure alarms would indicated the need to throttle HPI	Crew might not immediately throttle if they perform additional investigation to confirm that the event they are responding to is a stuck-open valve (for which throttling is appropriate) vs. a pipe break (for which throttling is not appropriate.			
	Crew would be alerted to changing plant conditions by the slow pressure rise that follows valve reclosure and precedes the rapid pressure increase.				
Beaver Valley	Before valve reclosure the crew has successfully stabilized a SLOCA, and they remain in a SLOCA condition until the valve recluses. SLOCA procedures make it reasonable to expect that the crew is thinking about PTS and is carefully monitoring plant parameters.	Simulator observations suggest that the crews do not have a sense of urgency associated with throttling/terminating HHSI. Rather, they trust that their procedures will tell them to throttle in time.	40%	56%	4%
	Simulator observations confirm that procedures are attended to and the crew carefully monitors critical parameters.	Crew might have adopted a LOCA mindset and therefore not be attentive to the possibility of rapid repressurization.			
		Emergency safeguards logic must be reset before HPI can be throttled, so throttling might be delayed while logic is being reset.			
		Crew might not immediately throttle if they perform additional investigation to confirm that the event they are responding to is a stuck-open valve (for which throttling is appropriate) vs. a pipe break (for which throttling is not appropriate.			
Palisades	**Throttling of the charging system (pressurizes from 1,250 psi to full system pressure)** is very likely because it is a simple action that is linked procedurally to securing HPSI.	**Throttling of HPSI (pressurizes to 1,250 psi)** is unlikely because the time available in which to throttle is very short.	0% for throttling HPSI within 5 minutes		100% for never throttling HPSI
			99% for throttling charging system within 5 minutes		1% for never throttling charging system

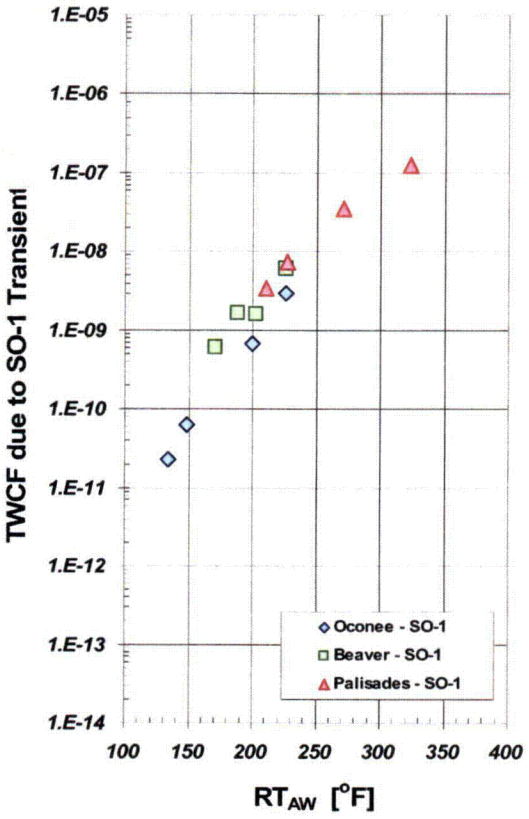

Figure 8.32. The TWCF attributable solely to stuck-open valves on the primary side that later reclose

8.5.3.5 Comparison with Previous Studies

8.5.3.5.1 As Reported by [Kirk 12-02]

Previously, we reported that stuck-open valves on the primary side were dominant contributors to TWCF only in Oconee; in both Beaver Valley and Palisades, the contribution of such transients was 20% or less [***Kirk 12-02***]. Figure 8-11 and Figure 8.32 demonstrate that stuck-open valves on the primary side now contribute significantly to the TWCF of all three plants. This change results from an inadequacy in our previous approach to determining the group of transients we use in FAVOR to represent the behavior of the plant. Previously, we performed our first FAVOR calculation for each plant for a highly embrittled condition, determined which transients contributed ~1% or more to the TWCF, and conducted analyses at lower embrittlement levels using only this limited set of transients. As shown in Figure 8-11, our previous filtering strategy eliminated transients that provide significant contributions to PTS risk at lower embrittlement levels. Therefore, in this study, FAVOR analyses were performed on all transients at all embrittlement levels.

8.5.3.5.2 Studies Providing the Technical Basis of the Current PTS Rule

In analyses performed to establish the technical basis for the current PTS Rule, the three plants analyzed were Oconee, H.B. Robinson, and Calvert Cliffs. Analyses of Oconee and H.B. Robinson (which were performed first) did not consider the class of scenarios referred to herein as SO-1 [ORNL 85b, ORNL 86]. The Calvert Cliffs analysis, which was the last analysis performed, considered the possibility of both PORV and SRV reclosures, although not to the level of detail achieved in the current study [ORNL 85a]. Furthermore, all valve reclosure cases were binned together in the Calvert Cliffs study, which made it impossible to characterize the effects of power level, valve reclosure time, and operator action as we have in this study. Putting everything into one bin usually produces a conservative characterization; however, not investigating or understanding how various factors influence transient severity can lead to nonconservatisms when significant effects are not recognized and, therefore, not modeled.

In the 1986 analysis of Calvert Cliffs, SO-1 transients were among the two most important PTS scenarios (the other being small LOCAs) for the Calvert Cliffs analysis. This is in contrast to the 1985–1986 findings for Oconee and H.B. Robinson, which found secondary failures (either MSLBs or secondary valve openings) to be most important.

With regard to frequency estimates for SO-1 transients, our estimates rely on data that are representative of current operating practice. These estimates are lower than those used in the 1980s.

8.5.4 Large Diameter Secondary Side or Main Steam Line Breaks

8.5.4.1 General Description of MSLB Transients

MSLB transients all begin with a break in one of the main steam lines. As main steam lines are large pipes with diameters of multiple feet, the steam generator rapidly blows down (loses steam through the break). Because of the break, the affected steam generator can no longer maintain pressure above that existing at the break location. The depressurization of the generator from its 860 psi (5.92 MPa) operating pressure to the pressure at the break location causes a temperature drop in the primary from 550°F (288°C) to the saturation temperature at the pressure that exists at the break location (212°F (100°C) if the break is outside of containment, ~250°F (~121°C) if the break is inside of containment because containment is pressurized to ~50psi (345 kPa) by the steam escaping from the break). The temperature inside the still sealed primary system tracks that of the broken steam generator because of the very large heat transfer area provided by the steam generator tubes. (That is, the primary and secondary systems are coupled, so the temperature in the primary rapidly approaches that of the largest heat sink, which in this case, is the broken steam generator.) Thus, the inventory in the primary circuit cools rapidly to the temperature of the water boiling in the broken steam generator (as previously mentioned, 212°F (100°C) if the break is outside of containment, ~250°F (~121°C) if the break is inside of containment) for all durations of interest *from a PTS perspective*[†††††]. As explained below, this is true despite the fact that both the makeup water to the primary and the feedwater to the faulted generator are supplied at temperatures far below the boiling point of water:

- The rapid cooling of the primary in response to the MSLB shrinks the primary system inventory, causing a pressure drop. To compensate for the pressure drop, the ESFAS (an automatic function) initiates safety injection, causing the HPI pumps to supply makeup water to the primary system. HPI flow then refills and repressurizes the primary system. Even though the makeup water is drawn from external tanks and, so, is injected at a temperature far below the range of 212°F (100°C) to ~250°F (~121°C), the temperature of the primary remains at or above that of the broken steam generator because the heat transfer area provided by the steam generator tubes is so large that it overwhelms the lower temperature of the makeup water. At a later time, operators may be allowed to throttle HPI injection.
- At very long times after the beginning of an MSLB transient, the temperature in the primary system approaches that of the feed water to the faulted steam generator, or about 100°F (38°), because the reactor is no longer generating enough heat to boil the water in the faulted generator. This drop to temperatures below 212°F (100°C) does not occur until several hours or more have passed, long after isothermal conditions have been achieved in the RPV.

The primary aim of operators responding to an MSLB is to isolate the break (that is, to stop the feed to the faulted generator and/or to stop the flow out of the break). The steps the operators take to achieve this goal depends on the location of the break relative to both the main steam isolation valve and the containment structure (see Figure 2.1 for the arrangement of major plant components and a definition of the terms used in the following description):

- Break downstream of the MSIV: In this case, the operators' response is simply to isolate the affected generator by closing both the FWIV and MSIV. This reseals the secondary system and ends the transient. At this point, the temperature of the steam

[†††††] When the primary remains at approximately isothermal conditions for a long period of time, the temperatures of the ID and the OD of the RPV become approximately equal. Under these conditions, there is no thermal stress and, consquently, no risk of vessel failure attributable to PTS.

generator is controlled by the temperature of the primary.

- Break upstream of the MSIV outside of containment: In this case, the break flow cannot be stopped by shutting the MSIV, so the operators close both the FWIV and MSIV to isolate the affected generator. Without feedwater, the generator eventually boils dry, and the unaffected generator becomes the primary heat sink, thereby ending the transient.
- Break upstream of the MSIV inside of containment: The operators' response to this event is the same as when the break is upstream of the MSIV and outside of containment: the FWIVs are closed, stopping feed to the faulted generator. However, the venting of steam from the break inside the containment structure increases pressure inside of containment, causing an "adverse containment" condition. As a result of the increase in pressure inside of containment, the ESFAS generates a containment isolation signal. This signal automatically isolates all containment penetrations that could (potentially) lead to a radioactive release; however, the source of cooling water to the RCPs is one of these penetrations. Without cooling water, the RCPs would seize, so operators must secure (stop) the RCPs. Without RCPs to circulate water in the cold leg, the mixing of cooler and hotter water in the downcomer reduces significantly, resulting in lower downcomer temperatures.

Given the relative length of pipe runs, the ruggedness of the piping, and the pipe support system, MSLBs are most likely to occur downstream of the MSIVs. Also, as was the case with stuck-open valve transients (see Section 8.5.3), MSLBs can occur from either full power or HZP conditions.

8.5.4.2 Model of this Transient Class

As detailed in Table A.4 of Appendix A, our modeling of MSLB transients includes delayed operator actions, such as the following examples:

- allowing feed to continue to the faulted steam generator for 30 minutes or indefinitely
- throttling HPI to the primary, but only 30–60 minutes after the throttling criteria have been met

The model also includes exacerbating equipment failures, such as the following:

- failure of MSIVs to close

Additionally, the model adopts physically unrealistic temperatures, such as:

- Most MSLBs in Beaver Valley and Oconee are assumed to occur inside containment (worst case). When a main steam line breaks inside of containment, the containment building is pressurized to ~50psi (345 kPa), which elevates the boiling point of water to ~260°F (127°C). However, our model does not account for pressurization of containment by the break flow, so the boiling point of the secondary (and, consequently, the minimum temperature in the primary) is 212°F (100°C). This lower temperature increases the severity of the thermal shock to which the RPV wall is subjected and reduces the RPV's resistance against this thermal shock.

This conservative modeling approach was taken because PFM calculations performed early in the project indicated that even with these conservative assumptions, the contribution of MSLB transients to the total vessel risk was very small relative to the contribution of primary side pipe breaks and stuck-open primary side valves. Further refinement of the MSLB model to achieve increased realism would only reduce the risk-significance of the transients, and this refinement was not viewed as being necessary. Consequently, when considering the results presented in the following sections, the reader is reminded to view them as representing an upper bound to the vessel integrity challenge actually posed by MSLB transients.

8.5.4.3 Relationships between System Characteristics and Thermal-Hydraulic Response

In this section, we examine the effects of a variety of factors on the pressure and temperature transients associated with MSLBs:

- Effect of plant power level at event initiation: Figure 8.33 and Figure 8.34 show the effect of an MSLB initiating from full power vs. HZP conditions. The initial cooldown rate associated with the HZP transients is more rapid than for the full-power transients expected as a result of a lack of heat in the system, but only slightly so. The rapidity of the cooldown caused by the large break area of the main steam line mitigates the potential cooling rate boost associated with transient initiation from HZP.
- Effect of break location: Figure 8.35 shows that MSLBs occurring inside containment experience considerably faster cooldown rates than when the break is outside of containment. As previously discussed, the break of a main steam line inside containment is expected to produce more rapid cooling of the downcomer because the RCPs will be shut down, resulting in less mixing of the hot and cold water in the downcomer.
- Isolation of feedwater flow: Figure 8.36 shows that failure to isolate feedwater flow allows temperatures in the primary to continue to drop because feedwater flowing to the affected generator is still steaming and, therefore, still cooling the primary.
- Timing of HHSI control: Safety injection flow initiates automatically following an MSLB to repressurize the primary. Figure 8.37 shows that when the operators throttle HHSI effects directly how long high pressures are maintained.

In terms of plant-specific effects on MSLB transients, B&W plants (Oconee) differ from other plants because of the much smaller steam generator volume in the B&W design than in Combustion Engineering or Westinghouse designs. Consequently, the blowdown from an MSLB at Oconee concludes almost instantaneously, whereas the blowdown in Beaver Valley and Palisades takes approximately 250 seconds. The rapid blowdown in Oconee produces a much more rapid cooling rate than in the other two plants, but the minimum temperature associated with this rapid cooling is so high (far above 400°F (204°C)) that the risk of vessel failure is very very low. Thus, the vessel failure probability estimates discussed in the following section arise almost exclusively from the non-B&W plants.

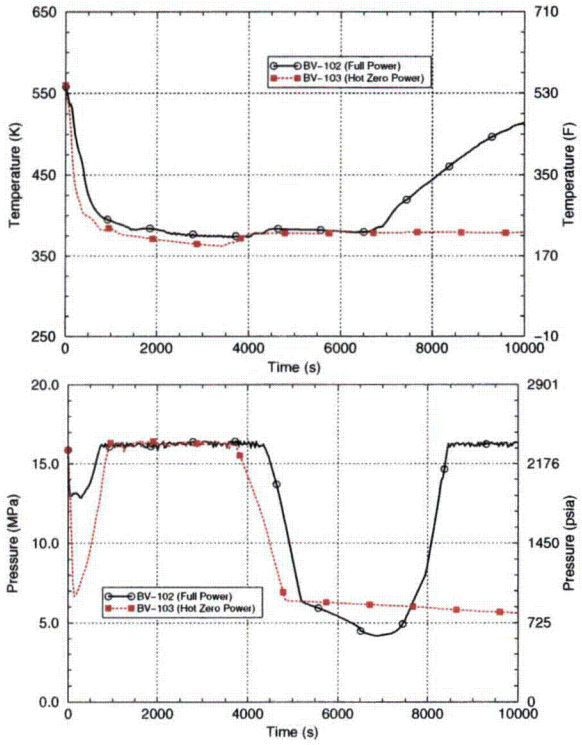

Figure 8.33. Power level effects on MSLB transients at Beaver Valley. Both breaks are in containment and have AUX feed continuing to the faulted generator for 30 minutes. The operator throttles HPSI 30 minutes after allowed.

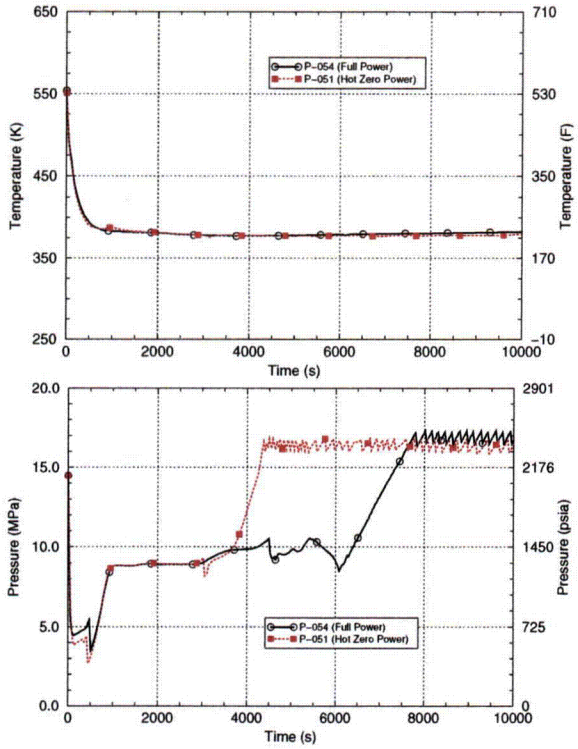

Figure 8.34. Power level effects on MSLB transients at Palisades. Both breaks are in containment and include failures of both MSIVs to close. The operator takes no actions to either isolate AUX feed or to throttle HPI.

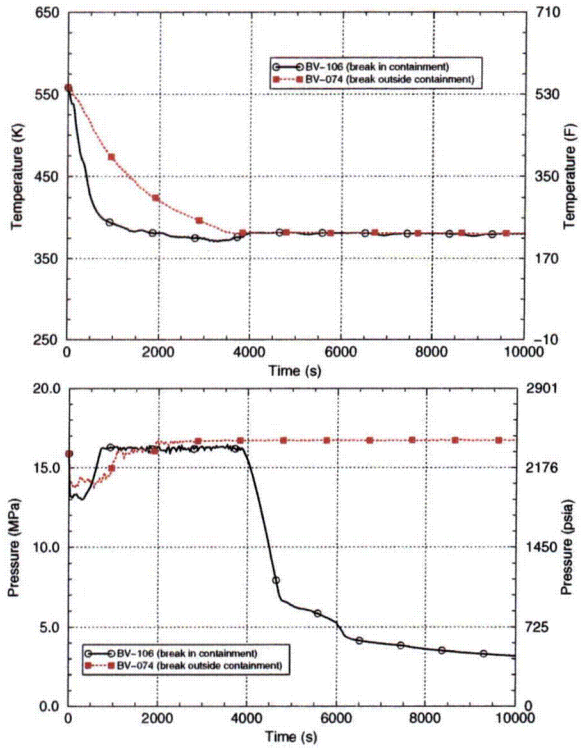

Figure 8.35. Break location effects on MSLB transients at Beaver Valley. Both breaks include continuous AUX feed and are initiated from full-power conditions. In transient 106, the operator controls HPSI 30 minutes after allowed.

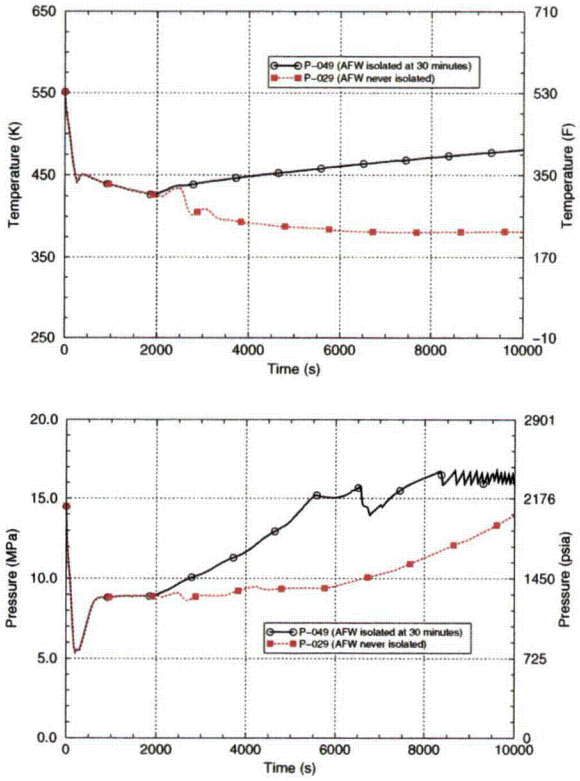

Figure 8.36. Break isolation effects on MSLB transients at Palisades. Both breaks occur inside containment and are initiated from HZP conditions.

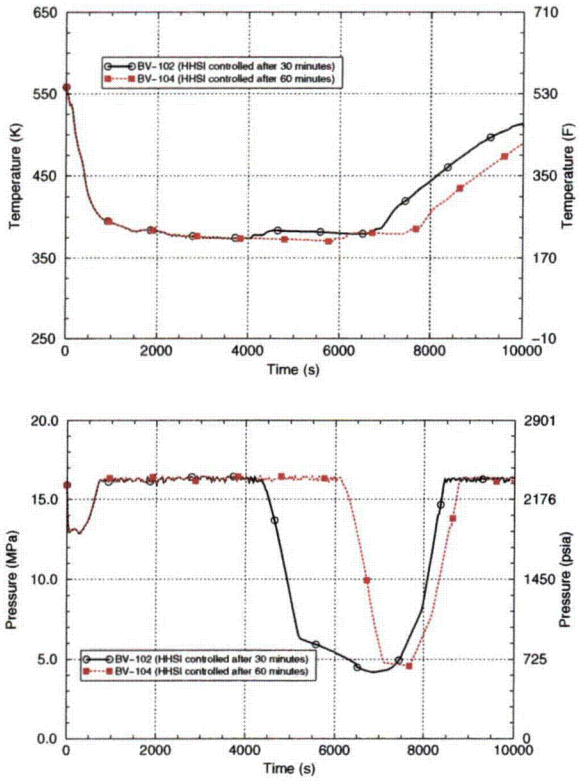

Figure 8.37. Effect of HHSI control on MSLB transients at Beaver Valley. In both breaks, AUX feed is isolated 30 minutes after the break occurs. Both breaks are initiated from full-power conditions.

8.5.4.4 Estimates of Vessel Failure Probability

8.5.4.4.1 General Observations

In the preceding section the effect of the following factors on the pressure and temperature transients associated with main steam line breaks was examined:

- effect of plant power level at event initiation
- effect of break location
- isolation of feedwater flow
- timing of HHSI control

All of the long-time effects (isolation of feedwater flow, timing of HSSI control) have no effect on the vessel failure probability because these factors influence the progression of the thermal-hydraulic transient after failure has occurred (*if* it occurs). In almost all of the transients discussed in the previous section, vessel failure is predicted to occur between 10 and 15 minutes after transient initiation (rare cases have failures as late as 30 minutes after initiation). Thus, operator actions (as modeled) cannot affect vessel failure probability. Only factors affecting the initial cooling rate can have any influence on CPTWC values. These factors include the plant power level at event initiation and the location of the break (inside or outside of containment). As shown in Figure 8.33 and Figure 8.34, the plant power level has only a slight influence on the initial cooling rate, and (so) only a slight influence on the CPTWC (less than a factor of 2 increase). The location of the break (inside or outside of containment, see Figure 8.35) has a somewhat larger effect. For this comparison, the break inside containment has a CPTWC ~3 times higher than the break outside of containment.

Figure 8.38 presents a distribution describing the percentage of cracks initiated by MSLB transients that subsequently propagate through-wall. The large thermal component to the loading at the time of failure (10–15 minutes into the transient) allows a large percentage of the initiated cracks to experience a stable arrest. However, because there is a pressure component to MSLB transients (the relative proportion of pressure loading to thermal loading depends on the time of failure experienced by a particular simulation), in some situations, once the cracks initiate they almost always propagate entirely through the vessel wall.

8.5.4.4.2 Applicability of these Findings to PWRs in General

These results can be applied with confidence to PWRs in general for the following reasons:

- Even though our model of MSLBs is intentionally conservative, the estimated conditional failure probabilities are low (10^{-9} to 10^{-5}); realistic estimates can be expected to be lower (perhaps considerably so) because of the physically unrealistic aspects of our modeling (e.g., we have not modeled the pressure buildup inside of containment attributable to the MSLB, which would raise the minimum temperature of the primary system, thereby reducing the severity of the transient).
- Operator actions (as modeled) have no influence whatsoever on the estimated failure probabilities reported here.
- The part of the MSLB transient responsible for the reported failure probabilities is the rapid initial cooldown caused by depressurization of the secondary through the break. Since main steam lines are so large, the rapidity of this cooldown should not vary much from plant-to-plant, nor should it be influenced by other factors (plant power level at event initiation, operator actions, etc.)

Figure 8.39 compares the portion of the TWCF attributable to MSLBs at the three study plants. Based on the factors discussed above, the plant-to-plant consistency in the level MSLBs challenge is expected.

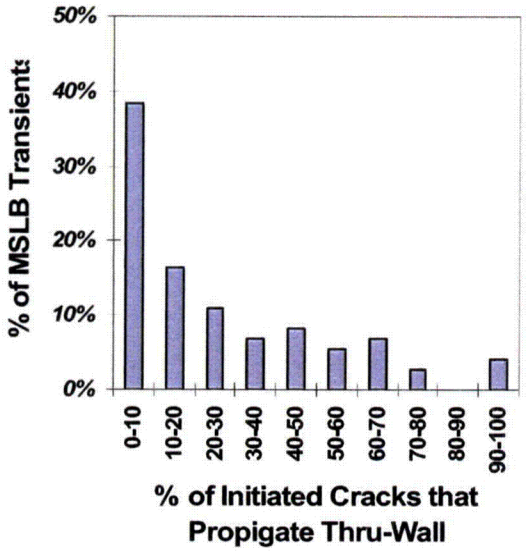

Figure 8.38. Percentage of initiated cracks that propagate through-wall for MSLB transients

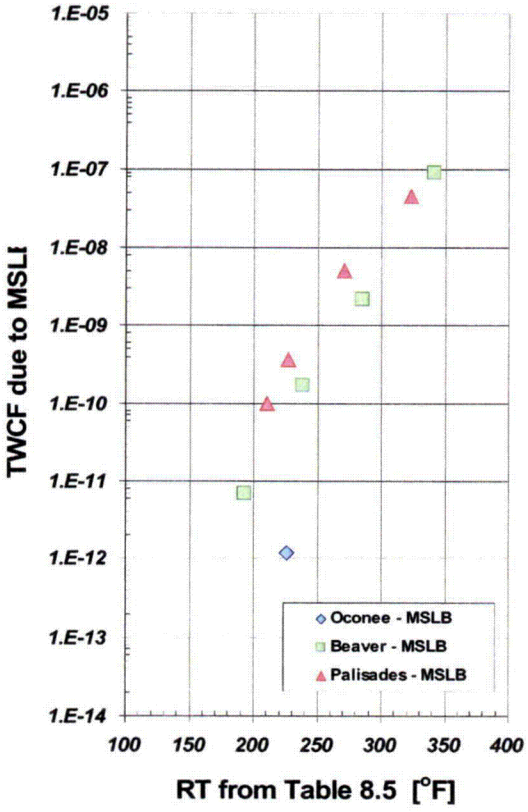

Figure 8.39. TWCF attributable to MSLB transients

8.5.4.5 Comparison with Previous Studies

8.5.4.5.1 As Reported by [Kirk 12-02]

While the specific numerical results reported herein differ from those in our interim report [***Kirk 12-02***], the general trends discussed in this section have not changed substantively from those reported earlier.

8.5.4.5.2 Studies Providing the Technical Basis of the Current PTS Rule

In analyses performed to establish the technical basis for the current PTS Rule three plants were analyzed: Oconee, H.B. Robinson, and Calvert Cliffs [ORNL-86, ORNL-85b, ORNL-85a, respectively]. Analyses of Oconee and H.B. Robinson revealed secondary failures (either MSLBs or secondary valve openings) to be the most dominant class of transient (following the "residual" categorization in Oconee), in contrast to the information reported here, which shows the contribution of MSLBs to be much less than that associated with either primary side pipe breaks or with stuck-open primary side relief valves that reclose after a significant cooling period. (See Figure 8.40 for a summary of current TWCF predictions divided by transient class.)

In the previous analyses of Oconee and H.B. Robinson, MSLBs ***had to be*** more risk-significant than either (1) medium–large diameter pipe breaks or (2) stuck-open relief valves on the primary side that reclose after a significant cooling period simply because these classes of transients were not modeled in the earlier studies. At the time of these previous analyses, the prevalent technical belief regarding vessel failure was that *"rapid depressurization will severely limit the potential for a vessel failure"* [ORNL-85b]. Consequently, no breaks larger than 2.5-in. (6.4-cm) in diameter were considered in these analyses. Further, while stuck-open primary side valve scenarios were analyzed, and *early* isolation of stuck-open pressurizer pilot-operated relief valve scenarios were also examined, late reclosures of primary

side valves after significant cooling has occurred were not analyzed in the Oconee and H.B. Robinson analyses.

In the Calvert Cliffs analysis [ORNL-85a], the LOCAs considered included pipe diameters only up to 3-in. (7.6-cm). However, for Calvert Cliffs, "late" reclosures of stuck-open pressurizer relief valves (i.e., reclosures occurring 1½ hours into the transient) were analyzed. In the 1985 ORNL analysis of Calvert Cliffs, such a reclosure event (similar to those we analyzed in this updated study), especially at HZP, was found to be the highest or among the top three highest "dominant risk sequences" depending on the EFPY of the vessel (including being more important than steam line breaks, as we have found in this updated study). Hence, the early Calvert Cliffs analysis [ORNL-85a] shows trends similar to those reported herein.

Additionally, even though our treatment of MSLBs has been conservative, it is still more refined than in previous studies largely because of the evolution of computer capabilities and the ability to analyze many more scenarios more completely today than was available more than 20 years ago. For example, the secondary side break models adopted in the previous analyses often represented a full spectrum of secondary side breaks from small breaks and valve opening scenarios through a break of the main steam line using the bounding pressure/temperature *vs.* time transient characteristic of an MSLB. This approach overestimated both the severity of many secondary side events and the frequency of their occurrence. Furthermore, many of the TH profiles (e.g., for downcomer temperature vs. time) were based, in part, on extrapolations of the early timing profile trends and other hand calculations that tended to conservatively predict the degree of cooling in the downcomer region.

Based on the above along with advances in our technical understanding and modeling of cooling scenarios, the associated thermal-hydraulics, and vessel fracture mechanics, it is understandable that the early belief that secondary failures dominate PTS risk has changed to that provided in this study.

8.5.5 Stuck-Open Valves on the Secondary Side (SO-2)

8.5.5.1 General Description of SO-2 Transients

The steam supply system contains several valves to control pressure. All of these valves have opening areas much smaller than the main steam line, so opening any one (or even several) of them does not produce nearly as rapid a depressurization rate (and consequently cooling rate) as that associated with MSLB transients (see Section 8.5.4). The general progress of a transient associated with one (or many) secondary side valves sticking open is, therefore, similar to that described for MSLBs (see Section 8.5.4.1), with the exception that all of these valves are outside of containment, so the considerations associated with a break in containment discussed in Section 8.5.4.1 do not apply to stuck-open secondary side valves.

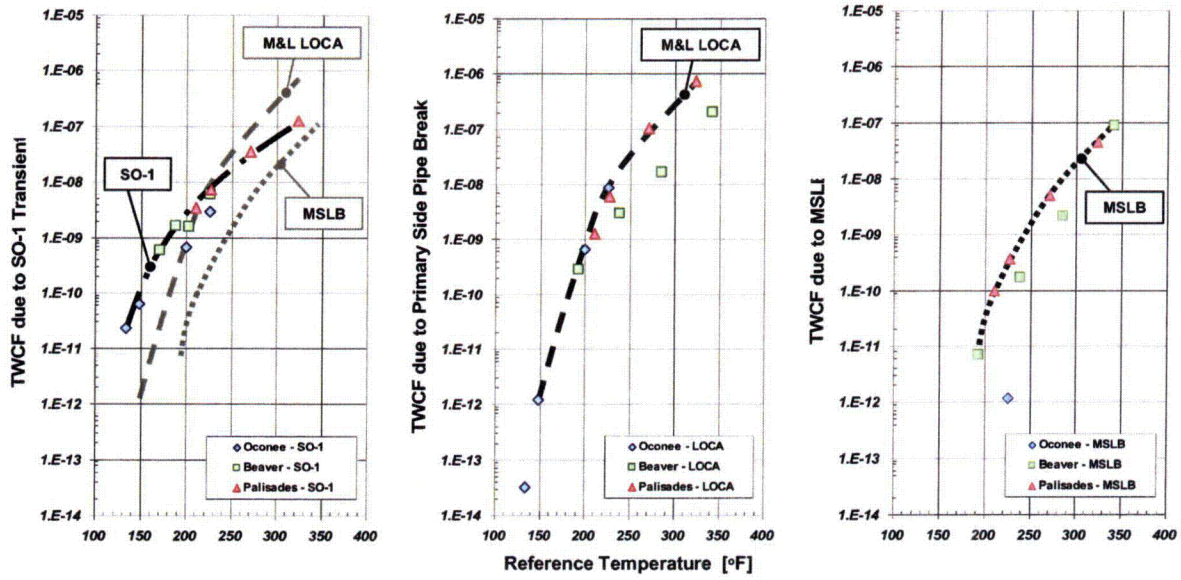

Figure 8.40. Comparison of TWCF attributable to primary side stuck-open valves, primary side pipe breaks, and MSLBs. Note that the contribution of MSLBs here overrepresents their actual contributions to TWCF because of conservatisms in their modeling. On each graph, an upper-bound curve is hand drawn to the data originally presented in Figure 8.23, Figure 8.32, and Figure 8.39. On the left hand graph, all three upper-bound curves are placed together for easy comparison.

8.5.5.2 Model of this Transient Class

Tables A.5 and A.6 in Appendix A detail the transients analyzed as SO-2s. The transients in Table A.5 include the sticking open of *all* main steam safety valves (MSSVs) or turbine bypass valves (TBVs). The opening of all TBVs is an action taken to depressurize the secondary in response to complete loss of both main and emergency feedwater to a single steam generator. Different scenarios are selected to assess the effect of smaller breaks of the steam line than those discussed in Section 8.5.4, including all MSSVs sticking open, one MSSV sticking open, or an ADV sticking open. The transients in Table A.6 begin with the trip of the reactor/turbine. This is followed by one or two of the TBVs or ADVs being opened to purge energy from the system. If these valves stick open, an overcooling transient begins. In both sets of transients (Table A.5 and A.6), the effects of operator actions and plant power level at event initiation are modeled.

Our modeling of this class of transients is not "best estimate." Rather, we have tended to examine bounding cases. This approach was motivated by the knowledge that MSLB transients (which are more severe than SO-2 transients because of the larger break area) contribute very little to the overall TWCF. (See Figure 8.41 for a comparison of cooldown rates of all transient classes.) Consequently, detailed analysis of SO-2 transients was not viewed as being warranted. When considering the results presented for SO-2 transients, the reader is reminded (1) to view them as representing an upper bound to the vessel integrity challenge actually posed by SO-2 transients, and (2) to *expect* a greater apparent risk-significance of SO-2 transients in Palisades than in the other two plants as a result of the lack of refinement in the Palisades model of this transient class.

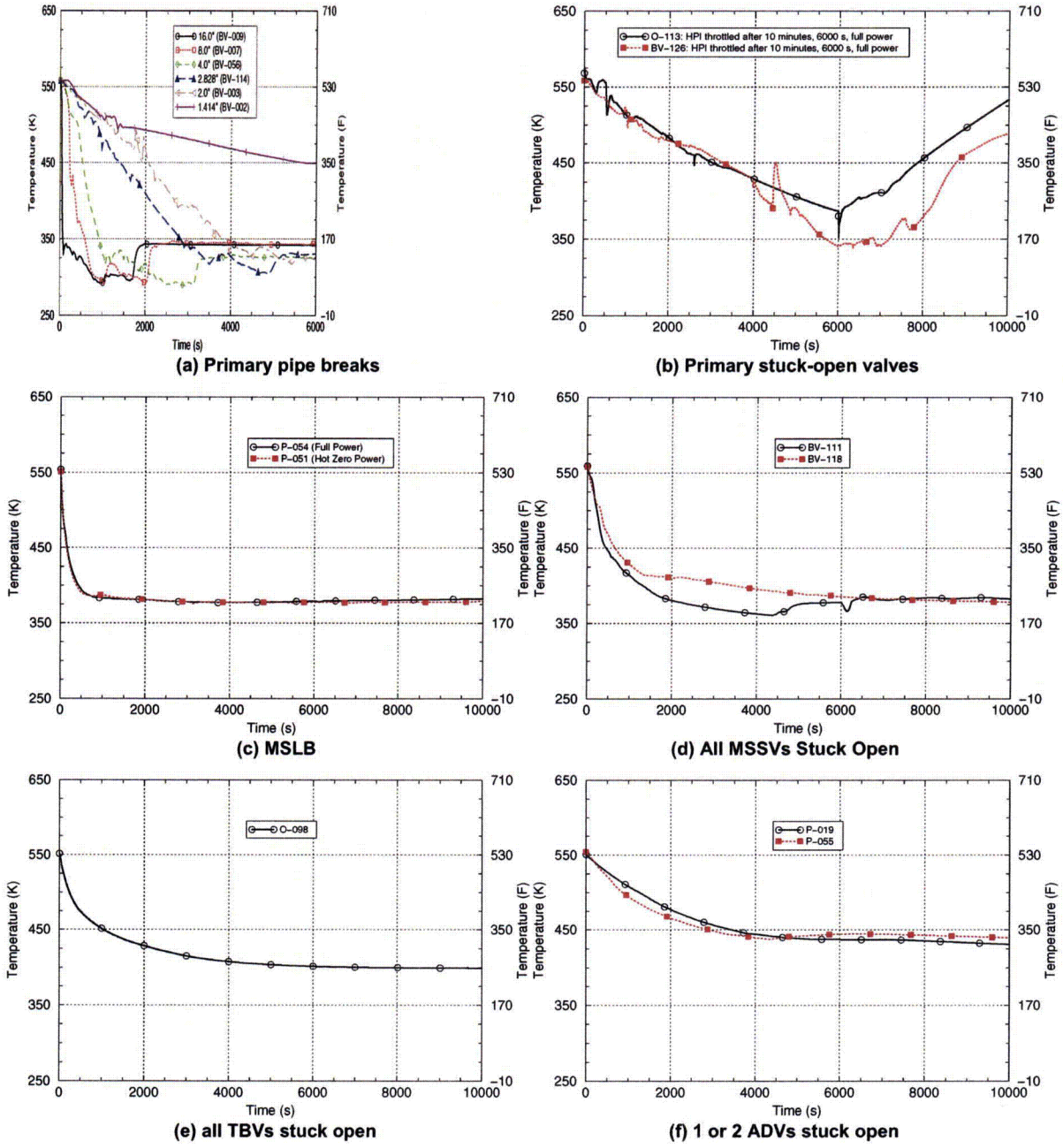

Figure 8.41. The cooldown rate of various SO-2 transients, graphs (d) through (f), compared to MSLBs, graph (c), and primary side transients, graphs (a) and (b).

8.5.5.3 Relationships between System Characteristics and Thermal-Hydraulic Response

As illustrated in Figure 8.41, the cooling rate associated with SO-2 transients is slower than for MSLBs and, in general, decreases with decreasing valve opening area. Additionally, while the minimum temperature experienced when MSSVs are open is the same as during an MSLB, the minimum temperature produced by opening TBVs or ADVs is higher (nearly 100°F (55.5°C) higher), further redacting the severity of these transients relative to MSLBs. Figure

8.42 through Figure 8.45 show both the temperature and pressure characteristics of a variety of different transients in the SO-2 category. These graphs show that for a number of different reasons (HHSI into the primary and failure to throttle same, AUX feed, etc.) SO-2 transients generally experience some (or even full) system pressure in the primary.

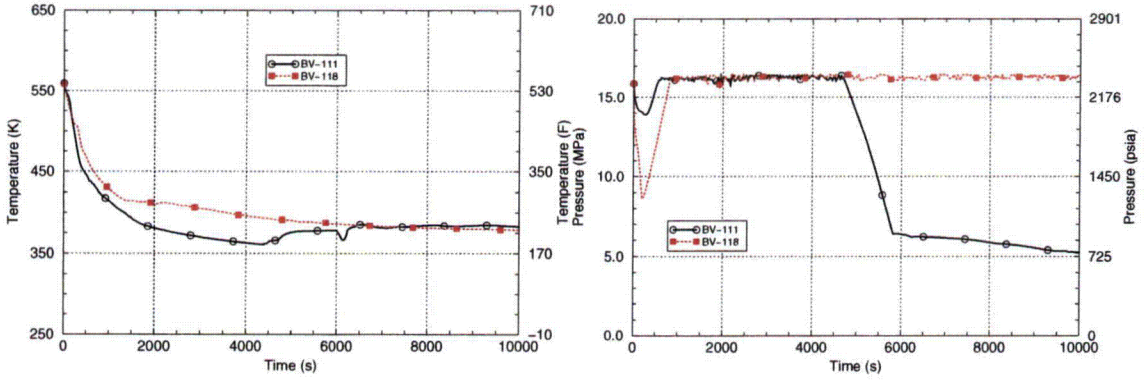

Figure 8.42. Small steam line break simulated by sticking open all MSSVs in steam generator A with AFW continuing to feed affected generator for 30 minutes. Beaver Valley transient 111 occurs at HZP, while Beaver Valley transient 118 occurs at full power.

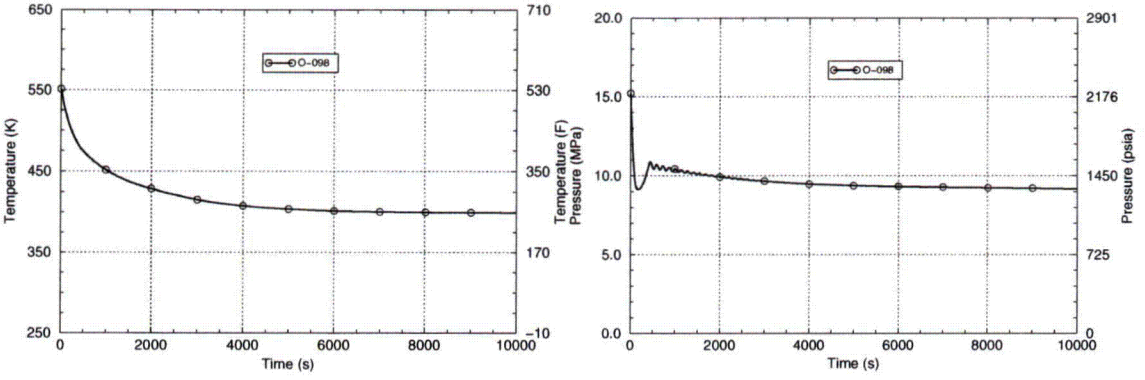

Figure 8.43. Reactor/turbine trip with loss of MFW and EFW in Oconee. Operator opens all TBVs to depressurize the secondary side.

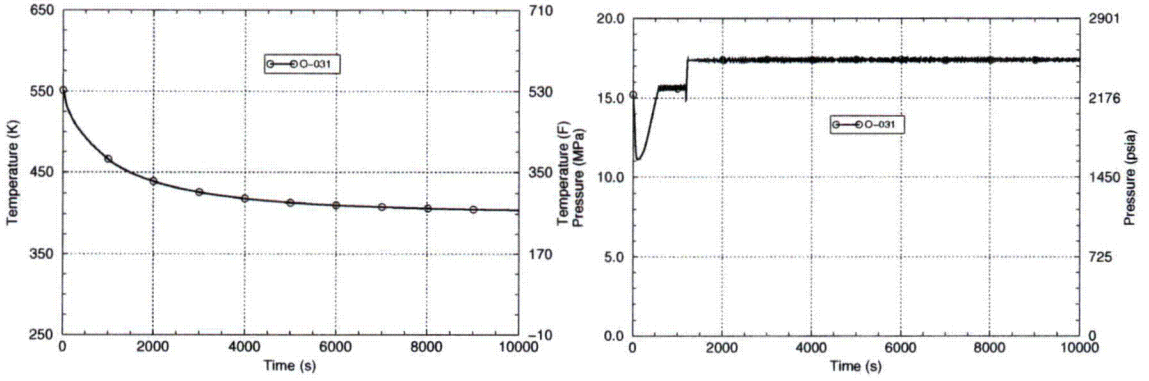

Figure 8.44. Reactor/turbine trip with two stuck-open safety valves in Oconee.

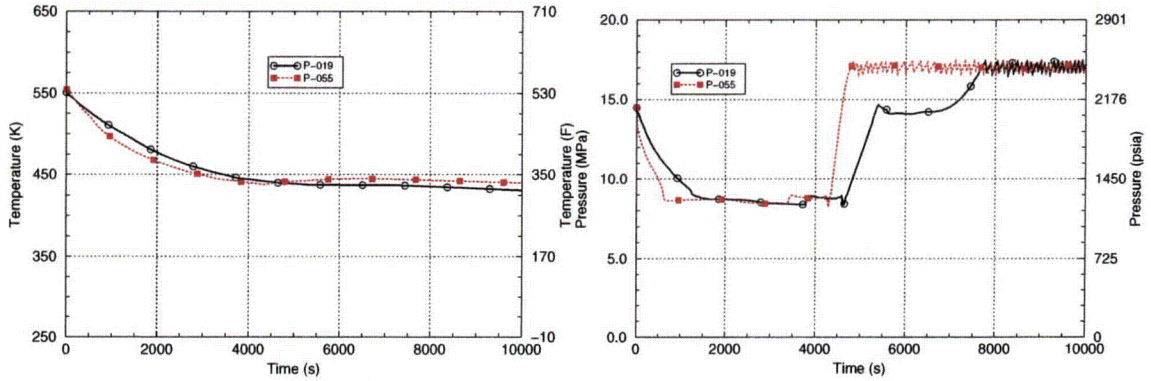

Figure 8.45. Reactor/turbine trip with one or two stuck-open ADVs (P-019 and P-055, respectively) in Palisades.

8.5.5.4 Estimates of Vessel Failure Probability

The CPTWC of SO-2 transients tends to be very low, consistent with the more gradual cooling rates caused by these transients relative to other transient classes (see Figure 8.41). Ranges of SO-2 CPTWC values for different transients are as follows (different plants are compared at roughly equivalent levels of embrittlement, see

Table 8.6):

- Many stuck-open valves: CPTWC ranges from E-13 to E-10.
- One or two stuck-open valves: CPTWC ranges from E-13 to E-7.

Comparing these values with the E-5 to E-4 CPTWC values associated with the significant transients in the dominant classes (primary side pipe breaks and stuck-open valves on the primary side) provides a perspective on the limited influence of SO-2 transients to the total TWCF estimated for a vessel. As stated earlier, it is only the conservative binning of Palisades transients, this leading to high estimates of bin frequencies (see section 8.5.5.2), that has led SO-2 transients to contribute non-negligibly to the percentage total TWCF in Palisades (see Figure 8-11). More refined analysis of SO-2 transients for Palisades would reduce their influence to the point of being immeasurable, as was the case for Beaver Valley and Oconee.

Two factors in our analysis suggest that these findings can be applied to PWRs in general:

- the conservative modeling of SO-2 frequencies in Palisades
- the fact that the CPTWC values that result from ***all*** secondary side valves sticking open produces values that are negligible (E-13 to E-10) relative to significant transients in the dominant classes (E-5 to E-4).

Section 9.3 provides further discussion of the similarities and differences between the SO-2 modeling employed here and the general conditions in the operating fleet.

8.5.5.5 Comparison with Previous Studies

8.5.5.5.1 As Reported by [Kirk 12-02]

While the specific numerical results reported herein differ from those in our interim report [***Kirk 12-02***], the general trends discussed in this section have not changed substantively from those previously reported.

8.5.5.5.2 Studies Providing the Technical Basis of the Current PTS Rule

In the preceding analysis of the Oconee plant [ORNL 86], relevant operator action HEPs were applied to a wide spectrum of scenarios (i.e., not so scenario-specific). This analysis used generic

probabilities for a limited number of operator events and did not consider all of the various times that we investigated. Thus, the preceding analysis of the Oconee plant for SO-2 transients should be viewed as being conservative relative to that reported herein. In the preceding analyses of Robinson and Calvert Cliffs [ORNL 85b, ORNL 85a], the HRA became more sophisticated, in that the HEPs were assigned on a more scenario-specific basis than for Oconee. However, these analyses still did not model different action times, as was done in our analysis. For these reasons, the preceding analysis of both Oconee and or H.B. Robinson for SO-2 transients should be viewed as being conservative relative to that reported herein.

Other generic factors contribute to the conservatism of the preceding analyses:

- Today, we have more industry experience, providing a larger data basis upon which to establish initiating event frequency estimates. The number of initiating events per year has declined since the earlier analyses were performed.
- Procedures and training have improved considerably.
- Modern PRA and HRA techniques have allowed us to do more refined analyses and model industry improvements.
- Increased computational ability has enabled finer subdivision of the challenges to the plant (more bins). This has considerably reduced the conservatism inherent to the binning process.

8.5.6 Other Transient Classes

Tables A.7 and A.8 in Appendix A summarize the transients analyzed in the following classes:

- feed-and-bleed
- steam generator tube rupture
- overfeeds
- mixed primary and secondary side failures

In all cases, the combination of the low probability of these events occurring with the low consequence of the event produces transients that are not risk-significant.

8.6 Summary

This chapter provides the results of plant-specific analyses of Oconee Unit 1, Beaver Valley Unit 1, and Palisades. In the following list, which summarizes the information presented in this chapter, the ***conclusions*** are shown in ***bold italics*** while supporting information is shown in regular type:

- ***The degree of PTS challenge for currently anticipated lifetimes and operating conditions is low.***
    - Even at the end of license extension (60 operational years, or 48 EFPY at an 80% capacity factor), the mean estimated through-wall cracking frequency (*TWCF*) does not exceed 2×10^{-8}/year for the plants analyzed. Considering that the Beaver Valley and Palisades RPVs are constructed from some of the most irradiation-sensitive materials in commercial reactor service today, these results suggest that, provided that operating practices do not change dramatically in the future, the operating reactor fleet is in little danger of exceeding either the limit on *TWCF* of 5×10^{-6}/yr expressed by Regulatory Guide 1.154 [RG 1.154] or the 1×10^{-6}/yr value recommended in Chapter 10, even after license extension.
- ***Mean TWCF values are in fact upper bounds.***
    - Because of the skewness characteristic of the *TWCF* distributions that arise as a result of the physical processes responsible for steel fracture, mean *TWCF* values correspond to the 90th percentile (or higher) of the *TWCF* distribution. Thus, the mean *TWCF* values we report in this chapter are appropriately regarded as upper bounds to the uncertainty distribution on TWCF.

- ***Axial flaws, and the toughness properties that can be associated with such flaws, control nearly all of the TWCF.***
  - Axial flaws are much more likely to propagate through-wall than circumferential flaws because the applied driving force to fracture increases continuously with increasing crack depth for an axial flaw. Conversely, circumferentially oriented flaws experience a driving force peak mid-wall, providing a natural crack arrest mechanism. It should be noted that crack initiation from circumferentially oriented flaws is likely; it is only their through-wall propagation that is much less likely (relative to axially oriented flaws).
  - It is, therefore, the toughness properties that can be associated with axial flaws that control nearly all of the TWCF. These include the toughness properties of plates and axial welds at the flaw locations. Conversely, the toughness properties of both circumferential welds and forgings have little effect on TWCF because these can be associated only with circumferentially oriented flaws.
- ***Transients involving primary side faults are the dominant contributors to TWCF. Transients involving secondary side faults play a much smaller role.***
  - The severity of a transient is controlled by a combination of three factors:
    - the initial cooling rate, which controls the thermal stress in the RPV wall
    - the minimum temperature of the transient, which controls the resistance of the vessel to fracture
    - the pressure retained in the primary system, which controls the pressure stress in the RPV wall
  - The significance of a transient (i.e., how much it contributes to PTS risk) depends on these three factors and on the likelihood of the transient occurring.
  - Our analysis considered transients in the following classes:
    - primary side pipe breaks
    - stuck-open valves on the primary side
    - main steam line breaks
    - stuck-open valves on the secondary side
    - feed-and-bleed
    - steam generator tube rupture
    - mixed primary and secondary initiators
  - Table 8.12 summarizes our results for these transient classes in terms of both transient severity indicators and the likelihood of the transient occurring. The color-coding of table entries indicates the contribution (or not) of these factors to the TWCF of the different classes of transients. This summary indicates that the risk-dominant transients (medium- and large-diameter primary side pipe breaks, and stuck-open primary side valves that later reclose) all have multiple factors that, in combination, result in their significant contribution to TWCF.
    - For medium- to large-diameter primary side pipe breaks, the fast to moderate cooling rates and the low downcomer temperatures (generated by the rapid depressurization and emergency injection of low-temperature makeup water directly to the primary) combine to produce a high-severity transient. Despite the moderate to low likelihood of transient occurrence, the severity of these transients (if they occur) makes them significant contributors to the total TWCF.
    - For stuck-open primary side valves that later reclose, the repressurization associated with valve reclosure coupled with low temperatures in the primary combine to produce a high-severity transient. This coupled with a high likelihood of transient occurrence makes stuck-open primary side valves that later reclose significant contributors to the total TWCF.

Table 8.12. Factors contributing to the severity and risk-dominance of various transient classes

Transient Class		Transient Severity			Transient Likelihood	TWCF Contribution
		Cooling Rate	Minimum Temperature	Pressure		
Primary Side Pipe Breaks	Large-Diameter	Fast	Low	Low	Low	Large
	Medium-Diameter	Moderate	Low	Low	Moderate	Large
	Small-Diameter	Slow	High	Moderate	High	~0
Primary Stuck-Open Valves	Valve Recloses	Slow	Moderate	High	High	Large
	Valve Remains Open	Slow	Moderate	Low	High	~0
Main Steam Line Break		Fast	Moderate	High	High	Small
Stuck-Open Valve(s), Secondary Side		Moderate	High	High	High	~0
Feed-and-Bleed		Slow	Low	Low	Low	~0
Steam Generator Tube Rupture		Slow	High	Moderate	Low	~0
Mixed Primary & Secondary Initiators		Slow	Mixed		Very Low	~0
Color Key	Enhances TWCF Contribution		Intermediate		Diminishes TWCF Contribution	

- The small or negligible contribution of all secondary side transients (MSLBs, stuck-open secondary valves) results directly from the lack of low temperatures in the primary system. For these transients, the minimum temperature of the primary for times of relevance is controlled by the boiling point of water in the secondary (212°F (100°C) or above). At these temperatures, the fracture toughness of the RPV steel is sufficiently high to resist vessel failure in most cases.

- ***Credits for operator action, while included in our analysis, do not influence these findings in any significant way.*** Operator action credits can dramatically influence the risk-significance of ***individual*** transients. Appropriate credits for operator action, therefore, need to be included as part of a "best estimate" analysis because there is no way to establish *a priori* if a particular transient will make a large contribution to the total risk. Nonetheless, the results of our analyses demonstrate that the ***overall effect*** of these operator action credits on the ***total TWCF*** for a plant is small, for the following reasons:
  - Medium- and Large-Diameter Primary Side Pipe Breaks: No operator actions are modeled for any break diameter because, for these events, the safety injection systems do not fully refill the upper regions of the RCS. Consequently, operators would never take action to shut off the pumps.
  - Stuck-Open Primary Side Valves that May Later Reclose: Reasonable and appropriate credit for operator actions (throttling of HPI) has been included in the PRA model. However, the influence of these credits on the estimated values of vessel failure probability attributable to SO-1 transients is small because the operator actions credited only prevent repressurization when SO-1 transients initiate from HZP conditions and when the operators act promptly (within 1 minute) to throttle HPI. Complete removal of operator action credits from the model increases the total risk associated with SO-1 transients only slightly.
  - Main Steam Line Breaks: For the overwhelming majority of MSLB transients, vessel failure is predicted to occur between 10 and 15 minutes after transient initiation because it is within this timeframe that the thermal stresses associated with the rapid cooldown reach their maximum. Thus, all of the long-time effects (isolation of feedwater flow, timing of HSSI control) that can be influenced by operator actions have no effect on vessel failure probability because these factors influence the progression of the transient after failure has occurred (if it occurs). Only factors affecting the initial cooling rate (i.e., plant power level at transient initiation, break location inside or outside of containment) can influence the CPTWC values. These factors are not influenced in any way by operator actions.

- ***Because the severity of the most significant transients in the dominant transient classes are controlled by factors that are common to PWRs in general, the TWCF results presented in this chapter can be used with confidence to develop revised PTS screening criteria that apply to the entire fleet of operating PWRs.***
  - Medium- and Large-Diameter Primary Side Pipe Breaks: For these break diameters, the fluid in the primary cools faster than can the wall of the RPV. In this situation, ***only*** the thermal conductivity of the steel and the thickness of the RPV wall control the thermal stresses and, thus, the severity of the fracture challenge. Perturbations to the fluid cooldown rate controlled by break diameter, break location, and season of the year do not play a role. Thermal conductivity is a physical property, so it is very consistent for all

RPV steels, and the thicknesses of the three RPVs analyzed are typical of PWRs. Consequently, the TWCF contribution of medium- to large-diameter primary side pipe breaks is expected to be consistent from plant-to-plant and can be well-represented for all PWRs by the analyses reported herein.

- Stuck-Open Primary Side Valves that May Later Reclose: A major contributor to the risk-significance of SO-1 transients is the return to full system pressure once the valve recloses. The operating and safety relief valve pressures of all PWRs are similar. Additionally, as previously noted, operator action credits affect the total risk associated with this transient class only slightly.
- Main Steam Line Breaks: Since MSLBs fail early (within 10–15 minutes after transient initiation), only factors affecting the initial cooling rate can have any influence on CPTWC values. These factors include the plant power level at event initiation and the location of the break (inside or outside of containment). These factors are not influenced in any way by operator actions.

9 Generalization of the Baseline Results to All Pressurized-Water Reactors

In Chapter 8, we presented the results of three plant-specific analyses of Oconee Unit 1, Beaver Valley Unit 1, and Palisades. These analyses quantified the variation with material embrittlement level of the annual risk of developing a through-wall crack in an RPV. Since the objective of this project is to develop a revision to the PTS screening limit expressed in 10 CFR 50.61 that applies *in general* to all PWRs, it is critical that we understand the extent to whixh our analyses adequately address the range of conditions experienced by domestic PWRs. In this chapter, we therefore examine the generality of our results, focusing on four topics that address this goal:

- Sections 9.1 and 9.2 describe sensitivity studies performed on the TH and PFM models, respectively. These studies address the effect of credible changes to the model and/or its input parameters on the output of the model. Such results are needed to engender confidence in both the robustness of the results presented in Chapter 8 and their applicability to PWRs *in general.*
- Section 9.3 describes an effort in which we examine the plant design and operational characteristics of five additional plants. Our aim is to determine whether the design and operational features that are the key contributors to PTS risk (see Section 8.6) vary significantly enough in the general plant population to question the generality of our results.
- Throughout our analysis, we have assumed that the only possible causes of PTS events have origins that are *internal* to the plant. However, *external* events such as fires, floods, earthquakes, and so on, can also be PTS precursors. Therefore, in Section 9.4, we examine the potential for external initiating events to create significant additional risk relative to the internal initiating events we have already modeled in detail.

9.1 Thermal-Hydraulic Sensitivity Studies

9.1.1 Introduction

This section addresses the results and observations of the thermal-hydraulic analyses and sensitivity studies performed to support the PTS analysis. The sensitivity studies were performed to evaluate the effects of variations in parameters that can affect the downcomer conditions used as boundary conditions to the probabilistic fracture mechanics analysis. These conditions are the average downcomer fluid temperature, the system pressure and the average downcomer fluid to wall heat transfer coefficient.
The sensitivity studies were performed to achieve the following purposes:

(1) Determine the effect on average downcomer fluid temperature range attributable to variation of system parameters such as break size, break location, season, and others.

(2) Evaluate the impact of downcomer heat transfer coefficient on the downcomer conditions and, ultimately, on conditional probability of through-wall cracking (CPTWC).

The thermal-hydraulic analysis was performed using RELAP5/MOD3.2.2Gamma. Chapter 6 presents a discussion of RELAP5 as used in this analysis, along with a comparison of RELAP predictions of pressure, temperature, and heat transfer coefficient to the results of both separate effects and integral systems and tests (see Section 6.7). A discussion of how uncertainty was factored into the analysis is also presented in Chapter 6 (see Section 6.8.2).

9.1.2 Sensitivity Studies Performed for Uncertainty Analysis

Selection of sensitivity studies that were performed is based largely on previous experience with the types of transients being analyzed combined with variations in plant operating states that can affect the downcomer conditions. Sensitivity studies were performed for the Oconee, Beaver Valley, and Palisades plants to support the thermal-hydraulic uncertainty analyses. As previously noted, the uncertainty analysis approach is discussed in Chapter 6. This section focuses on the results of the sensitivity studies conducted to support the uncertainty analysis. [***Chang***] discusses the sensitivity and uncertainty analyses in detail.

9.1.2.1 LOCAs

Sensitivity analyses were performed on LOCAs ranging from 1.4-in. (3.59-cm) to 8-in. (20.32-cm) for the Oconee, Beaver Valley, and Palisades plants. Various sensitivity parameters were defined and a RELAP5 run was made for a selected parameter, changing only that parameter. The average downcomer fluid temperature over a 10,000-second period was then computed. The downcomer temperature difference between the nominal case (no parameters varied) and the cases where a parameter is varied is used in the uncertainty analysis.

Table 9.1, Table 9.2, and Table 9.3 present a summary of the key sensitivity parameters and the effects on downcomer temperature for the Oconee, Beaver Valley, and Palisades plants, respectively. The nominal temperatures are based on RELAP5 runs with no change in sensitivity parameters, while the other temperatures listed are the differences between the temperature results for the changed sensitivity parameter and the nominal temperature results. Several parameters were considered in the sensitivity analysis, including season of the year, decay heat load, heat transfer coefficient, break area, and break location. Season of the year considered the impact of winter and summer on the ECCS injection water temperature. Typically, the RWST (or equivalent), which is the source of HPI and LPI injection water, is located outdoors. The temperature range analyzed is listed below:

- Oconee: The HPI and LPI injection temperature used is 303 K [85°F], and the core flood tank temperature is 311 K [100°F] during the summer. During the winter, the HPI and LPI injection temperature used is 278 K [40°F], and the core flood tank temperature is 294 K [70°F]. For the nominal case, the HPI and LPI injection temperature used is 294 K [70°F], and the core flood tank temperature is 300 K [80°F].
- Beaver Valley: HPI and LPI injection temperature used is 286 K [55°F], and core flood tank temperature is 314 K [105°F] during the summer. During the winter, the HPI and LPI injection temperature used is 281 K [45°F], and the core flood tank temperature is 297 K [75°F]. For the nominal case, the HPI and LPI injection temperature used is 283 K [50°F], and core flood tank temperature is 305 K [90°F]. Note that Beaver Valley currently cools the RWST to meet LOCA safety limits.
- Palisades: The HPI and LPI injection temperature used is 311 K [100°F], and the safety injection tank temperature is 305 K [90°F] during the summer. During the winter, the HPI and LPI injection temperature used is 278 K [40°F], and the safety injection tank temperature is 289 K [60°F]. For the nominal case, the HPI and LPI injection temperature used is 304 K [87.9°F], and the safety injection tank temperature is 300 K [80°F].

Table 9.1. Summary of Oconee Downcomer Fluid Temperature Sensitivity Results for LOCA

Parameter	Break Diameter					
	3.6-cm [1.4 in]	5.1-cm [2 in]	7.2-cm [2.8 in]	10.2-cm [4 in]	14.4-cm [5.7 in]	20.3-cm [8 in]
Nominal	***414 K [285 °F]***	***394 K [250 °F]***	***388 K [239 °F]***	***363 K [194 °F]***	***329 K [133 °F]***	***317 K [111 °F]***
Winter	-12 K [-22°F]	-	-14 K [-25°F]	-	-15 K [-27°F]	-3 K [-5°F]
Summer	-	-	7 K [13°F]	-	7 K [13°F]	0 K [0°F]
0.7% Decay Heat Load	-16 K [-29°F]	-	-39 K [-70°F]	-	-8 K [-14°F]	-5 K [-9°F]
130% Heat Transfer Coeff	-	6 K [11°F]	8 K [14°F]	-	2 K [4°F]	-
70% Heat Transfer Coeff	-	-7 K [-13°F]	-8 K [-14°F]	-	-5 K [-9°F]	-
Cold Leg Break		61 K [110°F]	24 K [43°F]	13 K [23°F]	16 K [29°F]	0 K [0°F]

Note: The ***nominal*** temperatures listed above are based on RELAP5 runs with no change in sensitivity parameters. Other temperatures listed are the difference between the temperature results for the changed sensitivity parameter and the nominal temperature results.

Table 9.2. Summary of Beaver Valley Downcomer Fluid Temperature Sensitivity Results for LOCA

Parameter	Break Diameter					
	3.6-cm [1.4 in]	5.1-cm [2 in]	7.2-cm [2.8 in]	10.2-cm [4 in]	14.4-cm [5.7 in]	20.3-cm [8 in]
Nominal	***459 K [367 °F]***	***377 K [219 °F]***	***336 K [145 °F]***	***319 K [115 °F]***	***313 K [104 °F]***	***300 K [80 °F]***
Winter	-2 K [-4°F]	-11 K [-20°F]	-3 K [-5°F]	-1 K [-2°F]	3 K [5°F]	-3 K [-5°F]
Summer	1 K [2°F]	-7 K [-13°F]	8 K [14°F]	12 K [22°F]	5 K [9°F]	3 K [5°F]
0.7% Decay Heat Load	-99 K [-178°F]	-29 K [-52°F]	-11 K [-20°F]	-7 K [-13°F]	-9 K [-16°F]	-1 K [-2°F]
0.2% Decay Heat Load	-106 K [-191°F]	-40 K [-72°F]	-16 K [-29°F]	-10 K [-18°F]	-11 K [-20°F]	-2 K [-4°F]
130% Heat Transfer Coeff	3 K [5°F]	-3 K [-5°F]	6 K [11°F]	5 K [9°F]		0 K [0°F]
70% Heat Transfer Coeff	-4 K [-7°F]	-15 K [-27°F]	-5 K [-9°F]	2 K [4°F]		
130% Break Area		-48 K [-86°F]	-11 K [-20°F]	-12 K [-22°F]	-13 K [-23°F]	1 K [2°F]
70% Break Area		-18 K [-32°F]	23 K [41°F]	4 K [7°F]	-7 K [-13°F]	6 K [11°F]
Cold Leg Break	-4 K [-7°F]	76 K [137°F]	79 K [142°F]	50 K [90°F]	34 K [61°F]	40 K [72°F]

Note: The ***nominal*** temperatures listed above are based on RELAP5 runs with no change in sensitivity parameters. Other temperatures listed are the difference between the temperature results for the changed sensitivity parameter and the nominal temperature results.

Table 9.3. Summary of Palisades Downcomer Fluid Temperature Sensitivity Results for LOCA

Parameter	Break Diameter					
	3.6-cm [1.4 in]	5.1-cm [2 in]	7.2-cm [2.8 in]	10.2-cm [4 in]	14.4-cm [5.7 in]	20.3-cm [8 in]
Nominal	***482 K [408 °F]***	***427 K [309 °F]***	***391 K [244 °F]***	***350 K [170 °F]***	***320 K [116 °F]***	***310 K [98 °F]***
Winter	-6 K [-11°F]	-8 K [-14°F]	-17 K [-31°F]	-16 K [-29°F]	-16 K [-29°F]	-16 K [-29°F]
Summer	8 K [14°F]	10 K [18°F]	13 K [23°F]	14 K [25°F]	13 K [23°F]	15 K [27°F]
0.7% Decay Heat Load	-32 K [-58°F]	-21 K [-38°F]	-27 K [-49°F]	-17 K [-31°F]	-1 K [-2°F]	0 K [0°F]
0.2% Decay Heat Load	-66 K [-119°F]	-47 K [-85°F]	-40 K [-72°F]	-20 K [-36°F]	-2 K [-4°F]	-1 K [-2°F]
130% Heat Transfer Coeff	4 K [7°F]	6 K [11°F]	11 K [20°F]	5 K [9°F]		
70% Heat Transfer Coeff	-3 K [-5°F]	-2 K [-4°F]	-2 K [-4°F]	-4 K [-8°F]		
130% Break Area		13 K [23°F]	24 K [43°F]	20 K [36°F]	14 K [25°F]	3 K [5°F]
70% Break Area		-9 K [-16°F]	-18 K [-32°F]	-12 K [-22°F]	-6 K [-11°F]	-1 K [-2°F]
Cold Leg Break	9 K [16°F]	38 K [68°F]	39 K [70°F]	23 K [41°F]	32 K [58°F]	22 K [40°F]

Note: The ***nominal*** temperatures listed above are based on RELAP5 runs with no change in sensitivity parameters. Other temperatures listed are the difference between the temperature results for the changed sensitivity parameter and the nominal temperature results.

As listed in Table 9.1 through Table 9.3, the two levels of decay heat considered were 0.7% and 0.2% of full power. The heat transfer coefficient was varied by 70% and 130% of the RELAP5 computed value in the primary system except for the core and the steam generator tubes. The nominal break area was varied by a factor of 0.7 and 1.3 to evaluate possible uncertainty in the break flow. Finally, breaks of various sizes in the cold leg as well as the hot leg are considered.

Some overall trends in the results are seen from the results in Table 9.1, through Table 9.3. First, the magnitude of the variation from nominal generally decreases with increasing break size for all three plants regardless of the parameter being evaluated, because of the combined effects of increased break and ECCS flow that occurs as the break size increases. For break diameters of 4-in. (10.2-cm) or more, ECCS flow is at a maximum since the HPI and LPI pumps are generally operating at pump runout conditions. For breaks diameters less than 2.8-in. (7.2-cm), the pump flow begins to become limited by the break flow, with decreasing pump flow as the break diameter is decreased. In this range of break diameters, the downcomer fluid temperature is more sensitive to changes in break diameter.

Cold leg breaks generally show the greatest increase in downcomer fluid temperature for the three plants, principally because of partial ECCS bypass through the break.

The assumed decay heat load between hot full power and hot zero power cases shows the greatest decrease in downcomer fluid temperature. These sensitivity parameters are part of the definition of the boundary conditions that typically are provided as part of the transient definition.

Parameters that involve model sensitivity such as change in break area, change in heat transfer coefficient (system-wide) also significantly affect the downcomer fluid temperature. Of the two parameters, downcomer fluid temperature is more sensitive to changes in break flow. As a result, a number of transients with adjustments

in break area were included in the baseline models discussed in Chapter 8.

9.1.2.2 Stuck-Open Pressurizer SRVs That Reclose

Sensitivity cases for stuck-open primary side SRVs considered the following parameters:

- Number of valves stuck open (i.e., one or two valves)
- Timing of valve reclosure (Reclosure times of 3,000 s, 6,000 s, and no reclosure were analyzed. Additional sensitivity studies were conducted for longer reclosure times; see response to Peer Review Comment #76 in Appendix B.)
- Time for operator to start HPI throttling (i.e., 1 minute, 10 minutes, and not throttled)
- Decay heat (i.e., full-power and HZP)

The number of stuck-open valves analyzed for the three plants depended on the plant characteristics. For Oconee, analysis was performed for one stuck-open SRV, since the probability of two stuck-open valves was screened out on the basis of low probability. For Palisades, sensitivity analysis was not performed on the stuck-open valve scenarios.

For Beaver Valley, sensitivity studies were performed for one and two stuck-open valves considering various parameters, similar to the approach used for LOCA transients. The range used for each parameter is the same as used for the LOCA. The sensitivity of downcomer fluid temperature to each parameter is listed in Table 9.4. As in the LOCA case, the nominal temperatures are based on RELAP5 runs with no change in sensitivity parameters while the other temperatures listed are the difference between the changed and the nominal sensitivity parameter.

Table 9.4. Summary of Downcomer Fluid Temperature Sensitivity Results for Stuck-Open Primary Side Valves

	Number of Stuck-Open SRVs	
	1 valve	2 valves
Nominal	393 K [248°F]	349 K [169°F]
Winter	-5 K [-9°F]	-3 K [-5°F]
Summer	0 K [0°F]	6 K [11°F]
0.7% Decay Heat Load	-42 K [-76°F]	-15 K [-27°F]
0.2% Decay Heat Load	-52 K [-93°F]	-27 K [-49°F]
130% Heat Transfer Coeff	3 K [-5°F]	6 K [-11°F]
70% Heat Transfer Coeff	-8 K [-14°F]	-4 K [-7°F]
130% Valve Flow Area		-22 K [-40°F]
70% Valve Flow Area		10 K [18°F]

Some overall trends in the results are seen in Table 9.4. The largest change in temperature is from the variation in decay heat, a finding consistent with the observations made in Section 8.5.3.3.2 concerning the differences between HZP and full-power transients. This sensitivity parameter is part of the definition of the transient boundary conditions that are part of the definition of the transient being analyzed. Changes in valve flow area also significantly affect the downcomer fluid temperature. Parameters that involve model sensitivity such as change in break area, change in heat transfer coefficient (system-wide) also significantly affect the downcomer fluid temperature. Of the two parameters, downcomer fluid temperature is more sensitive to changes in break flow. Changes in these parameters are considered in defining the transients used in the risk assessment.

9.1.2.3 CPTWC Sensitivity During LOCA Transients

One of the trends identified in the sensitivity and uncertainty analysis performed in [***Chang***] is the relationship between the conditional probability of vessel failure (CPF) and the LOCA break diameter; see the related discussion in Sections 8.5.2.4.1 and 8.5.2.4.2. Figure 9.1 presents the Oconee, Beaver Valley, and Palisades CPTWC results at an approximately equivalent embrittlement level. The CPTWC data presented in Figure 9.1 for Oconee and Beaver Valley are for surge line or hot leg breaks with the indicated diameter. The transients were initiated from hot full-power conditions. The data presented for Palisades are for cold leg breaks, with the exception of the 16-in. (40.6-cm) results which represent a hot leg break. All of the Palisades cases are initiated from full-power conditions.

The results in Figure 9.1 show that CPTWC is relatively insensitive to thermal-hydraulic conditions in the primary system during LOCAs with a break diameter greater than 5.656-in. (14.4-cm). For these break diameters, the primary system cooldown rate is governed by the high rate of break and ECCS injection flow, which is a maximum at this break size range. The safety injection tanks discharge within a few minutes of accident initiation. Additionally, the high pressure and low-pressure injection systems will be at or near pump runout conditions. The combined flow of the injection systems and safety injection tank discharge will fill the downcomer with subcooled water after the initial blowdown for the duration of the transient. In this range of break sizes, the blowdown flow of the break is much greater than the ECCS flow delivery rate. The downcomer fluid temperature will be determined principally by the flow from the high and low-pressure injection systems, the safety injection tank discharge, and the initial temperature of the water used in the injection systems. In this range of break sizes, CPTWC reaches a maximum.

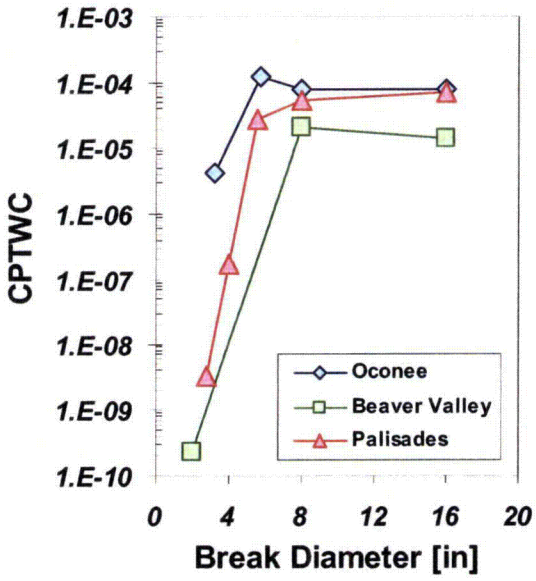

Figure 9.1. CPTWC Behavior for LOCAs of Various Break Diameters

The sensitivity of CPTWC to break size increases for break sizes below 5.656-in. (14.4-cm). This trend is seen for all of the results presented in Figure 9.1. For these smaller break diameters, the balance between break flow and the ECCS injection flow governs the primary system cooldown and depressurization rates. System depressurization is slower relative to the larger breaks (greater than 5.656-in. (14.4-cm)). As a result, safety injection tank discharge and initiation of low-pressure system injection begins later in the transient, and the injection rate is lower. At the lower end of this break diameter range (i.e., ≈2.5-in. or ≈5-cm), low-pressure system injection flow may not even be initiated, and the safety injection tanks may not totally discharge. In this range of break sizes, the depressurization limits the rate of high- and low-pressure injection system injection to the reactor system. The downcomer fluid temperature is principally determined by the break diameter (break flow), the flow from the high- and low-pressure injection systems, the safety injection tank discharge, and the initial temperature of the water used in these systems as in the larger breaks. However, water is injected at a slower rate, resulting in a slower cooldown and relative to the larger breaks.

One significant aspect of the results shown in Figure 9.1 is that there is a limit to the CPTWC value for each plant and, hence, to the risk of vessel failure produced by a primary side pipe break. Additionally, this limiting CPTWC behavior would be similar for any plant because the designs of the different vendors all have similar ratios of initial energy to RCS volume and core power to RCS volume.

The observations on CPTWC behavior suggest that the same CPTWC trend will occur for any plant with a shift in the break diameter at which the CPTWC curve bends over and reaches a maximum. This behavior is expected to occur regardless of plant power level given that the ECCS system for any plant is designed to cool the core under a wide variety of LOCA conditions. This observation is relevant to the applicability of these results to PWRs *in general.*

9.2 Fracture mechanics sensitivity studies

We have performed sensitivity studies on our PFM model (and on PFM-related variables) with two aims in mind:

- To provide confidence in the ***robustness*** of our PFM model, we assessed the effect of credible model and input perturbations on TWCF estimates.
- To provide confidence that the results of our calculations for three specific plants can be ***generalized*** to apply to all PWRs, we performed sensitivity studies to assess the influence of factors not fully considered in our baseline TWCF estimates (see Chapter 8).

Full details of sensitivity studies of our PFM model are available in a companion report [***EricksonKirk-SS***]. This section provides a brief summary of that information.

9.2.1 Sensitivity Studies Performed To Assess the Robustness of the PFM Model

9.2.1.1 Approach

The model used to generate TWCF estimates is a complex assemblage of many sub-models and parameter inputs. These combine to produce intermediate calculated results that, upon passing through yet more sub-models, eventually become an estimated distribution of TWCF. The existence of each sub-model and parameter input in the PFM model, and their arrangement with respect to one another, represents a decision to structure the overall model in a particular way. Changing any one of these decisions can, in principal, change the estimated output of the model (i.e., the distribution of TWCF values). Therefore, we investigated the degree to which the selection of ***credible*** alternative sub-models may influence the TWCF estimates. Additionally, many of the inputs parameters to the PFM cannot be known precisely. Therefore, we also investigated the degree to which ***credible*** variations in the input parameters change the TWCF estimates. This approach of basing sensitivity studies on ***credible*** alternative sub-models and/or on ***credible*** variations of the input parameters follows directly from two principles of our overall approach to model building (see Section 3.2):

- the use of realistic input values and sub-models
- an *explicit* treatment of uncertainties

These principles permitted calculation of TWCF estimates that are systematically biased neither high nor low (i.e., values that represent a *"best estimate"*) to the greatest extent practicable. By basing sensitivity studies on ***credible*** alternative sub-models and ***credible*** variations of the input parameters, we maintain these principals and, thereby, allow our TWCF estimates to maintain their "best estimate" label.

This approach to performing sensitivity studies deviates from that taken previously [SECY-82-465], wherein sensitivity studies either focused on "important" parameters and sub-models (i.e., those to which the TWCF was believed to be sensitive), or were performed seemingly without consideration of either the technical justification for the baseline sub-model or the credibility of the alternative sub-model used to motivate the sensitivity study. We feel it is, in most cases, important to avoid such *ad hoc* justifications for performing sensitivity studies. Low sensitivity of the output TWCF to a change in a sub-model or input having an inadequate technical justification does not provide a rational basis for accepting that sub-model or input as part of the overall model. Similarly, high sensitivity of the output to a well justified sub-model or input does not provide a basis for either condemning that sub-model/input or adopting arbitrary margins in an effort to compensate for the high sensitivity.

9.2.1.2 Sensitivity Studies Performed

As detailed in [***EricksonKirk-SS***], the following sensitivity studies were performed to provide confidence in the robustness of the PFM model:

- flaw distribution (size and density of simulated flaws)
- residual stresses assumed to exist in the RPV wall
- embrittlement shift model used and treatment of uncertainties
- re-sampling of chemical composition variables at the ¼T, ½T, and ¾T locations for welds
- crack face pressure
- upper shelf toughness model

The results of these sensitivities are summarized in the following sections.

9.2.1.2.1 Flaw Distribution

As detailed in Appendix C, the distributions of flaws that FAVOR simulates provide a conservative representation of both the sizes and densities of crack-like defects that exist in the general population of PWRs. Additionally, these flaw distributions were based on what is generally regarded as among the most comprehensive studies of flaws in RPV fabrication that is currently available [***Simonen***]. Consequently, it is difficult to find a ***credible*** alternative flaw model on which to motivate a sensitivity study. Nonetheless, it is informative to understand the characteristics of the flaws drawn from these distributions that contribute most significantly to the estimated values of FCI and TWCF. For example, the information presented in Figure 8.7 indicated that only axial flaws can contribute significantly to the TWCF atributable to differences in the through-wall variation of crack driving force between axial and circumferentially oriented flaws. Two other general statements can be made regarding the flaws that contribute most significantly to the estimated TWCF values:

(1) <u>They are located close to the inner diameter surface of the vessel</u>. The tensile thermal stresses produced by rapid cooling along the vessel ID do not penetrate far into the wall thickness of the RPV. A natural consequence of this, which is illustrated in Figure 9.3, is that the great majority of the cracks that are predicted to initiate and subsequently propagate through the vessel wall lie very close to the inner diameter surface. The information in Figure 9.3 indicates that almost all flaws that initiate lie less than 1/8-T from the vessel ID. Since they are driven by the thermal stresses characteristic of cooldown transients, these observations hold true independent of embrittlement level.

(2) <u>They have a small through-wall dimension</u>. This again occurs as a direct consequence of the fact that cooldown transients produce thermal stresses that (together with the pressure stresses) are only high enough to initiate cracks at locations close to the inner diameter of the vessel. Consequently, larger

flaws (which would generally be considered more deleterious in a fracture evaluation than would small flaws) tend to not initiate very frequently because their crack tips lie too far away from the inner diameter surface and, so, are subjected to low tensile loads, or even to compressive loads. In Figure 9.4 and Figure 9.5, we examine the effect of duration of irradiation exposure, flaw location (in plate or weld), and transient type on the flaw sizes that initiate fracture in our analyses. This information demonstrates that the combined effects of the duration of irradiation exposure and flaw location are small, and are entirely as expected for they correlate well with relative embrittlement levels. Transient type plays a minor role, with predominantly thermal transients such as large pipe breaks generally initiating fracture from smaller flaws while transients that involve a significant pressure component (such as stuck-open valves that may later reclose) tend to initiate fracture from larger flaws. Nonetheless, the flaws that contribute to the estimated through-wall cracking frequency are small, having median depths ranging from 0.1 to 0.3-in. (2.54 to 7.62-mm).

In combination, these observations help to allay concerns that the flaw distributions sampled in FAVOR do not simulate enough flaws of large dimensions, or that the postulated future discovery of a large (previously undetected) flaw in service could invalidate the results of this study. Neither of these concerns is valid because, given the dominant effects of thermal stresses in controlling crack driving force, large flaws do not play a role in establishing the risk of RPV failure attributable to PTS.

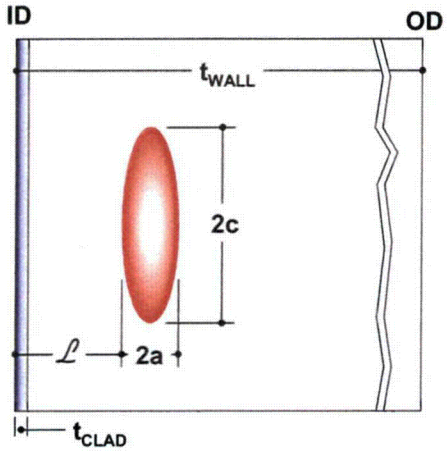

Figure 9.2. Flaw dimension and position descriptors adopted in FAVOR

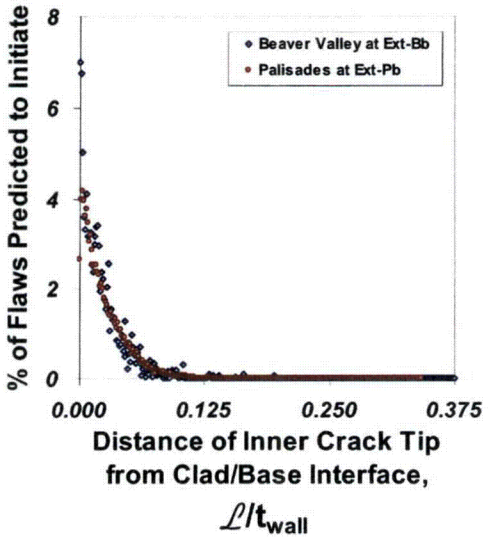

Figure 9.3. Distribution of through-wall position of cracks that initiate

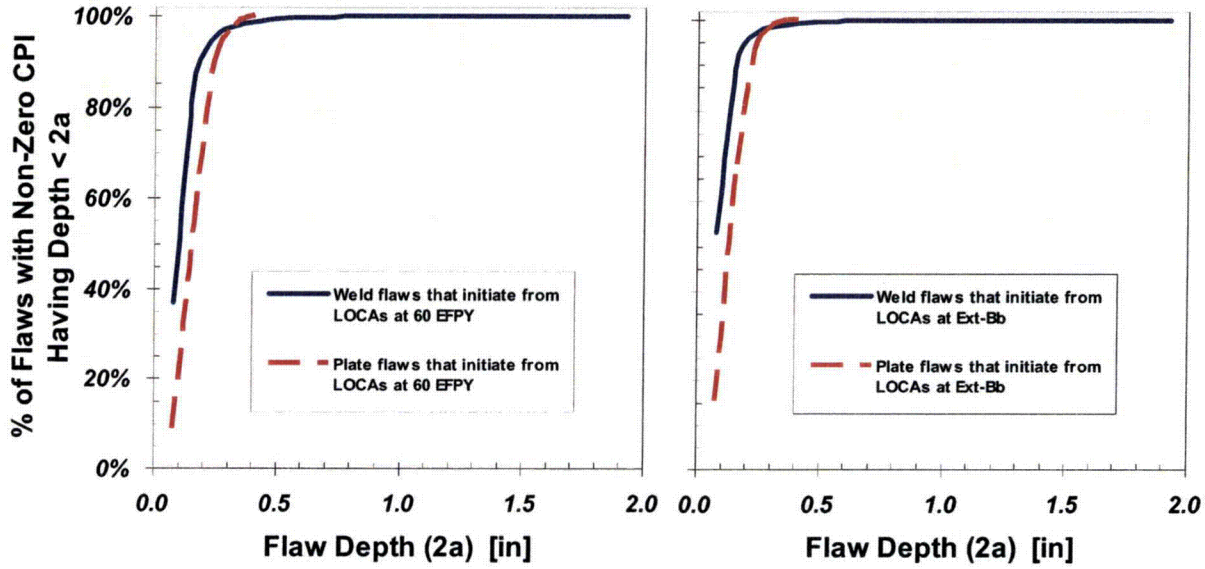

Figure 9.4. Flaw depths that contribute to crack initiation probability in Beaver Valley Unit 1 when subjected to medium- and large-diameter pipe break transients at two different embrittlement levels

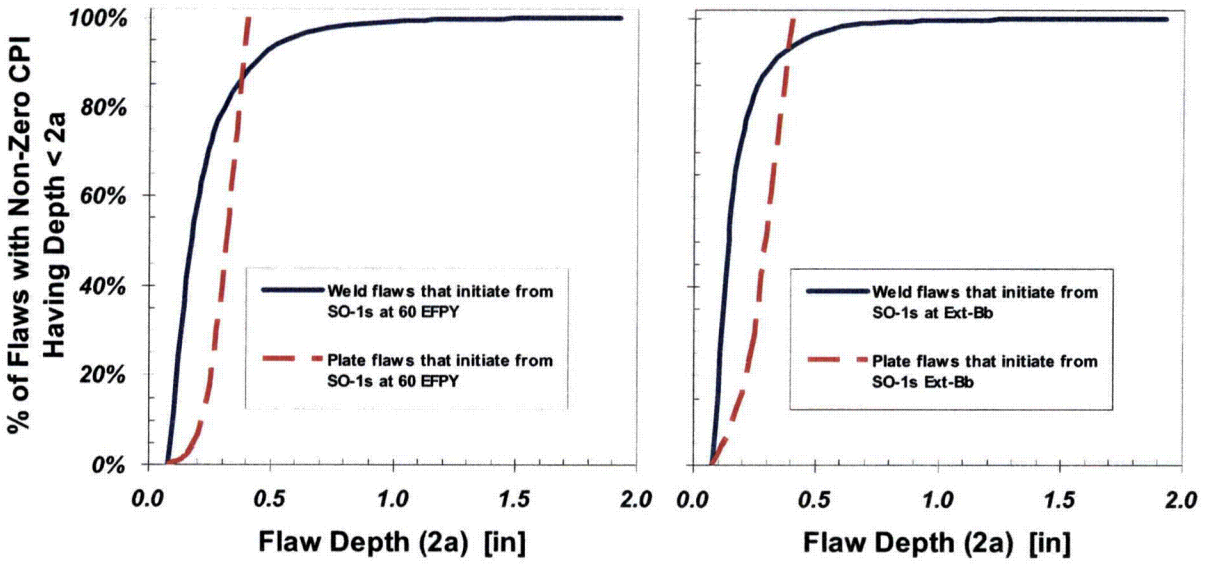

Figure 9.5. Flaw depths that contribute to crack initiation probability in Beaver Valley Unit 1 when subjected to stuck-open valve transients at two different embrittlement levels

9.2.1.2.2 Residual Stresses

FAVOR assumes that a single distribution quantifies the residual stresses produced by welding in both axial and circumferential welds [***Williams***]. These residual stresses were estimated from measurements made of how the width of a radial slot cut in the longitudinal weld in a shell segment from an RPV change with cut depth. These measurements were processed through a finite element analysis to determine the residual stress profile used by FAVOR [Dickson 99]. FAVOR also assumes that this residual stress distribution is not relieved by cracking of the vessel, (i.e., the residual stresses in the figure to the right are applied equally

irrespective of *a/t*). Since residual stresses would have to be relieved were a crack to develop through the weld in an RPV, the effect of this conservative assumption was be assessed by performing a sensitivity study wherein the weld residual stresses are retained in the crack initiation calculation but are removed from the through-wall cracking calculation. In this sensitivity study, we performed analyses of both the Beaver Valley and the Palisades RPVs at two embrittlement levels each (32 EFPY and the Ext-B embrittlement conditions). The effect of relieving the residual stresses in the through-wall cracking calculations was to entirely negligible, reducing the TWCF values by less than 1% (on average). This limited sensitivity of the TWCF values on residual stresses occurs because the crack driving force cause by the residual stress is very small relative to that caused by the combination of thermal and pressure loading.

9.2.1.2.3 Embrittlement Shift Model

The embrittlement shift model relates compositional and neutron exposure variables to the amount by which irradiation shifts the Charpy V-notch (CVN) transition temperature curve to higher temperatures. FAVOR adopts a model developed under an NRC Research contract by Eason in 2000 [Eason]. Since that time a similar, albeit not identical, embrittlement trend curve had been adopted by the American Society for Testing and Materials in the E900-02 standard [ASTM E900]. A sensitivity study was, therefore, performed to assess the effect of adopting the ASTM embrittlement trend curve, rather than that proposed by Eason (again analyzing Beaver Valley and Palisades at two different embrittlement levels). The ASTM E900-02 embrittlement shift model produces TWCF estimates that are systematically lower (approximately one-third) of those estimated using the Eason shift model. This reduction in TWCF is almost entirely attributable to the existence of a "long-term bias" in the Eason model that does not exist in the ASTM E900-02 model. Activity is currently underway within ASTM Committee E10.02 to revise the E900 model. Representatives of both the industry and the NRC are involved in this code committee work, and the committee is expected to publish a revised model that incorporates features of both the current Eason and E900-02 relationships. Thus, for the purposes this report, we have continued to use the Eason correlation and accepted this approach as slightly conservative. At such time as a consensus emerges from the E10.02 Code committee process, it will be a simple matter to assess the effect of the new embrittlement shift model on the TWCF values reported herein. However, based on this sensitivity study, we expect this effect to be small (less than a factor of 3 reduction in TWCF).

9.2.1.2.4 Embrittlement Shift Uncertainty Treatment

In FAVOR, the uncertainty of the embrittlement shift model is not sampled. As argued in [***ErickssonKirk-SS***], this approach is appropriate because the uncertainty in the embrittlement shift model arises as a result of uncertainties in the input variables to the embrittlement shift model (i.e., copper content, nickel content, phosphorus content, and fluence), which are sampled in FAVOR. This is demonstrated by the results in Figure 9.6, which were generated as follows:

(1) Median values were assigned to all of the input variables to the Eason embrittlement shift equation (except for fluence).

(2) The FAVOR uncertainty distributions for Cu, Ni, P, and fluence were sampled about these medians for fluence medians ranging from 0.25×10^{19} to 5×10^{19} n/cm^2.

(3) At each different fluence value, 1,000 sets (Cu, Ni, P, and fluence) were simulated. Each set was used to estimate a value of embrittlement shift using the Eason embrittlement model. The standard deviation of these 1,000 embrittlement shift estimates was calculated and plotted in Figure 9.6.

The uncertainties simulated by FAVOR agree well with those in the embrittlement shift data used by Eason to develop the model. The lower uncertainties associated with lower fluence

values results from FAVOR setting to zero simulations of embrittlement shift that are negative, which is physically unrealistic.

This information confirms the appropriateness of the FAVOR approach to uncertainty simulation for this model. Simulation of both the embrittlement shift model uncertainties and the uncertainties in the input variables would produce a model that simulated a greater magnitude of uncertainty in embrittlement shift than is observed in test data.

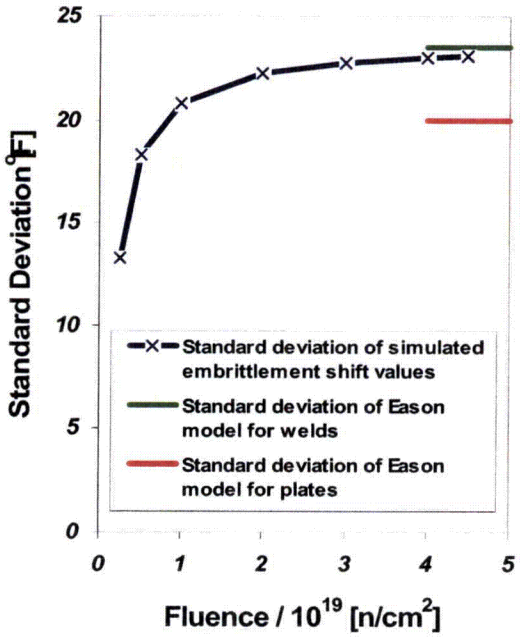

Figure 9.6. Comparison of embrittlement shift uncertainties simulated by FAVOR (blue line with X symbols) with the uncertainties in the experimental embrittlement shift database used by Eason to construct the model

9.2.1.2.5 Chemical Composition Re-Sampling for Welds

In welds, a gradient of properties is expected to exist through the thickness of the RPV because of through-wall changes in copper content. These copper content changes arise from the fact that, given the large volume of weld metal needed to fill an RPV weld, manufacturers often needed to use weld wire from multiple weld wire spools to completely fill the groove. Lack of control of the process used to copper plate the weld wires (a step taken for corrosion control) resulted in wide variability in copper coating thickness from spool to spool (variability that is manifested in measurable variations in Cu content through the RPV wall thickness). These copper variations produce variations in sensitivity to irradiation embrittlement, and consequent variations in resistance to fracture though the vessel wall.

FAVOR adopts a weld composition gradient model wherein the Cu content is re-sampled in a through-wall cracking calculation every time the crack passes the ¼ thickness, the ½ thickness, and the ¾ thickness locations in the vessel wall. A four-weld layer model was developed based on considerations of the volume of weld metal needed to fill an RPV weld. To assess the effect of this model on TWCF, a sensitivity study was performed wherein the Cu resampling in FAVOR was turned off. Again, the sensitivity study included analysis of Beaver Valley and Palisades at two different embrittlement levels. The results of this study show that turning off the FAVOR 4-weld layer model increase the estimated TWCF by a small amount (factor of 2.5 on average).

9.2.1.2.6 Crack Face Pressure

As part of the peer review, Dr. Schultz noted that FAVOR had inappropriately not accounted for the effects of crack face pressure loading (see Appendix B, Reviewer Comment #23). FAVOR Ver. 04.1 (which was used to generate all of the results reported in Chapter 8) now accounts for the effects of crack face pressure. The effect of including crack-face pressure on non-SO-1 transients is a negligible (a 0% to 6% increase in CPTWC) because pressure does not contribute significantly to the failure probability of these transients. For SO-1 transients, larger increases (25% to 75%) in the CPTWC are seen. The effect of including crack face pressure in an integrated analysis of PTS risk (all transients) is, however, small. An analysis of Beaver Valley at 60 EFPY showed that including crack face pressure increased the estimated TWCF by only 6%.

9.2.1.2.7 Upper Shelf Toughness Model

In FAVOR Version 03.1, upper shelf fracture toughness values (J_{Ic}, *J-R*) were estimated through correlations with Charpy V-notch energy. These empirical relationships had very low correlation coefficients and high scatter, reflecting the different underlying physical processes that control Charpy energy and fracture toughness on the upper shelf. Comments from the peer review group (see Comment #40, Appendix B) questioned the appropriateness of this approach. After reviewing the existing FAVOR model and other available alternatives, the staff adopted a new upper shelf model and implemented it in FAVOR Version 04.1 to address this concern. This new model does not rely on Charpy correlations in any way, and features an explicit treatment of the uncertainty in upper shelf toughness (both the ductile initiation toughness as measured by J_{Ic} and the resistance to further crack extension as measured by *J-R*). Additionally, the new model links transition toughness and upper shelf toughness properties, a relationship motivated by trends in fracture toughness data and physical considerations, and a feature the FAVOR Version 03.1 models did not have. This upper shelf model is based on work recently completed by EPRI [EricksonKirk 04]. Details of the FAVOR implementation of this new model can be found in [***EricksonKirk-PFM***] and [***Williams***].

The new upper shelf model does not change the TWCF values in any substantive way. On average, the TWCF values estimated using the new model are ~5% lower than the values estimated using the correlative approaches used in FAVOR 03.1. However, the linkage between transition toughness and upper shelf toughness properties in the new model has eliminated FAVOR predictions of physically implausible results (e.g., predicting that flaws in a particular axial weld (say Axial Weld A) of the RPV beltline contribute more to the TWCF than do flaws in another axial weld (say Axial Weld B) even though the toughness of Axial Weld A exceeds that of Axial Weld B).

9.2.2 Sensitivity Studies Performed to Assess the Applicability of the Results in Chapter 8 to PWRs in General

As detailed in [***EricksonKirk-SS***], the following sensitivity studies were performed to assess the applicability of the TWCF results presented in Chapter 8 to PWRs *in general*:

- method for simulating increased levels of embrittlement
- assessment of the applicability of these results to forged vessels
- effect of vessel thickness

The results of these sensitivities are summarized in the following sections.

9.2.2.1 Simulating Increased Levels of Embrittlement

Use of more realistic models and input values than were used in the calculations that provide the technical basis for the current PTS Rule produces a considerable reduction in the estimated values of TWCF. As detailed in Table 8.4, at 60 EFPY (an operational lifetime beyond that anticipated after a single license extension), the TWCF values estimates for the three study plants lie between 10^{-11} and 10^{-8} events/year. However, the through-wall cracking frequency limit recommended in Chapter 10 as being consistent with Regulatory Guide 1.174 is 10^{-6} events/year. Consequently, to develop a reference temperature based screening limit (see Chapter 11), it was necessary to somehow artificially increase the level of embrittlement of the vessels and, thereby, the estimated TWCF values so that they would approach the 10^{-6} events/year limit. In the baseline calculations reported in Chapter 8, embrittlement was artificially increased by increasing EFPY (increasing time) and extrapolating fluence in linear proportion to time. An alternative procedure for artificially increasing embrittlement would be to allow the temporal and irradiation exposure parameters to remain within realistic ranges and, instead, increase the unirradiated transition temperature (the $RT_{NDT(u)}$)

of the beltline materials. To determine what effect these two procedures have on estimated TWCF values, we performed a sensitivity study using the Beaver Valley and Palisades plants. In this sensitivity study, the 32 EFPY analyses reported in Table 8.4 were treated as a baseline above which embrittlement was increased. Increases in embrittlement achieved by increasing EFPY/time are also reported in Table 8.4. Each EFPY/time increase in this table can be quantified as an increase in the reference temperature by subtracting from the reference temperature associated with a particular EFPY/time increment the reference temperature associated with 32 EFPY. In this sensitivity study, we compared the TWCF increases produced by these EFPY/time-driven reference temperature increases with TWCF increases driven by simply increasing the $RT_{NDT(u)}$ of the beltline materials by some fixed increment. Figure 9.7 shows the result of this analysis, which demonstrates that the EFPY/time method of artificially increasing embrittlement results in TWCF estimates that exceed those produced by the alternative method of increasing $RT_{NDT(u)}$.

It must be emphasized that both of these procedures (as well as any other alternative procedures) extrapolate outside of the empirical bounds of the database used to establish the embrittlement shift model. We selected the EFPY/time extrapolation method over the $RT_{NDT(u)}$ extrapolation method because the embrittlement shift model includes explicitly both time and irradiation exposure variables. During the development of this model, the known physical bases for time/exposure trends were explicitly considered, and this knowledge was incorporated into the functional form of the model [Eason]. Thus, there is some reason to expect that time and irradiation exposure variables will extrapolate better than the fracture toughness before irradiation begins (as quantified by $RT_{NDT(u)}$), which was not considered in the development of the embrittlement shift model.

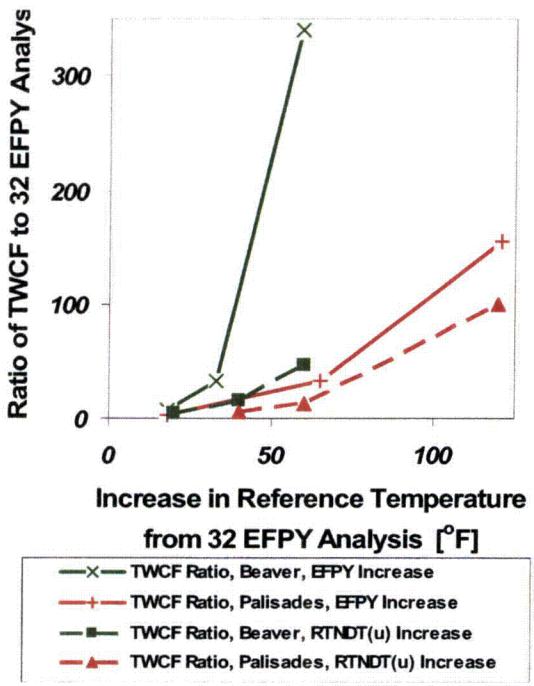

Figure 9.7. Effect of different methods to artificially increase embrittlement on the predicted TWCF values

9.2.2.2 Applicability to Forged Vessels

All three of our study plants are plate vessels. However, 21 of the operating PWRs have beltline regions made of ring-forgings. As such, these vessels have no axial welds. The lack of the large axially oriented axial flaws from such vessels indicates that they should, in general, have much lower values of TWCF than a comparable plate vessel of equivalent embrittlement. However, forgings have a population of embedded flaws that is particular in density and size to their method of manufacture. Additionally, under certain conditions forgings are subject to subclad cracking associated with the deposition of the austenitic stainless steel cladding layer. Thus, to investigate the applicability of the results reported in Chapter 8 to forged vessels, we performed a number of analyses on vessels using properties ($RT_{NDT(u)}$, Cu, Ni, P) and flaw populations appropriate to forgings.

Appendix G details the technical basis for the distributions of flaws used in these sensitivity studies. The distribution of embedded forging flaws is based on destructive examination of an RPV forging [Schuster 02]. These flaws are similar in both size and in density to plate flaws. The distribution of subclad cracks is based on a review of the literature on subclad flaws, in particular that appearing in a summary article [Dhooge 78]. Subclad cracks occur as dense arrays of shallow cracks extending into the vessel wall from the clad to basemetal interface to depths limited by the heat affected zone (~0.08-in. (~2mm)). These cracks are oriented normal to the direction of welding for clad deposition, producing axially oriented cracks in the vessel beltline. They are clustered where the passes of strip clad contact each other. Subclad flaws are much more likely to occur in particular grades of pressure vessel steels that have chemical compositions that enhance the likelihood of cracking. Forging grades such as A508 are more susceptible than plate materials such as A533. High levels of heat input during the cladding process also enhance the likelihood of subclad cracking.

9.2.2.2.1 Embedded Forging Flaw Sensitivity Study

This sensitivity study was constructed as follows:

(1) Two sets of forging properties were selected: those of the Sequoyah 1 and Watts Bar 1 RPVs [RVID2]. These properties were selected because they are among the most irradiation-sensitive of all the forging materials in RVID.

(2) Two hypothetical models of forged vessels were constructed based on our existing models of the Beaver Valley and Palisades vessels. In each case, the hypothetical forged vessels were constructed by removing the axial welds and combining these regions with the surrounding plates to make "forgings." These "forgings" were assigned the properties from Step 1.

(3) A FAVOR analysis of each vessel/forging combination from Steps 1 and 2 was analyzed at two embrittlement levels: 32 EFPY and Ext-B. Thus, a total of 2^3 (or 8) FAVOR analyses were performed (2 material property definitions x 2 vessel definitions x 2 embrittlement levels).

On average, the TWCF of the "forging" vessels was only 3% of the plate welded vessels; at most, it was 15%. These reductions are consistent with those expected when the large axial weld flaws are removed from the analysis.

9.2.2.2.2 Subclad Crack Sensitivity Study

This sensitivity study was constructed as follows:

(1) One set of forging properties was selected: that of the Sequoyah 1 RPV [RVID2].

(2) One hypothetical model of a forged vessel was constructed based on our existing model of the Beaver Valley vessel. The hypothetical forged vessel was constructed by removing the axial welds and combining these regions with the surrounding plates to make a "forging." This "forging" was assigned the properties from Step 1.

(3) A FAVOR analysis of each vessel/forging combination from Steps 1 and 2 was analyzed at three embrittlement levels: 32 EFPY, 60 EFPY, and Ext-B. Thus, a total of 3 FAVOR analyses were performed (1 material property definition x 1 vessel definition x 3 embrittlement levels).

At 32 and 60 EFPY the TWCF of the "forging" vessels was ~0.2% and 18% of the plate welded vessels. However, at the much higher embrittlement level represented by the Ext-B condition the "forging" vessels had TWCF values 10 times higher than that characteristic of plate welded vessels at an equivalent level of embrittlement. While these very high embrittlement levels are unlikely to be approached in the foreseeable future, these results indicate that a more detailed assessment of vessel failure probabilities associated with subclad cracks would be warranted should a

subclad cracking prone forging ever in future be subjected to very high embrittlement levels.

9.2.2.3 Effect of RPV Wall Thickness on TWCF

In Section 8.5.2.4.1, we noted in the FAVOR results for primary side pipe breaks a potential effect of vessel wall thickness on the conditional probability of through-wall cracking. This affect can be expected for the following reasons:

- The magnitude of thermal stress scales in proportion to the thickness, with thicker vessels generating higher levels of thermal stress. Figure 9.8 shows the effect of this increased thermal stress on the applied driving force to fracture associated with a large-diameter pipe break. This effect will tend to increase the probability of through-wall cracking for thicker vessels.
- Because thicker vessels will have a larger volume of plate material and a larger weld fusion line area, they will also have a larger number of flaws. This effect will also tend to increase the probability of through-wall cracking for thicker vessels.
- There is more distance in a thicker vessel over which an initiated crack can arrest, thereby not failing the vessel. Also, thicker vessels would tend to have more weld layers with different Cu contents. This effect will tend to reduce the probability of through-wall cracking for thicker vessels.

To investigate the effect of these first two factors (the third could not be investigated without modifying the structure of the FAVOR code), we increased the thickness of the Beaver Valley vessel from 7.875-in. (20-cm) (its actual thickness) in 5 increments up to 11-in. (27.9-cm) (characteristic of the thickest PWRs in service, see Figure 9.9). For each of these 5 thicker versions of Beaver Valley, we used FAVOR to estimate the CPTWC of the following four transients (all of which are dominant contributors to the TWCF of Beaver Valley):

- BV9: 16-in. diameter hot leg break
- BV56: 4-in. diameter surge line break
- BV126: stuck-open safety relief valve that recloses after 100 minutes resulting in repressurization of the primary system
- BV102: main steam line break

Figure 9.10 shows that increasing the vessel wall thickness increases the CPTWC for all four transients. Recalling that these CPTWC values would be weighted by their bin frequencies (and those of other transients) to obtain a TWCF estimate, these results suggest that through a wall thickness of 9.5-in. (24.13-cm) (thicker than all but three of the in-service PWRs), the integrated effect of wall thickness on TWCF should be modest (factor of ~3 increase at most) relative to our analyses (see Chapter 8) of one 7.875-in. (20-cm) thick vessel and two 8.5-in. (21.6-cm) thick vessels. For vessels of greater wall thicknesses, a plant-specific analysis is warranted to properly capture all aspects of increased vessel wall thickness on TWCF. However, given that the three plants of 11-in. (27.9-cm) and greater thickness are Palo Verde Units 1, 2, and 3, and these vessels have very low embrittlement projected at either EOL or EOLE, the practical need for such plant-specific analysis is mitigated. It can also be noted that using the TWCF results from Chapter 8 will overestimate the TWCF of the seven thinner operating PWRs (7-in. (17.78-cm) thick or less).

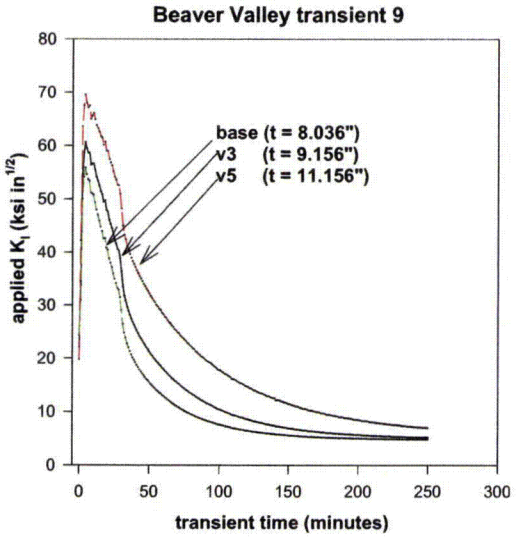

Figure 9.8. Effect of vessel wall thickness on the variation of applied-K_I *vs.* time for a 16-in. (40.64-cm) diameter hot leg break in Beaver Valley. The flaw has the following dimensions: ℓ=0.35-in., $2a$=0.50-in., $2c$=1.5-in. (ℓ=8.89-mm, $2a$=12.7-mm, $2c$=38.1-mm)

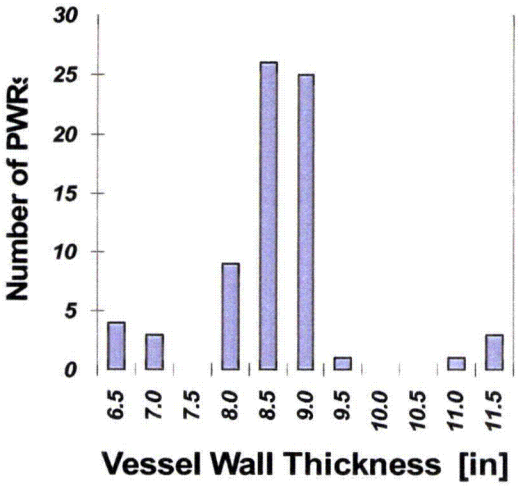

Figure 9.9. Distribution of RPV wall thicknesses for PWRs currently in service [RVID2]

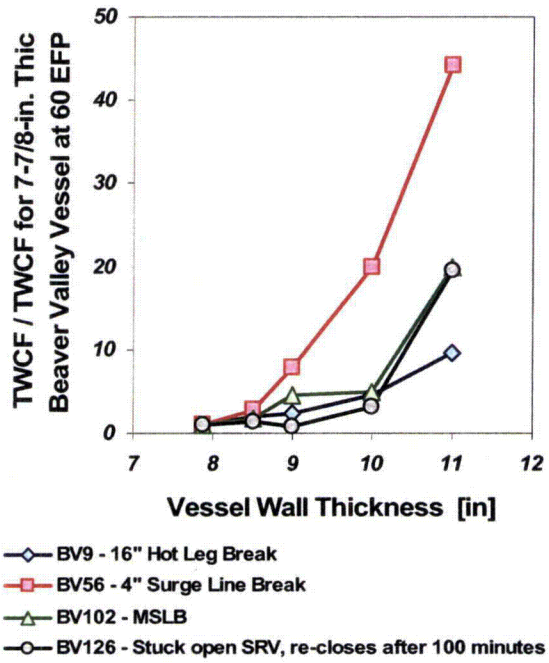

Figure 9.10. Effect of vessel wall thickness on the TWCF of various transients in Beaver Valley (all analyses at 60 EFPY)

9.2.3 Summary and Conclusions

This section summarized sensitivity studies on our PFM model (and on PFM-related variables) performed with two aims in mind:

- To provide confidence in the ***robustness*** of our PFM model we assessed the effect of credible model and input perturbations on TWCF estimates:
  - flaw distribution (size and density of simulated flaws)
  - residual stresses assumed to exist in the RPV wall
  - embrittlement shift model: model used and treatment of uncertainties
  - re-sampling of chemical composition variables at the ¼T, ½T, and ¾T locations for welds
  - crack face pressure
  - upper shelf toughness model

- To provide confidence that the results of our calculations for three specific plants can be ***generalized*** to apply to all PWRs, we performed sensitivity studies to assess the influence of factors not fully considered in our baseline TWCF estimates (see Chapter 8):
  - method for simulating increased levels of embrittlement
  - assessment of the applicability of these results to forged vessels
  - effect of vessel thickness

In the former category, all effects were negligible or small. The small effects included our adoption of an embrittlement shift model different from that in ASTM E900-02 (which increases TWCF by ~3x) and our model that accounts for distinctly different Cu contents in different weld layers (which reduces TWCF by ~ 2.5x relative to the assumption that the mean value of Cu does not vary through the vessel thickness). Neither of these effects is significant enough to warrant a change to our baseline model, or to recommend a caution regarding its robustness.

Sensitivity studies in the latter category suggest the following minor cautions regarding the applicability of the results in Chapter 8 to PWRs *in general*:

- In general, the TWCF of forged PWRs can be assessed using the Chapter 8 results by ignoring the TWCF contribution of axial welds. However, should changes in future operating conditions result in a forged vessel being subjected to very high levels of embrittlement, a plant-specific analysis to assess the effect of subclad flaws on TWCF would be warranted.
- For PWRs with thicknesses of 7.5 to 9.5-in. (19.05 to 24.13-cm), the TWCF results in Chapter 8 are realistic. The Chapter 8 results overestimate the TWCF of the seven thinner vessels (wall thicknesses below 7-in. (17.78-cm)) and underestimate the TWCF of Palo Verde Units 1, 2, and 3, all of which have wall thicknesses above 11-in. (27.94-cm). However, these vessels have very low embrittlement projected at either EOL or EOLE, suggesting little practical effect of this underestimation.

9.3 Plant-to-Plant Differences in Design/Operational Characteristics that Impact PTS Transient Severity

This section describes an effort in which we examined the plant design and operational characteristics of five additional high-embrittlement plants. Our aim was to identify whether the design and operational features that are the key contributors to PTS risk (see Section 8.6) vary significantly enough in the larger population of PWRs to question the generality of our results. Full details of this work are reported elsewhere [***Whitehead-Gen***].

In this activity, we focused on several plants beyond the three for which we have conducted detailed plant-specific analyses to assess PTS risk. To identify which additional plants to study, Table 9.5 was constructed early in 2002. At the time, we understood from our plant-specific analyses of Oconee that circumferential welds did not contribute significantly to through-wall cracking. Therefore, we calculated a reference temperature metric for each plant equal to the sum of the un-irradiated RT_{NDT} plus the embrittlement shift after 40 years of operation [Eason] calculated for the most irradiation-sensitive region in the beltline (i.e., most irradiation-sensitive axial weld, plate, or forging; circumferential welds were excluded). This metric, shown as a column in Table 9.5, provided an approximate ranking of the PTS sensitivity of the plants based on information we had available at the time. Since the goal of this activity was to determine whether the design and operational features that we have identified as being the key contributors to PTS risk (see Section 8.6) vary significantly enough in the larger population of PWRs to question the generality of our findings from Chapter 8, we felt it important to select the most embrittled plants from the list. In the end, we selected the following five plants:

- Salem 1 (W-4[1]) [comparable to Beaver Valley (W-3[2])]
- TMI 1 (B&W[3]) [comparable to Oconee]
- Ft. Calhoun (CE[4]) [comparable to Palisades]
- Diablo Canyon 1 (W-4) [comparable to Beaver Valley]
- Sequoyah 1 (W-4) [comparable to Beaver Valley]

Following identification of the study plants, we conducted the following three activities:

- A questionnaire was developed to elicit PTS-relevant information about the additional PWRs.
- Responses to the questionnaire were examined to determine whether results from the detailed analyses were generically applicable to the additional PWRs.
- Conclusions were generated as to the generic applicability of the detailed results.

We compared potentially important design and operational features (as related to PTS) of these five PWRs to the same features from the three plants on which we have performed detailed analyses to determine whether these features are similar or different. Based on these comparisons, we made judgments regarding the appropriateness of treating the results presented in Chapter 8 as being representative of PWRs *in general.*

Section 9.3.1 details the questionnaire we developed and sent to the five plants, while Section 9.3.2 details our analysis of the results we obtained. Combined observations and overall conclusions are provided in Section 9.3.3.

9.3.1 Generalization Questionnaire

Based on the insights obtained during an examination of the results from the three plant-specific studies, the analysts identified five general event scenarios for which plant design and operational features should be obtained. Plant design and operational features were examined to identify those that play a role in determining the importance of these five overcooling scenarios.

Table 9.6 identifies the scenarios and their corresponding plant design and operational features. Once the scenarios and the design and operational features were identified, a questionnaire was constructed. Collection of the information via this questionnaire was facilitated by an industry representative working under the auspices of the Electric Power Research Institute (EPRI).

9.3.2 Analysis of Collected Information

Our analysis of the plant design and operational information collected via the questionnaire entails both PRA/HRA and TH information. Judgmental analysis of the comparable design and operational information between Oconee, Beaver Valley, and Palisades and the generalization plants (i.e., Ft. Calhoun, TMI, Diablo Canyon, Sequoyah, and Salem) was performed to determine if there are any differences that would be expected to have a significant impact on any conclusions that would be reached by the activity if it were to be performed in detail (i.e., to the same level of rigor as was done in the plant-specific analyses). The following subsections summarize the results of the PRA/HRA (9.3.2.1) and TH judgmental analyses (9.3.2.2)

---

1 W-4 denotes a Westinghouse 4-loop design.
2 W-3 denotes a Westinghouse 3-loop design.
3 B&W denotes Babcock and Wilcox.
4 CE denotes Combustion Engineering.

9.3.2.1 PRA/HRA Judgmental Analyses

For **secondary breaches**, the following observations were made:

- For generalization issue (GI) 1[‡‡‡‡‡], each of the generalization plants is similar to or better than their corresponding detailed plant. Thus, for GI 1, we conclude that there would be no significant adverse differences between the generalization plants and their corresponding detailed plant.
- For GI 2, each of the generalization plants is similar to their corresponding detailed plant. Thus, for GI 2, we conclude that there would be no significant adverse differences between the generalization plants and their corresponding detailed plant.
- For GI 3, each of the generalization plants is similar to their corresponding detailed plant with one possible exception. For Salem, it appears that early isolation opportunities exist; however, exactly when these occur is not clear. Nonetheless, since Salem's procedures are based on Westinghouse Owners Group (WOG) Emergency Response Guidelines, it is expected that Salem is similar to its corresponding detailed analyzed plant, Beaver Valley. Thus, for GI 3, we conclude that there would be no significant adverse differences between the generalization plants and their corresponding detailed plant.

‡‡‡‡‡ GI # refers to the number assigned to each generic issue. For example, GI 1 refers to *number of MSIVs* and GI 26 refers to *emergency operating procedure (EOP) criteria for initiation of feed-and-bleed.*

Table 9.5. Plant list for generalization study

Tolerance to a PTS Challenge		Plant Name	NSSS Vendor	Most Embrittled Material	$RT_{NDT(u)}$ + Irradiation Shift at 40 years [°F]	Vessel Manufacturer
The estimated tolerance to a PTS challenge increases as the number in the next column increases (i.e., plants with the lowest ranking have the most embrittled materials).	1	Salem 1	Westinghouse	Plate	204	Combustion Engineering
	2	Beaver Valley 1	Westinghouse	Plate	194	Combustion Engineering
	3	TMI-1	Babcock & Wilcox	Axial Weld	186	Babcock & Wilcox
	4	Fort Calhoun	Combustion Engineering	Axial Weld	181	Combustion Engineering
	5	Palisades	Combustion Engineering	Axial Weld	179	Combustion Engineering
	6	Calvert Cliffs 1	Combustion Engineering	Axial Weld	178	Combustion Engineering
	7	Diablo Canyon 1	Westinghouse	Axial Weld	171	Combustion Engineering
	8	Diablo Canyon 2	Westinghouse	Plate	170	Combustion Engineering
	9	Sequoyah 1	Westinghouse	Forging	167	Rotterdam Dockyard
	10	Watts Bar 1	Westinghouse	Forging	164	Rotterdam Dockyard
	11	St. Lucie 1	Combustion Engineering	Axial Weld	164	Combustion Engineering
	12	Surry 1	Westinghouse	Axial Weld	163	Babcock & Wilcox
	13	Indian Point 2	Westinghouse	Plate	162	Combustion Engineering
	14	Ginna	Westinghouse	Forging	161	Babcock & Wilcox
	15	Point Beach 1	Westinghouse	Axial Weld	159	Babcock & Wilcox
	16	Farley 2	Westinghouse	Plate	158	Combustion Engineering
	17	Mcguire 1	Westinghouse	Axial Weld	158	Combustion Engineering
	18	Oconee 1	Babcock & Wilcox	Axial Weld	157	Babcock & Wilcox
	19	North Anna 2	Westinghouse	Forging	155	Rotterdam Dockyard
	20	Shearon Harris	Westinghouse	Plate	153	Chicago Bridge & Iron
	21	North Anna 1	Westinghouse	Forging	153	Rotterdam Dockyard
	22	Cook 2	Westinghouse	Plate	152	Chicago Bridge & Iron
	23	Salem 2	Westinghouse	Axial Weld	148	Combustion Engineering
	24	Crystal River 3	Babcock & Wilcox	Axial Weld	141	Babcock & Wilcox
	25	Calvert Cliffs 2	Combustion Engineering	Plate	139	Combustion Engineering
	26	Robinson 2	Westinghouse	Plate	138	Combustion Engineering
	27	Cook 1	Westinghouse	Axial Weld	138	Combustion Engineering
	28	Farley 2	Westinghouse	Plate	133	Combustion Engineering
	29	Farley 1	Westinghouse	Plate	133	Combustion Engineering
	30	Arkansas Nuclear 1	Babcock & Wilcox	Axial Weld	129	Babcock & Wilcox

Notes:

Plants analyzed in the PTS reevaluation effort.

Plants compared in the Generalization activity.

Table 9.6 Important PTS scenarios and corresponding plant design and operational features

		Scenario Types				
		Secondary Breach	**Secondary Overfeed**	**LOCA Related**	**PORV and SRV Related**	**Feed and Bleed Related**
Generalization Issues (Number)		Number of MSIVs (1)	Information on the feed (MFW and AFW or emergency feedwater (EFW)) capabilities to the steam generators including inventory of water available to continue MFW or AFW/EFW (8)	Allowable range of safety injection water temperatures (11)	Number and sizes of PORVs and SRVs, whether each plant operates with PORV block valves normally shut, and if there are any auto-operation features of the PORVs (20)	Number of AFW/EFW pumps/flow paths versus minimum success criteria for adequate feed to the steam generators (hints to reliability of AFW/EFW and, hence, probability for going to feed-and-bleed) (25)
		Isolation capability with regards to other paths (2)	Information on normal steam generator inventory (9)	Information to estimate recirculation water temperature (12)	Instrumentation available (e.g., acoustic monitors, differential pressure, etc.) to identify open PORVs or SRVs and to notice if they have reclosed (21)	Emergency operating procedure (EOP) criteria for initiation of feed-and-bleed (26)
		Identification of procedures, steps, and location of steps within procedures that ensure likelihood of early identification and isolation of faulted steam generators (3)	Information on possible feed temperatures for all feed sources (especially how cold they could be) (10)	Safety injection/ accumulators water source size (i.e., inventory) (13)	Procedures for addressing LOCAs resulting from stuck-open PORVs or SRVs (22)	Number of PORVs opened out of total available (or even SRVs if pumps can open SRVs) when in feed-and-bleed mode (27)
		Operator training or procedural allowances that support early isolation of steam generators (4)		Safety injection flow rate versus LOCA break size (14)	Procedures for addressing the sudden reclosure of such valves, including safety injection (SI) throttling/termination guidance (23)	Number of HPI pumps used in feed-and-bleed and is actual flow rate equivalent to number of pumps (28)
		Location and size of steamline flow restrictors (5)		Charging, high-pressure injection (HPI), and low-pressure injection (LPI) shutoff heads (15)	Operating characteristics of the charging system when pressurizer level goes back high (e.g., stop, keep running) (24)	
	Key Assumptions Relative to MSLB Analysis	Auxiliary feedwater (AFW) and main feedwater (MFW) control during steamline break (or similar) (6)		Actuation requirements for containment spray and flow rate once running (16)		
		Determination of whether turbine-driven AFW pump (auto) isolates in MSLB (7)		Impact on HPI, LPI, and charging when sump switchover occurs (which pumps on vs. off) (17)		
				Any significant changes in flow rates going from injection to recirculation (18)		
				Accumulator (e.g., safety injection tank (SIT), core flood tank (CFT)) discharge pressure (19)		

- For GI 4, each of the generalization plants is similar to their corresponding detailed plant with one possible exception. For Salem, it appears that training supports early action, even though it is unclear exactly when the actions would occur. Since Salem's procedures are based on Westinghouse Owners Group (WOG) Emergency Response Guidelines, it is expected that Salem is similar to its corresponding detailed analyzed plant, Beaver Valley. Thus, for GI 4, we conclude that there would be no significant adverse differences between the generalization plants and their corresponding detailed plant.
- GI 5 is not a PRA/HRA issue. This issue is examined in section 9.3.2.2.
- For GI 6, each of the generalization plants is similar to or as good as their corresponding detailed plant. Thus, for GI 6, we conclude that there would be no significant adverse differences between the generalization plants and their corresponding detailed plant.
- For GI 7, each of the generalization plants is similar to their corresponding detailed plant with one exception. For TMI the turbine-driven AFW pump is not automatically isolated while it is automatically isolated for the corresponding detailed analyzed plant, Oconee. Thus, for GI 7, this could increase the importance of a faulted steam generator for the Babcock & Wilcox (B&W) generalization plant.

From the observations provided above, only GI 7 has the potential for a significant adverse difference between the generalization plants and their corresponding detailed plant — and that only for the B&W generalization plant (i.e., TMI). However, when observations for GI 3 and GI 4 are considered in combination, we expect the importance of the GI 7 difference to be minimal, since operators would be expected to isolate the feed flow. Thus, we conclude that for secondary breaches, no significant adverse differences exist.

For **secondary overfeed**, the GIs are not PRA/HRA issues. These issues are examined in section 9.3.2.2.

For **LOCA-related**, the GIs are not PRA/HRA issues. These issues are examined in the in section 9.3.2.2.

For **PORV- and SRV-related**, the following observations are made:

- For GI 20, generic data were used to estimate the probabilities associated with the sticking open and subsequent closure of either PORVs or SRVs [Poloski 99]. No significant differences are expected for Westinghouse and B&W plants. For the Combusting Engineering (CE) generalization plant, Fort Calhoun, we might expect a higher estimated probability of having a stuck-open valve. This expectation comes from the fact that Fort Calhoun experienced one of the two stuck-open valve events that were used to estimate the generic probability of a stuck-open valve (1.6E-3). If we approximate the probability by using one event in the 12 years covered by [Poloski 99] (the most conservative interpretation of the data), we get approximately 0.08. Using this approximate value for Fort Calhoun, the probability associated with stuck-open valves would increase by about a factor of 50. This ignores the fact that there may be appropriate reasons to combine both generic PWR experience and the Fort Calhoun plant-specific experience (such as through a Bayesian analysis) or to obtain other information to arrive at a more realistic estimate of a stuck-open valve event at Fort Calhoun.

  In an effort to determine a more realistic estimate, additional information was obtained with the help from staff at Fort Calhoun Station about the SRV opening event that actually happened in 1992, subsequent analyses of the root cause, and the corrective actions. This additional information [LER 92-023, LER 92-028, and NRC-IR] including phone conversations with plant staff, revealed that the causes of

the actual event are well-understood, and actions have been taken that should make Fort Calhoun no more susceptible to SRV demand events than other PWRs.
In particular, the event was caused by both a SRV setpoint drift as a result of movement of an adjusting nut during valve vibrations that resulted in a lower setpoint for valve opening, and determination that setpoint calibration of the SRVs at an outside laboratory was not being done under laboratory conditions (particularly temperature conditions) that sufficiently approximated actual plant installation conditions closely enough. This latter situation was unknowingly contributing to the SRV setpoint being lower than what was specified.

The SRVs at Fort Calhoun are manufactured by Crosby (one of the manufacturers used in other plants), so Fort Calhoun is not unique from this perspective. The specific corrective actions included adding a torque setting for the adjusting nut that did not exist in the procedures, adding a locking nut that prevents inadvertent movement of the adjusting nut, and changes in the laboratory setup and procedures during valve calibration that now allow for sufficient approximation of actual installation conditions. Additionally, Fort Calhoun, like other plants, has lowered the plant's high-pressurizer pressure trip setpoint, making it less likely to cause an SRV demand.

Considering the use of a valve manufacturer not uncommon among PWRs, changes in the plant's high-pressure setpoint to be like other PWRs, the specific "fixes" for the identified Fort Calhoun SRV problems, and a history of no subsequent SRV events or significant problems at Fort Calhoun since 1992, we conclude that no evidence exists to suggest that Fort Calhoun is any more susceptible to SRV events than other PWRs. Hence, our best estimate of Fort Calhoun's frequency of stuck-open SRV events looking to the future, is that Fort Calhoun can be treated as among the "generic" population of PWRs, and the generic value used for such events in our PTS models can be used for Fort Calhoun. Hence, there is no identifiable frequency difference to be considered in this generalization study.

Thus, for GI 20, we conclude that there would be no significant adverse differences between the generalization plants and their corresponding detailed plant.

- For GI 21, except for possibly Salem, all plants have multiple indications to know when pressurizer PORV/SRVs are open and/or reclose. Thus, it would be appropriate to postulate that for Salem, there might be some increase in the human error probability (HEP) associated with the failure to throttle because operators have less direct indication of stuck-open valves (e.g., no acoustic monitors) and, thus, less indication of valve reclosure than for Beaver Valley (the corresponding detailed plant). Without a detailed analysis of the specifics associated with stuck-open valves that reclose at Salem, it is difficult to estimate the amount of increase in the throttling HEP. Nonetheless, given the fact that there are indications available at Salem (although they are neither as redundant nor as direct as for other plants), we expect the HEP for failure to throttle should not increase by more than a factor of 5 (at most). Thus, for GI 21, we conclude that Salem is the only generalization plant that might have a significant adverse difference compared to the corresponding detailed plant.
- For GI 22, it appears that procedural guidance is sufficiently similar among all plants. From this similarity, we do not expect significant differences in operator response or large delays in attempting to isolate paths (e.g., >15–20 minutes). Thus, for GI 22, we conclude that there would be no significant adverse differences between the generalization plants and their corresponding detailed plant.
- For GI 23, all plants have throttling guidance and specific steps; particularly once a transition to the appropriate procedure occurs. For the very rapid rise in RCS pressure and subcooling that would occur with an unexpected/sudden reclosure

of PORVs or SRVs, it would seem that there is likely to be some delay in responding to the very quick transition from a saturated RCS to a filled RCS (as we have seen for the analyzed plants). Thus, for GI 23, we conclude that there would be no significant adverse differences between the generalization plants and their corresponding detailed plant.

- For GI 24, all plants require (or appear to require) manual action to control charging flow. Thus, for GI 24, we conclude that there would be no significant adverse differences between the generalization plants and their corresponding detailed plant.

From the observations provided above, one potential difference has been found between the detailed analysis plants and the generalization plants. For Salem, the frequency could increase by at most a factor of 5 (GI 21).

For **feed-and-bleed-related**, the following observations are made:

- For GI 25, all plants appear to have a similar "over-capacity" of feed than what is needed for sufficient heat removal. Hence, losing all feedwater and having to go to feed-and-bleed would seem similarly "unlikely." To test this, information in Table D-5 of NUREG/CR-5500, Vol. 1 [Poloski 98] was examined. From this examination, we found that for B&W plants, the generalization plant (TMI) has an AFW/EFW unavailability that is a factor of 1.2 higher than the detailed plant (Oconee). For the Westinghouse plants, the unavailability is either lower for the generalization plants (Diablo Canyon and Salem) or higher by a factor of 1.1 (for Sequoyah) compared to the detailed plant (Beaver Valley). For the CE plants, the unavailability for the generalization plant (Ft. Calhoun) is a factor of 26 higher than the detailed analysis plant (Palisades). However, this does not include credit for the diesel-driven AFW pump at the generalization plant. If we conservatively assign a 0.1 probability of failure to the diesel-driven pump, this difference becomes a factor of 3. Thus, for GI 25, we conclude that only the CE generalization plant would have a frequency that is somewhat higher than its detailed analysis plant.
- For GI 26, all plants have specific criteria that direct the operators to go to feed-and-bleed. While there are some differences in the specifics, it is unlikely that such specifics would substantially affect the operators' response. Thus, for GI 26, we conclude that there would be no significant adverse differences between the generalization plants and their corresponding detailed plant.
- GI 27 is not a PRA/HRA issue. This issue is examined in in section 9.3.2.2.
- GI 28 is not a PRA/HRA issue. This issue is examined in section 9.3.2.2.

From the observations provided above, one potential difference has been found between the detailed analysis plants and the generalization plants. For Fort Calhoun, the frequency could increase by about a factor of 3 (GI 25).

9.3.2.2 TH Judgmental Analyses

9.3.2.2.1 Introduction

To facilitate the performance of the individual judgmental TH analyses, the five general scenarios identified in Table 9.6 of Section 9.3.1 were recategorized into four basic groups based on (1) more global examination of the dominant types of scenarios in more detail and the less-dominant scenarios, (2) the TH characteristics of the scenarios in the group, and (3) the systems that determine the downcomer fluid temperature behavior. These groups are described in the following subsections.

9.3.2.2.1.1 Group 1: Large-Diameter Pipe Breaks

Group 1 consists of LOCAs with a break diameter of 8-in. (20.32-cm) or greater. This group of LOCAs results in rapid system cooldown and complete system depressurization. The operator trips the reactor coolant pumps in these transients because of loss of primary system subcooling. The high- and low-pressure injection systems are running at or near pump runout conditions within several minutes of initiation. The safety injection tanks also discharge within several minutes. With the combined flow of the injection systems and safety injection tank discharge, the downcomer is filled with subcooled water after the initial blowdown for the duration of the transient[§§§§§]. The downcomer fluid temperature is principally determined by the flow from the high- and low-pressure injection systems, the safety injection tank discharge, and the initial temperature of the water used in the injection systems.

9.3.2.2.1.2 Group 2: Small- to Medium-Diameter Pipe Breaks

Group 2 consists of LOCAs with a break diameter of 2.0 to 5.7-in. (5.08 to 14.37-cm). This group of LOCAs results in slower cooldown and depressurization than the Group 1 transients. For this break diameter range, the balance between break flow and ECCS injection flow governs the primary system cooldown and depressurization rate. The operator trips the reactor coolant pumps in these transients because of loss of primary system subcooling, although there is some trip time variation for different break sizes. Safety injection tank discharge and initiation of low-pressure injection occur later in the sequence, relative to Group 1 transients. In cases where the break diameters are small, low-pressure injection flow may not be initiated at all. Also, the safety injection tanks may not totally discharge, again depending on the break size. In this range of break sizes, the system pressure limits the rate of high- and low-pressure injection system injection to the reactor system. The downcomer fluid conditions are principally determined by the break diameter, the flow from the high- and low-pressure injection systems, the safety injection tank discharge, and the initial temperature of the water used in these systems. The break location plays a role in the downcomer fluid conditions. In the case of a cold leg break, some of the ECCS goes directly out the break instead of into the downcomer, resulting in warmer downcomer fluid temperatures over an equivalent-sized hot leg break. Note that the use of feed-and-bleed can be considered to "fit" within this group, since this involves one or more open pressurizer valves (hence, like a LOCA) with successful safety injection. Since feed-and-bleed can be controlled by the operator, it cannot be worse than an equivalent-sized break.

9.3.2.2.1.3 Group 3: Stuck-Open Valves in the Primary System that Reclose

Group 3 consists of transients involving stuck-open primary side SRVs that reclose. This group of transients results in cooldown and depressurization characteristics of a LOCA with a diameter at the low end of the Group 2 range. Once the valve recloses, the system heats up as a result of the loss of primary system coolant flow out the valve, and repressurizes as a result of charging or high-pressure injection flow. The operator trips the reactor coolant pumps in these transients because of loss of primary system subcooling, although there may be some time separation when individual pumps are tripped depending on the trip criteria used. In Group 3 transients, low-pressure injection flow is not initiated. Safety injection tanks do not generally totally discharge because the system remains at relatively high pressure, compared to Groups 1 and 2. The high-pressure injection system is not operating near pump runout conditions, especially once the valve recloses. In this range of break sizes, the break flow limits the rate of high-pressure injection system injection to the reactor system.

§§§§§ The term "transient" is used in its generic sense to represent the occurrence of a set of events that lead to a specific outcome

9.3.2.2.1.4 Group 4: Main Steam Line Breaks and Other Secondary Side Failures

Group 4 consists of main steam line breaks and other secondary side failures (e.g., valve openings, overfeed). This group of transients results in overcooling of the primary system through the steam generator loop affected by the failure of the steam line or other secondary fault. The response of these events is determined by numerous factors, including break location and operator actions. If the operator isolates the affected steam generator within a reasonable time, the primary system cooldown stops. The secondary side pressure equalizes with the containment pressure (slightly above atmospheric), and the secondary side fluid is near saturation temperature (somewhat subcooled as a result of adverse containment conditions). On the primary side, the operator does not trip the reactor coolant pumps, as subcooling is not lost; however, if the break is inside containment, the reactor coolant pumps are manually tripped as a result of adverse containment conditions. High-pressure injection starts but does not operate at runout conditions, as the primary system pressure remains high. Low-pressure injection initiation and safety injection tank discharge do not occur. The downcomer fluid conditions generally remain subcooled throughout the transient.

Included in Group 4 are transients involving stuck-open secondary side SRVs and overfeeds. Like the main steam line break, this group of transients results in overcooling of the primary system through the steam generator loop affected by the stuck-open valve or overfeed. The cooldown rate is much slower because the flow through the valve is much lower than the flow through the failed steam line, and the consequences of any overfeed are not significant, particularly if isolated by the time the SG(s) are full. The operator does not trip the reactor coolant pumps, as subcooling is not lost. High-pressure injection starts but does not operate at runout conditions, as the primary system pressure remains high. Low-pressure injection initiation and safety injection tank discharge are not likely to occur. The downcomer fluid conditions generally remain subcooled throughout the transient.

9.3.2.2.2 Analysis

The approach used for the plant TH generalization is to compare key design features in conjunction with the RELAP5 TH results for the Oconee, Beaver Valley, and Palisades plants against the comparable designs in the generalization plants to determine whether there are any differences that would have a significant impact on the downcomer fluid temperature prediction. System pressure is considered in those transients where repressurization occurs. Further information and data on the four groups of TH sequences is presented in [***Whitehead-Gen***].

9.3.2.2.2.1 Group 1: Large Diameter Pipe Breaks

Group 1 sequences result in the most rapid cooldown and depressurization of any of the dominant sequences analyzed for the Oconee, Beaver Valley, and Palisades plants. S ystem cooldown and depressurization is essentially complete by about 150 seconds for 16-in. (40.64-cm) diameter LOCAs. For 8-in. (20.32-cm) LOCAs, the time for system depressurization to occur is longer because the break area is a factor of 4 lower than in the case of a 16-in. (40.64-cm) break. For the 8-in. (20.32-cm) break, the system depressurizes to 1.38 MPa [200 psia] in about 300 seconds for the Beaver Valley and Palisades plants. For Oconee, the system depressurizes to under 1.38 MPa [200 psia] in about 600 seconds.

Similar downcomer temperature characteristics are expected in the generalization plants, factoring in the plants' power level, primary system volume and ECCS design differences. For the CE designs, the comparable plants are Fort Calhoun and Palisades. Some differences are found in the injection system capacities and safety injection tank water volume as a result of the difference in power level between these plants, although differences in the reactor vessel volume may also be a factor as a key function of

the safety injection tanks is to refill the reactor vessel after blowdown. In any event, the safety injection tanks are designed to refill the system in large-break LOCAs.

In the case of B&W plants, the Oconee and TMI plants are comparable. These plants have about the same power level (2,568 MWt for Oconee compared to 2,530 MWt for TMI). The ECCS flow and safety injection tank volumes are comparable, which is not surprising, given that these plants operate at about the same power level.

The comparable Westinghouse plants are Beaver Valley, Diablo Canyon, Sequoyah, and Salem. These plants have significant basic design differences, including the core power level and number of loops in the plant. The core power level in Beaver Valley is 2,652 MWt compared to 3,338 MWt for Diablo Canyon (Unit 1) and 3,411 MWt for the Salem and Sequoyah plants. Beaver Valley is a 3-loop design, while Diablo Canyon, Salem, and Sequoyah are 4-loop designs. As a result, the system volume for Beaver Valley is less than the 4-loop plants[7]. The Beaver Valley plant has three safety injection tanks (one for each loop), compared to four injection tanks for the other plants. As noted earlier, reactor vessel volume is a factor since a key function of the tanks is to refill the vessel after blowdown. Because of the higher power levels, ECC injection flow is higher in the comparison plants compared to Beaver Valley.

The initial water temperature in the high- and low-pressure injection system and safety injection tanks is a factor in the cooldown rate and in the final downcomer fluid temperature. A review of the data obtained from the generalization plants show that the temperatures used in the plant analyses for Oconee, Beaver Valley, and Palisades is in the range of injection temperatures used in all plants. All the plants operate with injection temperatures within a range set in the plant technical specifications, which is represented by the temperatures used in the analysis.

In summary, no differences in the plant system designs have been found that will cause significant differences in the downcomer fluid temperature from a thermal-hydraulic perspective. It is possible that there will be temperature variations attributable to the power level (i.e., MWt), although breaks in the range of 8 to 16-in. (20.32 to 40.64-cm) are sufficiently large that the water injected into the system as a result of combined high- and low-pressure injection and safety injection tank discharge largely governs the downcomer fluid temperature. Also, the conditional probability of vessel failure is at a maximum in this break size diameter range, as discussed in Sections 8.5.2.4.1 and 9.1.2.1of this report.

9.3.2.2.2.2 Group 2: Small- to Medium-Diameter Pipe Breaks

The Group 2 sequences result in a slower cooldown and depressurization rate compared to the Group 1 dominant sequences for the Oconee, Beaver Valley, and Palisades plants. No general behavior pattern emerges in downcomer temperature for this mix of transients compared to the Group 1 transients. This lack of a general pattern is attributable to variations in such factors as break location, assumed injection temperature, and initial reactor power level. In addition, different operator actions, pump shutoff heads, and trip setpoints are also factors.

Although the downcomer temperature results are highly variable among the plant types, generalization among plants by a given vendor can still be made. In the range of break sizes from 2.0 to 5.7-in. (5.08 to 14.37-cm) from hot full-power conditions, the rate of injection is limited by the size of the break, particularly as the break sizes becomes smaller. As a result, variations in reactor power level have more of an impact on downcomer temperature predictions compared to Group 1. Safety injection tank discharge and low-pressure injection flow initiation occur later, if at all.

[7] The plant design factors in the power level when selecting ECCS injection and safety injection tank capacities.

The tendency of the injection flow to be limited by the break flow in Group 2 transients also limits the amount of energy that can be discharged through the break. Higher-power systems have a larger system volume with more steel mass and more water in the steam generators on the secondary side. Consequently, for a given break size, the higher-power systems should result in a slower cooldown and depressurization rate and, hence, somewhat warmer downcomer temperatures, particularly during depressurization, given comparable ECC injection rates. In general, the cooldown rate should be slower for the Salem, Sequoyah, and Diablo Canyon plants (compared to Beaver Valley), as these plants operate at higher reactor power relative to Beaver Valley. Conversely, a reactor system that operates at lower power could have a faster cooldown rate, which is the situation between the Palisades and Fort Calhoun plants. However, the capacity of the high- and low-pressure injection systems is smaller and generally scaled to the core power. Comparing Palisades and Fort Calhoun, for example, the high-pressure injection system pump at Palisades has about twice the flow capacity as at Fort Calhoun, so these plants should have comparable depressurization and cooldown rates. Once the system has depressurized and reached an equilibrium pressure, the downcomer temperature becomes comparable among the plants and is principally governed by the injection water temperature.

For hot zero power conditions, downcomer temperature behavior should be less sensitive to the power level, simply because the power level is low. For the analyzed plants, the assumed power level is 0.2% of rated core power (about 5 MWth) for hot zero power operation. If analyses were performed for the generalization plants, the models could be initialized to the same power level. In this case, the difference among plants of similar design would be small.

An issue that needs to be considered for the thermal-hydraulic generalization is the switchover of the ECCS injection suction from the refueling water storage tank (or equivalent) to the containment sump. The increase in downcomer fluid temperature later in the transient is attributable to this switchover at a point in time after system cooldown and depressurization has occurred, so the downcomer temperature is governed by the injection temperature. Many times, however, vessel failure is predicted to occur *before* switchover of ECCS suction. As a result, ECCS suction switchover to the containment sump is generally unimportant to the vessel failure prediction.

In summary, break flow and energy released through the break govern the rate of cooldown and depressurization in the reactor system. For hot full-power cases, the cooldown and depressurization rates are expected to be slower for reactor systems that operate at higher powers and faster for systems that operate at lower powers. However, since the flow capacity of the high-pressure injection pumps at Fort Calhoun is about one-half that of Palisades, all generalization plants should have depressurization and cooldown rates that are comparable to their corresponding detailed analysis plant. The difference in cooldown and depressurization rates should have less of an impact on downcomer temperature if the transient begins from hot zero power operation.

It should be noted that the feed-and-bleed LOCA scenarios have a thermal-hydraulic behavior that is similar to the small LOCA described above.

9.3.2.2.2.3 Group 3: Stuck-Open Valves in the Primary System

Transients involving stuck-open primary side SRVs that reclose have cooldown and depressurization characteristics of a LOCA with a diameter at the low end of the Group 2 range. A key difference, however, is the reclosure of the stuck-open valve after significant cooldown and depressurization has occurred. Once the valve recloses, rapid system repressurization occurs as a result of continued operation of the high-pressure injection system or charging system. The rate of repressurization depends on the flow characteristics of the high-pressure

injection or charging pumps. The operator action to control system pressure by controlling the high-pressure injection system pumps is important to determining system response in this group of transients.

The system cooldown and depressurization rates are governed by the capacity of the PORVs or SRVs, power level, system volume, and ECCS injection temperatures/rates. For the B&W design, the Oconee PORV and SRV capacities are slightly larger than the TMI capacities, so the cooldown and depressurization rates would be slightly faster for Oconee. For the Westinghouse designs, the capacity of the Beaver Valley PORV is higher than Sequoyah and Salem, even though the reactor power for both Salem and Sequoyah is more than 750 MWth higher. The cooldown and depressurization rates for Salem and Sequoyah would be slower, and the downcomer fluid temperature would remain higher throughout the transient if the PORV fails. The results are similar, comparing the relief valve capacity for these plants, as Beaver Valley has a higher relief capacity than Sequoyah or Salem.

Compared to Beaver Valley, the Diablo Canyon PORV has a 25% higher flow capacity. However, the reactor power is also about 25% higher, so the cooldown and depressurization rates would be about the same for both plants if the PORV fails. In the case of the SRVs, Beaver Valley has a higher capacity valve than Diablo Canyon, so the cooldown and depressurization rates for Diablo Canyon should be slower than for Beaver Valley.

For the CE designs, Fort Calhoun has a higher SRV capacity per valve than Palisades, even though its core power is lower. As a result, the cooldown and depressurization rates for Fort Calhoun are higher than for Palisades, given failure of a single valve. Palisades has large PORVs, but operates with closed block valves that prevent the function of pressure relief through these valves, so no comparison is made using PORV capacity for these plants.

As in the case of the Group 2 LOCAs, downcomer temperature behavior should be less sensitive to the power level for hot zero power conditions, simply because the power level is low for the reasons cited at the end of the Group 2 discussion.

In contrast to the Group 2 transients, late stage repressurization and operator actions to control the subcooling and system pressure must be factored into the evaluation. In LOCAs, the system pressure is low and does not play a significant role in the prediction of vessel failure. However, in the case of a stuck-open primary relief valve that subsequently recloses, the primary repressurizes (without operator intervention), and the resulting pressure rise can drive cracks through the vessel wall. The pump head of the high-pressure injection system is also a factor in determining the primary pressure. The Oconee, Beaver Valley, Diablo Canyon, and TMI plants have high-head pumps that can repressurize the system to the setpoint of the PORV or pressurizer SRV. The Palisades, Fort Calhoun, Sequoyah, and Salem plants have low-head pumps that can repressurize the system to the range of 8.9 to 10.3 MPa (1,290 to 1,500 psia). However, the charging systems of these plants can also repressurize the system, albeit at a slower rate. Primary system reheating after the valve recloses as a result of decay heat also contributes to system repressurization. For hot zero power cases, the system can also repressurize after the valve recluses, although throttling of the high-pressure injection system allows the system to eventually depressurize.

Operators are trained to control system pressure and subcooling by controlling high-pressure injection flow and to reestablish normal charging and letdown flow (see Table 9.7, GI 23). The criteria used to establish when the operator starts high-pressure injection system throttling and continues to throttle varies significantly from plant-to-plant. It is not possible to generalize system response to the variety of possible throttling strategies without further analysis.

In summary, the system cooldown and depressurization rates are higher for Oconee (B&W) and Beaver Valley (W-3) than for the generalization plants from the same NSSS vendor (i.e., the generalization plants are

warmer). However, Fort Calhoun (CE) has higher system cooldown and depressurization rates than its corresponding detailed analysis plant, Palisades. The impact of high-pressure injection system throttling strategies among the plants is discussed in Section 9.3.2.1.

9.3.2.2.2.4 Group 4: Main Steam Line Breaks and Other Secondary Side Failures

Group 4 transients includes large steam line breaks and stuck-open secondary side valves, as well as consideration of overfeeds such as the unexpected opening of the feed regulating valves. The secondary breaches can vary from double-ended guillotine breaks of the main steam line to a single stuck-open turbine bypass valve. There are many factors that influence the thermal-hydraulic response of the reactor system during such events.. Key factors are operator actions, the location of the break, and steam line flow restrictors. If the operator can isolate the affected steam generator in a reasonable amount of time, primary system cooldown is stopped and there may not be a primary system overcooling problem. In all plants, the operator is instructed to isolate the affected steam generator, and training and procedures support early operator actions (see more on this above under the PRA/HRA discussion). In order for main steam line breaks and other secondary faults to become a PTS problem, feedwater must be continued to the affected steam generator.

Break location is another factor in system response during a main steam line break transient. Plant response is different depending on whether the break is inside or outside containment because of effects on reactor trip, containment spray actuation, safety injection and reactor coolant pump trips, and other adverse condition issues. If the break/stuck valve is downstream of the MSIV, the valves should close and the primary system cooldown is stopped. While the MSIV closure setpoints vary from plant-to-plant, they all close relatively early in the transient. Note that some B&W plants (such as Oconee) do not have MSIVs, so the break location is less important. If the break occurs inside containment, the operators should trip the RCPs in response to adverse containment conditions. In general, RCP trip makes conditions worse as the downcomer fluid is not as well-mixed as when the pumps are running so lower downcomer fluid temperatures may result. The flow restrictors (if available) are in place to limit the break flow during steam line breaks and determine the cooldown rate. Note that the B&W plants (Oconee and TMI) do not have flow restrictors, and the break flow is determined by the flow area of the steam line.

Starting with the B&W plants designs (Oconee and TMI) some comparisons and observations are made. Both plants use the once-through steam generator design and have comparable power levels (2,568 MWt for Oconee and 2,533 MWt for TMI). The steam generator water mass in the Oconee plant is estimated between 35,000 to 40,000 lbm (15,875 to 18,143 kg), while TMI is estimated between 42,000 and 45,000 lbm (19,050 and 20,411 kg). Neither plant has flow restrictors, so the steam line break flow is limited by steam line size (34-in. (86.4-cm) for Oconee, and 24-in. (61.0-cm) for TMI). Since the steam line flow area is smaller in TMI, the break flow is expected to be less than at Oconee, thus leading to a slower primary side cooldown. In addition, neither the Oconee nor TMI plants have MSIVs, so the break location is relatively unimportant. Both plants have main feedwater automatically isolated after an MSLB, so main feedwater temperature and flow rate are unimportant.

On the primary system side, the high-pressure injection system has a major effect on downcomer fluid temperature during a main steam line break transient. The two B&W plants have similar high-pressure injection systems. Based on an overall general comparison, the Oconee and TMI plants are expected to have similar thermal-hydraulic responses to an MSLB transient. Given that TMI has smaller-diameter steam lines, the average downcomer fluid temperature is expected to be slightly warmer than at Oconee.

Next, comparisons are made between the two CE plants: Palisades and Ft. Calhoun. Both plants utilize vertical U-tube steam generators. These two plants have significantly different power levels (2,530 MWt for Palisades and 1,500 MWt for Ft. Calhoun). Consequently, Ft. Calhoun has smaller steam generators. The normal full power water mass in the steam generator for Palisades is 142,138 lbm (64,472 kg), compared to 82,000 lbm (37,194 kg) for Ft. Calhoun. Both plants have flow restrictors at the steam generator outlets with a flow area of approximately 2.0 ft^2 (0.18 m^2). In Palisades, the MFW is typically isolated by the operator; however, MFW is runback automatically if the operator does not take control in time. In Ft. Calhoun, MFW is isolated automatically during an MSLB. Auxiliary feedwater temperature can vary from 294 to 311 K (70 to 100°F). The Palisades analysis uses a nominal temperature of 305 K (90°F). In the Palisades plant, a control system limits the total AFW flow to the affected steam generator. In other plants, this type of control system is not used, so total AFW flow to a single steam generator is possible.

The high-pressure injection pumps at Palisades have a shutoff head of 8.9 MPa (1,291.7 psia), while Ft. Calhoun pumps are slightly higher at 9.6 MPa (1,390 psia). However, both plants have charging pumps capable of pressurizing the primary system to above the PORV setpoint. Note that Palisades normally operates with the PORV block valves closed. The flow capacity of the Palisades HPI pumps is about twice that of the Ft. Calhoun pumps. The Ft. Calhoun plant probably has a smaller primary side fluid volume than Palisades, consistent with the difference in power level.

Based on an overall general comparison, the Palisades and Ft. Calhoun plants are expected to have similar thermal-hydraulic responses to an MSLB transient.

Finally, comparisons are made between the Westinghouse-designed plants, Beaver Valley (3-loop), Diablo Canyon (4-loop), Sequoyah (4-loop), and Salem (4-loop). All plants utilize vertical U-tube steam generators. The power levels vary from 2,652 MWt for Beaver Valley to 3,411 MWt for Sequoyah and Salem. Note that the power levels are larger on the 4-loop plants than on the 3-loop Beaver Valley plant. The steam generator mass varies from 100,000 lbm (45,360 kg) for Salem to 115,000 lbm (52,160 kg) for Diablo Canyon. All plants use a flow restrictor at the steam generator outlet. For the 4-loop plants, the flow area is 1.4 ft^2 (0.13 m^2), but is much larger (4.7 ft^2 (0.44 m^2)) on the 3-loop Beaver Valley plant. Based on its larger flow restrictor, Beaver Valley is expected to have a much faster cooldown rate than the other Westinghouse plants.

The main feedwater temperature for the Westinghouse plants is typically around 497 K (435°F), and decreases to 311 K (100°F) after a reactor trip. In all four plants, main feedwater should automatically trip on a main steam line break. Auxiliary feedwater temperature varies from 275 to 322 K (35 to 120°F) among the four plants. The Beaver Valley analysis uses a temperature of 295 K (72°F). In all four plants, the AFW is capable of maintaining steam generator level even during an MSLB.

The four plants have somewhat different high-pressure injection systems. At Beaver Valley, the charging and high-pressure injection systems use the same pumps. These pumps have a shutoff head greater than 18 MPa (2,600 psia) and are capable of pressurizing the primary system to above the PORV setpoint. The other Westinghouse plants use high-head charging pumps but intermediate-pressure HPI pumps. These intermediate-pressure pumps have a shutoff head of approximately 10.3 MPa (1,500 psia). The minimum HPI temperature varies from 275 to 289 K (35 to 60°F) among the four plants. In the Beaver Valley analysis, 283 K (50°F) was used for HPI temperature.

Based on an overall general comparison, the four Westinghouse plants are expected to have similar thermal-hydraulic responses to an MSLB transient.

Stuck-open valves on the secondary side are equated to smaller steam line breaks. Transients with stuck-open secondary side (turbine bypass, atmospheric dump, and safety relief) valves are less severe thermal-hydraulically than the larger steam line breaks discussed above. For all plants evaluated, all secondary side valves can be isolated with the exception of the SRVs.

In summary, the generalization plants should be warmer (or about the same) when compared to the plants analyzed in detail.

The simple overfeeds are worth a brief mention. In these events, an unexpected overfeed of one or more SGs occurs. If such an overfeed condition is allowed to continue for many tens of minutes, the secondary temperature will ultimately drive toward the main condenser water temperature (~311 K (100°F)) following a plant trip and likely isolation of warming (i.e., steam addition) of the feedwater. This causes depressurization and cooldown of the primary system. However, as discussed in the above comparable PRA/HRA section, the likelihood of a continuing overfeed, which would involve failure of automatic high SG level trips backed by operator action to either close feed valves or shutdown pumps as necessary, makes such an event very unlikely. Further, the plant-specific plant analyses show that the PTS challenge, if the feed is not controlled even until the SGs are completely full, is not significant. For these reasons, simple overfeed scenarios are not important and, hence, not discussed any further.

9.3.3 Combined Observations and Overall Conclusion

Group 1 (Large-Diameter Primary Side Pipe Breaks): No differences were found that would cause significant changes in either the progression or frequencies of the PTS scenarios. From the TH perspective, no differences in the plant system designs were found that would cause significant changes in the downcomer fluid temperature. While some temperature variations could be expected because of the initial power level, breaks in this range are sufficiently large that the water injected into the system due to combined high- and low-pressure injection and safety injection tank discharge should largely govern the downcomer fluid temperature. Thus, we expect that the generalization plants can be bounded (or represented) by the detailed analysis plants.

Group 2 (Small- to Medium-Diameter Primary Side Pipe Breaks): No differences were found that would cause significant changes in either the progression or frequency of the pipe break LOCAs. For the feed-and-bleed LOCAs, the only identified difference affected the frequency for the CE generalization plant (i.e., Fort Calhoun). The frequency for these types of scenarios could be higher by a factor of ~3; however, this increase would not prevent the generalization plants from being bounded (or represented) by the detailed analysis plants. All generalization plants should have depressurization and cooldown rates associated with pipe break and feed-and-bleed transients that are comparable to their corresponding detailed analysis plant. Thus, we expect that the generalization plants can be bounded (or represented) by the detailed analysis plants.

Group 3 (Stuck-Open Valves on the Primary Side that May Later Reclose): The progression of accident scenarios should be the same across all plants. However, the frequencies associated with these scenarios could increase by at most a factor of 5 for one of the Westinghouse plants (i.e., Salem). The importance of this factor of 5 increase at Salem was approximated by increasing the failure probability assigned to the operator fails to throttle basic event in the Beaver Valley model and requantifying the Beaver Valley results. The total point estimate for Beaver Valley increased by a factor of 1.02; thus, we conclude that this difference is unimportant.

Only Fort Calhoun is expected to have a downcomer temperature that is cooler than its corresponding detailed analysis plant (Palisades). The downcomer temperature for the other generalization plants is actually

expected to be somewhat warmer. Given the expected Fort Calhoun results, a surrogate analysis was performed. This analysis used the Palisades TH model, adjusting the model to account for the differences in thermal power to primary system volume and size of the relief valve opening(s). Results from the analysis indicated that Fort Calhoun would have a lower downcomer temperature, as expected. The results from the surrogate TH calculation were then analyzed using FAVOR and the Palisades embrittlement map. Results from the FAVOR calculation indicated an increase in conditional probability of through-wall cracking. While this resulted in much higher TWCFs for Fort Calhoun than for Palisades for the same type of sequence, the TWCFs were still small in an absolute sense (low E-08/yr or lower range). These values are comparable to but not higher than the highest TWCFs estimated for all types of sequences (LOCAs, SRV openings, MSLBs, etc.), which are also in the E-08/yr range. Thus, the TWCF of Fort Calhoun can be bounded by Palisades.

Group 4 (Main Steam Line Breaks and Secondary Side Breaks, in General): No differences were found that would cause significant differences in either the progression or frequency of the PTS scenarios. The downcomer temperature for the generalization plants should be about the same (Westinghouse and CE) or warmer (B&W). Thus, we expect that the generalizations plants can be bounded (or represented) by the detailed analysis plants.

These combined observations support the overall conclusion that the TWCF estimates produced for the detailed analysis plants are sufficient to characterize (or bound) the TWCF estimates for the five generalization plants and, thus, by inference, PWRs *in general*.

9.4 Consideration of External Events

9.4.1 Introduction

In examining the potential for a revised PTS screening limit, it is important to also consider the potential risk from external events. External events are those in which spatial interactions may be important to the propagation of the accident sequence, and these can contribute to the PTS risk. External events include such scenarios as those involving fires, floods, high winds and tornados, and seismic events, among others. As an example, a fire could start in an electrical cabinet causing the spurious opening of one or more secondary relief valves such as turbine bypass (steam dump) valves, which could induce a serious overcooling and a potential PTS concern depending on subsequent plant equipment and operator responses. Since external events can affect multiple plant equipment and operator actions as well, they could be important to PTS.

Because (1) the specific effects of external events are very plant-specific (e.g., into which rooms the water from an internal flood propagates and, thus, what equipment is affected), and (2) since these analyses can be resource-intensive, requiring the gathering of significant spatial information about each plant, it was not practical to perform plant-specific external event PTS analyses. Instead, conservative analyses were performed with the goal of *bounding* the potential PTS TWCFs from external events. This is in contrast to the internal event PTS analyses results, which are generally "best-estimate" analyses meant to determine a realistic assessment of PTS TWCFs attributable to scenarios initiated by such events as turbine trips, loss of feedwater, etc. (i.e., internal events). In contrast, the contribution from external events was assessed by using conservative assumptions to bound the PTS TWCFs from external events and, hopefully, demonstrates that the bounding TWCFs from external events are at least no higher than the highest best-estimate internal events TWCFs. Such a result would provide reasonable assurance that the total external event-caused

PTS TWCF is no worse than the total internal event-caused PTS TWCF (which is as high as the low E-8/yr range at 60 EFPY based on the three detailed plant analyses).

As a result, the numerical results from the external events analyses (described in detail in [***Kolaczkowski-Ext***] and which contains the references to the other documents cited here) should not be taken as best-estimate or realistic values; they are intended to provide bounding TWCF estimates for the pertinent external event scenarios. Also note that in following this approach, no particular plant was taken as a representative model for the analysis (with the exception of earthquake hazard, where H.B. Robinson and Diablo Canyon were used as surrogates). Therefore, because these results are intended to bound the worst situation that might arise at virtually any plant, they may be extremely conservative for many plants. The degree of conservatism cannot be determined without performing plant-specific analyses.

9.4.2 Approach

A multi-faceted approach was used to gain insight as to the potential contribution of external events to the PTS TWCFs. This approach included the following:

(1) A review was performed of the late 2001 – early 2002 version of the Calvert Cliffs PRA model, with cooperation from the utility, which includes not only core damage scenarios, but also PTS scenarios. The model includes contributions from both internal and external events for both core damage frequencies and PTS TWCFs and can offer insight into the potential importance of external events.

(2) As further evidence of the potential importance of external events, a review of licensee event reports (LERs) was performed of actual overcooling events in U.S. plant operating experience covering a recent approximately twenty year period.

(3) Further, a review was conducted of a sampling of (just two) individual plant examinations for external events (IPEEE) submittals, one for Salem and one for Ginna, to determine what insights could be gained from those studies that might be applicable to PTS.

(4) With all of the above as background, it was nonetheless decided that additional analytical analyses were necessary to be able to bound the potential TWCFs from external event overcooling scenarios.

9.4.3 Findings Based on the Reviews

The late 2001 – early 2002 version of the Calvert Cliffs PRA suggests that the TWCFs as a result of PTS caused by external events are low compared to that caused by internal events (i.e., less than 10%). The PRA shows fire as the external event of greatest concern. While this is an indicator of the potential relative contributions, it is only one plant's result and the finding is subject to some modifications that would need to be made to the model in order to be more comparable to the three analyses conducted as part of this work. For instance, the Calvert Cliffs model needs modifications in the areas of the sequences being modeled, and some human failure probabilities may need to be reconsidered during certain external events. Additionally, the latest CPTWC information from this study needs to be reflected in any update of the Calvert Cliffs PRA. Hence, while encouraging, the relative importance of external events to the PTS TWCFs cannot be generically determined based on this one input alone.

The LER review of events occurring in a recent 20-year period identified a total of 128 PTS-relevant (i.e., cooldown) events. Of these, only three events could be potentially categorized as involving an external event, although only one (a switchgear fire) was clearly an external event (LER No. 26989002). This evidence suggests that external events will be involved in no more than approximately 2% of all PTS occurrences. While this is a valuable insight in that it suggests that experience shows that cooldowns are more likely to be caused by internal events rather than external events, it still does not address the potential TWCFs from external events even if they do occur less frequently. This is because

external events could still lead to more serious scenarios with higher CPTWC values, thereby resulting in potentially higher TWCFs.

The two IPEEEs were originally conducted to determine core damage frequencies as a result of undercooling (rather than overcooling events); hence, there were very limited insights from these reports applicable to PTS. Nonetheless, during the review of the IPEEEs, one general type of interaction between external events and effects of interest to PTS was noted to be included in both studies. This was a fire-induced opening of one or more pressurizer PORVs — a possible serious overcooling event. This indicates that any estimation of the external event contribution to PTS needs to include consideration of spurious actions such as that described as a result of fire scenarios. However, no other meaningful insights were gained from reviewing the two IPEEEs that would be applicable to this PTS work.

9.4.4 Additional Analyses

9.4.4.1 Overview

The above reviews provided some insights with regard to how important external events may be to PTS. However, the set of insights was incomplete. As a result, additional analytical analyses were performed. These additional analyses involved comparisons of the following factors:

(1) TWCF results from the internal events analyses for the three plants

(2) conservatively estimated corresponding external event TWCF results

This comparative analysis was structured based on the following *broad* types of overcooling scenarios analyzed in this PTS work:

- *Category 1: Loss-of-Coolant Accidents (LOCAs).* These are scenarios that involve primary system breaches (such as pipe breaks and open pressurizer valves) but without any secondary anomalies or faults.
- *Category 2: Secondary Anomalies or Faults.* These are scenarios that involve such events as stuck-open secondary valves, main steam line breaks, and steam generator overfeeds but without any primary system anomalies or faults.
- *Category 3: Coexisting LOCA - Secondary Faults.* These are scenarios that involve both primary system breaches and secondary faults at the same time.

As required, the analyses further divided these broad categories of scenarios into more specific types of scenarios. Table 9.7 summarizes all types of scenarios for which TWCF comparisons were made. These were examined for both full-power and hot zero power conditions. For each type of scenario, conservative judgments were made with regard to the type of external event that could directly contribute to the cause of such a scenario. In addition, conservative estimates were made with regard to the applicable external event frequencies, plant equipment responses, and operator effects. With regard to operator actions, little or no credit was given in these analyses in response to the external event-induced PTS challenges; this further contributed to the conservative estimations of external event TWCFs, thereby making them artificially more important. Finally, the resulting TWCFs from both internal event contributions and the conservatively assessed external event contributions were compared. The following is provided as just one example of such a comparison.

9.4.4.2 A Representative Comparison

Category 1 - LOCAs; Scenario Type #3: In this scenario, a small LOCA (with an equivalent diameter of ~1.5 to 3-in. (~3.8 to 7.6-cm)) occurs as a result of a pipe break, and everything else functions as designed. (Other small LOCAs, such as those caused by an open PORV, are a different scenario type that is analyzed elsewhere.) By this, we mean that HPI operates (so cold water enters the vessel downcomer region) and the system likely continues to provide full flow, since throttling criteria are not likely to be met for most breaks

in this size range during the time period of interest to PTS when large temperature gradients occur across the vessel wall. It is assumed the operator does shut down the RCPs as procedurally required (this is worse for PTS since there is less mixing of the primary coolant), and there are no secondary anomalies or other operator errors that induce secondary complications.

Table 9.8 summarizes the major inputs and resulting TWCFs from such a scenario caused by a random small-break LOCA (i.e., an internal event initiator) based on results from the three plant analyses.

Table 9.7. Scenarios covered under the external event analyses

Overall Scenario Category	Scenario Types
Category 1: LOCAs	Large LOCA pipe break
	Medium LOCA pipe break
	Small LOCA pipe break
	Scenario with single stuck-open pressurizer PORV
	Scenario with single stuck-open pressurizer SRV
	Scenario with two stuck-open pressurizer PORVs
	Scenario with two stuck-open pressurizer SRVs
	Scenario with two stuck-open pressurizer PORVs that reclose
	Scenario with one or two stuck-open pressurizer SRVs that reclose
	Total loss of secondary heat sink with subsequent use of feed-and-bleed
	Small LOCA, or PORV or SRV opening, with initial loss of primary system injection
Category 2: Secondary Anomalies or Faults	Steam generator(s) overfeeds
	Uncontrolled secondary depressurization to feed steam generator(s) with condensate
	Two or fewer valves open upstream of MSIVs
	Turbine bypass (steam dump) valves open downstream of MSIVs
	Large steamline break upstream of MSIVs
	Large steamline break downstream of MSIVs
Category 3: Coexisting LOCA - Secondary Faults	Consideration of combinations of above

Table 9.8. Small-break LOCA internal event results

Scenario	Internal Event Frequency (yr^{-1})	CPTWC at 60 EFPY	Internal Event TWCF (yr^{-1})
Small LOCA at Full Power	Up to 1E-3	Up to 1E-5	Up to 2E-9*
Small LOCA at Hot Zero Power	Up to 2E-5	<1E-4 (conservative estimate)	<2E-9

* Highest CPTWC does not necessarily correspond to the highest frequency shown, so one cannot simply multiply the highest frequency in the table with the highest CPTWC shown in the table.

Consideration was given to how external events might directly induce a small pipe break LOCA. Seismic, flooding, fire, high wind/tornado, and other (e.g., aircraft crash) external events were considered. In large part because of the nature of the primary coolant system and containment designs, and their relative location to the rest of the plant (e.g., a fire in the auxiliary building

should not be able to induce a pipe break in the primary coolant housed inside the containment), we concluded that only a seismic event might be able to induce a small pipe break LOCA. Hence an analysis of a seismic-induced small pipe break LOCA was conducted.

Possible Seismic-Small Loca Scenario:

For the small LOCA case, a 0.3g high confidence of low probability of failure (HCLPF) is assumed to be representative of the seismic strength of the primary piping and other components for which failure as a result of a seismic event could result in a small LOCA. This corresponds to the review-level earthquake (RLE) peak ground acceleration for most plants in the IPEEE program. Most (if not all) IPEEEs concluded that primary piping and components have higher seismic strengths than that corresponding to a 0.3g HCLPF; thus, use of the 0.3g HCLPF in this analysis is conservative. It is further assumed that both β_R and β_u (which define the uncertainty in the HCLPF) are 0.3 (typical), giving a median fragility of about 0.5g. Using the H.B. Robinson site as a surrogate for Eastern plants, because it has the largest hazard of any Eastern PWR, this corresponds to a mean accidence frequency of 1.6E-4/yr. An analysis was performed using the SAPHIRE computer code to convolve the above fragility information with the revised Lawrence Livermore National Laboratory (LLNL) hazard curve for H.B. Robinson, resulting in a mean seismic-induced small pipe break LOCA frequency estimated to be 1.1E-4/yr.

As an additional sensitivity, the hazard curve for Diablo Canyon was also used as representative of a high-seismicity site. A corresponding HCLPF for a small pipe break LOCA at such a site was assumed to be 0.5g, because of the more rugged plant design (higher RLE). Maintaining β_R and β_u of 0.3, and convolving this fragility information for a small pipe break LOCA with the mean hazard curve from the Diablo Canyon IPEEE submittal results in a mean seismic-induced small pipe break LOCA frequency of 5.0E-4/yr[******].

Using a value of 0.02 (i.e., 2%) as the fraction of the year the plant is at HZP conditions, as done in the internal events analysis, yields 1E-5/yr as the highest estimated frequency (5.0E-4/yr from above x 0.02 = 1E-5/yr) of a seismic event causing a small pipe break LOCA while the plant is at HZP conditions.

By using the frequencies conservatively estimated above, and the same maximum CPTWC from the internal events analyses of the three plants (the CPTWC will be the same whether the event is caused by an internal event initiator or a seismic event), the corresponding seismically induced small pipe break LOCA TWCFs are as shown in Table 9.9.

Note that the conservative external event contributions to the TWCFs for this type of accident are either less than or not significantly greater than the internal event TWCFs.

9.4.5 Overall Findings

In spite of the conservative nature of the external event analyses, no external event scenarios were found where the TWCFs significantly exceed that of the worst internal event scenarios (contributions from LOCA-type and SRV open-reclose-type accidents) as discussed in detail in the companion report [***Kolaczkowski-Ext***]. From that report, and as reiterated in this summary section, the highest total best-estimate TWCF across all internal event scenarios for the three plants analyzed at 60 EFPY is approximately 2E-8/yr and is used as part of the basis for proposing revised PTS Rule criteria. The comparable *bounding* total TWCF across all external event scenarios is also approximately 2E-8/yr. Therefore, given the bounding nature of the external event analyses, there is

[******] The hazard curve in the Diablo Canyon IPEEE is given in terms of peak spectral acceleration in the range of 3.5–8Hz. This was converted to a zero-period peak ground acceleration by dividing the accelerations by a factor of 2.

considerable assurance that the external event contribution to overall TWCF as a result of PTS is at least no greater than the highest best-estimate contribution from internal events. In fact, given the conservative probabilities and dependencies assumed in the external event analyses, with the addition of little or no credit for any operator actions for the external event scenarios, it is more likely that the "realistic" external event contribution to overall TWCF is much less than the highest internal event contribution. It is, therefore, our view that the contribution of external initiating events to the overall TWCF attributable to PTS is enveloped by the internal event results. Hence, for general purposes, it is recommended that the overall PTS TWCF can be estimated by neglecting the potential contribution from external events. To the extent it may be necessary or desirable, individual plants could provide a detailed external events PTS analysis to ensure that the plant staff understands the specific contributions to PTS TWCF from external events.

Table 9.9. Small-break LOCA TWCF comparison

Scenario	Internal Event Frequency (yr^{-1})	CPTWC at 60 EFPY	Internal Event TWCF (yr^{-1})	Bounding External Event Frequency (yr^{-1})	Bounding External Event TWCF (yr^{-1})
Small LOCA at Full Power	Up to 1E-3	Up to 1E-5	Up to 2E-9	5E-4	5E-9
Small LOCA at Hot Zero Power	Up to 2E-5	<1E-4 (conservative estimate)	<2E-9	1E-5	<1E-9

9.5 Summary of Generalization Studies

In this chapter, we examined the applicability of the TWCF estimates presented in Chapter 8 for Oconee Unit 1, Beaver Valley Unit 1, and Palisades to PWRs *in general*. The information presented focused on the following topics:

- Sensitivity studies performed on the TH and PFM models to engender confidence in both the robustness of the results presented in Chapter 8 and their applicability to PWRs *in general*.
- An examination of the plant design and operational characteristics of five additional plants to determine whether the design and operational features that are the key contributors to PTS risk vary significantly enough in the general plant population to question the generality of our results.
- An examination of the effects of external events (e.g., fires, floods, earthquakes) to PTS risk.

Except for a few situations that are not expected to occur, none of these analyses revealed any reason to question the applicability of the results presented in Chapter 8 to the general population of operating PWRs in the United States. The information developed in these analyses is summarized as follows:

TH Sensitivity Studies

- Changes to the RELAP heat transfer coefficient model to account for low-flow situations where mixed convection heat transfer may be occurring in the downcomer were made based on the Petukhov-Gnielinski heat transfer correlation. This change in the heat transfer coefficient increases the CPTWC by a factor ~3 (averaged across all transients analyzed) compared to using the default heat transfer correlations in RELAP5/MOD3.3 Version ei. There is some variability from the average CPF factor, depending upon the transient being considered.

PFM Sensitivity Studies

- An examination of the effects of all postulated credible perturbations to our PFM model revealed no effects significant enough to warrant a change to our baseline model, or to recommend a caution regarding its robustness.
- In general, the TWCF of forged PWRs can be assessed using the Chapter 8 results (for plate welded PWRs) by ignoring the TWCF contribution of axial welds. However, should changes in future operating conditions result in a forged vessel being subjected to very high levels of embrittlement (far beyond any currently anticipated at EOL or EOLE) a plant-specific analysis to assess the effect of subclad flaws on TWCF would be warranted.
- For PWRs with vessel thicknesses of 7.5 to 9 .5-in. (19.05 to 24.13-cm), the TWCF results in Chapter 8 are realistic. The Chapter 8 results overestimate the TWCF of the seven thinner vessels (with wall thicknesses below 7-in. (17.78-cm)) and underestimate the TWCF of Palo Verde Units 1, 2, and 3, all of which have wall thicknesses above 11-in (27.94-cm). However, these vessels have very low embrittlement projected at either EOL or EOLE, suggesting little practical effect of this underestimation.

Plant Design and Operational Characteristics

- *Large-Diameter Primary Side Pipe Breaks*: No differences were found that would cause significant changes in either the progression or frequencies of the PTS scenarios. Additionally, no differences in the plant system designs were found that would cause significant changes in the downcomer fluid temperature.
- *Small- to Medium-Diameter Primary Side Pipe Breaks*: No differences were found that would cause significant changes in either the progression or frequency of the pipe break LOCAs. For the feed-and-bleed LOCAs, the only difference that was found affected the frequency for the CE generalization plant (i.e., Fort Calhoun). The frequency for these types of scenarios could be higher by a factor of ~3; however, this increase would not prevent the generalization plants from being bounded (or represented) by the detailed analysis plants.
- *Stuck-Open Valves on the Primary Side that May Later Reclose*: The progression of the accident scenarios should be the same across all plants. While, the frequency associated with this type of scenarios could increase at some Westinghouse plants, the integrated effect of this increase was determined to be small. Fort Calhoun is expected to have a downcomer temperature that is cooler than its corresponding detailed analysis plant (Palisades) because of the smaller size of the plant. The downcomer temperature for the other generalization plants is actually expected to be somewhat warmer. PFM calculations performed to quantify the effect of the colder temperatures in Ft. Calhoun determined that while the conditional through-wall cracking probabilities would increase (as expected), the increase was not so substantial as to prevent the Palisades plant analysis from upper-bounding the Ft. Calhoun plant analysis. Thus, the colder downcomer temperature for smaller plants was not viewed as impeding the applicability of the TWCF values in Chapter 8 to PWRs in general.
- *Main Steam Line and other Secondary Side Breaks*: No differences were found that would cause significant differences in either the progression or frequency of the PTS scenarios.
- *Summary*: These observations support the conclusion that the Chapter 8 TWCF estimates produced can be used to characterize (or bound) the TWCF of PWRs in general.

External Events

- No external event scenarios were found where the TWCFs significantly exceed that of the worst internal event scenarios (contributions from LOCA-type and SRV open-reclose-type accidents). Given the bounding nature of the external event analyses, there is considerable assurance that the external event contribution to overall TWCF as a result of PTS does not exceed than the highest best-estimate contribution from internal events. Given the conservative probabilities and dependencies assumed in the external event analyses, with the addition of little or no credit for any operator actions for the external event scenarios, it is more likely that the "realistic" external event contribution to overall TWCF is much less than the highest internal event contribution. Therefore, the contribution of external initiating events to the overall TWCF attributable to PTS can be considered negligible.

10 Risk-Informed Reactor Vessel Failure Frequency Acceptance Criteria

10.1 Introduction

As discussed in Chapter 2, the current PTS Rule establishes a series of steps that PWR licensees must perform. The initial step involves a deterministic evaluation of the RPV's RT_{PTS} for welds and plate materials (RT_{NDT} evaluated at EOL). If the computed RT_{PTS} values exceed the screening limit established in 10 CFR 50.61, licensees are directed to accomplish reasonably practicable neutron flux reduction to avoid exceeding the screening limit during the RPV's licensed life. Plants for which the computed RT_{PTS} values still exceed the screening limit, even with neutron flux reduction, are required, at least 3 years before exceeding the criteria, to submit a plant-specific safety analysis demonstrating that the risk associated with PTS events is acceptably low. Regulatory Guide 1.154 [RG 1.154], describes one acceptable method for performing such safety analyses.

Two key aspects of the PTS safety analysis approach described in RG 1.154 are the estimation of RPV TWCF and comparison of the estimated TWCF with an acceptance criterion of 5×10^{-6} per reactor year (ry). Neither RG 1.154 nor Enclosure A to SECY-82-465 [SECY-82-465] provides a detailed discussion regarding this specific value, although Enclosure A to SECY-82-465 does argue that an even higher TWCF value (i.e., 1×10^{-5}/ry) is consistent with the then-proposed Safety Goal Policy guidelines on "core melt frequency" and the desire that the core melt frequency ascribable to "one sequence" (such as PTS) should be a small fraction of the overall core melt frequency. Based on the assessed likelihood of potential PTS challenges, predicted TH response of the plant, and predicted behavior of the RPV, the RT_{NDT} screening limits recommended by the staff in 1982 and subsequently incorporated in 10 CFR 50.61 were determined to be consistent with a TWCF of around 5×10^{-6}/ry.

The NRC has established a considerable amount of guidance on the use of risk information in regulation since it issued SECY-82-465 and published the original PTS Rule. In light of this more recent guidance, and as part of the PTS technical basis reevaluation project, the staff has identified and assessed options for a risk-informed criterion for the reactor vessel failure frequency (RVFF) associated with PTS (currently specified in RG 1.154 in terms of TWCF). The assessment includes a scoping study of the issue of containment performance during PTS accidents, which has implications for the specification of the acceptance criterion. The resulting conclusions and their bases are provided in this chapter.

10.2 Current Guidance on Risk-Informed Regulation

Key documents published since the issuance of the original PTS Rule include the Commission's Safety Goal Policy Statement (issued in 1986); a June 1990 Staff Requirements Memorandum (SRM) [NRC 90]; and RG 1.174 [RG 1.174], as well as the associated revision of Chapter 19 of NUREG-0800, "Standard Review Plan for the Review of Safety Analysis Reports for Nuclear Power Plants (LWR Edition)" (SRP) [NRC 98b].

The Safety Goal Policy Statement [NRC FR 86] defines qualitative goals and quantitative health objectives (QHOs) for the acceptable risk of nuclear power plant operations. The QHOs address the prompt fatality risk to individuals, and the cancer fatality risk to society. For both the individual and societal risks, the QHOs are defined to ensure that the public health and safety risk arising from nuclear power plant

operations is a very small fraction (0.1% or less) of the total risk to the public.

The June 1990 SRM [NRC 90] discusses subsequent Commission decisions with respect to the policy statement. Of particular interest, the SRM establishes a subsidiary core damage frequency (CDF) goal of $1x10^{-4}$/ry. At the time it was developed, this subsidiary goal, as well as the qualitative safety goals and QHOs, was intended for use in generic agency decisions such as rulemakings. It was not aimed at plant-specific applications.

RG 1.174 [RG 1.174] and SRP Chapter 19 [NRC 98b] describe a risk-informed process by which licensee-proposed license amendments that act to change regulatory requirements can be submitted, reviewed, and, if appropriate, approved. Toward that end, RG 1.174 fulfills the following purposes:

- Describe a set of general principles for this process.
- Extend the policies established in the Safety Goal Policy Statement, by providing a large early release frequency (LERF) subsidiary objective and making use of the QHOs in plant-specific decision-making.
- Provide a set of probabilistic guidelines defining acceptable changes in CDF and LERF associated with proposed reductions in regulatory requirements.

RG 1.174 applies to voluntary changes to a plant's licensing basis. However, it provides a general template for improving consistency in regulatory decisions in areas in which the results of risk analyses are used to help justify regulatory action. The principles of integrated, risk-informed decision-making (involving consideration of risk information, defense-in-depth, safety margins, and uncertainties) discussed in that RG apply broadly to risk-informed regulatory activities. RG 1.174 provides acceptance guidelines for changes in CDF and LERF. These guidelines were developed to provide assurance that proposed increases in CDF and LERF are small and consistent with the intent of the Safety Goal Policy Statement. If the baseline risk can be shown to be acceptable (as indicated by a total mean CDF of less than 1×10^{-4}/ry and a total mean LERF less than 1×10^{-5}/ry), applications for plant changes leading to small increases in mean CDF (up to 1×10^{-5}/ry) and mean LERF (up to 1×10^{-6}/ry) will be considered for regulatory approval.

The relationship between the RG 1.174 LERF criterion and the QHOs is discussed in Appendix A to NUREG/CR-6595 [Pratt 99]. In particular, that appendix argues that, for certain large early releases (involving the release of 2.5% to 3% of the reactor's iodine and/or tellurium inventory within 4 hours of accident initiation), a LERF of 1×10^{-5}/ry roughly corresponds to the prompt fatality QHO (currently around 5×10^{-7}/yr). The calculations supporting NUREG/CR-6094 [Hanson 94] and SECY-93-138 [SECY-93-138] are cited as the basis for these conclusions.

The staff's current activities on Option 3 for risk-informing 10 CFR Part 50, as described in SECY-00-0198 [SECY-00-0198], takes advantage of the groundwork laid by RG 1.174. The Option 3 framework being developed employs the total mean CDF and mean LERF guidelines mentioned above (1×10^{-4}/ry and 1×10^{-5}/ry, respectively). The framework also provides guidelines to limit the CDF and LERF associated with any single accident type from being a large fraction of the plant's total CDF and LERF.

10.3 Containment Performance During PTS Accidents

As discussed in Section 10.1, the current TWCF criterion of 5×10^{-6}/ry provided in RG 1.154 was established to ensure that the risk associated with PTS is a small fraction of the acceptable level of risk established by the Safety Goals and is consistent with the philosophy of distributing risk among accident types. However, the relationship between this criterion and the CDF and LERF guidelines established in RG 1.174 and those proposed in the draft Option 3 framework is not clear because there is currently an incomplete understanding regarding the

progression of an accident following a postulated PTS-induced RPV failure.

10.3.1 Previous Research Results

Several previous research efforts have addressed potential PTS-induced RPV failure modes and their effects on core cooling and containment integrity. In the late 1970s and 1980s, large-scale experiments, in which prototypic RPVs were subjected to pressure and temperature transients characteristic of PTS loadings, were conducted as part of the NRC-sponsored Heavy Steel Section Technology (HSST) research program. These experiments demonstrated three potential outcomes of a PTS event (depending on the particulars of the transient, material embrittlement, etc.):

- No cracks initiate, and the vessel remains intact.
- A crack initiates, propagates to some depth into the entire vessel wall, and stops. The vessel remains intact with little additional deformation.
- A crack initiates and propagates entirely through the vessel wall. In addition to large openings in the reactor vessel, this outcome involves significant additional deformation of the vessel.

In the context of RPVs, the third outcome presents a potentially significant challenge to core cooling and containment integrity.

In the mid-1980s, following the promulgation of the initial versions of 10 CFR 50.61 and RG 1.154, the NRC sponsored a number of studies on the risk associated with PTS. One such study, documented in NUREG/CR-4483 [Simonen 86], evaluated the current state of knowledge regarding post-vessel failure accident progression. The study considered such issues as the axial and azimuthal extent of crack propagation, depressurization of the reactor coolant system, RPV vertical movement resulting from postulated full circumferential breaks of the vessel wall, and the possibility of missiles generated during the RPV failure. From the perspective of an RVFF acceptance criterion, NUREG/CR-4483 offers two key findings:

(1) The possibility of axial cracks propagating into embrittled circumferential welds and then propagating along these welds cannot be neglected.

(2) The effects of PTS-induced missiles (including the RPV in extreme cases) are likely to be contained within the concrete barriers surrounding the RPV.

In 2001, the NRC sponsored a study of the potential structural consequences of PTS events. This study [Theofanous 2001] assumed the instantaneous opening of a very large axially oriented hole (4-m x 0.4-m, ~2,480-in.^{2}) in the RPV as a postulated result of PTS. Under these conditions, and given the relatively low energy of the fluid, the impulse on the RPV and piping resulting from the blowdown was predicted to be within the bounds of a design-basis safe-shutdown earthquake (SSE). However, the study did not model either the effects of internal structures (fuel supports, fuel assemblies, etc.) on the blowdown loads, or the possible effects of blowdown on the internal structures themselves.

The study also explored a simplified crack opening model that predicts a small hole (~110-in^2 (0.07-m^2)) resulting from a postulated 157.48-in. (4-m) long axial crack, rather than the very large hole (~2,480-in^2 (1.6-m^2)) assumed in the analysis of blowdown loads. The study found that ECCS injection would not be challenged by a crack (and predicted hole area) of this size. However, the study did not address either the possibility of more extensive axial crack propagation, or the possibility of circumferential cracks that could challenge the ECCS. The staff's evaluation, summarized in Section 10.3.2, addresses these issues.

On July 18, 2002, the Advisory Committee on Reactor Safeguards (ACRS) wrote a letter on the issue of PTS acceptance criteria [Apostolakis 02]. The letter noted that the LERF criterion provided in RG 1.174 is not a proper starting point for PTS considerations, since the "...source terms used to develop the current goal do not

reflect the air-oxidation phenomena that would be a likely outcome of a PTS event."

The concern with air-oxidation events is associated with potential scenarios where fuel cooling has been lost and the fuel rods are exposed to air (as opposed to steam). Should such a situation arise, some portion of the reactor fuel will eventually be oxidized in an air environment. Based upon currently available information, this oxidation is expected to result in release fractions for key fission products (ruthenium being of primary concern) that may be significantly (e.g., a factor of 20) larger than those associated with fuel oxidation in steam environments, and these larger release fractions could lead to a larger number of prompt fatalities than predicted for non-PTS risk-significant scenarios.

10.3.2 Post-RPV Failure Scenarios Scoping Study

In order to support the assessment of options for an RVFF acceptance criterion (see Section 10.4 for a description of the options considered), the staff conducted a limited scoping study of PTS-induced post-RPV failure scenarios. The specific aim of the study was to develop an initial qualitative assessment of the potential impact (both positive and negative) of the unique characteristics of such scenarios on the likelihood of severe source terms, especially source terms beyond those typically assessed for non-PTS-associated risk-significant scenarios.

The study involved the structured identification of technical issues underlying the assessment of the margins to core damage and large early release following potentially significant PTS-induced RPV failure scenarios (dominant scenarios for the pilot plants addressed by the PTS reevaluation project are discussed in Chapter 8 of this report), and the collection and evaluation of currently available information relevant to these issues. Of particular interest was the identification of PTS-unique physical mechanisms that could lead to dependent failures of accident mitigation features. To better inform the evaluation, a small number of limited-scope TH and structural calculations were performed.

The scoping study focused on differences between post-PTS-induced RPV failure accident progression and accident progression associated with non-PTS core damage events. Thus, in addition to the previously mentioned air-oxidation issue, the scoping study addressed issues associated with the development and characteristics of the postulated opening in the RPV, the resulting blowdown forces, the effect on key structural components (e.g., the RPV, containment penetrations), and the potential for damaging missiles. Table 10.1 lists and briefly describes the issues addressed.

To support the identification and semi-quantitative analysis of the issues, an accident progression event tree (APET) was developed. This tree, shown in Figure 10.1, identifies potentially important phenomena and possible scenarios following PTS-induced RPV failure.††††††

In general, the APET explicitly addresses the issues listed in Table 10.1. Two notable exceptions are the issues of missiles and early overpressure. Regarding missiles, activities performed as part of the scoping study indicate that the possibility of a PTS-induced RPV failure leading to energetic missiles that could affect important top events in the APET (i.e., those associated with containment isolation, sprays, and ECCS) is sufficiently remote to allow exclusion of this issue from the APET. Missile generation attributable to a PTS event would result in an object being directed laterally into the reactor vessel cavity wall by the blowdown forces associated with the breach in the RPV. For a missile to affect the containment spray systems, ECCS systems or containment penetrations, it would have to traverse a tortuous

†††††† Note that the APET includes branches for issues whose uncertainties are more epistemic in character (e.g., the blowdown forces associated with a given break size), as well as branches associated with issues for which the uncertainties are more aleatory in character (e.g., the availability of ECCS).

path through tight clearances of the RPV cavity (between the reactor vessel and the concrete of the cavity wall). It would then have to hit an extremely small target (either ECCS piping, containment penetration or containment spray piping). The missile's energy would be dissipated through its multiple contacts with the RPV cavity wall, as well as the distance it traveled.

Table 10.1. Post-RPV-failure technical issues

Dominant PTS scenarios	This issue concerns the relative likelihood and characteristics of the scenarios predicted to contribute most to PTS-induced RPV failure. The characteristics of the PTS scenario (e.g., pressure, temperature, timing) directly affect the issues of crack propagation, blowdown forces, and ECCS status (see below).
Relative contribution of axial and circumferential welds	This issue concerns the relative frequencies of PTS-induced RPV failures attributable to flaws in axial welds vs. flaws in circumferential welds. The orientation of the crack affects crack propagation and the characteristics of the resulting hole.
Crack propagation, hole size, hole location	This issue concerns the characteristics of the crack and the resulting hole in the RPV (including the rate of opening and the shape of the hole). This issue directly affects the issues of blowdown forces, fuel coolability, and fuel environment (see below).
Blowdown forces	This issue concerns the pressure differential driving fluid out of the RPV and the associated forces on the RPV, its internals, and connected piping. This issue directly affects the issues of containment isolation, missiles, ECCS status, core status, and fuel dispersal (see below).
Containment isolation	Early failure of containment isolation (e.g., by the failure of containment penetrations) is a contributing factor to the occurrence of a large early release.
Missiles	This issue concerns the possibility of a PTS-induced RPV failure leading to energetic missiles that could affect accident progression. This issue directly affects the issues of ECCS status and containment spray status (see below).
ECCS status (injection, recirculation)	This issue concerns the reliability of ECCS (given that ECCS was working prior to RPV failure). Potential contributors to ECCS failure include random hardware failure, failure to switch over properly to recirculation, failure of ECCS piping, and containment sump clogging.
Containment spray status	Early failure of containment spray is a contributing factor to the occurrence of a large early release. This issue concerns the reliability of containment spray (given that ECCS was working prior to RPV failure). Potential contributors to failure include random hardware failure, failure of piping (attributable to missiles), and containment sump clogging.
Core status (intact, distorted, disrupted)	This issue concerns whether the fuel geometry is distorted or severely disrupted as a result of the blowdown forces associated with a PTS-induced RPV failure.
Fuel dispersal	This issue concerns the location of fuel, should it be dispersed from the core as a consequence of a PTS-induced RPV failure.
Fuel coolability	This issue concerns fuel coolability, given its location and the core status.
RPV water level	This issue concerns the availability of water to cool the fuel (even if the ECCS is not working). It is affected by a number of factors, including the characteristics of the RPV cavity and the inventory of water available.
Fuel environment (steam, air)	This issue concerns the possibility of large-scale air oxidation of fuel. It is strongly dependent on the development of the accident scenario.
Early overpressure	This issue concerns the possibility of early containment failure attributable to (1) overpressures resulting from PTS-induced RPV failure events, and (2) overpressure caused by other mechanisms (e.g., hydrogen combustion).

Figure 10.1. Post-RPV failure accident progression tree

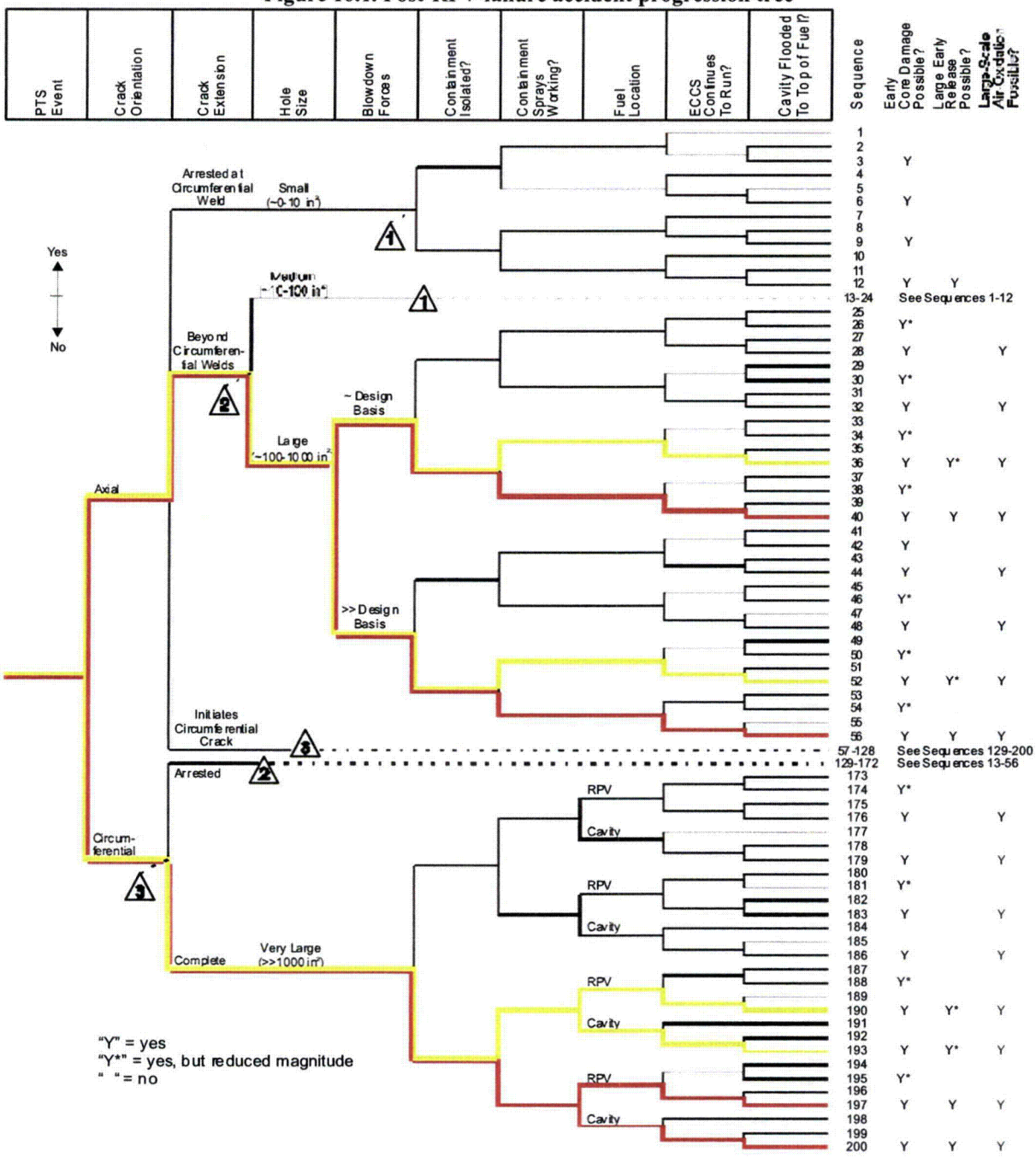

Therefore, there is little chance that the missile would possess the energy to damage the ECCS, containment spray system, or any containment penetrations. Additional activities regarding missiles included a review of NUREG/CR-4483 [Simonen 86] in light of currently available information on missile generation and penetration potential, a review of the reactor cavity designs of the plants considered in this study, and limited calculations to estimate plastic strains associated with a postulated, instantaneous large (~4 m x 0.3 m, 1,728 in.^{2}) hole in the side of a representative RPV.

To address scenarios involving early overpressure, limited-scope RELAP5 calculations (performed for a representative plant) were performed. These calculations indicate that the initial containment pressure rise associated with a range of PTS-induced RPV failures should be small, relative to the containment design pressure. PTS-initiated scenarios involving large amounts of hydrogen generation are possible (e.g., see Scenario 56 in the APET), but are not likely to lead to failure of either large, dry containments or ice condenser containments. The former are capable of withstanding the overpressure associated with a severe accident hydrogen burn, and the principal failure mode of the hydrogen igniters for the latter is a loss of station power, which is not a concern for PTS scenarios. (Loss of power is, of course, an issue for core overheating scenarios typically addressed by PRAs, in which possible RPV failures occur after core damage.)

Figure 10.1 identifies scenarios that have the potential to lead to source terms significantly worse than those associated with risk-significant, non-PTS related accident scenarios. Scenarios that are judged to have a possibility of leading to an early (e.g., less than 4 hours after RPV failure) release with a severe source term (i.e., a source term associated with large-scale air-oxidation of fuel) are highlighted in red. Scenarios that are judged to have a possibility of leading to an early release with a containment-spray-scrubbed, air-oxidation source term are highlighted in yellow.

Table 10.2 summarizes the key characteristics associated with each of the highlighted scenarios. The common characteristics of these scenarios are also shared with risk-significant non-PTS scenarios: they require the loss of fuel cooling (either from ECCS or from water in the reactor cavity), the loss of containment isolation, and, in the case of the most severe scenarios, the loss of containment spray. Table 10.2 also provides a summary assessment of the conditional likelihood of each scenario, given the occurrence of a PTS event.

The discussion in Table 10.2 identifies two classes of plants, including (1) those for which it is expected that, following a PTS-initiated RPV failure, the reactor cavity will be flooded above the top of the active fuel, and (2) all other plants. For the first class, it is believed that, for all scenarios identified by the APET, the conditional probability of PTS-induced fuel damage and subsequent large early release is extremely small (i.e., less than 0.001).

For the second class of plants, the most important APET postulated scenarios appear to be Scenarios 96, 100, 118, and 125. These scenarios all involve the following factors:

- an initial crack in an axial weld that propagates to the circumferential weld, and then initiates a circumferential crack
- blowdown forces above those anticipated for design-basis events
- the possibility of containment penetration failures as a result of RPV movement
- the possibility of ECCS failure attributable to RPV movement

Table 10.3 identifies the key differences between the four scenarios and their assessed likelihoods. A likelihood rating of "extremely small" corresponds to a conditional probability less than 0.001, while a rating of "very small" corresponds to a conditional probability less than 0.01, and a rating of "small" corresponds to a conditional probability less than 0.1.

Table 10.2. Potentially risk-significant post-RPV failure accident progression scenarios

Scenario	Characteristics	Potential Consequential Failures[b]	Independent Failures[c]	Conditional Probability Rating[d,e]
36	- Axial crack that extends beyond circumferential weld - Medium-to-large (~100-1,000 in^2) hole in RPV - Blowdown forces within design basis - Failed containment isolation - Operating containment spray - Loss of fuel cooling		- Containment Isolation - ECCS	Extremely small
40	- Axial crack that extends beyond circumferential weld - Medium-to-large (~100-1000 in^2) hole in RPV - Blowdown forces within design basis - Failed containment isolation - Failed containment spray - Loss of fuel cooling		- Containment Isolation - Containment Spray - ECCS	Extremely small
52	- Axial crack that extends beyond circumferential weld - Medium-to-large (~100-1000 in^2) hole in RPV - Blowdown forces greater than design basis - Failed containment isolation - Operating containment spray - Loss of fuel cooling	- Containment Penetration - ECCS piping		- Extremely small for plants where cavity flooding above the top of the fuel is expected - May be very small for other plants, depending on effect of blowdown forces
56	- Axial crack that extends beyond circumferential weld - Medium-to-large (~100-1000 in^2) hole in RPV - Blowdown forces greater than design basis - Failed containment isolation - Failed containment spray - Loss of fuel cooling	- Containment Penetration - ECCS piping	- Containment Spray	Extremely small
80	- Axial crack that initiates a circumferential crack that arrests after limited propagation - Medium-to-large (~100-1000 in^2) hole in RPV - Blowdown forces within design basis - Failed containment isolation - Operating containment spray - Loss of fuel cooling		- Containment Isolation - ECCS	Extremely small
84	- Axial crack that initiates a circumferential crack that arrests after limited propagation - Medium-to-large (~100-1000 in^2) hole in RPV - Blowdown forces within design basis - Failed containment isolation - Failed containment spray - Loss of fuel cooling		- Containment Isolation - Containment Spray - ECCS	Extremely small
96	- Axial crack that initiates a circumferential crack that arrests after limited propagation - Medium-to-large (~100-1000 in^2) hole in RPV - Blowdown forces greater than design basis - Failed containment isolation - Operating containment spray - Loss of fuel cooling	- Containment Penetration - ECCS piping		- Extremely small for plants where cavity flooding above the top of the fuel is expected - May be small to very small for other plants, depending on effect of blowdown forces
100	- Axial crack that initiates a circumferential crack that arrests after limited propagation - Medium-to-large (~100-1000 in^2) hole in RPV - Blowdown forces greater than design basis - Failed containment isolation - Failed containment spray - Loss of fuel cooling	- Containment Penetration - ECCS piping	- Containment Spray	- Extremely small for plants where cavity flooding above the top of the fuel is expected - May be very small to extremely small for other plants, depending on effect of blowdown

Scenario	Characteristics	Potential Consequential Failures[b]	Independent Failures[c]	Conditional Probability Rating[d,e]
				forces
118	- Axial crack that initiates a circumferential crack that subsequently progresses around the entire RPV - Very large (>>1000 in^2) hole - Blowdown forces greater than design basis - Failed containment isolation - Operating containment spray - Majority of fuel retained in RPV - Loss of fuel cooling	- Containment Penetration - ECCS piping		- Extremely small for plants where cavity flooding above the top of the fuel is expected - May be small to very small for other plants, depending on effect of blowdown forces
121	- Axial crack that initiates a circumferential crack that subsequently progresses around the entire RPV - Very large (>>1000 in^2) hole - Blowdown forces greater than design basis - Failed containment isolation - Operating containment spray - Majority of fuel dispersed into reactor cavity - Loss of fuel cooling	- Containment Penetration - ECCS piping		- Extremely small for plants where cavity flooding above the top of the fuel is expected - May be very small to extremely small for other plants, depending on effect of blowdown forces
125	- Axial crack that initiates a circumferential crack that subsequently progresses around the entire RPV - Very large (>>1000 in^2) hole - Blowdown forces greater than design basis - Failed containment isolation - Failed containment spray - Majority of fuel retained in RPV - Loss of fuel cooling	- Containment Penetration - ECCS piping	- Containment Spray	- Extremely small for plants where cavity flooding above the top of the fuel is expected - May be very small to extremely small for other plants, depending on effect of blowdown forces
128	- Axial crack that initiates a circumferential crack that subsequently progresses around the entire RPV - Very large (>>1000 in^2) hole - Blowdown forces greater than design basis - Failed containment isolation - Failed containment spray - Majority of fuel dispersed into reactor cavity - Loss of fuel cooling	- Containment Penetration - ECCS piping	- Containment Spray	Extremely small
152	- Circumferential crack that arrests - Medium-to-large (~100-1000 in^2) hole in RPV - Blowdown forces within design basis - Failed containment isolation - Operating containment spray - Loss of fuel cooling		- Containment Isolation - ECCS	Extremely small
156	- Circumferential crack that arrests - Medium-to-large (~100-1000 in^2) hole in RPV - Blowdown forces within design basis - Failed containment isolation - Failed containment spray - Loss of fuel cooling		- Containment Isolation - Containment Spray - ECCS	Extremely small
168	- Circumferential crack that arrests - Medium-to-large (~100-1000 in^2) hole in RPV - Blowdown forces greater than design basis - Failed containment isolation - Operating containment spray - Loss of fuel cooling	- Containment Penetration - ECCS piping		- Extremely small for plants where cavity flooding above the top of the fuel is expected - May be very small to extremely small for other plants, depending on effect of blowdown forces
172	- Circumferential crack that arrests - Medium-to-large (~100-1000 in^2) hole in RPV - Blowdown forces greater than design basis	- Containment Penetration - ECCS piping	- Containment Spray	Extremely small

Scenario	Characteristics	Potential Consequential Failures[b]	Independent Failures[c]	Conditional Probability Rating[d,e]
	- Failed containment isolation - Failed containment spray - Loss of fuel cooling			
190	- Circumferential crack that progresses around the entire RPV - Very large (>>1000 in^2) hole - Blowdown forces greater than design basis - Failed containment isolation - Operating containment spray - Majority of fuel retained in RPV - Loss of fuel cooling	- Containment Penetration - ECCS piping		- Extremely small for plants where cavity flooding above the top of the fuel is expected - May be very small to extremely small for other plants, depending on effect of blowdown forces
193	- Axial crack that initiates a circumferential crack that subsequently progresses around the entire RPV - Very large (>>1000 in^2) hole - Blowdown forces greater than design basis - Failed containment isolation - Operating containment spray - Majority of fuel dispersed into reactor cavity - Loss of fuel cooling	- Containment Penetration - ECCS piping		Extremely small
197	- Axial crack that initiates a circumferential crack that subsequently progresses around the entire RPV - Very large (>>1000 in^2) hole - Blowdown forces greater than design basis - Failed containment isolation - Failed containment spray - Majority of fuel retained in RPV - Loss of fuel cooling	- Containment Penetration - ECCS piping	- Containment Spray	Extremely small
200	- Axial crack that initiates a circumferential crack that subsequently progresses around the entire RPV - Very large (>>1000 in^2) hole - Blowdown forces greater than design basis - Failed containment isolation - Failed containment spray - Majority of fuel dispersed into reactor cavity - Loss of fuel cooling	- Containment Penetration - ECCS piping	- Containment Spray	Extremely small

Table 10.3. Key APET scenarios

Scenario	Circumferential Crack Arrested?	Containment Spray Status	Likelihood Rating
96	Yes	Operating	Very small to small
100	Yes	Failed	Extremely small to very small
118	No	Operating	Very small to small
125	No	Failed	Extremely small to very small

The ratings are based largely on the following considerations:

- Containment spray operation is not expected to be adversely affected by the occurrence of a PTS event. In fact, its reliability may be higher than for non-PTS risk-significant scenarios, since support system availability is not generally a concern for PTS scenarios.[‡‡‡‡‡‡]
- As shown in Chapter 8, PTS scenarios generally involve situations where the RCS is at relatively low temperature. Consequently, the stored energy in the RCS is relatively low, and there is little driving force to directly cause the damage postulated in the scenarios.
- An initial assessment of the RPV deformation associated with a (conservatively assumed) instantaneous hole opening in the RPV indicates that substantial deformations will not occur and, therefore, the movement of the pipes connected to the RPV will be limited by the gap between the RPV and the cavity wall.
- Since reactor vessel movement attributable to blowdown forces is limited, damage of ECCS piping, containment spray or containment penetrations is not expected. The limited vessel movement would be compensated for by the pipe ductility, long runs of piping with many bends, and the hanger and support systems.

Table 10.3 is based upon currently available information. Resolution of the following key uncertainties could affect the assessment:

- the likelihood that an axial crack will indeed initiate a propagating circumferential crack
- the potential effect of "external events" (e.g., earthquakes) and other environmental hazards (e.g., internal fires) on PTS-induced LERF that were not addressed in the scoping study

10.4 Acceptance Criteria Options

The staff has developed two sets of options for PTS-associated RVFF acceptance guidelines. The first set of options concerns the specific definition of RPV failure to be used. The second concerns possible quantitative acceptance limits for that metric. Note that any potential changes to the RT_{NDT} screening limits discussed in Chapter 11 may affect RVFF, but are not likely to affect the conditional probability of core damage (given a PTS-induced RPV failure) or the conditional probability of large, early release (given a PTS-induced core damage event). Thus, they will likely have little effect on the level of defense-in-depth against PTS challenges already provided by the current rule.

The following two options were considered for defining RPV failure:

(1) RPV failure occurs when a PTS-induced crack penetrates the RPV wall (i.e., RVFF = TWCF).

(2) RPV failure occurs when a PTS event initiates a crack in the RPV wall (i.e., RVFF = Vessel Crack Initiation Frequency, or VCIF).

The first option uses the current definition of RPV failure. The second reflects the position adopted by non-U.S. regulatory bodies.

‡‡‡‡‡‡ This assessment is based on an assumption that any potential recirculation sump clogging issues, as identified under GSI-191, are addressed.

In developing the possible quantitative acceptance limits for RVFF (denoted by RVFF*), the staff considered the following four options:

A. RVFF* = 5 x 10^{-6}/ry
B. RVFF* = 1 x 10^{-5}/ry
C. RVFF* = 1 x 10^{-6}/ry
D. RVFF* << 1 x 10^{-6}/ry

Option A is suggested by the current value in RG 1.154. Option B is suggested by current guidelines on CDF provided by RG 1.174 and the Option 3 framework for risk-informing 10 CFR Part 50. Option C is suggested by current guidelines on LERF provided by RG 1.174 and the Option 3 framework for risk-informing 10 CFR Part 50. Option D is suggested by the possibility of significantly worse consequences for PTS events (as opposed to other risk-significant scenarios), as discussed by the July 2002 letter from ACRS [Bonaca 02].

10.5 Conclusions

The staff's analysis has led to the following conclusions regarding the establishment of a criterion for RVFF:

(1) The analysis supports a definition of RVFF as being equivalent to TWCF (i.e., for PTS considerations, RPV "failure" can be defined as an occurrence of a through-wall crack). This conclusion is based on the following two factors:

   (a) TWCF is a more direct measure than VCIF of the likelihood of events with potentially significant public health consequences. This is desirable from a risk-informed decision-making perspective.

   (b) The uncertainties associated with the prediction of a through-wall crack (under PTS conditions) are only slightly larger than those associated with the prediction of crack initiation (also under PTS conditions). For example, at the 10 CFR 50.61 RT_{PTS} screening limit, the separation between the 50th and 95th percentiles in the distribution of *VCIF* ranges from 0.8 to 1.8 orders of magnitude, while the separation between the 50th and 95th percentiles in the distribution of *TWCF* ranges from 0.9 to 2.6 orders of magnitude. This slight increase in uncertainty is a natural and expected consequence of a cleavage failure mechanism and does not reflect a state of knowledge limitation regarding crack arrest. (See [***EricksonKirk-PFM***] for details of the crack arrest model.)

(2) The analysis supports an acceptance criterion for *RVFF*, *RVFF**, of 1x10^{-6}/ry. This is based on the following observations:

   (a) The conditional probability of an unscrubbed, large early release with a large air-oxidation source term (given a PTS-induced RPV failure) appears to be very small (i.e., less than 0.01). It is particularly small for plants where water in the reactor cavity (following a PTS-induced RPV failure) will cover the fuel. For plants with larger cavities, the low probability of the scenario is largely attributable to the independence and reliability of containment sprays.

   (b) The assessment underlying the above observation does not account for potential dependencies associated with PTS-events initiated by "external events" (e.g., earthquakes) or internal fires.

   (c) For plants with cavities such that fuel cooling is not assured following a PTS-induced RPV failure, the APET (Figure 10.1) identifies the most probable scenarios where limited fuel damage might occur, even if ECCS operates as designed.

Observation (a), taken in isolation, supports the use of an *RVFF** based on considerations of core damage consistent with those proposed in current activities for risk-informing 10 CFR Part 50 [SECY-00-0198]. However, Observation (b) identifies a potentially significant uncertainty regarding the margin between PTS-induced RPV failure and large early release, and Observation (c) raises a potential concern

regarding defense-in-depth. Therefore, RG 1.174 guidelines on CDF supporting a value for *RVFF** of $1x10^{-5}$ events/year may not have sufficient justification, whereas the scoping study developed for RG 1.174 guidelines on LERF is more defensible given currently available information. This rationale supports our recommended value of $1x10^{-6}$ events/year for *RVFF**, which is consistent with the RG 1.174 guidelines on LERF.

When assessing the acceptability of the PTS-associated risk at a given plant, the mean value of the plant's PTS-induced *RVFF* (i.e., the mean *TWCF*) should be compared with *RVFF**. This conclusion is based on how other NRC risk-informed decisions use risk information (e.g., see RG 1.174).

(3) Should additional work be performed to address the key post-RPV failure accident progression uncertainties identified in this study, the following issues are of principal importance:

(a) the likelihood that a PTS-induced axial crack will, upon reaching a circumferential weld, turn and progress along the circumferential weld

(b) the likelihood of PTS-induced containment isolation failure (especially failures associated with failure of containment penetrations) and ECCS failure (especially ECCS piping failures)

(c) the magnitude of potential source terms and consequences associated with PTS events

(d) substantiation of conditional probability values in Table 10.2 and Table 10.3

(e) the impact of external events on PTS-induced LERF.

It is anticipated that state-of-knowledge improvements in any of these areas will strengthen this study's conclusions regarding the margin between a PTS-induced RPV failure and consequent large early releases. Although not quantified, several aspects of our analysis performed to support an RVFF* value $1x10^{-6}$ events/year have a known conservative bias. The following is a summary of a few of these areas identified earlier in this chapter:

- Given the relatively low energy of the fluid following a postulated PTS event, the impulse on the RPV and piping resulting from a blowdown was predicted to be within the bounds of a design-basis SSE. The limited vessel movement from a blowdown forces would be compensated for by the pipe ductility, long runs of piping with many bends, and the hanger and support systems. For these reasons, damage of ECCS piping or containment penetrations is not expected.
- Missile generation attributable to a postulated PTS event would result in an object being directed laterally into the reactor vessel cavity wall by the blowdown forces associated with the breach in the reactor vessel. For a missile to affect the containment spray system or containment penetrations, it would have to traverse a tortuous path through tight clearances of the reactor vessel cavity. The missile's energy would be dissipated by multiple contacts with the reactor cavity wall, as well as the distance it travels, and it would have to hit an extremely small target to render the containment spray system inoperable.
- Through-wall crack frequency is assumed to equal core damage, which is assumed to equal a release. The through-wall cracks may cover a wide spectrum of sizes, from very large to very small. Very small cracks would result in only minor leakage that would not significantly challenge the reactor safety systems.

11 Reference Temperature (*RT*)-Based PTS Screening Criteria

11.1 Introduction

In Chapter 8, we presented our baseline estimates of the variation of TWCF in the three study plants over a range of embrittlement levels. These estimates demonstrated that the challenge to the structural integrity of the RPV posed by the dominant transient classes (i.e., large-diameter primary side pipe breaks, stuck-open primary side valves that later reclose, and breaks of the main steam line) is approximately equal (at equivalent levels of embrittlement) across the three plants. We also identified why the structural integrity challenges posed by these dominant transients are *not expected* to vary from plant-to-plant, and are *not expected* to be influenced by factors that may differ between the three study plants and the general population of PWRs (see Sections 8.5.2.4.5, 8.5.3.4.3, and 8.5.4.4.2, respectively). This finding was further reinforced in Section 9.3, which included a survey of five additional plants having high levels of embrittlement. This survey assessed the factors in these plants that could influence either the severity of the transients or the frequency of their occurrence, with the aim of identifying the potential for situations in the general PWR population having greater severity and/or frequency than in the three study plants. The survey's outcome supported the view presented in Chapter 8. In the great majority of cases, the severity and frequency of transients in the general PWR population is no greater, and is often less, than in the three study plants. A few situations were identified where greater severities or frequencies did occur, but never both. Thus, the effect of these situations not being considered in the baseline TWCF results presented in Chapter 8 can be regarded as negligible.

Overall, the evidence presented in both Chapter 8 and Chapter 9 supports the use of the TWCF values presented in Table 8.5, together with the reactor vessel failure frequency acceptance criterion of 1×10^{-6} events per year proposed in Chapter 10 to develop a materials-based screening limit applicable to PWRs *in general*. In this chapter, we propose such a limit, making use of the reference temperature (*RT*) metrics also found in Table 8.5. As illustrated in Figure 8-4, an *RT* establishes a material's resistance to fracture, the variability in this resistance, and how this resistance varies with temperature. Since *RT* values can be estimated from information on vessel materials available in the RVID database [RVID2], as well as surveillance programs conducted in accordance with Appendix H to 10 CFR Part 50, they provide a means to estimate the fracture resistance of vessel materials and how this resistance diminishes with increased neutron irradiation.

The remainder of the chapter is organized as follows:

- Section 11.2 addresses *RT* metrics. We review the discussion of Section 8.4.1, which concerns the characteristics an *RT* metric needs so that it can be expected to correlate/predict the probability of vessel failure. This section also includes a critique of how well the *RT* metric currently used in 10 CFR 50.61, RT_{PTS}, meets these characteristics.
- In Section 11.3, we develop relationships between the RT_{AW}, RT_{PL}, and RT_{CW} metrics (see Table 8.5) and TWCF.
- Section 11.4 includes our proposed PTS screening criteria derived from the relationship developed in Section 11.3. We discuss the applicability of these screening criteria to PWRs in general, and we assess

the proximity of currently operating PWRs to this proposal at both end of license (40 years of operation) and end of license extension (60 years of operation).

11.2 Reference Temperature (*RT*) Metrics

As discussed in Section 8.4.1, in order to correlate and/or predict a RPV's resistance to fracture, we need some measure of the fracture resistance of the materials in the vessel at the location of the flaws in the vessel. *RT* values characterize fracture resistance, as illustrated in Figure 8-4. In Section 8.4.1, we proposed three *RT* metrics (RT_{AW}, RT_{PL}, and RT_{CW}), each of which is associated with a different flaw population (flaws on the axial weld fusion lines, flaws in plates, and flaws on the circumferential weld fusion lines, respectively). These three *RT* metrics were defined as follows (see Eq. 8-1, Eq. 8-2, and Eq. 8-3 for mathematical definitions):

- The **axial weld reference temperature** RT_{AW} characterizes the RPV's resistance to fracture initiating from flaws found along the axial weld fusion lines. It corresponds to the maximum RT_{NDT} of the plate/weld that lies to either side of each weld fusion lines, and is weighted to account for differences in weld fusion line length (and, therefore, the number of simulated flaws).
- The **plate reference temperature** RT_{PL} characterizes the RPV's resistance to fracture initiating from flaws found in plates that are not associated with welds. It corresponds to the maximum RT_{NDT} occurring in each plate, and is weighted to account for differences in plate volumes (and, therefore, the number of simulated flaws).
- The **circumferential weld reference temperature** RT_{CW} characterizes the RPV's resistance to fracture initiating from flaws found along the circumferential weld fusion lines. It corresponds to the maximum RT_{NDT} of the plate/weld that lies to either side of each weld fusion lines, and is weighted to account for differences in weld fusion line length (and, therefore, the number of simulated flaws).

We proposed these ***three*** different *RT*s in recognition of the fact that the probability of vessel fracture initiating from these three different flaw populations varies considerably as a result of the following known factors.

- Different regions of the vessel have flaw populations that differ in size (weld flaws are considerably larger than plate flaws), density (weld flaws are more numerous than plate flaws), and orientation (axial and circumferential welds have flaws of corresponding orientations, whereas plate flaws may be either axial or circumferential). The driving force to fracture depends on both flaw size and flaw orientation, so different vessel regions experience different fracture driving forces.
- The degree of irradiation damage suffered by the material at the flaw tips varies with location in the vessel because of differences in chemistry and fluence.

These differences indicate that it is impossible for a single *RT* to accurately represent the RPV's resistance to fracture in the general case. Indeed, this is precisely the liability associated with the 10 CFR 50.61 *RT* value RT_{PTS}. 10 CFR 50.61 defines RT_{PTS} as the maximum RT_{NDT} of any region in the vessel (a region is an axial weld, a circumferential weld, a plate, or a forging) evaluated at the peak fluence occurring in that region. Consequently, the RT_{PTS} value currently assigned to a vessel may only coincidentally correspond to the toughness properties of the material region responsible for the bulk of the TWCF, as illustrated by the following examples:

- Out of 71 operating PWRs, 14 have their RT_{PTS} values established based on circumferential weld properties [RVID2]. However, our results show that the probability of a vessel failing as a consequence of a crack in a circumferential weld is extremely remote because of the lack of through-wall fracture driving force associated with circumferentially oriented

cracks. For these 14 vessels, the RT_{PTS} value is unrelated to any material that has any significant chance of causing vessel failure.

- Out of 71 operating PWRs, 32 have their RT_{PTS} values established based on plate properties [RVID2]. Certainly, plate properties influence vessel failure probability; however, the 10 CFR 50.61 practice of evaluating RT_{PTS} at the peak fluence occurring in the plate is likely to estimate a toughness value that cannot be associated with any large flaws because the location of the peak fluence may not correspond to an axial weld fusion line. While the RT_{PTS} value for these 32 vessels is related to a material that contributes significantly to the vessel failure probability, it is likely that RT_{PTS} has been overestimated (perhaps significantly so) because the fluence assumed in the RT_{PTS} calculation does not correspond to the fluence at a likely flaw location.
- Out of 71 operating PWRs, 10 have their RT_{PTS} values established based on forgings [RVID2]. Forged vessels do not have axial welds, and consequently do not have the large flaws associated with axial weld fusion lines that account for a large portion of the TWCF. As discussed in Section 9.2 of this report and in [***EricksonKirk-SS***], flaws in forgings arise either as a consequence of the forging process itself or as "subclad" defects associated with the stainless steel cladding. Forging flaws are approximately equivalent to plate flaws in terms of both size and density, while subclad flaws occur as dense arrays of axially oriented flaws with a depth of ≈0.08-in. (≈2mm). Our sensitivity studies show that at an equivalent level of embrittlement, a forged vessel will have a through-wall cracking frequency that is ***at most*** ~15% that of an equivalent plate vessel (with axial welds). Thus, while forgings do contribute to the risk of vessel failure, the RT_{PTS} value for a forging-limited plant could considerably exceed the 10 CFR 50.61 screening criteria and still have a TWCF value below that of a plate vessel.
- Out of 71 operating PWRs, 15 have their RT_{PTS} values established based on axial weld properties [RVID2]. It is only for these vessels where the RT_{PTS} value is clearly associated with a material region that contributes significantly to the vessel failure probability, and is evaluated at a fluence that is clearly associated with a potential location of large flaws.

11.3 Relationship between *RT* Metrics and TWCF

11.3.1 Weighted *RT* Values

The information in Table 8.5 provides the percent contribution to the total TWCF attributable to axial weld flaws, circumferential weld flaws, and plate flaws. We use this information in Table 11.1 to determine the TWCF attributable to each flaw population. Figure 11-1 shows the relationships between the weighted *RT* metrics RT_{AW}, RT_{PL}, and RT_{CW} (described in Section 8.4.1 and quantified by Eq. 8-1, Eq. 8-2, and Eq. 8-3) and the TWCF values presented in Table 11.1. At a fixed reference temperature, the TWCF increases ≈50-fold between circumferential weld flaws and plate flaws, and ≈100-fold between plate flaws and axial weld flaws, reflecting the differences in fracture driving force caused by the different flaw sizes and orientations associated with the three flaw populations. The close agreement between TWCF values for different plants shown in Figure 11-1 is attributable to two factors:

- the similarity in both the frequency of, and the structural integrity challenge posed by, the most aggressive transients (i.e., large-diameter primary side pipe breaks, stuck-open primary side valves that later reclose, and breaks of the main steam line), as discussed in Section 8.5
- the fact that the weighted *RT* metrics appropriately reflect the toughness of the vessel at the location of postulated flaws

The fits shown in Figure 11-1 can be combined to estimate the TWCF of other PWRs, as follows:

Eq. 11-1 $$TWCF_{TOTAL} = TWCF_{AXIAL-WELD} + \alpha_{PL} \cdot TWCF_{PLATE} + TWCF_{CIRC-WELD}$$

where

$$TWCF_{AXIAL-WELD} = 4\text{x}10^{-26} \cdot \exp\{0.0585 \cdot (RT_{AW} + 459.69)\}$$ (see Eq. 8-1 for RT_{AW})

$$\alpha_{PL} = 1.7, \quad TWCF_{PLATE} = 4\text{x}10^{-29} \cdot \exp\{0.064 \cdot (RT_{PL} + 459.69)\}$$ (see Eq. 8-2 for RT_{PL})

$$TWCF_{CIRC-WELD} = 3\text{x}10^{-27} \cdot \exp\{0.051 \cdot (RT_{CW} + 459.69)\}$$ (see Eq. 8-3 for RT_{CW})

Table 11.1. Contributions of different flaw populations to the TWCF values estimated by FAVOR Version 04.1

EFPY	Weighted Reference Temperatures [°F]			Maximum Reference Temperatures [°F]			% TWCF Due to Flaws in			Mean TWCF, events/yr.			
	RT_{AW}	RT_{CW}	RT_{PL}	RT_{MAX-AW}	RT_{MAX-CW}	RT_{MAX-PL}	Axial Welds	Circ Welds	Plates	Total	Axial Welds	Circ Welds	Plates
Oconee Unit 1													
32	134	136	72	152	175	79	100.00%	0.00%	0.00%	2.30E-11	2.30E-11	0.00E+00	0.00E+00
60	149	156	83	171	193	89	99.90%	0.10%	0.00%	6.47E-11	6.46E-11	6.47E-14	0.00E+00
Ext-Oa	200	207	134	232	251	136	99.83%	0.16%	0.00%	1.30E-09	1.30E-09	2.08E-12	0.00E+00
Ext-Ob	227	229	164	263	281	170	99.81%	0.11%	0.08%	1.16E-08	1.16E-08	1.28E-11	9.28E-12
Beaver Valley Unit 1													
32	171	243	217	192	243	243	68.44%	0.33%	31.23%	8.89E-10	6.08E-10	2.93E-12	2.78E-10
60	188	272	244	210	272	272	39.19%	0.72%	60.09%	4.84E-09	1.90E-09	3.48E-11	2.91E-09
Ext-Ba	203	301	273	225	301	301	15.69%	1.74%	82.55%	2.02E-08	3.17E-09	3.51E-10	1.67E-08
Ext-Bb	226	354	324	250	354	354	9.21%	6.18%	84.62%	3.00E-07	2.76E-08	1.85E-08	2.54E-07
Palisades													
32	210	201	165	212	201	189	99.95%	0.05%	0.00%	4.90E-09	4.90E-09	2.45E-12	0.00E+00
60	227	215	181	230	215	205	99.97%	0.04%	0.00%	1.55E-08	1.55E-08	6.20E-12	0.00E+00
Ext-Pa	271	259	231	277	259	259	99.91%	0.02%	0.08%	1.88E-07	1.88E-07	3.76E-11	1.50E-10
Ext-Pb	324	335	293	333	335	335	98.62%	0.01%	1.37%	1.26E-06	1.24E-06	1.26E-10	1.73E-08

Note: See Eq. 8-1, Eq. 8-2, and Eq. 8-3 for reference temperature definitions.

In Eq. 11-1, the *RT* values are expressed in °F; the formula converts Fahrenheit to Rankine to prevent the introduction of negative numbers to the exponential terms. The TWCF attributable to plate flaws is multiplied by a factor of 1.7 to prevent a systematic underestimation of the TWCF results for Beaver Valley. Averaged across all embrittlement levels analyzed, Eq. 11-1 overpredicts the Oconee, Beaver Valley, and Palisades results by 65%, 1%, and 25%, respectively. Figure 11-3 compares the FAVOR 04.1 TWCF estimates with the predictions of Eq. 11-1, showing good agreement overall.

11.3.2 Maximum *RT* Values

The TWCF estimation formula (Eq. 11-1) developed in the preceding Section is based on weighted *RT* values; it provides a means to estimate with reasonable accuracy how TWCF changes with embrittlement level. However, information from construction drawings regarding the dimensions and placement of the welds, plates, and forgings in the beltline region is needed to estimate the weighted reference temperatures (RT_{AW}, RT_{CW}, and RT_{PL}) used in Eq. 11-1, *in addition to* information available in the RVID database concerning chemical composition, fluence, and the RT_{NDT} before irradiation [RVID2]. While this additional information is readily available to licensees, and indeed has been docketed with the NRC, not having this information available in one place for all PWRs makes it difficult to estimate TWCF using Eq. 11-1 for the operating fleet. Conversely, the *maximum* reference temperatures $RT_{MAX\text{-}AW}$, $RT_{MAX\text{-}CW}$, and $RT_{MAX\text{-}PL}$ that are used to estimate the weighted reference temperatures (RT_{AW}, RT_{CW}, and RT_{PL}, respectively) can be evaluated based only on information in RVID. Consequently, in Figure 11-2, we examine the relationships between these maximum reference temperatures and the TWCF values presented in Table 11.1 for each of the three flaw populations. The uncertainty in the correlations of TWCF with maximum *RT* values exceeds slightly the uncertainty in the correlations of TWCF with weighted *RT* values (compare Figure 11-2 to Figure 11-1). Nonetheless, the relationships in Figure 11-2 do provide a basis for estimating TWCF when only the information in RVID is available. The fits shown in Figure 11-2 can be combined to estimate the TWCF of other PWRs, as follows:

Eq. 11-2 $$TWCF_{TOTAL} = \alpha_{AW} \cdot TWCF_{AXIAL-WELD} + \alpha_{PL} \cdot TWCF_{PLATE} + TWCF_{CIRC-WELD}$$

where

$$\alpha_{AW} = 1.6,\ TWCF_{AXIAL-WELD} = 3\text{x}10^{-27} \cdot \exp\{0.0605 \cdot (RT_{MAX-AW} + 459.69)\}$$

$$\alpha_{PL} = 1.7,\ TWCF_{PLATE} = 9\text{x}10^{-27} \cdot \exp\{0.0543 \cdot (RT_{MAX-PL} + 459.69)\}$$

$$TWCF_{CIRC-WELD} = 4\text{x}10^{-29} \cdot \exp\{0.0561 \cdot (RT_{MAX-CW} + 459.69)\}$$

(see Eq. 8-1, Eq. 8-2, and Eq. 8-3 for the definitions of $RT_{MAX\text{-}AW}$, $RT_{MAX\text{-}PL}$, and $RT_{MAX\text{-}CW}$, respectively)

In Eq. 11-2, the *RT* values are again expressed in °F; the formula converts Fahrenheit to Rankine to prevent the introduction of negative numbers to the exponential terms. The TWCF attributable to axial weld flaws and to plate flaws are multiplied by factors of 1.6 and 1.7, respectively, to prevent a systematic underestimation of the TWCF results of Palisades and of Beaver Valley, respectively. Averaged across all embrittlement levels analyzed, Eq. 11-2 overpredicts the Oconee, Beaver Valley, and Palisades results by 278%, 1%, and 2%,respectively. Figure 11-4 compares the FAVOR 04.1 TWCF estimates with the predictions of Eq. 11-2. As expected, based on the lower correlation coefficients of the TWCF *vs.* maximum *RT* relationships shown in Figure 11-2, the estimation accuracy of Eq. 11-2 is not quite as good as that of Eq. 11-1.

11.4 Proposed *RT*-Based Screening Limits

A *RT*-based screening limit can be established by setting the total TWCF in either Eq. 11-1 or Eq. 11-2 equal to the reactor vessel failure frequency acceptance criterion of $1x10^{-6}$ events per year proposed in Chapter 10. In the following two subsections we propose two *RT*-based screening limits: first in Section 11.4.1 for plate vessels (which have axial welds), and second in Section 11.4.2 for forged vessels (which do not have axial welds). In both sections, we compare our proposed screening limits to the *RT* values for currently operating PWRs at both EOL and EOLE. This section concludes with a discussion of the need for margins when using these screening limits to assess operating PWRs (see Section 11.4.3).

11.4.1 Plate Vessels

Plate vessels are made up of axial welds, plates, and circumferential welds, so in principal flaws in all of these regions will contribute to the through-wall cracking frequency. However, as revealed by our results (see Table 8.5) and as reflected in Eq. 11-1 and Eq. 11-2, the contribution of flaws in circumferential welds to TWCF is negligible relative to that of flaws in axial welds and in plates. A *RT*-based screening limit for PTS can therefore be derived from Eq. 11-1 by the following procedure:

(1) Set RT_{CW} to a fixed value.

(2) Set $TWCF_{TOTAL}$ to the $1x10^{-6}$ value proposed in Chapter 10.

(3) Solve the equation to establish (RT_{AW}, RT_{PL}) pairs that satisfy equality.

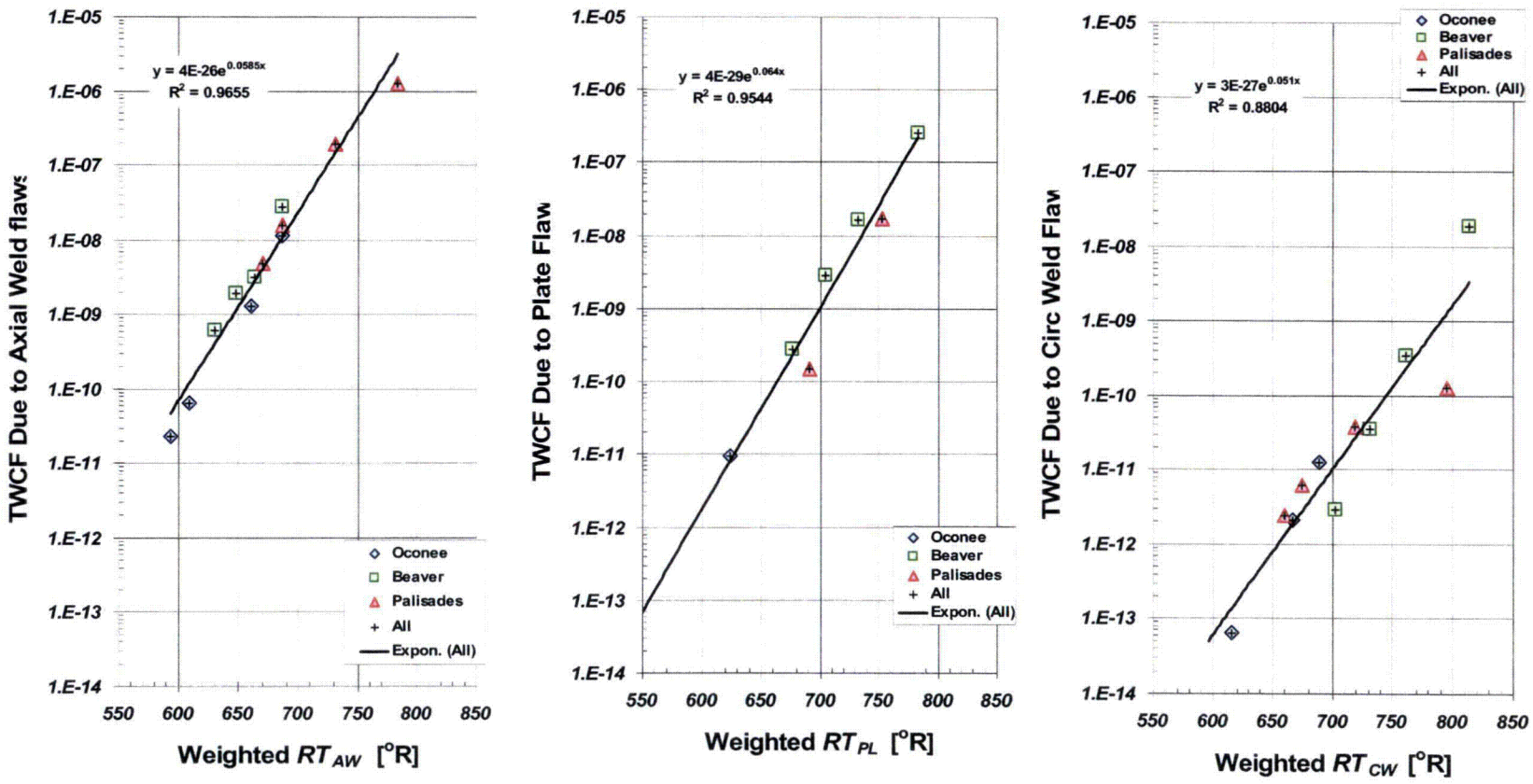

Figure 11-1. Correlation of through-wall cracking frequencies with weighted reference temperature metrics for the three study plants (°R = °F + 459.69)

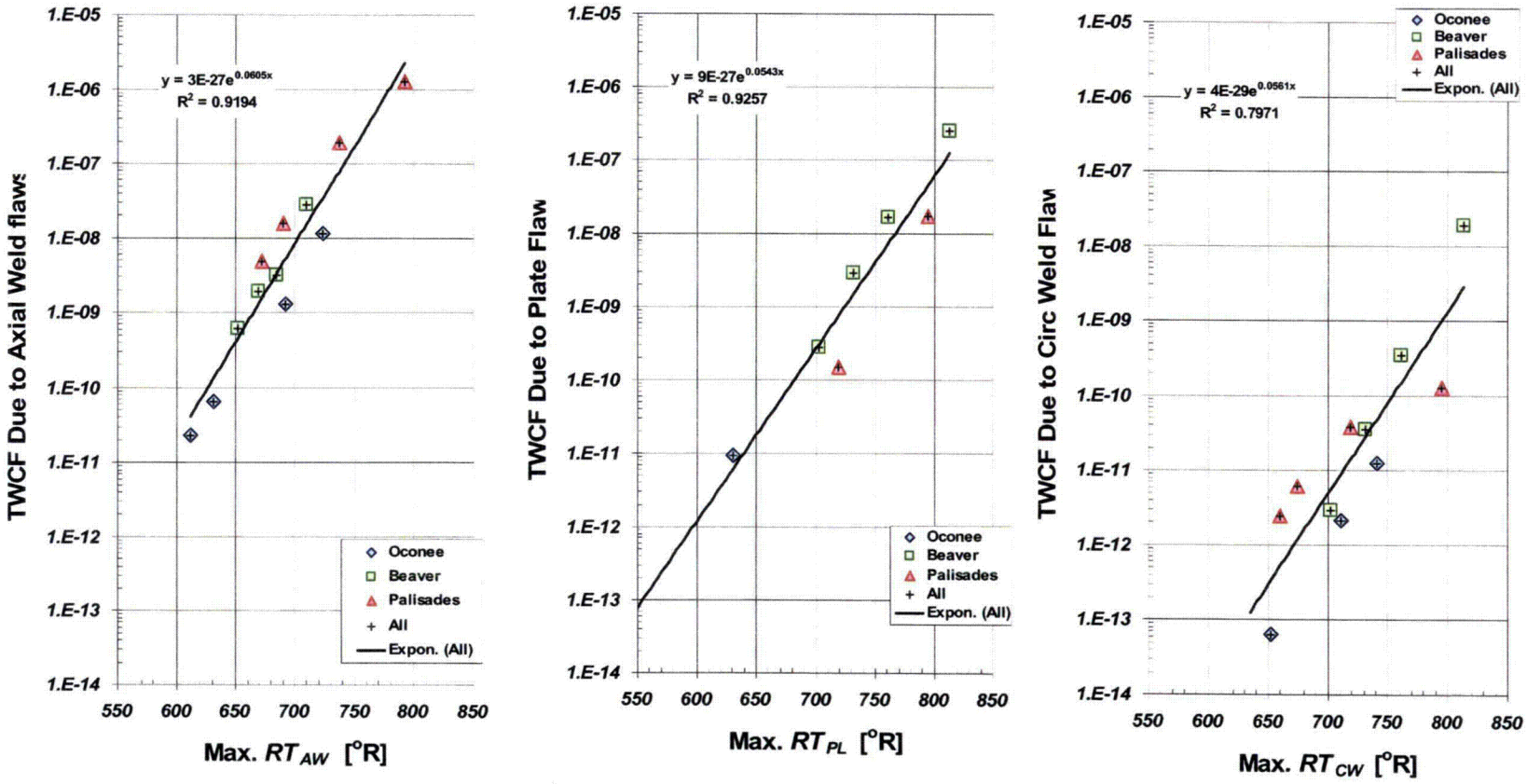

Figure 11-2. Correlation of through-wall cracking frequencies with maximum reference temperature metrics for the three study plants (°R = °F + 459.69)

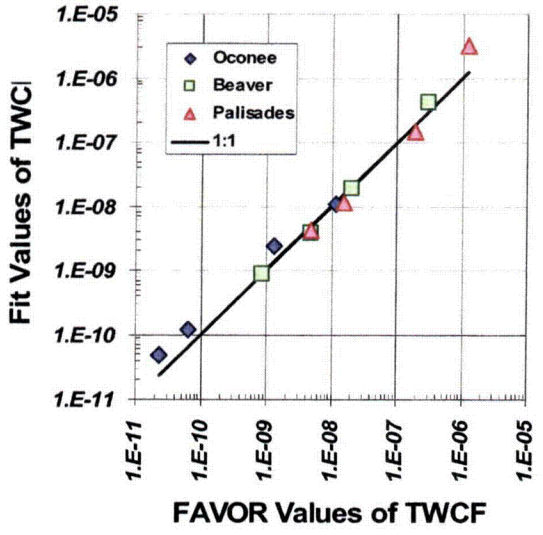

Figure 11-3. Comparison of FAVOR 04.1 TWCF estimates with TWCF values estimated using weighted *RT* values (Eq. 11-1)

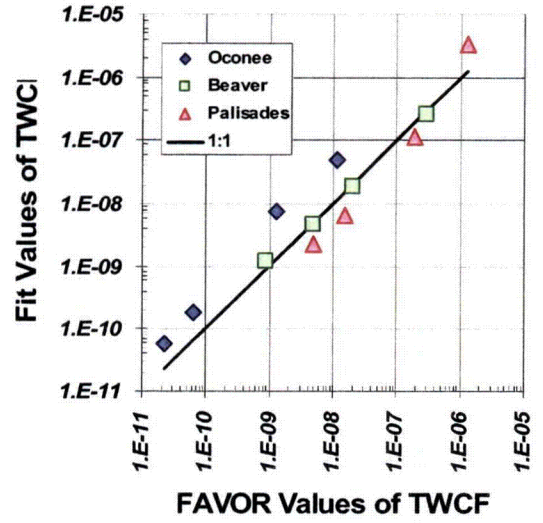

Figure 11-4. Comparison of FAVOR 04.1 TWCF estimates with TWCF values estimated using maximum *RT* values (Eq. 11-2)

As graphically illustrated in Figure 11-5, this procedure establishes a locus of (RT_{AW}, RT_{PL}) pairs. In the region of the graph between the locus and the origin, the TWCF is below the $1x10^{-6}$ acceptance criterion, so these combinations of RT_{AW} and RT_{PL} would be considered acceptable and require no further analysis. In the region of the graph outside of the locus, the TWCF is above the $1x10^{-6}$ acceptance criterion, indicating the need for additional analysis or other measures to justify continued plant operation. Figure 11-5 also indicates the effects of the RT_{CW} value (left-hand graph) and the $TWCF_{TOTAL}$ value (right-hand graph) on the position of the RT_{AW} *vs.* RT_{PL} locus. As previously mentioned, the RT_{CW} value has little effect on the location of the $1x10^{-6}$ locus for any RT_{CW} value that is likely to occur within the foreseeable future.

Figure 11-6 provides loci of ($RT_{MAX\text{-}AW}$, $RT_{MAX\text{-}PL}$) similar to those shown in Figure 11-5, but based instead on Eq. 11-2 (that is, on maximum *RT* values rather than on weighted *RT* values). These loci are used to assess the condition of currently operating PWRs relative to *RT*-based screening limits derived from the results of this investigation because maximum *RT* values can be estimated using only the information available in the RVID database [RVID2]. We assess the condition of operating PWRs at EOL (40 years, or 32 EFPY) and EOLE (60 years of operation, or 48 EFPY). The ID fluence at EOLE was assumed to be 1.5 times the value reported in RVID at EOL. This assumption implies that no changes in core loading will be made during the period of license extension. Were any licensee to change their core loading (e.g., remove their halfnium suppression to increase power), these changes would be reflected in both calculated fluence values and in the results of the surveillance programs conducted under Appendix H to 10 CFR Part 50, and so could easily be accounted for by recalculating the various *RT* metrics based on these different input values.

The results of these calculations are reported in Appendix D and are compared to the proposed screening limit for plate vessels in Figure 11-7. At EOL, at least 70°F (21°C) and up to 290°F (143°C) separate operating PWRs from the proposed screening limit; these values reduce by between 10 and 20°F (5.5 to 11°C) at EOLE. The wide separation of operating plants at EOL from these proposed screening limits contrasts sharply with the current regulatory situation (see Figure 1.1), where some operating plants lie within less than a single degree Fahrenheit of the

10 CFR 50.61 RT_{PTS} screening limits. This increase in estimated "distance" from a RT screening limit occurs as a direct consequence of the more accurate models used throughout this investigation. Figure 11-8 points out that these improvements can, equivalently, be quantified in terms of a reduction in the estimated annual frequency of through-wall cracking associated with operating PWRs. As shown in the figure, even at EOLE no currently operating plant is projected to exceed a annual TWCF of $1x10^{-7}$ (again, most plants have projected TWCFs far below this value, see Figure 11-8).

11.4.2 Forged Vessels

Forged vessels are comprised of forgings and circumferential welds; they contain no axial welds and so there can be no contribution to TWCF from the $RT_{MAX\text{-}AW}$ term in Eq. 11-2. While we have not performed a detailed analysis of a forged vessel, the sensitivity studies on forging flaw distributions reported in Section 9.2 of this report and in [***EricksonKirk-SS***] support the use of the $RT_{MAX\text{-}PL}$ term (evaluated using forging properties) in Eq. 11-2 to estimate the contribution of TWCF of forgings.

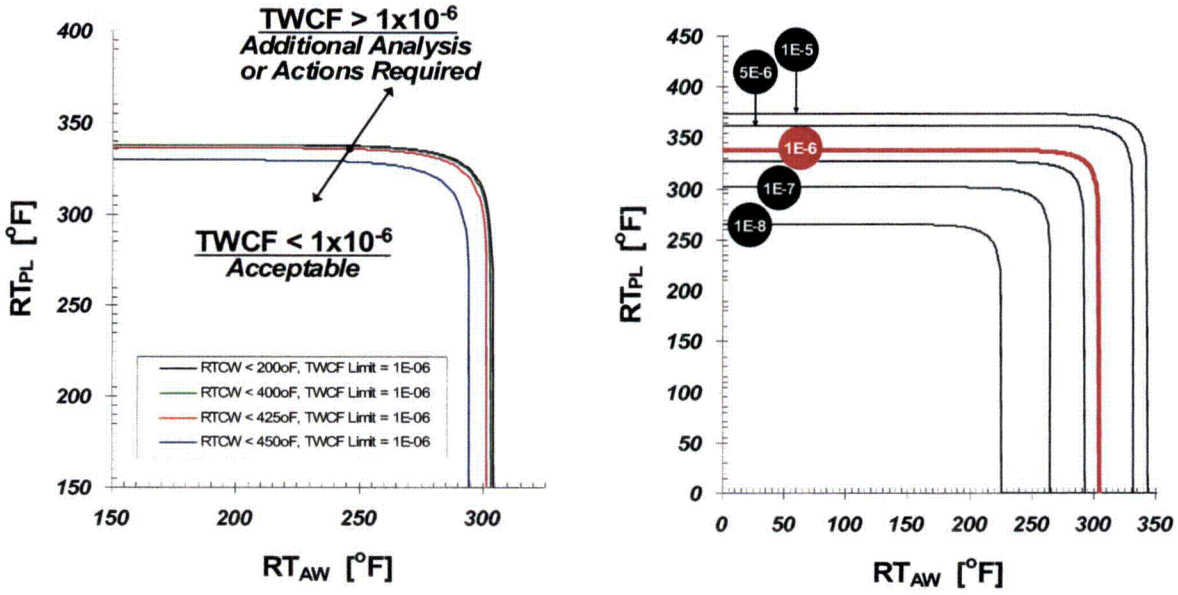

Figure 11-5. Weighted RT-based screening criterion for plate vessels based on Eq. 11-1 (Left: Effect of RT_{CW} value for a fixed $TWCF_{TOTAL}$ value of $1x10^{-6}$; Right: Effect of $TWCF_{TOTAL}$ for a fixed RT_{CW} value of 300°F (149°C))

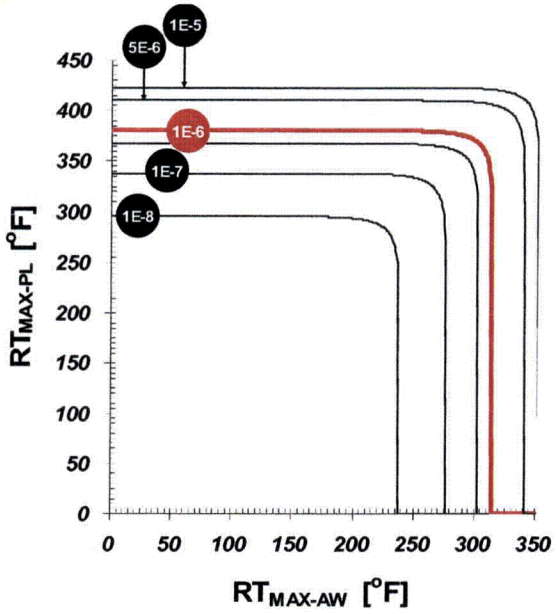

Figure 11-6. Maximum *RT*-based screening criterion for plate vessels based on Eq. 11-2

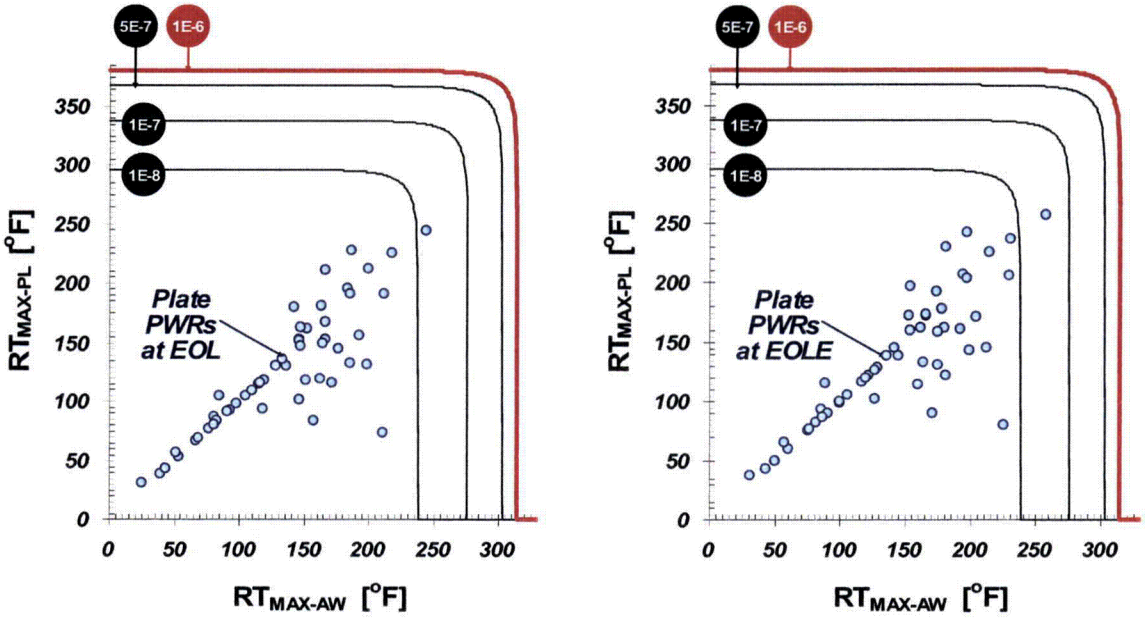

Figure 11-7. Comparison of the maximum *RT*-based screening limit for plate vessels based on Eq. 11-2 with assessment points for all operating PWRs at EOL (32 EFPY, 40 operating years) (left) and EOLE (48 EFPY, 60 operating years) (right) (Plant RT values estimated from information in [RVID2]. $RT_{MAX\text{-}CW}$ is 300°F (149°C) for both graphs, exceeding the calculated $RT_{MAX\text{-}CW}$ value for any plant at EOL or EOLE.)

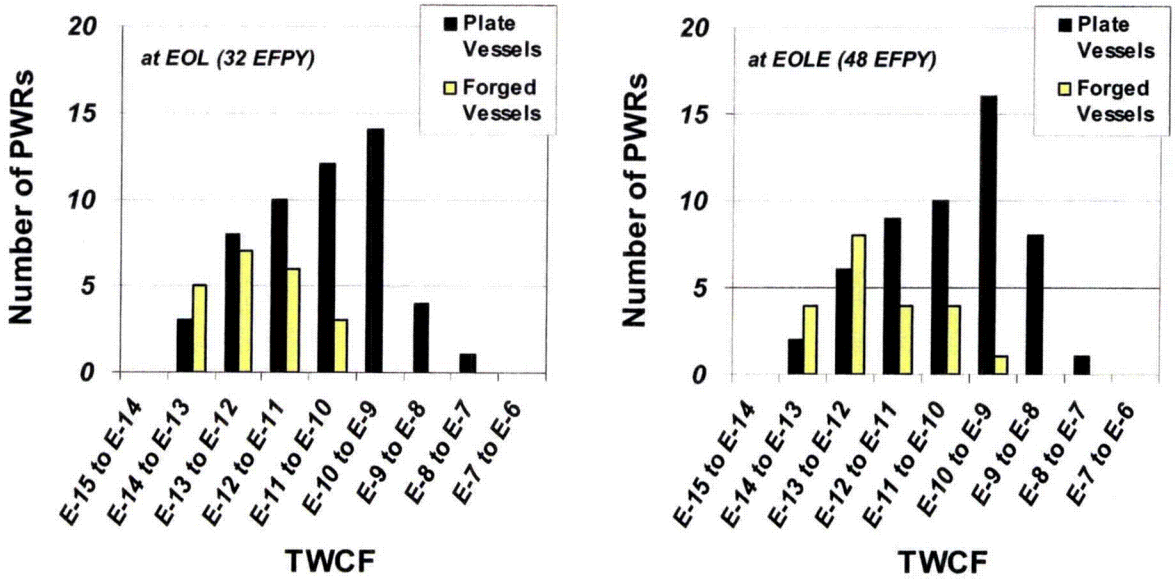

Figure 11-8. TWCF values for operating PWRs estimated using Eq. 11-1 at EOL (left) and EOLE (right) (Values for individual plants are reported in Appendix D.)

Figure 11-9 provides the locus of ($RT_{MAX\text{-}CW}$, $RT_{MAX\text{-}PL}$) pairs that can be used to assess the compliance of forged vessels with the reactor vessel failure frequency limit of $1x10^{-6}$ events/year proposed in Chapter 10. Figure 11-9 is interpreted in the same way as the proposed screening limit for plate vessels (Figure 11-6).

Figure 11-10 compares this proposed screening limit with the $RT_{MAX\text{-}CW}$ and $RT_{MAX\text{-}PL}$ values for currently operating forged vessels at EOL and at EOLE (see Appendix D for plant-specific values of $RT_{MAX\text{-}CW}$ and $RT_{MAX\text{-}PL}$). These results demonstrate that no forged plant is anywhere close to screening limits based on a reactor vessel failure frequency limit of $1x10^{-6}$ events/year (see also Figure 11-8, which expresses these results in terms of frequency, rather than in terms or reference temperature).

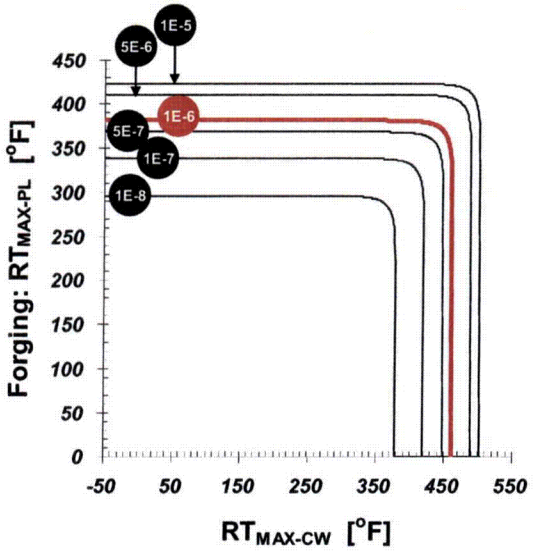

Figure 11-9. Maximum *RT*-based screening criterion for forged vessels based on Eq. 11-1, illustrating the effect of $TWCF_{TOTAL}$

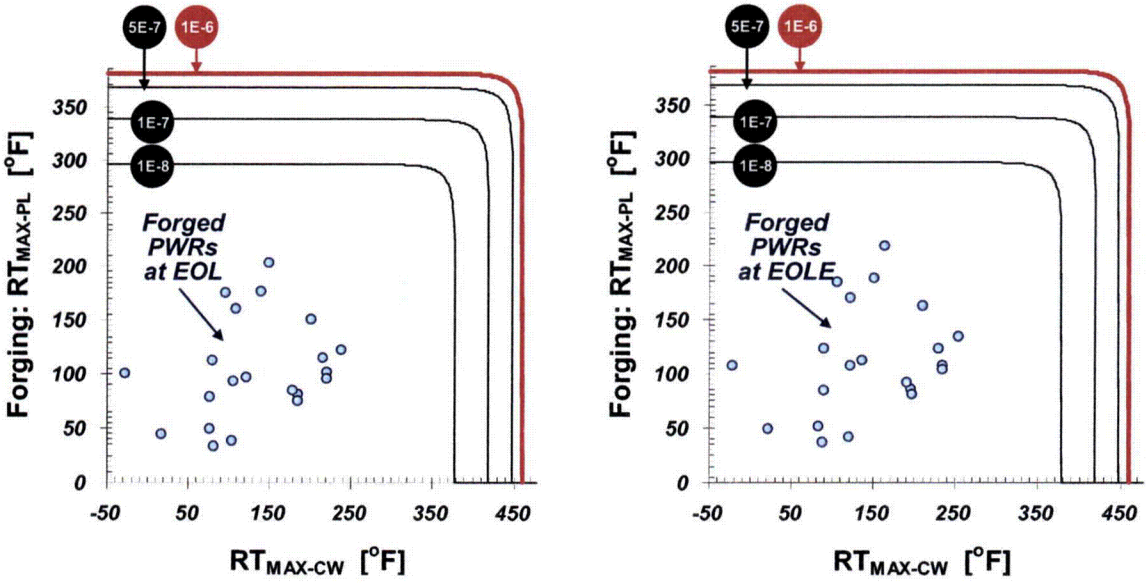

Figure 11-10. Comparison of maximum *RT*-based screening limit for forged vessels based on Eq. 11-2 with operating PWRs at EOL (32 EFPY, 40 operating years) (left) and EOLE (48 EFPY, 60 operating years) (right) (Plant *RT* values estimated from information in [RVID2]. $RT_{MAX\text{-}PL}$ is estimated based on forging properties.)

11.4.3 Need for Margin

Aside from relying on different *RT* metrics, the PTS screening limits proposed in Figure 11-6 and Figure 11-9 differs from the 10 CFR 50.61 RT_{PTS} screening limit by the absence of a "margin term." Use of a margin term is appropriate to account (at least approximately) for factors that occur in application that were not considered in the analyses upon which these proposed screening limits are based. For example, the 10 CFR 50.61 margin term (see **Eq. 2-4**) accounts for uncertainty in copper, in nickel, and in initial RT_{NDT}. However, as summarized in Chapter 7 and discussed in detail by [***ErickssonKirk-PFM***], our model explicitly considers uncertainty in all of these variables, and represents these uncertainties as being larger

(a conservative representation) than would be appropriate in any plant-specific application of the proposed screening limit. Consequently, use of the 10 CFR 50.61 margin term with the screening limits proposed in Figure 11-6 and Figure 11-9 would be inappropriate.

In general, the following additional reasons suggest that use of any margin term with the proposed screening limits is inappropriate:

(1) The *TWCF* values used to establish the screening limit represent 90th percentile values or greater (see Figure 8-3).

(2) Chapter 8 and Chapter 9 demonstrate that the results from our three plant-specific analyses apply to PWRs in general.

(3) Certain aspects of our modeling cannot be reasonably represented as "best estimates." On balance, there is a conservative bias to these non-best estimate aspects of our analysis, as discussed in the following section.

11.4.4 Non-Best Estimate Aspects of the Model

Throughout this project, every effort has been made to perform a "best estimate" analysis. Nonetheless, comparison of the analytical models upon which the screening limits proposed in Sections 11.4.1 and 11.4.2, with the actual situation being assessed, reveals that certain features of that situation have not been represented as realistically as possible. These parts of the model may be judged as providing either a conservative representation (i.e., tending to increase the estimated TWCF) or a nonconservative representation (i.e., tending to decrease the estimated TWCF) relative to the actual situation in service. Table 11.2 summarizes these conservatisms and nonconservatisms, which are discussed in greater detail in Section 11.4.4.1 and Section 11.4.4.2, respectively. This discussion does not include factors that our models do not accurately represent when these inaccuracies have been demonstrated not to significantly influence the TWCF results. This information demonstrates that, on balance, more conservatisms than nonconservatisms remain in the model, suggesting the appropriateness of applying the proposed screening limits (see Figure 11-6 and Figure 11-9) without an additional margin term.

11.4.4.1 Residual Conservatisms

In the reactor vessel failure frequency limit

- The reactor vessel failure frequency limit of $1x10^{-6}$ events/year was established based on the assumption that through-wall cracking of the RPV will produce a large early release in all circumstances. As discussed in Chapter 10, through-wall cracking of the RPV is likely to lead to core damage, but large early release is unlikely because of reactor safety systems and the multiple barriers that block radioactive release to the environment (e.g., containment). Current guidelines on core damage frequency provided by RG 1.174 and the Option 3 framework for risk-informing 10 CFR Part 50 suggest a reactor vessel failure frequency limit of $1x10^{-5}$ events/year [RG1.174]. As illustrated in Figure 11-6 and Figure 11-9 changing from a $1x10^{-6}$ to a $1x10^{-5}$ limit would increase all of the proposed *RT* limits by ≈40°F (22°C)

Table 11.2. Non-best estimate aspects of the models used to develop the RT-based screening limits for PTS shown in Figure 11-5 and Figure 11-9

Situation in Service	Potential Conservatism in the Analytical Model
If the vessel fails, what happens next?	The model assumes that all failures produce a large early release; however, in the APET (Ch. 10), most sequences lead only to core damage.
	An initiated axial crack is assumed to instantly propagate to infinite length. In reality, the crack length will be finite and limited to the length of a single shell course because the cracks will most likely arrest when they encounter higher toughness materials in either the adjacent circumferential welds or plates.
	An initiated circumferential crack is assumed to instantly propagate 360° around the vessel ID. In reality, the crack length is limited because the azimuthal fluence variation places strips of tougher material in the path of the extending crack.
How the many possible PTS initiators are binned, and how TH transient are selected to represent each bin to the PFM analysis.	When uncertainty of how to bin existed, consistently conservative decisions were made
Characterization of secondary side failures	The minimum temperature of main steam line break inside containment is modeled as ~50°F (28°C) colder than it can be because containment pressurizes as a result of the steam escaping from the break.
	Stuck-open valves on the secondary side are conservatively modeled in Palisades.
Through-wall attenuation of neutron damage	Attenuation is assumed to be less-significant than measured in experiments.
Model of material unirradiated toughness and chemical composition variability.	The statistical distributions sampled produce more uncertainty than could ever occur in a specific weld, plate, or forging.
Correction for systematic conservative bias in RT_{NDT}	Model corrects for mean bias, but over represents uncertainty in RT_{NDT}.
Embrittlement shift model	Model used produces systematically higher TWCF than that estimated by the embrittlement shift model adopted by ASTM.
Flaw model	All defects found were assumed to be planar.
	Systematically conservative judgments were made when developing the flaw distribution model.
Interdependency of between initiation toughness and arrest toughness.	Model employed allows all initiated flaws a chance to propagate into the vessel.
Extrapolation of irradiation damage	Most conservative approach taken (increasing time, vs. increasing unirradiated RT_{NDT}).

Situation in Service	Potential Non-Conservatism in the Analytical Model
If the vessel fails, what happens next?	The potential for air oxidation has been ignored.
External PTS initiators	The potential for external events (e.g., fires, earthquakes) initiating PTS transients has been ignored. A conservative bounding analysis (see Section 9.4) estimates the effect of external events to be at most a factor of 2 increase in TWCF, but the likely increase is expected to be much less than 2x.
Through-wall chemistry layering	Model assumes that the mean level of copper can change four times through the vessel wall thickness. If copper layering is not present, the TWCF would increase.

In the PRA model

- In the PRA binning process, when there was uncertainty regarding what bin to place a particular scenario in, the scenario was intentionally binned in a conservative manner. Thus, the loading severity has a tendency toward being overestimated.

In the thermal-hydraulics model

- The temperature of water held in the safety injection accumulators was assumed to be 60°F (15.6°C). These accumulators are inside containment and (so) exist at temperatures of 80–90°F (26.7–32.2°C) in the winter and above 110°F (43.3°C) in the summer. Again, this conservative estimate of injection water temperature increases the magnitude of the thermal stresses that occur during of pipe breaks and reduces the fracture resistance of the vessel steel.
- When a main steam line breaks inside of containment the release of steam from the break pressurizes the containment structure to ~50psi (335 kPa). Consequently, the minimum temperature for MSLBs is bounded by the boiling point of water at ~50psi (335 kPa), or ~260°F (126.7°C). However, our models of secondary side breaks do not account for pressurization of containment, so the minimum temperature calculated by RELAP for these transients is 212°F (100°C), or approximately 50°F (28°C) too cold. This conservative estimate of the minimum temperature associated with an MSLB increases the magnitude of the thermal stresses that occur during pipe breaks and reduces the fracture resistance of the vessel steel.

In the fracture model

- Once a circumferential crack initiates, it is assumed to instantly propagate 360° around the vessel wall. However, full circumferential propagation is highly unlikely because of the azimuthal variation in fluence, which causes alternating regions of more embrittled and less embrittled material to exist circumferentially around the vessel wall. Thus, our model tends to overestimate the extent of cracking initiated from circumferentially oriented defects because it ignores this natural crack arrest mechanism.
- Once an axial flaw initiates, it is assumed to instantly become infinitely long. In reality, it only propagates to the length of an axial shell course (~8 to 12–ft (~2.4 to 3.7-m)), at which point, it encounters tougher material and arrests. Even though a shell course is very long, flaws of finite length tend to arrest more readily than do flaws of infinite length because of systematic differences in the through-wall variation of crack driving force. Because of this approximation, our model tends to overestimate the likelihood of through-wall cracking.
- As detailed in Section 4.2.3.1.3 of [***EricksonKirk-PFM***] and in [English 02], the adopted FAVOR model of how fluence attenuates through the RPV wall is conservative relative to experimental data.
- As detailed in Section 4.2.2.2 of [***EricksonKirk-SS***] and in Appendix D to [***EricksonKirk-PFM***], the statistical distributions of Cu, Ni, P, and RT_{NDT} sampled by FAVOR overestimate the degree of uncertainty in these variables relative to what can actually exist in any particular weld, plate, or forging.
- While the FAVOR model corrects (on average) for the systematic conservative bias in RT_{NDT}, the model overestimates the uncertainty associated with the fracture toughness transition temperature metric.
- As detailed in Section 9.2.1.2.3, the embrittlement shift model adopted by FAVOR systematically overestimates the TWCF relative to the embrittlement shift model currently recommended by the ASTM (an international consensus body).

In the flaw model

- In the experimental data upon which the flaw distribution is based, all detected defects were modeled as being crack-like and, therefore, potentially deleterious to the

fracture integrity of the vessel. However, many of these defects are actually volumetric rather than planar, making them either benign or, at a minimum, much less of a challenge to the fracture integrity of the vessel. Thus, the model we have adopted overestimates the seriousness of the defect population in RPV materials, which leads to overly pessissimistic assessments of the fracture resistance of the vessel.

- FAVOR incorporates an interdependence between initiation and arrest fracture toughness values premised on physical arguments (see Sections 5.3.1.1 and 5.3.1.2 of [***EricksonKirk-PFM***]). While the staff believes these models are appropriate, this view is not universally held (see reviewer comment 40D in Appendix B). The alternative model, with no interdependence between initiation and arrest fracture toughness values, would reduce the estimated values of TWCF.
- As detailed in Section 9.2.2.1, we have simulated levels of irradiation damage beyond those occurring over currently anticipated lifetimes using the most conservative available techniques.

11.4.4.2 Residual Non-Conservatisms

In the reactor vessel failure frequency limit

- Air oxidation. The LERF criterion provided in RG 1.174, which was used to establish the 1×10^{-6}/ry TWCF limit, assumes source terms that do not reflect scenarios where fuel cooling has been lost, exposing the fuel rods to air (rather than steam). Should such a situation arise, some portion of the reactor fuel would eventually be oxidized in an air environment, which would result in release fractions for key fission products (ruthenium being of primary concern) that may be significantly (e.g., a factor of 20) larger than those associated with fuel oxidation in steam environments. These larger release fractions could lead to larger numbers of prompt fatalities than predicted for non-PTS risk-significant scenarios. Nonetheless, the APET developed in Chapter 10 demonstrates that the number of scenarios where air oxidation is possible is extremely small, certainly far smaller than the number of scenarios where only core damage (not LERF) is the only plausible outcome. Thus, the nonconservatism introduced by not explicitly considering the potential for air oxidation is more than compensated for by the conservatism of establishing a TWCF limit based on LERF when many accident sequences can only plausibly result in core damage.

In the PRA model

- External initiating events. As detailed in Section 9.4, our analysis hast not considered the potential for a PTS transient to be started by an initiating event external to the plant (e.g., fire, earthquake). The bounding analyses reported in Section 9.4 demonstrate that this would increase the TWCF values reported herein by at most a factor of 2. However, the bounding nature of our external events analysis suggests strongly that the actual effect of ignoring the contribution of external initiating events would be much smaller than 2x.

In the fracture model

- Through-wall chemistry layering. As detailed in Section 9.2.1.2.5, FAVOR models the existence of a gradient of properties through the thickness of the RPV because of through-wall changes in copper content. These copper content changes arise from the fact that, given the large volume of weld metal needed to fill an RPV weld, manufacturers often need to use weld wire from multiple weld wire spools (having different amounts of copper coating) to completely fill the groove. The model adopted in FAVOR resamples the mean copper content of the weld at the ¼T, ½T, and ¾T locations through the thickness. This resampling increases the probability of crack arrest because it allows the simulation of less irradiation-sensitive materials, which could arrest the running crack before it fails the vessel. If these weld layers did not occur in a real vessel, the TWCF would increase

relative to those reported herein by a small factor (~2.5 based on the limited sensitivity studies performed).

12 Summary of Findings and Considerations for Rulemaking

The investigation documented by this report reevaluates the technical basis of the PTS Rule and its associated screening criteria. Our approach considers the factors that influence the risk of vessel failure during a PTS event, while accounting for uncertainties as an integrated part of a quantitative PRA. Two central features of our approach are a focus on the use of realistic input values and models (wherever possible), and an *explicit* treatment of uncertainties (to the greatest extent practicable). Thus, our approach differs markedly from that employed in developing 10 CFR 50.61, in which many aspects of the analysis included intentional and unquantified conservatisms, and uncertainties were *implicitly* treated by incorporating them into the models.

In this chapter, we summarize the results of our findings in the following four areas:

- baseline analysis of the likelihood of PTS-induced RPV failure at three plants (Oconee 1, Beaver Valley, and Palisades), as presented in Chapter 8
- examination of the applicability of the results from Chapter 8 to PWRs *in general*, as presented in Chapter 9
- assessment of a annual per plant limit on through-wall cracking frequency that is consistent with current NRC guidelines on risk-informed regulation, as presented in Chapter 10
- use of information from Chapters 8, 9, and 10 to develop a reference temperature (RT)-based PTS screening criteria, as presented in Chapter 11

This chapter concludes with a short discussion of considerations for rulemaking and possible regulatory implications of this work beyond those associated with 10 CFR 50.61.

12.1 Plant-Specific Baseline Analysis of the PTS Risk at Oconee Unit 1, Beaver Valley Unit 1, and Palisades

Chapter 8 provided the results of plant-specific analyses of Oconee Unit 1, Beaver Valley Unit 1, and Palisades. In the following list, which summarizes the information presented in Chapter 8, the ***conclusions*** are shown in ***bold italics***, while supporting information is shown in regular type:

- ***The degree of PTS challenge for currently anticipated lifetimes and operating conditions is low.***
  - Even at the end of license extension (60 operational years, or 48 EFPY at an 80% capacity factor), the mean estimated through-wall cracking frequency (*TWCF*) does not exceed 2×10^{-8}/year for the plants analyzed. Considering that the Beaver Valley and Palisades RPVs are constructed from some of the most irradiation-sensitive materials in commercial reactor service today, these results suggest that, provided that operating practices do not change dramatically in the future, the operating reactor fleet is in little danger of exceeding either the limit on *TWCF* of 5×10^{-6}/yr expressed by Regulatory Guide 1.154 [RG 1.154] or the 1×10^{-6}/yr value recommended in Chapter 10, even after license extension.
- ***Mean TWCF values are in fact upper bounds.***
  - Because of the skewness characteristic of the *TWCF* distributions that arise as a result of the physical processes responsible for steel fracture, mean *TWCF* values correspond to the 90th

percentile (or higher) of the *TWCF* distribution. Thus, the mean *TWCF* values we report in this chapter are appropriately regarded as upper bounds to the uncertainty distribution on TWCF.

- ***Axial flaws, and the toughness properties that can be associated with such flaws, control nearly all of the TWCF.***
  - Axial flaws are much more likely to propagate through-wall than circumferential flaws because the applied driving force to fracture increases continuously with increasing crack depth for an axial flaw. Conversely, circumferentially oriented flaws experience a driving force peak mid-wall, providing a natural crack arrest mechanism. It should be noted that crack initiation from circumferentially oriented flaws is likely; it is only their through-wall propagation that is much less likely (relative to axially oriented flaws).
  - It is, therefore, the toughness properties that can be associated with axial flaws that control nearly all of the TWCF. These include the toughness properties of plates and axial welds at the flaw locations. Conversely, the toughness properties of both circumferential welds and forgings have little effect on TWCF because these can be associated only with circumferentially oriented flaws.
- ***Transients involving primary side faults are the dominant contributors to TWCF. Transients involving secondary side faults play a much smaller role.***
  - The severity of a transient is controlled by a combination of three factors:
    - the initial cooling rate, which controls the thermal stress in the RPV wall
    - the minimum temperature of the transient, which controls the resistance of the vessel to fracture
    - the pressure retained in the primary system, which controls the pressure stress in the RPV wall
  - The significance of a transient (i.e., how much it contributes to PTS risk) depends on these three factors and on the likelihood of the transient occurring.
  - Our analysis considered transients in the following classes:
    - primary side pipe breaks
    - stuck-open valves on the primary side
    - main steam line breaks
    - stuck-open valves on the secondary side
    - feed-and-bleed
    - steam generator tube rupture
    - mixed primary and secondary initiators
  - Table 12.1 summarizes our results for these transient classes in terms of both transient severity indicators and the likelihood of the transient occurring. The color-coding of table entries indicates the contribution (or not) of these factors to the TWCF of the different classes of transients. This summary indicates that the risk-dominant transients (medium- and large-diameter primary side pipe breaks, and stuck-open primary side valves that later reclose) all have multiple factors that, in combination, result in their significant contribution to TWCF.
    - For medium- to large-diameter primary side pipe breaks, the fast to moderate cooling rates and the low downcomer temperatures (generated by the rapid depressurization and emergency injection of low-temperature makeup water directly to the primary) combine to produce a high-severity transient. Despite the moderate to low likelihood of transient occurrence, the severity of these transients (if they occur) makes them significant contributors to the total TWCF.
    - For stuck-open primary side valves that later reclose, the repressurization associated with valve reclosure

coupled with low temperatures in the primary combine to produce a high-severity transient. This coupled with a high likelihood of transient occurrence makes stuck-open primary side valves that later reclose significant contributors to the total TWCF.

Table 12.1. Factors contributing the severity and risk dominance of various transient classes.

Transient Class		Transient Severity			Transient Likelihood	TWCF Contribution
		Cooling Rate	Minimum Temperature	Pressure		
Primary Side Pipe Breaks	Large Diameter	Fast	Low	Low	Low	Large
	Medium Diameter	Moderate	Low	Low	Moderate	Large
	Small Diameter	Slow	High	Moderate	High	~0
Primary Stuck-Open Valves	Valve Recloses	Slow	Moderate	High	High	Large
	Valve Remains Open	Slow	Moderate	Low	High	~0
Main Steam Line Break		Fast	Moderate	High	High	Small
Stuck-Open Valve(s), Secondary Side		Moderate	High	High	High	~0
Feed-and-Bleed		Slow	Low	Low	Low	~0
Steam Generator Tube Rupture		Slow	High	Moderate	Low	~0
Mixed Primary & Secondary Initiators		Slow	Mixed		Very Low	~0
Color Key	Enhances TWCF Contribution		Intermediate		Diminishes TWCF Contribution	

- The small or negligible contribution of all secondary side transients (MSLBs, stuck-open secondary valves) results directly from the lack of low temperatures in the primary system. For these transients, the minimum temperature of the primary for times of relevance is controlled by the boiling point of water in the secondary (212°F (100°C) or above). At these temperatures, the fracture toughness of the RPV steel is sufficiently high to resist vessel failure in most cases.

- ***Credits for operator action, while included in our analysis, do not influence these findings in any significant way.*** Operator action credits can dramatically influence the risk-significance of ***individual*** transients. Appropriate credits for operator action, therefore, need to be included as part of a "best estimate" analysis because there is no way to establish *a priori* if a particular transient will make a large contribution to the total risk. Nonetheless, the results of our analyses demonstrate that the ***overall effect*** of these operator action credits on the ***total TWCF*** for a plant is small, for the following reasons:

  - Medium- and Large-Diameter Primary Side Pipe Breaks: No operator actions are modeled for any break diameter because, for these events, the safety injection systems do not fully refill the upper regions of the RCS. Consequently, operators would never take action to shut off the pumps.

  - Stuck-Open Primary Side Valves that May Later Reclose: Reasonable and appropriate credit for operator actions (throttling of HPI) has been included in the PRA model. However, the influence of these credits on the estimated values of vessel failure probability attributable to SO-1 transients is small because the operator actions credited only prevent repressurization when SO-1 transients initiate from HZP conditions and when the operators act promptly (within 1 minute) to throttle HPI. Complete removal of operator action credits from the model increases the total risk associated with SO-1 transients only slightly.

  - Main Steam Line Breaks: For the overwhelming majority of MSLB transients, vessel failure is predicted to occur between 10 and 15 minutes after transient initiation because it is within this timeframe that the thermal stresses associated with the rapid cooldown reach their maximum. Thus, all of the long-time effects (isolation of feedwater flow, timing of HSSI control) that can be influenced by operator actions have no effect on vessel failure probability because these factors influence the progression of the transient after failure has occurred (if it occurs). Only factors affecting the initial cooling rate (i.e., plant power level at transient initiation, break location inside or outside of containment) can influence the CPTWC values. These factors are not influenced in any way by operator actions.

- ***Because the severity of the most significant transients in the dominant transient classes are controlled by factors that are common to PWRs in general, the TWCF results presented in this chapter can be used with confidence to develop revised PTS screening criteria that apply to the entire fleet of operating PWRs.***

  - Medium- and Large-Diameter Primary Side Pipe Breaks: For these break diameters, the fluid in the primary cools faster than can the wall of the RPV. In this situation, ***only*** the thermal conductivity of the steel and the thickness of the RPV wall control the thermal stresses and, thus, the severity of the fracture challenge. Perturbations to the fluid cooldown rate controlled by break diameter, break location, and season of the year do not play a role. Thermal conductivity is a physical property, so it is very consistent for all

RPV steels, and the thicknesses of the three RPVs analyzed are typical of PWRs. Consequently, the TWCF contribution of medium- to large-diameter primary side pipe breaks is expected to be consistent from plant-to-plant and can be well-represented for all PWRs by the analyses reported herein.

- Stuck-Open Primary Side Valves that May Later Reclose: A major contributor to the risk-significance of SO-1 transients is the return to full system pressure once the valve recloses. The operating and safety relief valve pressures of all PWRs are similar. Additionally, as previously noted, operator action credits affect the total risk associated with this transient class only slightly.
- Main Steam Line Breaks: Since MSLBs fail early (within 10–15 minutes after transient initiation), only factors affecting the initial cooling rate can have any influence on CPTWC values. These factors include the plant power level at event initiation and the location of the break (inside or outside of containment). These factors are not influenced in any way by operator actions.

12.2 Applicability of these Plant Specific Results to Estimating the PTS Risk at PWRs in General

In Chapter 9, we examined the applicability of the TWCF estimates presented in Chapter 8 for Oconee Unit 1, Beaver Valley Unit 1, and Palisades to PWRs *in general.* The information presented focused on the following topics:

- Sensitivity studies performed on the TH and PFM models to engender confidence in both the robustness of the results presented in Chapter 8 and their applicability to PWRs *in general.*
- An examination of the plant design and operational characteristics of five additional plants to determine whether the design and operational features that are the key contributors to PTS risk vary significantly enough in the general plant population to question the generality of our results.
- An examination of the effects of external events (e.g., fires, floods, earthquakes) to PTS risk.

Except for a few situations that are not expected to occur, none of these analyses revealed any reason to question the applicability of the results presented in Chapter 8 to the general population of operating PWRs in the United States. The information developed in these analyses is summarized as follows:

TH Sensitivity Studies

- Changes to the RELAP heat transfer coefficient model to account for low-flow situations where mixed convection heat transfer may be occurring in the downcomer were made based on the Petukhov-Gnielinski heat transfer correlation. This change in the heat transfer coefficient increases the CPTWC by a factor ~3 (averaged across all transients analyzed) compared to using the default heat transfer correlations in RELAP5/MOD3.3 Version ei. There is some variability from the average CPF factor, depending upon the transient being considered.

PFM Sensitivity Studies

- An examination of the effects of all postulated credible perturbations to our PFM model revealed no effects significant enough to warrant a change to our baseline model, or to recommend a caution regarding its robustness.
- In general, the TWCF of forged PWRs can be assessed using the Chapter 8 results (for plate welded PWRs) by ignoring the TWCF contribution of axial welds. However, should changes in future operating conditions result in a forged vessel being subjected to very high levels of embrittlement (far beyond any currently anticipated at EOL or EOLE) a plant-specific analysis to assess the effect of subclad flaws on TWCF would be warranted.
- For PWRs with vessel thicknesses of 7.5 to 9 .5-in. (19.05 to 24.13-cm), the TWCF results in Chapter 8 are realistic. The Chapter 8 results overestimate the TWCF of the seven thinner vessels (with wall thicknesses below 7-in. (17.78-cm)) and underestimate the TWCF of Palo Verde Units 1, 2, and 3, all of which have wall thicknesses above 11-in (27.94-cm). However, these vessels have very low embrittlement projected at either EOL or EOLE, suggesting little practical effect of this underestimation.

Plant Design and Operational Characteristics

- *Large-Diameter Primary Side Pipe Breaks*: No differences were found that would cause significant changes in either the progression or frequencies of the PTS scenarios. Additionally, no differences in the plant system designs were found that would cause significant changes in the downcomer fluid temperature.
- *Small- to Medium-Diameter Primary Side Pipe Breaks*: No differences were found that would cause significant changes in either the progression or frequency of the pipe break LOCAs. For the feed-and-bleed LOCAs, the only difference that was found affected the frequency for the CE generalization plant (i.e., Fort Calhoun). The frequency for these types of scenarios could be higher by a factor of ~3; however, this increase would not prevent the generalization plants from being bounded (or represented) by the detailed analysis plants.
- *Stuck-Open Valves on the Primary Side that May Later Reclose*: The progression of the accident scenarios should be the same across all plants. While, the frequency associated with this type of scenarios could increase at some Westinghouse plants, the integrated effect of this increase was determined to be small. Fort Calhoun is expected to have a downcomer temperature that is cooler than its corresponding detailed analysis plant (Palisades) because of the smaller size of the plant. The downcomer temperature for the other generalization plants is actually expected to be somewhat warmer. PFM calculations performed to quantify the effect of the colder temperatures in Ft. Calhoun determined that while the conditional through-wall cracking probabilities would increase (as expected), the increase was not so substantial as to prevent the Palisades plant analysis from upper-bounding the Ft. Calhoun plant analysis. Thus, the colder downcomer temperature for smaller plants was not viewed as impeding the applicability of the TWCF values in Chapter 8 to PWRs in general.
- *Main Steam Line and other Secondary Side Breaks*: No differences were found that would cause significant differences in either the progression or frequency of the PTS scenarios.
- *Summary*: These observations support the conclusion that the Chapter 8 TWCF estimates produced can be used to characterize (or bound) the TWCF of PWRs in general.

External Events

- No external event scenarios were found where the TWCFs significantly exceed that of the worst internal event scenarios (contributions from LOCA-type and SRV open-reclose-type accidents). Given the bounding nature of the external event analyses, there is considerable assurance that the external event contribution to overall TWCF as a result of PTS does not exceed than the highest best-estimate contribution from internal events. Given the conservative probabilities and dependencies assumed in the external event analyses, with the addition of little or no credit for any operator actions for the external event scenarios, it is more likely that the "realistic" external event contribution to overall TWCF is much less than the highest internal event contribution. Therefore, the contribution of external initiating events to the overall TWCF attributable to PTS can be considered negligible.

12.3 An Anual Per-Plant Limit on Through-Wall Cracking Frequency Consistent with Current Regulatory Guidance on Risk-Informed Regulation

The analysis presented in Chapter 10 produced the following conclusions regarding the establishment of an annual per-plant limit on through-wall cracking frequency (i.e., a criterion for RVFF):

(1) The analysis supports a definition of RVFF as being equivalent to TWCF (i.e., for PTS considerations, RPV "failure" can be defined as an occurrence of a through-wall crack). This conclusion is based on the following two factors:

(a) TWCF is a more direct measure than VCIF of the likelihood of events with potentially significant public health consequences. This is desirable from a risk-informed decision-making perspective.

(b) The uncertainties associated with the prediction of a through-wall crack (under PTS conditions) are only slightly larger than those associated with the prediction of crack initiation (also under PTS conditions). For example, at the 10 CFR 50.61 RT_{PTS} screening limit, the separation between the 50th and 95th percentiles in the distribution of *VCIF* ranges from 0.8 to 1.8 orders of magnitude, while the separation between the 50th and 95th percentiles in the distribution of *TWCF* ranges from 0.9 to 2.6 orders of magnitude. This slight increase in uncertainty is a natural and expected consequence of a cleavage failure mechanism and does not reflect a state of knowledge limitation regarding crack arrest. (See [***EricksonKirk-PFM***] for details of the crack arrest model.)

(2) The analysis supports an acceptance criterion for *RVFF*, *RVFF**, of 1×10^{-6}/ry. This is based on the following observations:

(a) The conditional probability of an unscrubbed, large early release with a large air-oxidation source term (given a PTS-induced RPV failure) appears to be very small (i.e., less than 0.01). It is particularly small for plants where water in the reactor cavity (following a PTS-induced RPV failure) will cover the fuel. For plants with larger cavities, the low probability of the scenario is largely attributable to the independence and reliability of containment sprays.

(b) The assessment underlying the above observation does not account for potential dependencies associated with PTS-events initiated by "external events" (e.g., earthquakes) or internal fires.

(c) For plants with cavities such that fuel cooling is not assured following a PTS-induced RPV failure, the APET (Figure 10.1) identifies the most probable scenarios where limited fuel damage might occur, even if ECCS operates as designed.

Observation (a), taken in isolation, supports the use of an *RVFF** based on considerations of core damage consistent with those proposed in current activities for risk-informing 10 CFR Part 50 [SECY-00-0198]. However, Observation (b) identifies a potentially significant uncertainty regarding the margin between PTS-induced RPV failure and large early release, and Observation (c) raises a potential concern regarding defense-in-depth. Therefore, RG 1.174 guidelines on CDF supporting a value for *RVFF** of $1x10^{-5}$ events/year may not have sufficient justification, whereas the scoping study developed for RG 1.174 guidelines on LERF is more defensible given currently available information. This rationale supports our recommended value of $1x10^{-6}$ events/year for *RVFF**, which is consistent with the RG 1.174 guidelines on LERF.

When assessing the acceptability of the PTS-associated risk at a given plant, the mean value of the plant's PTS-induced *RVFF* (i.e., the mean *TWCF*) should be compared with *RVFF**. This conclusion is based on how other NRC risk-informed decisions use risk information (e.g., see RG 1.174).

(3) Should additional work be performed to address the key post-RPV failure accident progression uncertainties identified in this study, the following issues are of principal importance:

(a) the likelihood that a PTS-induced axial crack will, upon reaching a circumferential weld, turn and progress along the circumferential weld

(b) the likelihood of PTS-induced containment isolation failure (especially failures associated with failure of containment penetrations) and ECCS failure (especially ECCS piping failures)

(c) the magnitude of potential source terms and consequences associated with PTS events

(d) substantiation of conditional probability values in Table 10.2 and Table 10.3

(e) the impact of external events on PTS-induced LERF

It is anticipated that state-of-knowledge improvements in any of these areas will strengthen this study's conclusions regarding the margin between a PTS-induced RPV failure and consequent large early releases. Although not quantified, several aspects of our analysis performed to support an RVFF* value $1x10^{-6}$ events/year have a known conservative bias. The following is a summary of a few of these areas identified earlier in this chapter:

- Given the relatively low energy of the fluid following a postulated PTS event, the impulse on the RPV and piping resulting from a blowdown was predicted to be within the bounds of a design-basis SSE. The limited vessel movement from a blowdown forces would be compensated for by the pipe ductility, long runs of piping with many bends, and the hanger and support systems. For these reasons, damage of ECCS piping or containment penetrations is not expected.
- Missile generation attributable to a postulated PTS event would result in an object being directed laterally into the reactor vessel cavity wall by the blowdown forces associated with the breach in the reactor vessel. For a missile to affect the containment spray system or containment penetrations, it would have to traverse a tortuous path through tight clearances of the reactor vessel cavity. The missile's energy would be dissipated by multiple contacts with the reactor cavity wall, as well as the distance it travels, and it would have to hit an extremely small target to render the containment spray system inoperable.
- Through-wall crack frequency is assumed to equal core damage, which is assumed to equal a release. The through-wall cracks may cover a wide spectrum of sizes, from very large to very small. Very small cracks would

result in only minor leakage that would not significantly challenge the reactor safety systems.

12.4 A Reference Temperature Based PTS Screening Criteria

In Chapter 11, we proposed the use of different reference temperatures (*RT*) metrics to characterize the resistance of an RPV to fracture initiating from different flaws at different locations in the vessel:

- To characterize the contribution of flaws in **axial welds** to vessel fracture probability, we have proposed two reference temperature metrics: RT_{AW} and $RT_{AW\text{-}MAX}$. $RT_{AW\text{-}MAX}$ can be estimated for any plant based solely on the information contained in the NRC's RVID database [RVID], while estimation of RT_{AW} requires information from plant drawings concerning the dimensions and placement of axial welds in the beltline region of the RPV.
- To characterize the contribution of flaws in **plates** to vessel fracture probability, we have proposed two reference temperature metrics: RT_{PL} and $RT_{PL\text{-}MAX}$. $RT_{PL\text{-}MAX}$ can be estimated for any plant based solely on the information contained in the NRC's RVID database [RVID], while estimation of RT_{PL} requires information from plant drawings concerning the dimensions and placement of plates in the beltline region of the RPV.
- To characterize the contribution of flaws in **circumferential welds** to vessel fracture probability we have proposed two reference temperature metrics: RT_{CW} and $RT_{CW\text{-}MAX}$. $RT_{CW\text{-}MAX}$ can be estimated for any plant based solely on the information contained in the NRC's RVID database [RVID], while estimation of RT_{CW} requires information from plant drawings concerning the dimensions and placement of circumferential welds in the beltline region of the RPV.

These different *RT* values were proposed in recognition of the fact that the probability of vessel fracture starting from different flaw populations varies considerably as a result of factors that are both understood and predictable:

- Different regions of the vessel have flaw populations that differ in size (weld flaws are considerably larger than plate flaws) and orientation (axial and circumferential welds have flaws of corresponding orientations, whereas plate flaws may be either axial or circumferential). The driving force to fracture depends on both flaw size and flaw orientation, so different vessel regions experience different fracture driving forces.
- The degree of irradiation damage suffered by the material at the flaw tips varies with location in the vessel as a result of differences in chemistry and fluence.

Correlations between these *RT*-metrics and the TWCF attributable to axial weld flaws, plate flaws, and circumferential weld flaws showed little plant-to-plant variability as a result of the general similarity of PTS challenge between plants detailed in Chapters 8 and 9 and summarized in Sections 12.2 and 12.3. The following two relationships were developed based on these correlations:

TWCF estimated from weighted RT metrics

$$TWCF_{TOTAL} = TWCF_{AXIAL-WELD} + \alpha_{PL} \cdot TWCF_{PLATE} + TWCF_{CIRC-WELD}$$

where

$$TWCF_{AXIAL-WELD} = 4\text{x}10^{-26} \cdot \exp\{0.0585 \cdot (RT_{AW} + 459.69)\}$$ (see Eq. 8-1 for RT_{AW})

$$\alpha_{PL} = 1.7, \quad TWCF_{PLATE} = 4\text{x}10^{-29} \cdot \exp\{0.064 \cdot (RT_{PL} + 459.69)\}$$ (see Eq. 8-2 for RT_{PL})

$$TWCF_{CIRC-WELD} = 3\text{x}10^{-27} \cdot \exp\{0.051 \cdot (RT_{CW} + 459.69)\}$$ (see Eq. 8-3 for RT_{CW})

TWCF estimated from maximum RT metrics

$$TWCF_{TOTAL} = \alpha_{AW} \cdot TWCF_{AXIAL-WELD} + \alpha_{PL} \cdot TWCF_{PLATE} + TWCF_{CIRC-WELD}$$

where

$$\alpha_{PL} = 1.6, \; TWCF_{AXIAL-WELD} = 3\text{x}10^{-27} \cdot \exp\{0.0605 \cdot (RT_{MAX-AW} + 459.69)\}$$

$$\alpha_{PL} = 1.7, \; TWCF_{PLATE} = 9\text{x}10^{-27} \cdot \exp\{0.0543 \cdot (RT_{MAX-PL} + 459.69)\}$$

$$TWCF_{CIRC-WELD} = 4\text{x}10^{-29} \cdot \exp\{0.0561 \cdot (RT_{MAX-CW} + 459.69)\}$$

(see Eq. 8-1, Eq. 8-2, and Eq. 8-3 for the definitions of RT_{MAX-AW}, RT_{MAX-PL}, and RT_{MAX-CW}, respectively)

In these relationships, all temperatures are in °F. *RT*-based screening limits were established by setting the total TWCF in these equations equal to the reactor vessel failure frequency acceptance criterion of $1\text{x}10^{-6}$ events per year proposed in Chapter 10. Two different *RT*-based screening limits were developed from each of the above relationships: one for plate welded vessels based on axial weld and plate properties (the contribution of circumferential welds at realistic embrittlement levels is so small that it can be neglected), and one for forged vessels based on circumferential weld and plate properties (there are no axial welds in these vessels so their contribution to TWCF is, by definition, zero). Figure 12-1 provides graphical representations of these screening criteria along with an assessment of all operating PWRs relative to limits based on the maximum *RT* embrittlement metrics[§§§§§§]. In these figures, the region of the graph between the red locus and the origin has TWCF values below the $1\text{x}10^{-6}$ acceptance criterion, so these combinations of reference temperatures would be considered acceptable and require no further analysis. In the region of the graph outside of the red locus, the TWCF is above the $1\text{x}10^{-6}$ acceptance criterion, indicating the need for additional analysis or other measures to justify continued plant operation.

To compare the condition of currently operating PWRs with this proposed screening limit, we used the information in the RVID database [RVID2] to estimate values of RT_{MAX-AW}, RT_{MAX-PL}, and RT_{MAX-CW} for each operating PWR. At EOL, at least 70°F (21°C) and up to 290°F (143°C) separate operating PWRs from the proposed screening limit; these values reduce by between 10 and 20°F (5.5 to 11°C) at EOLE. Even at EOLE, no plate-welded PWR is projected to exceed an annual TWCF of $1\text{x}10^{-7}$ (again, most plants have projected TWCFs far below this value, see Figure 11-8). Additionally, no forged plant is anywhere close to the limit of $1\text{x}10^{-6}$ events per year at either EOL or EOLE. This separation of operating plants from the proposed

[§§§§§§] Maximum *RT* embrittlement metrics are used in these comparisons because these metrics can be estimated based only on the information in RVID. In principal PTS limits based on weighted *RT* embrittlement metrics should provide a somewhat more accurate estimate of plant risk.

screening limits can be compared with the current situation where the most embrittled plants are within 1°F of the 10 CFR 50.61 screening limit. As noted in Sections 9.2.2.2 and 9.2.2.3, these *RT*-based screening limits apply to PWRs in general subject to the following three provisos:

- When assessing a forged vessel where the forging has a very high reference temperature (RT_{PL} above 225°F (107°C)) ***and*** the forging is believed to be susceptible to subclad cracking, a plant-specific analysis of the TWCF produced by the subclad cracks should be performed. However, no forging is projected to reach this level of embrittlement, even at EOLE.
- When assessing an RPV having a wall thickness of 7-in. (18-cm) or less (7 vessels), the proposed *RT* limits are conservative.
- When assessing an RPV having a wall thickness of 11-in. (28-cm) or greater, the proposed *RT* limits may be nonconservative. For the three plants meeting this criterion, either the *RT* limits would need to be reduced or known conservatisms in the current analysis would have to be removed to demonstrate compliance with the TWCF limit of $1x10^{-6}$ event/year.

Aside from relying on different *RT* metrics than 10 CFR 50.61, the proposed revision to the PTS screening limit differs from that used currently in the absence of a "margin term." Use of a margin term is appropriate to account (at least approximately) for factors that occur in application that were not considered in the analysis upon which the screening limit is based. For example, the 10 CFR 50.61 margin term accounts for uncertainty in copper, in nickel, and in initial RT_{NDT}. However, our model considers explicitly uncertainty in all of these variables, and represents these uncertainties as being larger (a conservative representation) than would be appropriate in any plant-specific application of the proposed screening limit. Consequently, use of the 10 CFR 50.61 margin term with the new screening limits is inappropriate. In general, the following additional reasons suggest that use of any margin term with the proposed screening limits is inappropriate:

(1) The *TWCF* values used to establish the screening limit represent 90th percentile values or greater (see Figure 8-3).

(2) Chapter 8 and Chapter 9 demonstrate that the results from our three plant-specific analyses apply to PWRs in general.

(3) Certain aspects of our modeling cannot be reasonably represented as "best estimates." On balance, there is a conservative bias to these non-best estimate aspects of our analysis. Residual conservatisms and nonconservatisms in our model are as follows:

Conservatisms

(a) The assumption that all vessel failures lead to LERF, when in fact many would lead only to core damage.

(b) The assumption that once initiated all circumferential cracks instantly propagate 360° around the vessel ID. In reality, crack length is limited because the azimuthal fluence variation places strips of tougher material in the path of the extending crack.

(c) The assumption that once initiated, an axial crack will instantly propagate to infinite length. In reality, crack length is finite and limited to the length of a single shell course because axial cracks most likely arrest when they encounter higher toughness materials in either the adjacent circumferential welds or plates.

(d) The systematically conservative judgments made when placing potential PTS initiators into bins.

(e) The systematic underestimation of the minimum temperature associated with secondary side breaks (MSLBs) because the pressurization of containment (attributable to steam escaping from the break) is not modeled.

(f) The attenuation of neutron damage by steel in the vessel wall is assumed to be less than that measured in experiments.

(g) The distributions used to represent the statistical uncertainty in unirradiated transition temperature and chemical composition variables contain more uncertainty than could ever occur in a given weld, plate, or forging.

(h) The systematic modeling overestimation in the uncertainty in used to correct for the mean bias in the RT_{NDT} index temperature.

(i) The production of systematically higher TWCF values by the model used to estimate the increase in RT_{NDT} index temperature caused by irradiation damage (compared to those estimated by the model adopted by ASTM).

(j) The flaw model assumption that all defects are planar (when many are actually volumetric), as well as the use of systematically conservative judgments when developing the flaw model (in the absence of definitive evidence).

(k) Use of the most conservative available extrapolation schemes when the effects of irradiation damage were extrapolated forward in time.

Nonconservatisms

(a) The fact that the small potential for air oxidation has been ignored.

(b) The fact that the small possibility of external events (e.g., fire) initiating PTS has been ignored.

(c) The assumption that the mean level of copper can change four times through the vessel wall thickness, consistent with measurements made on thick-section RPV welds. (If copper layering is not present, the TWCF would actually increase slightly.)

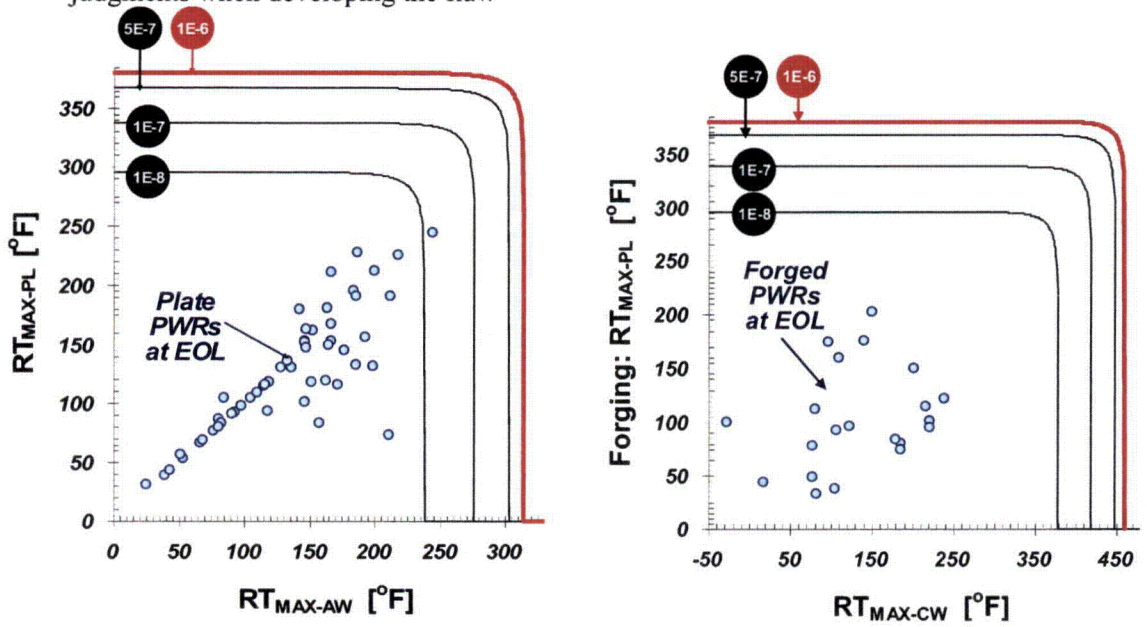

Figure 12-1. Comparison of *RT*-based screening limit (curves) with assessment points for operating PWRs at EOL in plate vessels (left) and forged vessels (right)

12.5 Considerations for Rulemaking

The calculations reported herein demonstrate that PTS events are associated with an extremely small risk of vessel failure, suggesting the existence of considerable safety margin in the current PTS Rule. The magnitude of this margin appears to justify consideration of rulemaking. Should rulemaking proceed, it appears feasible to use improved (i.e., more risk-informed) metrics to represent RPV embrittlement. The metrics proposed herein reflect the principal contributors to PTS-induced RPV failure. A numeric value can be established for an *RT*-based screening limit based on the information provided herein, as well as considerations of risk in current NRC guidance and other non-PTS-related risk-informed regulatory activities.

While numerous factors should be addressed in any revision of 10 CFR 50.61, our research shows that a significant increase in the PTS screening limit can be justified. Such a change could be implemented without imposing on licensees either new material testing requirements or new inspection programs.

13 References

13.1 Citations Summarized by this Report

The following three sections provide the citations that are summarized by this report (see also Figure 4-1). Taken together, these documents provide complete documentation of the NRC's PTS reevaluation project. When these reports are cited in the text, the citations appear in ***italicized boldface*** to distinguish them from the related literature citations.

13.1.1 Probabilistic Risk Assessment

Kolaczkowski-Oco Kolaczkowski, A.M., et al., "Oconee Pressurized Thermal Shock (PTS) Probabilistic Risk Assessment (PRA)," 9-28-2004, available in the NRC's Agencywide Documents Access and Management System (ADAMS) under Accession #ML042880452.

Kolaczkowski-Ext Kolaczkowski, A. et al., "Estimate of External Events Contribution to Pressurized Thermal Shock (PTS) Risk," Letter Report, 10-1-2004, available in ADAMS under Accession #ML042880476.

Siu 99 Sui, N., "Uncertainty Analysis and Pressurized Thermal Shock: An Opinion," U.S. Nuclear Regulatory Commission, 1999, available in ADAMS under Accession #ML992710066.

Whitehead-PRA Whitehead, D.L. and A.M. Kolaczkowski, "PRA Procedures and Uncertainty for PTS Analysis," NUREG/CR-6859, U.S. Nuclear Regulatory Commission, 12-31-2004.

Whitehead-BV Whitehead, D.L., et al., "Beaver Valley Pressurized Thermal Shock (PTS) Probabilistic Risk Assessment (PRA)," 9-28-2004, available in ADAMS under Accession #ML042880454.

Whitehead-Gen Whitehead, D.W., et al., "Generalization of Plant-Specific Pressurized Thermal Shock (PTS) Risk Results to Additional Plants," 10-14-2004, available in ADAMS under Accession #ML042880482.

Whitehead-Pal Whitehead, D.L., et al., "Palisades Pressurized Thermal Shock (PTS) Probabilistic Risk Assessment (PRA)," 10-6-2004, available in ADAMS under Accession #ML042880473.

13.1.2 Thermal-Hydraulics

Arcieri-Base Arcieri, W.C., R.M. Beaton, C.D. Fletcher, and D.E. Bessette, "RELAP5 Thermal-Hydraulic Analysis to Support PTS Evaluations for the Oconee-1, Beaver Valley-1, and Pallisades Nuclear Power Plants," NUREG/CR-6858, U.S. Nuclear Regulatory Commission, 9-30-2004.

Arcieri-SS Arcieri, W.C., et al., "RELAP5/MOD3.2.2Gamma Results for Palisades 1D Downcomer Sensitivity Study," August 31, 2004, available in ADAMS under Accession #ML061170401.

Bessette Bessette, D.E., "Thermal-Hydraulic Evaluations of Pressurized Thermal Shock," NUREG-1809, U.S. Nuclear Regulatory Commission, 5-30-2005.

Chang Chang, Y.H., K. Almenas, A. Mosleh, and M. Pour-Gol, "Thermal-Hydraulic Uncertainty Analysis in Pressurized Thermal Shock Risk Assessment: Methodology and Implementation on Oconee-1, Beaver Valley, and Palisades Nuclear Power Plants," NUREG/CR-6899, U.S. Nuclear Regulatory Commission.

Fletcher Fletcher, C.D., D.A. Prelewicz, and W.C., Arcieri, "RELAP5/MOD3.2.2γ Assessment for Pressurized Thermal Shock Applications," NUREG/CR-6857, U.S. Nuclear Regulatory Commission, 9-30-2004.

Junge "PTS Consistency Effort," Staff Letter Report to file, 10-1-2004, available in ADAMS under Accession #ML042880480.

Reyes-APEX Reyes, J.N., et al., "Final Report for the OSU APEX-CE Integral Test Facility," NUREG/CR-6856, U.S. Nuclear Regulatory Commission, 12-16-2004.

Reyes-Scale Reyes, J.N., et al., "Scaling Analysis for the OSU APEX-CE Integral Test Facility," NUREG/CR-6731, U.S. Nuclear Regulatory Commission, 11-30-2004.

13.1.3 Probabilistic Fracture Mechanics

Dickson-Base Dickson, T.L., and S. Yin, "Electronic Archival of the Results of Pressurized Thermal Shock Analyses for Beaver Valley, Oconee, and Palisades Reactor Pressure Vessels Generated with the 04.1 Version of FAVOR," ORNL/NRC/LTR-04/18, 10-15-2004, available in ADAMS under Accession #ML042960391

Dickson-UG Dickson, T.L., and P.T.Williams, "Fracture Analysis of Vessels Oak Ridge, FAVOR v04.1, Computer Code: User's Guide," NUREG/CR-6855, U.S. Nuclear Regulatory Commission, 10-21-2004.

EricksonKirk-PFM EricksonKirk, M.T., "Probabilistic Fracture Mechanics: Models, Parameters, and Uncertainty Treatment Used in FAVOR Version 04.1," NUREG-1807, U.S. Nuclear Regulatory Commission, 1-26-2005.

EricksonKirk-SS EricksonKirk, M.T., et al., "Sensitivity Studies of the Probabilistic Fracture Mechanics Model Used in FAVOR Version 03.1," NUREG-1808, U.S. Nuclear Regulatory Commission, 11-30-2004.

Kirk 12-02 EricksonKirk, M.T., "Technical Basis for Revision of the Pressurized Thermal Shock (PTS) Screening Limit in the PTS Rule (10 CFR 50.61)," December 2002, available in ADAMS under Accession #ML030090626.

Malik Malik, S.N.M., "FAVOR Code Versions 2.4 and 3.1: Verification and Validation Summary Report," NUREG-1795, U.S. Nuclear Regulatory Commission, 10-31-2004.

Simonen F.A. Simonen, S.R. Doctor, G.J. Schuster, and P.G. Heasler, "A Generalized Procedure for Generating Flaw Related Inputs for the FAVOR Code," NUREG/CR-6817, Rev. 1, U.S. Nuclear Regulatory Commission, October 2003, available in ADAMS under Accession #ML051790410.

Williams Williams, P.T., and T.L. Dickson, "Fracture Analysis of Vessels Oak Ridge, FAVOR v04.1: Computer Code: Theory and Implementation of Algorithms, Methods, and Correlations," NUREG/CR-6854, U.S. Nuclear Regulatory Commission, 10-21-2004.

13.2 Literature Citations

10 CFR 50.61 Title 10, Section 50.61, of the *Code of Federal Regulations*, "Fracture Toughness Requirements for Protection Against Pressurized Thermal Shock Events," promulgated June 26, 1984.

10 CFR Part 50 App. H. Appendix H to Title 10, Part 50, of the *Code of Federal Regulations*, "Reactor Vessel Material Surveillance Program Requirements."

ASME NB2331 ASME NB-2331, 1998 ASME Boiler and Pressure Vessel Code, Rules for Construction of Nuclear Power Plants, Division 1, Subsection NB, Class 1 Components, American Society of Mechanical Engineers.

ASTM E23 ASTM E23, "Standard Test Methods for Notched Bar Impact Testing of Metallic Materials," American Society for Testing and Materials, 1998.

ASTM E185 ASTM E185-94, "Standard Practice for Conducting Surveillance Tests for Light-Water Cooled Nuclear Power Reactor Vessels," American Society for Testing and Materials, 1998.

ASTM E208 ASTM E208, "Standard Test Method for Conducting Drop-Weight Test to Determine Nil-Ductility Transition Temperature of Ferritic Steels," American Society for Testing and Materials, 1998.

ASTM E399 ASTM E399, "Test Method for Plane-Strain Fracture Toughness Testing of Metallic Materials," American Society for Testing and Materials, 1998.

ASTM E900 ASTM E900-02, "Standard Guide for Predicting Radiation-Induced Transition Temperature Shift in Reactor Vessel Materials, E706 (IIF)," American Society for Testing and Materials, 2002.

ASTM E1221 ASTM E1221-96, "Standard Test Method for Plane-Strain Crack-Arrest Fracture Toughness, K_{Ia}, of Ferritic Steels," American Society for Testing and Materials, 1996.

ASTM E1921 ASTM E1921-02, "Test Method for Determination of Reference Temperature, T_o, for Ferritic Steels in the Transition Range," American Society for Testing and Materials, 2002.

Apostolakis 02 Apostakolis, G.E.., Chairman, Advisory Committee on Reactor Safeguards (ACRS), U.S. Nuclear Regulatory Commission, "Risk Metrics and Criteria

for Reevaluating the Technical Basis of the Pressurized Thermal Shock Rule," ADAMS ML0220406120, July 18, 2002.

Bass 04 — Bass, B.R., et al., "Experimental Program for Investigating the Influence of Cladding Defects on Burst Pressure," ORNL/NRC/LTR-04/13, NRC Adams Number ML042660206, 2004.

Bonaca 03 — Bonaca, M.V., Chairman, Advisory Committee on Reactor Safeguards (ACRS), U.S. Nuclear Regulatory Commission, "Pressurized Thermal Shock (PTS) Reevaluation Project: Technical Bases for Potential Revision to PTS Screening Criteria," February 21, 2003.

Brothers 63 — Brothers, A.J., and S. Yukawa, "The Effect of Warm Prestressing on Notch Fracture Strength," *Journal of Basic Engineering,* March 1963, p. 97.

Charpy — Charpy, M.G., "Note sur l'Essai des Metaux à la Flexion par Choc de Barreaux Entailles," *Soc. Ing. Francais*, June 1901, p. 848.

Cheverton 85a — Cheverton, R.D., et al., "Pressure Vessel Fracture Studies Pertaining to the PWR Thermal-Shock Issue: Experiments TSE-5, TSE-5A, and TSE-6," NUREG/CR-4249 (ORNL-6163), Oak Ridge National Laboratory, June 1985.

Cheverton 85b — Cheverton, R.D., et al., Pressure Vessel Fracture Studies Pertaining to the PWR Thermal-Shock Issue: Experiment TSE-7," NUREG/CR-4303 (ORNL-6177), Oak Ridge National Laboratory, August 1985.

Chopra 06 — Chopra, O.K., et al., "Crack Growth Rates of Irradiated Austenitic Stainless Steel Weld Heat Affected Zone in BWR Environments," NUREG/CR-6891, U.S. Nuclear Regulatory Commission, January 2006.

Congleton 85 — Congleton, J., T. Shoji, and R.N. Parkins, "The Stress Corrosion Cracking of Reactor Pressure Vessel Steel in High-Temperature Water" *Corrosion Science*, Vol. 25, No. 8/9: 1985.

CSAU — Boyack, B., et al., "Quantifying Reactor Safety Margins – Application of Code Scaling, Applicability, and Uncertainty Evaluation Methodology to a Large-Break Loss of Coolant Accident," NUREG/CR-5249, U.S. Nuclear Regulatory Commission, December 1989.

Dhooge 78 — A. Dhooge, R.E. Dolby, J. Sebille, R. Steinmetz, and A.G. Vinckier, "A Review of Work Related to Reheat Cracking in Nuclear Reactor Pressure Vessel Steels," *International Journal of Pressure Vessels and Piping*, Vol. 6, 1978, pp.329–409.

Dickson 87 — Dickson, T.L., "Sensitivity of Probabilistic Fracture Mechanics Analysis Results to Thermal-Hydraulic Variations," March 24, 1987.

Dickson 99 — Dickson, T.L., et al., "Evaluation of Margins in the ASME Rules for Defining the P-T Curve for an RPV," *Proceedings of the ASME Pressure Vessel and Piping Conference*, 1999.

Dickson 02 — Dickson, T.L. and Simonen, F.A., "The Impact of an Improved Flaw Model on Pressurized Thermal Shick Evaluation," *Proceedings of the ASME Pressure Vessel and Piping Conference*, Vancouver, British Columbia, 2002.

Dickson 03 — Dickson, T.L. and Simonen, F.A., "The Sensitivity of Pressurized Thermal Shock Results to Alternative Models for Weld Flaw Distributions,"

Proceedings of the ASME Pressure Vessel and Piping Conference, Cleveland, Ohio, 2002.

Dickson 03b — Bass, B.R., T.L. Dickson, P.T. Williams, A.-V. Phan, and K.L. Kruse, "Verification and Validation of the FAVOR Code: Deterministic Load Variables," Oak Ridge National Laboratory Report, ORNL/NRC/LTR-04/11, March 2004.

Eason — Eason, E., et al., "Updated Embrittlement Trend Curve for Reactor Pressure Vessel Steels," *Transactions of the 17th International Conference on Structural Mechanics in Reactor Technology (SMiRT 17)*, Prague, Czech Republic, August 17–22, 2003.

English 02 — English, C., and W. Server, "Attenuation in US RPV Steels – MRP-56," Electric Power Research Institute, June 2002.

EPRI 94 — EPRI Report TR-103837, "PWR Reactor Pressure Vessel License Renewal Industry Report, Revision 1," Electric Power Research Institute, July 1994

EricksonKirk 04 — EricksonKirk, MarjorieAnn, "*Materials Reliability Program: Implementation Strategy for Master Curve Reference Temperature, T_o (MRP-101),*" EPRI, Palo Alto, CA, and U.S. Department of Energy, Washington, DC: 2004. 1009543.

Fang 03 — Fang T., and M. Modarres, "Probabilistic and Deterministic Treatments for Multiple Flaws in Reactor Pressure Vessel Safety Analysis," *Transactions of the 17th International Conference on Structural Mechanics in Reactor Technology (SMiRT 17),* August 17–22, 2003, Prague, Czech Republic.

Fletcher 84 — Fletcher, C. D., et. al., RELAP5 Thermal-Hydraulic Analyses of Pressurized Thermal Shock Sequences for the Oconee-1 Pressurized-Water Reactor, NUREG/CR-3761, June 1984.

GL9201R1 — Generic Letter 92-01 Revision 1, "Reactor Vessel Structural Integrity, 10 CFR 50.54(f)," U.S. Nuclear Regulatory Commission, 1992.

GL9201R1S1 — Generic Letter 92-01 Revision 1, "Reactor Vessel Structural Integrity," U.S. Nuclear Regulatory Commission, May 19, 1995.

Hanson 94 — A.L. Hanson et al., "Calculations in Support of a Potential Definition of Large Release," NUREG/CR-6094, U.S. Nuclear Regulatory Commission, May 1994.

Hurst 85 — Hurst, P., D.A. Appleton, P. Banks, and A.S. Raffel. "Slow Strain Rate Stress Corrosion Tests on A508-III and A533B Steel in De-Ionized and PWR Water at 563K" *Corrosion Science*, Vol. 25, No. 8/9: 1985.

IAEA 90 — "Stress Corrosion Cracking of Pressure Vessel Steel in PWR Primary Water Environments." *Proceedings of the Third International Atomic Energy Agency Specialists' Meeting on Subcritical Crack Growth*, U.S. Nuclear Regulatory Commission (NRC), Moscow, 14–17 May 1990.

INEEL 00a — INEEL staff review of LERs for the Oconee PTS analysis conducted during March–April, 2000, based on keywords "overcooling," "thermal shock," and "excessive cooling." This includes a draft letter report, "Human Performance Insights for Overcooling Events in Support of PTS," D. Gertman and M. Parrish, INEEL, March 7, 2000.

Kasza 96	Kasza, K.E., et al., "Nuclear Plant Generic Aging Lessons Learned (GALL)," NUREG/CR-6490, U.S. Nuclear Regulatory Commission, October 1996.
Khaleel 00	Khaleel, M.A., et al., "Fatigue Analysis of Components for 60-Year Plant Life," NUREG/CR-6674, U.S. Nuclear Regulatory Commission, June 2000.
Kirk 01a	Kirk, M.T., M.E. Natishan, and M. Wagenhofer, "Microstructural Limits of Applicability of the Master Curve," *32nd Volume, ASTM STP-1406,* R. Chona, Ed., American Society for Testing and Materials, 2001.
Kirk 01b	Kirk, M., and M.E. Natishan, "Shift in Toughness Transition Temperature Due to Irradiation: ΔT_o *vs.* ΔT_{41J}, A Comparison and Rationalization of Differences," *Proceedings of the IAEA Specialists Meeting on Master Curve Technology*, Prague, Chech Republic, September 2001
Kirk 02a	Kirk, M. T., M.E. Natishan, and M. Wagenhofer, M., "A Physics-Based Model for the Crack Arrest Toughness of Ferritic Steels," *Fatigue and Fracture Mechanics, 33rd Volume, ASTM STP-1417,* W.G. Reuter and R.S. Piascik, Eds., American Society for Testing and Materials, 2002.
LER 92-023	Fort Calhoun Station, Docket No. 50-285, Licensee Event Report 92-023, submitted via letter from Omaha Public Power District to the USNRC on August 3, 1992.
LER 92-028	Fort Calhoun Station, Docket No. 50-285, Licensee Event Report 92-028, submitted via letter from Omaha Public Power District to the USNRC on September 21, 1992.
Marshall 82	"An Assessment of the Integrity of PWR Vessels," 2nd report by a study group under the chairmanship of D.W. Marshall, United Kingdom Atomic Eenergy Authority, 1982.
Meyer 03	Meyer, T., B. Bishop, P. Kotwicki, and N. Palm, "Materials Reliability Program: Pressurized Thermal Shock Sensitivity Studies Using the FAVOR Code (MRP-96)," Electric Power Research Institute, November 2003.
Natishan 01	Natishan, M.E.N., *Materials Reliability Program (MRP) Establishing a Physically Based, Predictive Model for Fracture Toughness Transition Behavior of Ferritic Steels (MRP-53)*, Electric Power Research Institute, 2001. 1003077.
NEI Comments	NEI Letter, dated June 23, 2003, from A. Marion to N. Chokshi. "Review of NRC Draft Report entitled *Technical Basis for Revision of the Pressurized Thermal Shock (PTS) Screening Limit in the PTS Rule (10 CFR 50.61).*"
NRC FR 86	51 FR 28044, August 4, 1986, and 51 FR 30028, August 21, 1986 (republication of 51 FR 28044 in its entirety at the Commission's request), "Safety Goals for the Operations of Nuclear Power Plants: Policy Statement."
NRC MEMO 82	Memorandum dated August 30 1982 from M. Vagans to S. Hanauer (DST/NRR).
NRC MTEB 5.2	METB 5-2, Branch Technical Position, "Fracture Toughness Requirements," Rev. 1, U.S. Nuclear Regulatory Commission, July 1981.

NRC 90	SRM - SECY-00-0077, STAFF REQUIREMENTS - SECY-00-0077 - "Modifications to the Reactor Safety Goal Policy Statement," U.S. Nuclear Regulatory Commission, June 27, 2000.
NRC 98b	NUREG-0800 (SRP Ch. 19), "Standard Review Plan for the Review of Safety Analysis Reports for Nuclear Power Plants," Chapter 19, Severe Accidents, U.S. Nuclear Regulatory Commission.
NRC 00	U.S. Nuclear Regulatory Commission, Technical Basis and Implementation Guidelines for A Technique for Human Event Analysis (ATHEANA), NUREG-1624, Rev. 1, U.S. Nuclear Regulatory Commission, May 2000.
NRC-IR	Inspection Report 50-285/92-18, U.S. Nuclear Regulatory Commission, August 6, 1992.
NRR Comments	Comments on [Kirk 12-02] provided from NRR to RES, March 2003.
NUREG/BR-0167	"Software Quality Assurance Program and Guidelines," Office of Information Resources Management, U.S. Nuclear Regulatory Commission, February 1993.
ORNL 85a	Oak Ridge National Laboratory, Pressurized Thermal Shock Evaluation of the Calvert Cliffs Unit 1 Nuclear Power Plant, NUREG/CR-4022, ORNL/TM-9408, for the U.S. Nuclear Regulatory Commission, September 1985.
ORNL 85b	Oak Ridge National Laboratory, Pressurized Thermal Shock Evaluation of the H.B. Robinson Unit 2 Nuclear Power Plant, NUREG/CR-4183, ORNL/TM-9567, for the U.S. Nuclear Regulatory Commission, September 1985.
ORNL 86	Oak Ridge National Laboratory, "Preliminary Development of an Integrated Approach to the Evaluation of Pressurized Thermal Shock as Applied to the Oconee Unit 1 Nuclear Power Plant, NUREG/CR-3770, ORNL/TM-9176, for the U.S. Nuclear Regulatory Commission, May 1986.
Poloski 98	J.P. Poloski et al., "Reliability Study: Auxiliary/Emergency Feedwater Systems, 1987–1995," NUREG/CR-5500, U.S. Nuclear Regulatory Commission, August 1998.
Poloski 99	Poloski, J.P., Marksberry, D.G., Atwood, C.L., and Galyean, W.J., "Rates of Initiating Events at U.S. Nuclear Power Plants: 1987-1995," NUREG/CR-5750, February 1999.
Pratt 99	Pratt W.T., et al., "An Approach for Estimating the Frequencies of Various Containment Failure Modes and Bypass Events," NUREG/CR-6595, U.S. Nuclear Regulatory Commission, October 2004.
PREP	"PREP4: Power Reactor Embrittlement Program, Version 1.0," Electric Power Research Institute, 1996. SW-106276.
PRODIGAL	Chapman, O.V.J., and F.A. Simonen, "RR-PRODIGAL – A Model for Estimating Probabilities of Defects in Welds," NUREG/CR-5505, U.S. Nuclear Regulatory Commission, October 1998.
Randall 87	Randall, P.N., "Basis for Revision 2 of the USNRC Reg. Guide 1.99, Radiation Embrittlement in Nuclear Pressure Vessel Steels: An International Review (2nd Volume)," ASTM STP-909, L.E. Steele, Ed., 1987.

RELAP 99	RELAP5/MOD3 Code Manual, Volume IV: Models and Correlations, June 1999.
RELAP 01	RELAP5/MOD3.3 Code Manual – Vol III: Developmental Assessment Problems, December 2001
RG 1.162	Regulatory Guide 1.162, "Thermal Annealing of Reactor Pressure Vessel Steels," U.S. Nuclear Regulatory Commission, February 1996.
RG 1.154	Regulatory Guide 1.154, "An Approach for Using Probabilistic Risk Assessment in Risk-Informed Decisions on Plant-Specific Changes to the Licensing Basis," U.S. Nuclear Regulatory Commission, January 1987.
RG 1.174 Rev 1	Regulatory Guide 1.174, Revision 1 "Format and Content of Plant-Specific Pressurized Thermal Shock Safety Analysis Reports for Pressurized-Water Reactors," U.S. Nuclear Regulatory Commission, November 2002.
RG 1.190	Regulatory Guide 1.190, "Calculational and Dosimetry Methods for Determining Pressure Vessel Neutron Fluence," U.S. Nuclear Regulatory Commission, March 2001.
RG 1.99	Regulatory Guide 1.99, Rev. 2, "Radiation Embrittlement of Reactor Vessel Materials," U.S. Nuclear Regulatory Commission, May 1988.
Rolfe	Rolfe, S.T., and J.T. Barson, *Fracture and Fatigue Control in Structures: Applicatins of Fracture Mechanics, Second Edition*, Prentice-Hall, 1987.
Rippstein 89	Rippstein, K., and H. Kaesche. "The Stress Corrosion Cracking of a Reactor Pressure Vessel Steel in High-Temperature Water at High Flow Rates," *Corrosion Science*, Vol. 29, No. 5: 1989
Ruther 84	Ruther, W.E., W.K. Soppet, and T.F. Kassner, "Evaluation of Environmental Corrective Actions," *Materials Science and Technology Division Light-Water-Reactor Safety Research Program: Quarterly Progress Report, October–December 1983*, NUREG/CR-3689, Vol. IV, ANL-83-85, Argonne National Laboratory, for the U.S. Nuclear Regulatory Commission, August 1984.
RVID2	Reactor Vessel Integrity Database, Version 2.1.1, U.S. Nuclear Regulatory Commission, July 6, 2000.
SAPHIRE	Systems Analysis Programs for Hands-on Integrated Reliability Evaluations (SAPHIRE) Version 7.0, Idaho National Engineering and Environmental Laboratory.
SECY-82-465	SECY-82-465, "Pressurized Thermal Shock," U.S. Nuclear Regulatory Commission, November 23, 1982.
SECY-93-138	SECY-93-138, "Recommendation on Large Release Definition," U.S. Nuclear Regulatory Commission, June 10, 1993.
SECY-00-0198	SECY-00-0198, "Status Report on Study of Risk-Informed Changes to the Technical Requirements of 10 CFR Part 50 (Option 3) and Recommendations on Risk-Informed Changes to 10 CFR 50.44 (Combustible Gas Control)," U.S. Nuclear Regulatory Commission, September 14, 2000.
SECY-02-0092	SECY-02-0092, "Status Report: Risk Metrics and Criteria for Pressurized Thermal Shock," U.S. Nuclear Regulatory Commission, May 30, 2002.

Schuster 02	Schuster, G.J., "Technical Letter Report – JCN-Y6604 – Validated Flaw Density and Distribution Within Reactor Pressure Vessel Base Metal Forged Rings," Pacific Northwest National Laboratory, for U.S. Nuclear Regulatory Commission, December 20, 2002.
Shaw 88	Shaw, R.A., et al., "Development of a Phenonmena Identificatioin and Ranking Table (PIRT) for Thermal-Hydraulic Phenomena During a PWR LBLOCA," NUREG/CR-5074, August 1988.
Simonen 86	Simonen, F.A., et al., "Reactor Pressure Vessel Failure Probability Following Through-Wall Cracks Due to Pressurized Thermal Shock Events," NUREG/CR-4483, U.S. Nuclear Regulatory Commission, March 1986.
Spiggs 85	Spriggs, G.D., Koenig, J. E., Smith, R.C., "TRAC-PF1 Analyses of Potential Pressurized Thermal Shock Transients at Calvert Cliffs Unit 1,". NUREG/CR-4109, February 1985
Strosnider 94	Strosnider, J., et al., "Reactor Pressure Vessel Status Report," NUREG-1511, U.S. Nuclear Regulatory Commission, 1994.
Swanson 87	Swanson, L.W., and I. Catton, "PWR Annulus Thermal-Hydraulics Important to Analysis of Pressurized Thermal Shock," *Nuclear Engineering and Design*, 102, 105–114, 1987
Theofanous 01	Theofanous, T.G., Dinh, A.T., Yuen, W.W., Nourgaliev, R.R., Dinh, T.N., "Consequences of Postulated PTS-Induced Brittle Failure of a Pressurized Water Reactor Vessel," University of California, Santa Barbara, CRSS-SA-01/4, April 5, 2001.
Travers 03	Travers, W.D., "Pressurized Thermal Shock (PTS) Reevaluation Project: Technical Bases for Potential Revision to PTS Screening Criteria," U.S. Nuclear Regulatory Commission, March 28, 2003.
Tregoning 05	Tregoning, R., Abramson, L., and Scott, P., "Estimating Loss-of-Coolant Accident (LOCA) Frequencies through the Elicitation Process," United States Nuclear Regulatory Commission, NUREG-1829, 2005.
Wagenhofer 01	Wagenhofer, M., and M.E. Natishan, "A Micromechanical Model for Predicting Fracture Toughness of Steels in the Transition Region," *33rd Volume, ASTM STP-1417*, Reuter and Piascik, Eds., American Society for Testing and Materials, 2002.
Wallin 93a	Wallin, K., "Irradiation Damage Effects on the Fracture Toughness Transition Curve Shape for Reactor Vessel Steels," *Int. J. Pres. Ves. & Piping*, 55, pp. 61–79, 1993.
Wallin 98b	Wallin, K., and R. Rintamaa, "Master Curve Based Correlation Between Static Initiation Toughness K_{Ic} and Crack Arrest Toughness K_{Ia}," *Proceedings of the 24th MPA-Seminar*, Stuttgart, October 8–9, 1998.
Westinghouse 99	"WOG Pilot-Plant Application of the EPRI Alternative Method for Reactor Vessel PTS," WCAP-15156, Westinghouse Electric Company, LLC, Nuclear Services Division, June 1999.
WRC 175	"PVRC Recommendations on Toughness Requirements for Ferritic Materials." Welding Research Council Bulletin No. 175, PVRC Ad Hoc Group on Toughness Requirements, August 1972.

Woods 01 — Woods, R., N. Siu, A. Kolaczkowski, and W. Galyean, "Selection of Pressurized Thermal Shock Transients To Include in PTS Risk Analysis," *IJPVP*, 78 (2001) 179–183.

Zuber 89 — Zuber, N. et al., "Quantifying Reactor Safety Margins, NUREG/CR-5249," December 1989.

NRC FORM 335 (9-2004) NRCMD 3.7

U.S. NUCLEAR REGULATORY COMMISSION

BIBLIOGRAPHIC DATA SHEET

(See instructions on the reverse)

1. REPORT NUMBER (Assigned by NRC, Add Vol., Supp., Rev., and Addendum Numbers, if any.)

NUREG-1806, Vol.1

2. TITLE AND SUBTITLE

Technical Basis for Revision of the Pressurized Thermal Shock (PTS) Screening Limit in the PTS Rule (10 CFR 50.61): Summary Report

3. DATE REPORT PUBLISHED

MONTH	YEAR
August	2007

4. FIN OR GRANT NUMBER

5. AUTHOR(S)

Mark EricksonKirk, Mike Junge, William Arcieri, B. Richard Bass, Robert Beaton, David Bessette, T.H.(James) Chang, Terry Dickson, C. Don Fletcher, Alan Kolaczkowski, Shah Malik, Todd Mintz, Claud Pugh, Fredric Simonen, Nathan Siu, Donnie Whitehead, Paul Williams, Roy Woods, Sean Yin

6. TYPE OF REPORT

Technical

7. PERIOD COVERED *(Inclusive Dates)*

6-99 to 6-06

8. PERFORMING ORGANIZATION - NAME AND ADDRESS *(If NRC, provide Division, Office or Region, U.S. Nuclear Regulatory Commission, and mailing address; if contractor, provide name and mailing address.)*

Division of Fuel, Engineering, and Radiological Research
Office of Nuclear Regulatory Research
U.S. Nuclear Regulatory Commission
Washington, DC 20555-0001

9. SPONSORING ORGANIZATION - NAME AND ADDRESS *(If NRC, type "Same as above"; if contractor, provide NRC Division, Office or Region, U.S. Nuclear Regulatory Commission, and mailing address.)*

Division of Fuel, Engineering, and Radiological Research
Office of Nuclear Regulatory Research
U.S. Nuclear Regulatory Commission
Washington, DC 20555-0001

10. SUPPLEMENTARY NOTES

M. EricksonKirk, NRC Project Manager

11. ABSTRACT *(200 words or less)*

During plant operation, the walls of reactor pressure vessels (RPVs) are exposed to neutron radiation, resulting in localized embrittlement of the vessel steel and weld materials in the core area. If an embrittled RPV had a flaw of critical size and certain severe system transients were to occur, the flaw could very rapidly propagate through the vessel, resulting in a through-wall crack and challenging the integrity of the RPV. The severe transients of concern, known as pressurized thermal shock (PTS), are characterized by a rapid cooling of the internal RPV surface in combination with repressurization of the RPV. Advancements in our understanding and knowledge of materials behavior, our ability to realistically model plant systems and operational characteristics, and our ability to better evaluate PTS transients to estimate loads on vessel walls led the NRC to realize that the earlier analysis, conducted in the course of developing the PTS Rule in the 1980s, contained significant conservatisms.

This report summarizes 21 supporting documents that describe the procedures used and results obtained in the probabilistic risk assessment, thermal hydraulic, and probabilistic fracture mechanics studies conducted in support of this investigation. Recommendations on toughness-based screening criteria for PTS are provided.

12. KEY WORDS/DESCRIPTORS *(List words or phrases that will assist researchers in locating the report.)*

pressurized thermal shock, probabilistic fracture mechanics, nuclear reactor pressure vessel pressurized water reactor

13. AVAILABILITY STATEMENT

unlimited

14. SECURITY CLASSIFICATION

(This Page)

unclassified

(This Report)

unclassified

15. NUMBER OF PAGES

16. PRICE

Federal Recycling Program